



Norwegian University
of Life Sciences

Master's Thesis 2017 30 ECTS
Faculty of Science and Technology

Seismic analysis of multistorey hybrid buildings.

Mohsen Shafighi
Structural Engineering and Architecture

ABSTRACT

Each cubic meter of timber added to a structure or a building accounts for an emission reduction of around 700-1000 kg¹ CO₂. This environmental advantage, in addition to increased interest in high-rise timber buildings and improved timber technologies, gives multistorey hybrid buildings of steel-timber and concrete-timber a more solid position in the Norwegian housing market. The benefits of prefabricated timber materials include a higher construction speed and efficiency, in addition to earthquake resistance, have led to timber construction establishing a more prominent role in building construction. Even though this position still is smaller than concrete and steel, and needs to overcome obstacles such as fire safety regulations and higher construction costs, building with timber is quickly gaining momentum. The additional costs associated with using timber will become less significant when the environmental aspects of a housing development gain more consideration.

The purpose of this thesis is to draw attention to some of the advantages adding timber has in terms of energy dissipation when subjected to earthquake-induced forces. This will be verified by analyzing different models and materials common in Norwegian construction.

The introductory part refers to the natural phenomenon of earthquakes and how Norway has been affected by it. The theory section deals with the dynamic aspects including systems with various degrees of freedom and the requirements from Eurocode 8, in addition to Norwegian National Annex. The methodology part of thesis deals with the calculation methodology used to determine the lateral forces a structure must resist in order to remain within a linearly elastic range of deformation without collapsing. Model analysis investigates the role of including timber elements in a seismic design, and how the ductility and strength provided by this material in a hybrid building is adequate. Finally, the result and conclusion section discusses the different results produced by various software packages and hand calculations.

¹ www.moelven.com

SAMMENDRAG

For hver kubikkmeter treverk som blir lagt i en konstruksjon eller ett bygg, oppnås utslippsreduksjon på rundt 700-1000 kg CO₂. Dette, i tillegg til vekst av interesser innen høyhus av tre, og forbedret dimensjoneringsteknologi, gir fleretasjes hybridbygninger av stål-massivtre og betong-massivtre en mer solid posisjon i den norske byggebransjen. Fordelen ved bruk av prefabrikkerte massive trelementer, oppnåelse av raskere byggetid og effektivitet på byggeplass, i tillegg til bedre jordskjelvmotstand har vært viktige for å nå denne posisjonen. Selv om massivtre har liten markedsandel i forhold til stål og betong, og hindringer som branntekniske begrensninger og høye byggekostnader, utbygging av nye trehus finner raskere enn noen gang sitt momentum. Ekstra kostnader ved bruk av tremateriale vil bli mindre avgjørende når miljøaspekter ved utbygging av trebygg blir enda viktigere.

Formålet med denne oppgaven er å rette fokus på noen av fordelene som oppnås ved bruk av massivtre i form av energidissipasjonsevne når de blir utsatt for jordskjelvinduserte krefter. Dette skal verifiseres ved analysering av flere modeller og materialer som er vanlig å bygge med i Norge.

Introduksjonsdelen omtaler blant annet fenomenet jordskjelv og hvordan Norge har blitt påvirket av dette. Teoridelen omhandler dynamikk, systemer med ulike frihetsgrader og kravene fra Eurokode 8, med tilhørende Nasjonalt tillegg. Metodologi omhandler beregningsmetoden som brukes til å finne horisontalkraft bygg må motstå for å forbli i et lineært elastisk område av deformasjon uten å kollapse. Analysedelen vil gjøre rede for hvor godt massivtre reduserer de seismiske kreftene, og at duktiliteten og styrken som tilbys i en hybridbygning er tilstrekkelig. Til slutt i resultat og diskusjonsdelen oppsummeres analysen, og vurderinger blir presentert.

ACKNOWLEDGEMENTS

This dissertation concludes the degree program at Norwegian University of Life Sciences (NMBU) for me. The work has been conducted in the spring semester of 2017. This has been a challenging, but very educational experience.

I would like to express my gratitude and sincere thanks to my thesis supervisors, Professor Roberto Tomasi and Associate Professor Themistoklis Tsalkatidis, for introducing this subject, encouraging me and coordinating the writing of this thesis.

My gratitude also goes to my colleagues at Multiconsult, who have supported me in different aspects of this work with their valuable advice.

Finally I would like to express my deepest gratuities to my father, Shahriar Shafighi and my mother, Mitra Gerami for their sacrifices, retaining their belief in me and their unfaltering love throughout my life. And at last but not least my wife Taban, who has stood by me like a supporting column in times of bewilderment and enabled me to complete this work.

Oslo, May 2017

Mohsen Shafighi

TABLE OF CONTENT

ABSTRACT	iii
SAMMENDRAG	v
ACKNOWLEDGEMENTS	vii
TABLE OF CONTENT	ix
LIST OF FIGURES.....	xii
LIST OF TABLES	xv
ABBREVIATION AND SYMBOLS	xvii
CHAPTER 1 INTRODUCTION	1
1.1 BACKGROUND.....	1
1.2 OBJECTIVE	2
1.3 LIMITATION.....	2
1.4 THESIS OUTLINE.....	2
CHAPTER 2 EARTHQUAKES	3
2.1 INTRODUCTION	3
2.2 EARTHQUAKES, THE PHENOMENON.....	3
2.3 EARTHQUAKE IN EUROPE	4
2.4 EARTHQUAKE IN NORWAY	5
2.5 EARTHQUAKE MAGNIUDE AND INTENSITY	6
CHAPTER 3 THEORY	7
3.1 STRUCTURAL DYNAMIC.....	7
3.1.1 INTRODUCTION	7
3.1.2 VIBRATION OF A SYSTEM.....	7
3.1.3 SINGLE-DEGREE-OF-FREEDOM SYSTEMS	15
3.1.4 GENERALIZED SDOF SYSTEMS	17
3.1.5 MULTI-DEGREE-OF-FREEDOM SYSTEMS.....	18
3.1.6 RESPONSE OF A MDOF SYSTEM.....	21
3.1.7 DUCTILITY OF STRUCTURE	23
3.1.8 FREQUENCY AND PERIOD	25
3.1.9 MASS AND STIFFNESS MATRIX.....	26
3.1.10 SECOND-ORDER EFFECTS.....	27
3.2 RESPONS AND DESIGN SPECTRA	31
3.2.1 INTRODUCTION	31
3.2.2 DEFINITION OF RESPONSE SPECTRUM.....	31
3.2.3 DIFFERENT RESPONSE SPECTRUM	33
3.2.4 DEFINITION OF DESING SPECTRUM.....	36
3.3 DESIGN GUIDELINES AND BUILDING CODES.....	39
3.3.1 INTRODUCTION	39

3.3.2	FUNDAMENTAL CRITERIA, FACTORS AND PARAMETERS	40
3.3.3	EARTHQUAKE CALCULATION ACCORDING TO EC8	48
3.3.4	DESIGN OF STRUCTURE.....	48
3.3.5	REGULARITY.....	49
3.3.6	TORSIONAL EFFECT.....	52
3.3.7	PRIMARY AND SECONDARY ELEMENTS	53
3.4	HYBRID BUILDING	53
3.4.1	INTRODUCTION	53
3.4.2	STEEL-CONCRETE.....	54
3.4.3	STEEL-TIMBER.....	55
3.4.4	EUROCODE 5	56
3.4.5	CROSS LAMINATED TIMBER (CLT).....	59
3.4.6	GLUED LAMINATED TIMBER (GLT).....	62
3.4.7	TIMBER BUILDINGS IN NORWAY	65
CHAPTER 4	METHOD	67
4.1	ANALYSING METHODS	67
4.1.1	INTRODUCTION	67
4.1.2	LATERAL FORCE METHOD.....	67
4.1.3	MODAL RESPONSE SPECTRUM.....	69
4.1.4	NONLINEAR ANALYSIS.....	71
CHAPTER 5	ANALYSIS	73
5.1	MODELLING	73
5.1.1	INTRODUCTION	73
5.1.2	PRESENTATION OF 3D MODELS	73
5.2	ANALYTICAL ANALYSIS OF 3D MODEL.....	77
5.3	MODAL ANALYSIS OF 3D MODELS	92
5.3.1	NATURAL FREQUENCY AND PERIOD	92
5.3.2	MODE SHAPES AND MODAL MASS	96
5.3.3	INTERSTOREY DRIFT.....	104
5.3.4	BASE SHEAR	113
5.4	SOFTWARE USAGE.....	118
5.4.1	FEM-DESIGN	118
5.4.2	CLTdesigner	119
5.4.3	OVE SLETTEN	120
5.4.4	MATHCAD PRIME.....	120
5.4.5	TIMBERTECH BUILDINGS.....	121
CHAPTER 6	RESULTS, DISCUSSION AND CONCLUSION.....	123
6.1	ASSESSMENT OF ANALYSIS AND RESULTS	123
6.2	ASSESSMENT OF WIND LOAD AND SEISMIC LOAD	125

6.3	CONCLUSION	126
6.4	PROPOSED FURTHER WORK.....	128
APPENDIX A	HAND CALCULATION	
APPENDIX B	PRESENTATION OF 3D MODELS	
APPENDIX C	WIND LOAD CALCULATION	
APPENDIX D	CLT FLOOR CALCULATION	
APPENDIX E	MEASUREMENT INSTRUMENTS	
APPENDIX F	CLT VALUES FROM MARTINSON	
	BIBLIOGRAPHY	

LIST OF FIGURES

FIGURE 1-1	WORLD'S MAP SHOWING BOUNDARIES OF DIFFERENT ZONE AND FAULTS (VISUAL.LY 2011).	1
FIGURE 2-1	DIFFERENT TYPES OF FAULTS (TFD.COM 2016).....	3
FIGURE 2-2	EUROPEAN SEISMIC HAZARD MAP (SHARE 2013).....	4
FIGURE 2-3	LAST FIVE LARGEST EARTHQUAKES IN NORWAY (JORDSKJELV.NO). MAP FROM MAPBOX.COM.....	5
FIGURE 3-1	SYSTEM CLASSIFICATION.	7
FIGURE 3-2	TRANSIENT AND STEADY-STATE DYNAMIC RESPONSE OF A SYSTEM (ANSYS.STUBA.SK 2016).	11
FIGURE 3-3	FREE VIBRATION OF SYSTEMS WITH FOUR LEVELS OF DAMPING (CHOPRA 2012).....	13
FIGURE 3-4	FREE VIBRATION OF CRITICALLY DAMPED, UNDER- AND OVERDAMPED SYSTEMS (CHOPRA 2012).	13
FIGURE 3-5	SINGLE-DEGREE-OF-FREEDOM SYSTEM: (A) APPLIED FORCE $p(t)$; (B) EARTHQUAKE-INDUCED GROUND MOTION (CHOPRA 2012).	15
FIGURE 3-6	SYSTEM WITH THE MASS DISTRIBUTED OVER TWO STOREY AND TWO POSSIBLE MODE SHAPES.	17
FIGURE 3-7	MULTI-DEGREE-OF-FREEDOM SYSTEM: (A) EARTHQUAKE INDUCED GROUND MOTION AND (B) EXTERNAL FORCES (CHOPRA 2012).....	18
FIGURE 3-8	TYPICAL STRESS-STRAIN CURVE OF TIMBER (KIRKEGAARD ET AL. 2010).....	24
FIGURE 3-9	ELASTOPLASTIC AND ITS CORRESPONDING LINEAR SYSTEM (CHOPRA 2012) & (JAVED 2015).	25
FIGURE 3-10	FREE VIBRATION OF A SYSTEM WITHOUT DAMPING WITH NATURAL PERIOD T_n (CHOPRA 2012).	26
FIGURE 3-11	COLUMN WITH HORIZONTAL DISPLACEMENT.	27
FIGURE 3-12	IDEALIZATION OF AXIAL-LOAD MECHANISM IN BEAM (CLOUGH & PENZIEN).....	29
FIGURE 3-13	FORCE ACTING ON A ROD ELEMENT.....	30
FIGURE 3-14	RECORDED GROUND MOTION BASED ON 1979 HUDSON (CHOPRA 2012).....	31
FIGURE 3-15	HORIZONTAL ELASTIC RESPONSE SPECTRA FOR USE IN NORWAY (EC8 2014).....	33
FIGURE 3-16	(A) GROUND ACCELERATION; (B) DEFORMATION RESPONSE OF THREE SDF SYSTEMS WITH $z = 2\%$ AND $T_n = 0.5, 1, \text{ AND } 2 \text{ SEC}$; (C) DEFORMATION RESPONSE SPECTRUM FOR $z = 2\%$ (CHOPRA 2012).	34
FIGURE 3-17	GRAPH THAT SHOWS DIFFERENT RESPONSE SPECTRUM BASED ON EL CENTRO GROUND MOTION WITH DAMPING RATION 0.02. (A) DEFORMATION RESPONSE SPECTRUM; (B) PSEUDO-VELOCITY RESPONSE SPECTRUM; (C) PSEUDO-ACCELERATION RESPONSE SPECTRUM (CHOPRA 2012).	35
FIGURE 3-18	D-V-A PLOT FOR EL CENTRO GROUND MOTION (CHOPRA 2012).....	36
FIGURE 3-19	NORWEGIAN SEISMIC ZONING MAPS (JORDSKJELV.NO).....	38
FIGURE 3-20	LIST OF CURRENT BEHAVIOR FACTO (EC8 2014).....	42
FIGURE 3-21	RECOMMENDED PARTIAL FACTORS (EC8 2014) & (EC5 1994).....	44
FIGURE 3-22	LOAD CASES AND THEIR CONVERSION OF MASS (FEM-DESIGN).	45
FIGURE 3-23	PRESENTATION OF INTERSTOREY DRIFT (SEO ET AL. 2015).	46

FIGURE 3-24	EXAMPLE OF HOW CRITERIA “V” WORKS. $SdT \leq 0,49$ LEADS TO ELIMINATION OF EARTHQUAKE CALCULATION. THE REGULARITY CRITERIA IS FULLFILED AND THE BUILDING ONLY HAVE ONE DOMINANT NATURAL PERIOD T (LØSET & RIF 2010).....	47
FIGURE 3-25	CONSEQUENCES OF STRUCTURAL REGULARITY ON SEISMIC ANALYSIS AND DESIGN (EC8 2014)	49
FIGURE 3-26	DEFINITION OF COMPACT SHAPE (ELGHAZOULI 2009).....	50
FIGURE 3-27	EXAMPLE OF DIFFERENT SOLUTIONS OF BRACING SYSTEMS (LØSET & RIF 2010).....	51
FIGURE 3-28	BASIC VALUES FOR BEHAVIOR FACTOR FOR SYSTEMS REGULAR IN ELEVATION (EC8 2014).	51
FIGURE 3-29	EXAMPLE OF STIFFNESS DISTRIBUTION (LØSET & RIF 2010).....	52
FIGURE 3-30	MATERIAL PROPERTIES FOR STEEL, CONCRETE AND TIMBER (KHORASANI 2011).....	54
FIGURE 3-31	STEEL–CONCRETE COMPOSITE BEAM-COLUMN MODEL (WANG ET AL. 2013).....	55
FIGURE 3-32	VALUES OF <i>kmod</i> (EC5 1994).....	57
FIGURE 3-33	LOAD-DURATION CLASSES (EC5 1994).....	58
FIGURE 3-34	SERVICE CLASSES (EC5 1994).....	58
FIGURE 3-35	VALUES OF <i>kdef</i> (EC5 1994).....	58
FIGURE 3-36	CLT ELEMENT (BCA.GOV.SG 2017).....	59
FIGURE 3-37	STRENGTH CLASSES FOR SOFTWOOD (NS-EN338 2016).....	60
FIGURE 3-38	GLUED LAMINATED TIMBER (BCA.GOV.SG 2017).....	62
FIGURE 3-39	DEFLECTION COMPONENTS (EC5 1994).....	63
FIGURE 3-40	EXAMPLE OF POSSIBLE BEAM DEFLECTION (EC5 1994) AND (BELL ET AL. 2015).....	63
FIGURE 3-41	INCREASE IN NUMBER OF STUDENT HOUSING UNITS IN NORWAY. DATA FROM ARKITEKTUR-N.NO	65
FIGURE 4-1	DISTRIBUTION OF HORIZONTAL FORCE (LØSET ET AL. 2011).....	69
FIGURE 4-2	MODAL RESPONSE ANALYSIS DESCRIBED (LØSET ET AL. 2011).....	70
FIGURE 5-1	MODEL #1 AS MODELED IN FEM-DESIGN VERSION 16.....	74
FIGURE 5-2	MODEL #2 AS MODELED IN FEM-DESIGN VERSION 16.....	75
FIGURE 5-3	MODEL #3 AS MODELED IN FEM-DESIGN VERSION 16.....	75
FIGURE 5-4	MODEL #4 AS MODELES IN FEM-DESIGN VERSION 16.....	76
FIGURE 5-5	HORIZONTAL SPECTRUM CREATED IN FEM-DESIGN VERSION 16.....	77
FIGURE 5-6	MODEL THAT HAND CALCULATION IS BASED ON IN THIS SECTION.....	77
FIGURE 5-7	BRACING IN X-DIRECTION.....	79
FIGURE 5-8	FACTOR δ IS FOUND BY MEASURING THE DISTANCE OF THE ELEMENT UNDER CONSIDERATION FROM COM PREPENDICULAR TO THE DIRECTION OF SEISMIC ACTION, IN THIS CASE X-DIRECTION. AND DISTANCE BETWEEN TEO OUTERMOST LATERAL LOAD RESISTIN ELEMENTS. (EC5 1994)	80
FIGURE 5-9	FIRST MODE SHAPE IN X-DIRECTION.....	82
FIGURE 5-10	SECOND MODE SHAPE IN X-DIRECTION.....	83
FIGURE 5-11	THIRD MODE SHAPE IN X-DIRECTION.....	83
FIGURE 5-12	FOURTH MODE SHAPE IN X-DIRECTION.....	83

FIGURE 5-13	BRACING IN Y-DIRECTION	85
FIGURE 5-14	DIFFERENCE IN TERMS OF ELASTIC RESPOSSPECTURM CALCULATED PERIODS GIVE (EC8 2014).	89
FIGURE 5-15	MODE SHAPES IN ABSENSE OF GEOMETRICAL MATRIX.	90
FIGURE 5-16	MODE SHAPES IN ABSENSE OF GEOMETRICAL MATRIX.	91
FIGURE 5-17	TIMBERTECH MODAL ANALYSIS RESULTS.	95
FIGURE 5-18	SCHEMATIC CALCULATION OF INTERSTOREY DRIFT IN X-DRECTION DIRECTION – FEM-DESIGN.	108
FIGURE 5-19	SCHEMATIC CALCULATION OF INTERSTOREY DRIFT IN Y-DRECTION	112
FIGURE 5-20	GRAPH SHOWING THE BASE SHEAR DIFFERENCE BETWEEN MODELS IN THE FIRST MODE AND THE EMPIRICAL FORMULA GIVEN BY EC8-1.	113
FIGURE 5-21	GRAPH SHOWING THE BASE SHEAR DIFFERENCE BETWEEN MODELS IN THE SECOND MODE.	114
FIGURE 5-22	GRAPH SHOWING THE TOTAL BASE SHEAR DIFFERENCE BETWEEN MODELS IN X-DIRECTION.	115
FIGURE 5-23	GRAPH SHOWING THE TOTAL BASE SHEAR DIFFERENCE BETWEEN MODELS IN Y-DIRECTION.	116
FIGURE 5-24	BASE SHEAR RESULTS FROM TIMBERTECH.	117
FIGURE 5-25	DIFFERENT ANALYSIS AND RESULTS IN FEM-DESIGN.....	118
FIGURE 5-26	CLTDESIGNER ENVIROMENT.	119
FIGURE 5-27	OVE SLETTEN SNOW LOAD CALCULATION MODUL.....	120
FIGURE 5-28	PTC MATHCAD PRIME 3.0 ENVIREMENT.	120
FIGURE 5-29	MODEL #4 AS PRESENTED IN TIMBERTECH.	121

LIST OF TABLES

TABLE 1	ELASTIC RESPONSE SPECTRUM VALUES (EC8 2014).....	38
TABLE 2	SUMMARY OF DESIGN GUIDELINES USED IN NORWAY (EC8 2014).....	39
TABLE 3	VALUES FOR IMPORTANCE FACTOR γ_1 AND TYPE OF STRUCTURES IT APPLIES TO (EC8 2014). 40	
TABLE 4	GROUND TYPES (EC8 2014).	41
TABLE 5	LOAD FACTOR FOR SEISMIC ACTION (LØSET ET AL. 2011).....	43
TABLE 6	LIMITATION OF INTERSTOREY DRIFT (EC8 2014).	46
TABLE 7	OVERVIEW OF MODELS DIFFERENT CONFIGURATION.	73
TABLE 8	NATURAL FREQUENCIES OF DIFFERENT MODELS FROM FEM-DESIGN.	92
TABLE 9	NATURAL PERIOD OF DIFFERENT MODELS FROM FEM-DESIGN.	92
TABLE 10	FREQUENCY AND PERIOD RESULTS FROM MODEL #1 IS COMPARED TO THE REST.	93
TABLE 11	FREQUENCY AND PERIOD RESULTS FROM MODEL #2 IS COMPARED TO THE REST.	93
TABLE 12	FREQUENCY AND PERIOD RESULTS FROM MODEL #3 IS COMPARED TO THE REST.	94
TABLE 13	FREQUENCY AND PERIOD RESULTS FROM MODEL #4 IS COMPARED TO THE REST.	94
TABLE 14	COMPARING THE NATURAL PERIODS TO SEE THE EFFECT OF STIFFNESS.....	95
TABLE 15	SELECTED SHAPES AND EFFECTIVE MASSES FROM FEM-DESIGN.....	97
TABLE 16	MODE SHAPE FOR THE FIRST MODE ACCORDING TO FEM-DESIGN VERSION 16. THIS MODE INDICATES DISPLACEMENT IN X-DIRECTION.	98
TABLE 17	MODE SHAPE FOR THE SECOND MODE ACCORDING TO FEM-DESIGN VERSION 16. THIS MODE INDICATES DISPLACEMENT IN Y-DIRECTION.	99
TABLE 18	MODE SHAPE FOR THE THIRD MODE ACCORDING TO FEM-DESIGN VERSION 16. THIS MODE INDICATES TORSIONAL EFFECT.	101
TABLE 19	MODE SHAPE FOR THE FOURTH MODE ACCORDING TO FEM-DESIGN VERSION 16. THIS MODE INDICATES DISPLACEMENT IN X-DIRECTION.	102
TABLE 20	MODE SHAPE FOR THE FIFTH MODE ACCORDING TO FEM-DESIGN VERSION 16. THIS MODE INDICATES DISPLACEMENT IN Y-DIRECTION.	103
TABLE 21	MAXIMUM HORIZONTAL FORCE ACTED ON BRACINGS (kN) AND SHEAR WALL (kN/M) IN X- DIRECTION – FEM-DESIGN.....	103
TABLE 22	MAXIMUM HORIZONTAL FORCE ACTED ON BRACINGS (kN) AND SHEAR WALL (kN/M) IN Y- DIRECTION – FEM-DESIGN.....	104
TABLE 23	TOTAL DISPLACEMENT OF MODEL #1 IN X-DIRECTION (MM) DIRECTION – FEM-DESIGN. 105	
TABLE 24	TOTAL DIPLACEMENT OF MODEL #2 IN X-DIRECTION (MM) DIRECTION – FEM-DESIGN. 106	
TABLE 25	TOTAL DISPLACEMENT OF MODEL #3 IN X-DIRECTION (MM) DIRECTION – FEM-DESIGN. 107	
TABLE 26	TOTAL DISPLACEMENT OF MODEL #4 IN X-DIRECTION (MM) DIRECTION – FEM-DESIGN. 107	
TABLE 27	DISPLACEMENTS OF DIFFERENT MODELS IN X-DIRECTION (MM) DIRECTION – FEM-DESIGN. 108	

TABLE 28	TOTAL DISPLACEMENT OF MODEL #1 IN Y-DIRECTION (MM) DIRECTION – FEM-DESIGN.	109
TABLE 29	TOTAL DISPLACEMENT OF MODEL #2 IN Y-DIRECTION (MM) DIRECTION – FEM-DESIGN.	110
TABLE 30	TOTAL DISPLACEMENT OF MODEL #3 IN Y-DIRECTION (MM) DIRECTION – FEM-DESIGN.	111
TABLE 31	TOTAL DISPLACEMENT OF MODEL #4 IN Y-DIRECTION (MM) DIRECTION – FEM-DESIGN.	112
TABLE 32	DISPLACEMENTS OF DIFFERENT MODELS IN Y-DIRECTION (MM).	112
TABLE 33	BASE SHEAR OF THE FIRST MODE BASED ON SEISMIC CALCUTAION FROM FEM-DESIGN AND HAND CALCULATION (kN).....	114
TABLE 34	BASE SHEAR OF THE SECOND MODE BASED ON SEISMIC CALCUTAION (kN) – FEM-DESIGN.	115
TABLE 35	CALCULATED MAXIMUM BASE SHEAR FORCE IN X DIRECTION FOR ALL FOUR MODELS (kN) – FEM-DESIGN.....	116
TABLE 36	CALCULATED MAXIMUM BASE SHEAR FORCE IN Y DIRECTION FOR ALL FOUR MODELS (kN) – FEM-DESIGN.....	117
TABLE 37	COMPARING BASE SHEAR OF MODEL #4 IN FEM-DESIGN AND TIMBERTECH.....	117
TABLE 38	COMPARISION OF LOADS IN X AND Y DIRECTION.....	125

ABBREVIATION AND SYMBOLS

Abbreviations

DCH	High ductility
DCL	Low ductility
DCM	Medium ductility
DOF	Degrees of freedom
EC5	Eurocode 5, NS-EN 1995
EC8	Eurocode 8, NS-EN 1998
EOM	Equation of motion
MDOF	Multi-degree-of-freedom
PGA	Peak ground acceleration
RSA	Response spectrum analysis
SDOF	Single-degree-of-freedom
SLS	Serviceability limit state
SRSS	Square root of Sum of Square
ULS	Ultimate limit state

Latin symbols

A	Cross sectional area
A	Peak pseudo-acceleration response spectrum
$a_g R$	Reference peak ground acceleration
a_g	Design ground acceleration
C	Modal damping matrix
c	Damping matrix

c	Damping coefficient
c_{cr}	Critical damping coefficient
c_u	Undrained shear strength of soil
D	Peak value of deformation
d_r	Design interstorey drift
d_s	Displacement of a point of the structural system induced by the design seismic action
$E_{0,05}$	Fifth percentile value of modulus of elasticity parallel to grain
$E_{0,mean}$	Mean value of modulus of elasticity along the grain
$E_{90,mean}$	Mean value of modulus of elasticity perpendicular to the grain
$e_{ox,y}$	Eccentricity between centers of stiffness and mass
e_{ai}	Accidental eccentricity
E_d	Design action effect
E_E	Seismic action effect under consideration
E_{E_i}	Value of seismic action effect due to the vibration mode i
E_{mean}	Mean value of modulus of elasticity
E_{S_0}	Peak value of strain energy
F_b	Shear force
f_0	Peak value of earthquake-induced resisting force
$f_{c,d}$	Design compression strength
$f_{c,0,k}$	Characteristic compressive strength along the grain
$f_{c,90,k}$	Characteristic compressive strength perpendicular to the grain
$f_D(t)$	Damping resisting force
f_G	Geometric-stiffness coefficients

$f_I(t)$	Inertia force
$f_{m,d}$	Design bending strength
$f_{m,k}$	Characteristic bending strength
f_n	Natural cyclic frequency of vibration
$f_S(t)$	Elastic resisting force
$f_{t,0,k}$	Characteristic tensile strength along the grain
$f_{t,90,k}$	Characteristic tensile strength perpendicular to the grain
$f_{v,k}$	Characteristic shear strength
\bar{f}_y	Normalized yield strength
f_y	Yield strength
G_{mean}	Mean value of shear modulus
h	Interstorey height
I_s	Radius of gyration
K	Modal stiffness matrix
k	Stiffness matrix
k_c	Coefficient of compression
k_{def}	Deformation factor related to creep characteristics
$k_{f,peak}$	Correction factor used in defining reference peak ground acceleration
\mathbf{k}_G	Geometric-stiffness matrix
k_h	Height factor
k_{mod}	Modification factor taking into account the effect of the duration of load and moisture content
K_{ser}	The slip modulus

L_i	Floor-dimension perpendicular to the direction of the seismic action
L_e	Distance between the two outermost lateral load resisting elements, measured perpendicularly to the direction of the seismic action considered
M	Modal matrix
m	Mass matrix
M_i^{eff}	Effective modal mass
N_{SPT}	Standard Penetration Test below-count
$p(t)$	External dynamic force
P_{cr}	Critical buckling load
$p_{eff}(t)$	Effective earthquake force
Q	Load
q	Behavior factor
q_o	Basic value of the behavior factor
q_d	Displacement behavior factor
r	Response
$r_{x,y}$	Torsional radius
R_y	Yield strength reduction factor
S	Soil factor
S_{clt}	CLT shear stiffness
$S_e(T)$	Elastic response spectrum
$S_d(T)$	Design spectrum
$S_{De}(T)$	Elastic displacement response spectrum
s_k	Contribution from mode k to load vector

$S_{ve}(T)$	Vertical elastic response spectrum
T_1	Fundamental period of the building in the horizontal direction of interest
T	Vibration period of a linear single-degree-of-freedom system
T_B	Lower limit of the period of the constant spectral acceleration branch
T_C	Upper limit of the period of the constant spectral acceleration branch
T_D	Value defining the beginning of the constant displacement response range of the spectrum depends on the magnitude of earthquake
T_k	Period of vibration of mode k
T_n	Natural period of vibration
$u(t)$	Displacement
u_0	Peak value of earthquake-induced deformation
$u^t(t)$	Total displacement
u_c	Complimentary function
$u_g(t)$	Earthquake-induced ground motion
u_m	Maximum deformation
u_p	Particular integral
u_y	Yield deformation
$\ddot{u}(t)$	Acceleration
$\ddot{u}_g(t)$	Ground acceleration
$\dot{u}(t)$	Velocity
v	Reduction factor (interstorey drift)
V	Peak pseudo-velocity
V_{bo}	Base shear

$V_{s,30}$	Average value of propagation velocity of S waves in the upper 30 m of the soil profile at shear strain 10^{-5} or less
w_c	Upward deflection
w_{creep}	Creep deflection
w_{fin}	Final deflection
w_{inst}	Instantaneous deflection
$w_{net,fin}$	Net final deflection
$z(t)$	Generalized coordinate response

Greek Symbols

α_1	Multiplier of horizontal seismic design action at formation of first hinge in the system.
α_u	Multiplier of horizontal seismic design action at formation of global plastic mechanism
β	Lower bound factor for the horizontal design spectrum
β_n	Frequency ratio
γ_1	Importance factor
γ_c	Partial factor for concrete
γ_s	Partial factor for steel
γ_M	Partial factor for a material property
δ	Torsional effect factor
η	Damping correction factor
θ	Angle between axes
ι	Influence vector
κ	Shear correction coefficient

λ	Slenderness ratio
λ_{rel}	Relative slenderness
μ	Ductility factor
ξ	Viscous damping ratio (in percent)
ρ_k	Characteristic density
ρ_{mean}	Mean density
$\sigma_{c,0,d}$	Design value of stress of compression along the grain
τ	Dummy time variable
ϕ_i	i th natural vibration mode
Φ	Matrix where each column is a shape mode
ψ	Shape vector
ψ_2	Factor for quasi-permanent value of a variable action
ω	Forcing frequency
ω_n	Natural circular frequency of vibration (undamped)
ω_D	Natural circular frequency of vibration (damped)

CHAPTER 1 INTRODUCTION

1.1 BACKGROUND

Norway is located in an area of low seismic activity, far away from the tectonic plate boundaries, and has not suffered the destructive effect of earthquake in the last century. Therefore, focus on modifying the structural design based on earthquakes and increasing the load carrying capacity of the construction has not been the main objective for Norwegian engineers. Wind load has traditionally been the main parameter considered in building design in Norway, and this provides enough resistance against the horizontal forces and ground's unexpected dynamic movement.

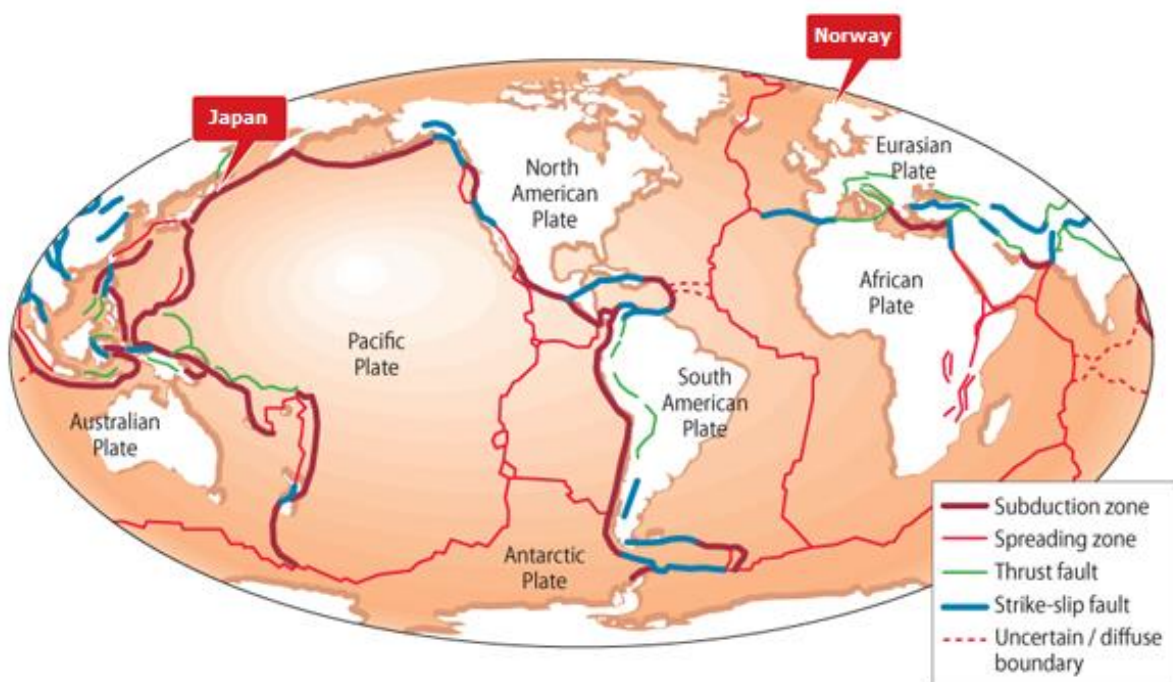


Figure 1-1 World's map showing boundaries of different zone and faults (Visual.ly 2011).

As discussed further in section 2.4 below, Norway has been exposed to several quakes with significant intensity in the past 100 years. The uncertainty of when the next earthquake will occur, and if it will be as intense as the Oslo Fjord quake of 1904 with a 5,4 magnitude on the Richter scale, provides the basis to consider that a similar incident can happen again.

By 2004 Norwegian standardization organization, Standards Norway has published the first edition of the rules and requirements that deal with loads from seismic influences, called NS 3491-12. With the introduction of Eurocode 8 and creating the *National Annex NS-EN 1998* in 2008, calculating the effect of seismic load became completely covered and even more prioritized. All these new regulations led to a need for more

competence and expertise related to earthquake resistant design of structures. The knowledge gap between knowing how to design a standard building with construction materials that react very differently under seismic force, has been something the industry worked to reduce by investing heavily in unconventional types of tall structures.

1.2 OBJECTIVE

The objective of this thesis is to create, through undertaking a detailed analysis and modelling in accordance with Eurocode 8, a better understanding of how a structure would react in case of earthquake in Norway.

The aim of this document is to compare and demonstrate the different structures made of steel, concrete and timber using the finite element modelling software FEM-DESIGN.

1.3 LIMITATION

During the presented analyses, materials were given the same amount of damping in order to give a uniform damping throughout the entire structure. Damping ratio is set to 5% as the recommended damping value given by most building codes for which earthquake-resistant design is intended (*Chopra 2012*)-table 11.2.1.

All connections and supports are considered hinged.

Effect of joint between the panel elements is neglected.

Vertical displacement is not reviewed.

Cross sections have been selected based on elements having less than 30% capacity.

1.4 THESIS OUTLINE

This dissertation is divided in six chapters with different subchapters.

Chapter 2: EARTHQUAKES, touches the basic facts.

Chapter 3: THEORY, gives a brief description of the earthquake phenomenon and the basics of dynamic analysis, which the thesis is founded upon.

Chapter 4: METHOD, sums up the different methods for calculations.

Chapter 5: FEM-DESIGN MODELLING, shows the different outcomes of the analysis.

Chapter 6: RESULTS, DISCUSSION AND CONCLUSIONS

CHAPTER 2 EARTHQUAKES

2.1 INTRODUCTION

The purpose of earthquake engineering as a branch of civil engineering is to give an in-depth knowledge of earthquakes, and how to use guidelines to minimize the damage to human life and property.

2.2 EARTHQUAKES, THE PHENOMENON

Seismic waves are the result of two tectonic plates on the Earth's crust moving relative to each other. This produces the phenomenon we know as earthquakes and is responsible for some of the most brutal natural disasters humanity has experienced.

This phenomenon originates when two sides of a plate boundary slips relative to each other and the increasing tension is so large that the fault line yields at the weakest point, and each side moves to a new position based on where the pressure is released. This movement is called faulting. Faulting can be divided in three types based on the direction tectonic plates move relative to each other, which has been shown in [Figure 2-1](#). With (a) they separate caused by tension forces and results in extension – Normal fault, at (b) they collide caused by compression forces and results in shortening – Reverse fault and at (c) they move laterally caused by shearing forces – Strike-Slip fault.

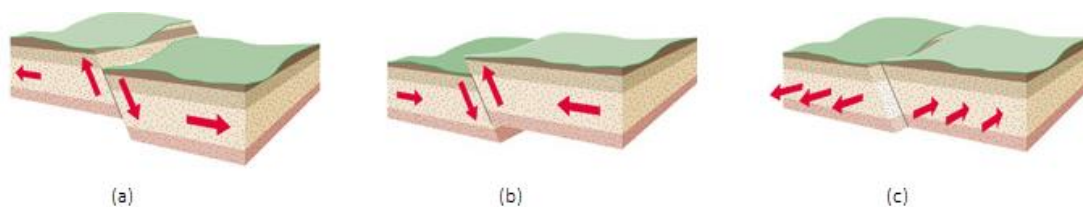


Figure 2-1 Different types of faults (TFD.com 2016).

Starting point of an earthquake called *Hypocenter* (focus) is the point where the slip starts. From here, deformational break spreads along the fault until the wave motion decreases. The force that causes the slip can be measured by basing the *Epicenter*, the point on the surface directly above the hypocenter. The distance between focus and the epicenter is called the *Focal depth* and the distance between epicenter and the site where earthquake waves have made an impact, is called *Epicentral distance*. These waves, also called seismic waves, can occur in different types and move in different ways. Body waves (*Primary* and *Secondary*) and Surface waves (*Love* and *Rayleigh*) are two main types. Primary waves are compression waves that travel at the speed of

sound, shaking things in their direction. Secondary waves, as the name indicates, are the second waves felt in an earthquake. While Surface waves are those travelling through the crust moving forward to back and side to side at the same time (Love) and/or rolling along the ground (Rayleigh). Surface waves are the main cause of destruction. And as far as the soil condition goes, ground displacement intensifies with decrease in soil stiffness (from solid bedrock to water-saturated sand and mud).

2.3 EARTHQUAKE IN EUROPE

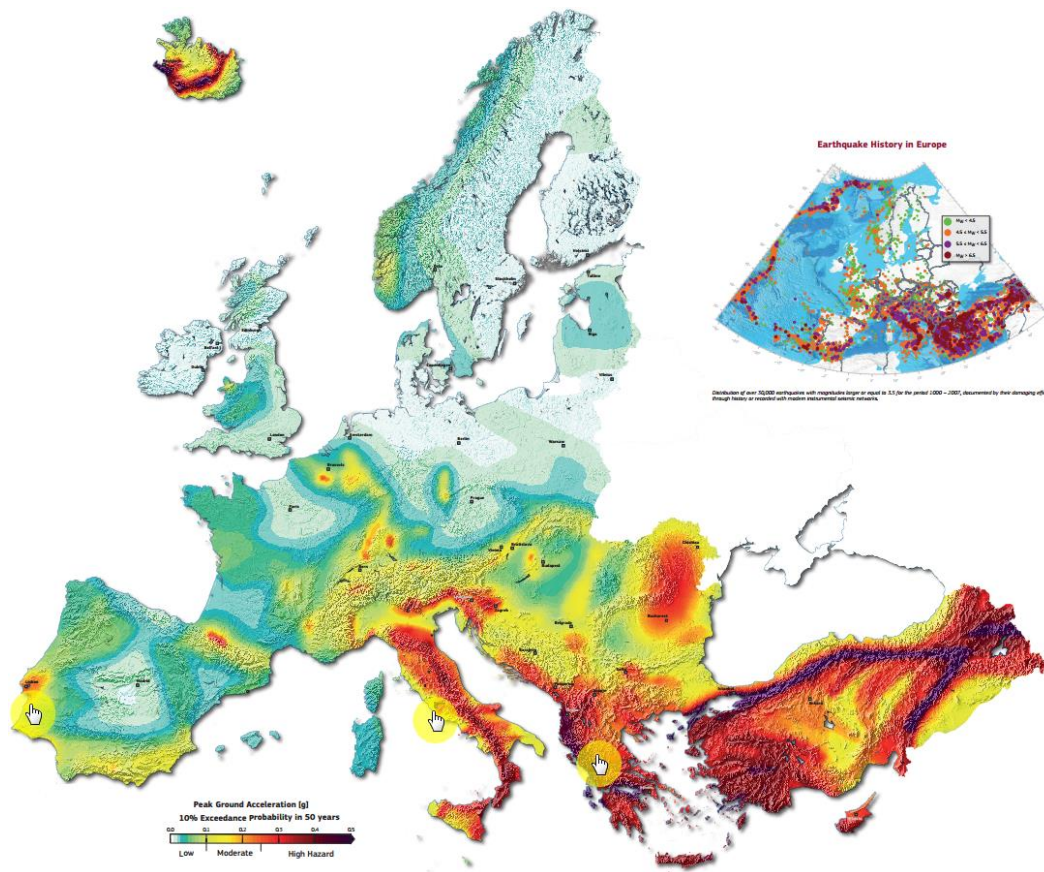


Figure 2-2 European seismic hazard map (SHARE 2013).

Earthquake forces have shaken other parts of Europe to a much greater extent than Norway. From ancient Greece where cities were destroyed (Kouskouna & Makropoulos 2004), to 15th century Portugal which experienced huge destruction related to an earthquake that was followed by a tsunami, and the devastating effect of the 1980 earthquake in Irpinia, southern Italy. These places, as Figure 2-2 displays, are in high hazard area. European continent is divided into low, moderate and high hazard areas based on a peak ground shaking with a 10% probability in 50 years of the region. It is clear that countries like Italy, Turkey and Greece are those with higher risk of experiencing earthquakes within their cities in the next 50 years. Located in a

subduction zone that expands from Mediterranean Sea and in fact being near the boundary of the African plate, makes southern Europe, and Italy in particular, vulnerable. The amount seismic activity in these territories calls for new and more innovative ways of engineering. One of these examples is the Energy Box passive house designed by architect Pierluigi Bonomo, which was introduced after the 2009 earthquake in the region Abruzzo, Italy. Bonomo introduced the earthquake-proof timber structure built on concrete foundation after thousands of traditional brick buildings collapsed. This type of material have replaced brick houses and is very common, with at least 4000 houses been rebuilt in timber (Bonomo 2013).

2.4 EARTHQUAKE IN NORWAY

The NORSAR seismic research institute, which monitors Norway's seismic activity, detected the biggest Norwegian earthquake of in recorded history in the 2012. This happened on Jan Mayen, an island 1506 km from Oslo, the capital city of Norway, which itself experienced its biggest earthquake in 1904 measuring 5,4 on Richter Scale (Jordskjelv.no).



Figure 2-3 Last five largest earthquakes in Norway (Jordskjelv.no). Map from mapbox.com.

Even though there is seismic activity in Norway, it is classified as a low seismic region with the most activity in Oslo-region, Agder-region in the south, Stad and Bergen-region in the west and Helgeland-region in the North(Løset et al. 2011). [Figure 2-3](#) shows Norway's five biggest quakes in the last 100 years.

Designing a more earthquake-resistant construction is based on collecting vital information from previous incidents. Data collected in Norway is less than in regions more affected by this phenomenon, and most of the requirements in building codes are adjusted after local conditions based on the European Standard EN 1998-1. Requiring every project, new builds and extension to undergo a seismic calculation, ensures that a building's stability is investigated regardless of size, material and ground conditions.

2.5 EARTHQUAKE MAGNIUDE AND INTENSITY

Earthquakes comes in huge variety of magnitudes and intensities that defines its characteristics. The magnitude scale is way of expressing the quantity of energy released by an earthquake. There are many different types of magnitudes, the most well-known is the Richter Scale which was developed by Charles Francis Richter and Beno Gutenberg at California Institute of Technology, USA, in 1935 (Splinter 2016). The Richter magnitude is a logarithmic number that increases in the size of the quake. For each level this number increases, the energy increases by a factor of 31. For example a magnitude 4.0 quake is about 30 times powerful than a 3,0 quake, and a magnitude of 5,0 is 900 times than the same 3,0 quake (Jordskjelv.no).

It is important to mention that the most correct method for measuring the magnitude of an earthquake is called " seismic moment". This quantity is calculated based on the area of fault rupture, the average amount of slip, and the required force to overcome the friction holding the rocks together, before they were offset by faulting (USGS.gov).

The intensity of an earthquake is based on several subjective interpretations. One of the two main factors is the shaking produced at the certain location. The second factor is the effect on people and their observations of the damages on structures and the environment around them, caused by the quake. This is known as the " Mercalli intensity scale" . This type of measurement is not precise due to lack of accuracy. These types of intensity observations are being collected all over the world and categorized by using a 12-part intensity scale which was developed back in the early 1900. The type of scale used in Norway called EMS98 or European micro seismic scale, defined in 1998, is the basis for evaluation in European countries.

CHAPTER 3 THEORY

3.1 STRUCTURAL DYNAMIC

3.1.1 INTRODUCTION

This chapter gives a brief look at the usual behavior of structures and the important aspect of dynamic in earthquake. The dissipated energy from an earthquake causes vibrations and loads on structures. These load cases varies by time and therefore we can say that seismic load is a dynamic type of load. It is possible to describe these loads by mathematical approaches based of the type of structure and how many degrees of freedom the system has.

Degrees of freedom describes the movement options a system has, based on the position of its mass. Systems with one degree of freedom are called SDOF-systems, which we look at in section 3.1.3. Generalized SDOF in a seismic context and MDOF-systems are each introduced in section 3.1.4 and 3.1.5. But first we look at vibration of systems in section 3.1.2. This part is mostly based on Dynamic of structure by Anil K. Chopra.

3.1.2 VIBRATION OF A SYSTEM

A system that vibrates can schematically be divided in two categories, free vibration and forced vibration, as shown in Figure 3-1.

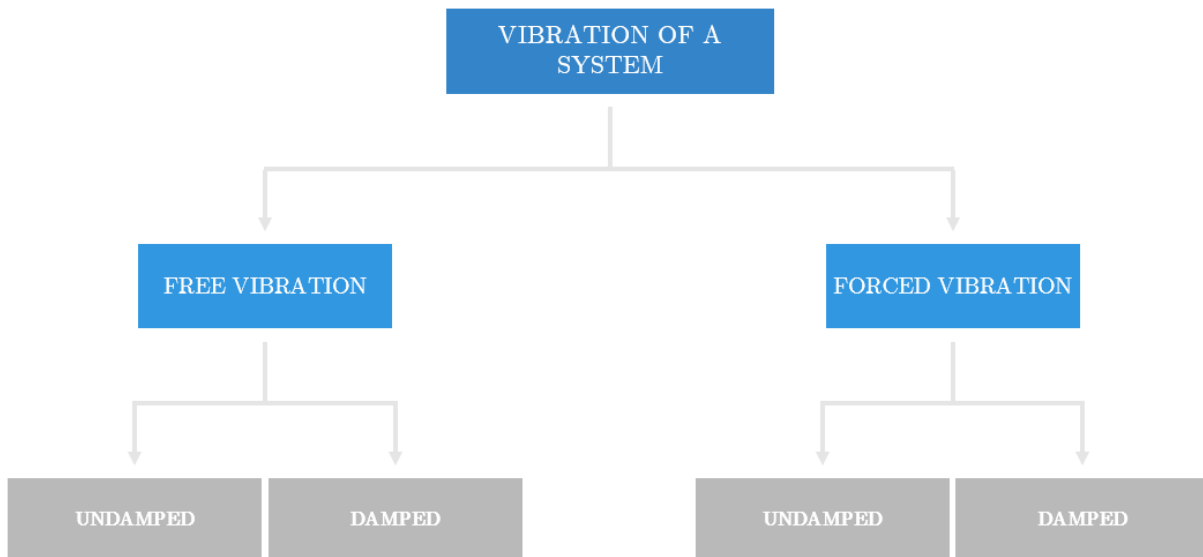


Figure 3-1 System classification.

Free vibration means that there is no externally applied force on the system as opposed to forced vibration where it indicates that force is present and not equal to zero, both with or without damping component in the system.

The general dynamic equation for a system in vibration or generally known as equation of motion (EOM) can be expressed as:

$$m\ddot{u}(t) + c\dot{u}(t) + ku(t) = p(t) \quad \text{for } t > 0 \quad 3-1$$

3.1.2.1 UDAMPED FREE VIBRATION

The equation of motion for an undamped free vibration is

$$m\ddot{u}(t) + ku(t) = 0 \quad 3-2$$

where both force and damping is removed from the system. System will oscillate with initial disturbance in form of initial displacement, initial velocity or both. The solution of EOM with these initial conditions by standard methods can be expressed by assuming that

$$u = e^{\lambda t} \quad 3-3$$

$$\dot{u} = \lambda e^{\lambda t} \quad 3-4$$

$$\ddot{u} = \lambda^2 e^{\lambda t} \quad 3-5$$

for simple harmonic motion problem, where constant λ is unknown. By substituting into equation 3-2, the new EOM can be rewritten as the characteristic equation shown here:

$$(m\lambda^2 + k)e^{\lambda t} = 0 \quad 3-6$$

with two roots $\lambda_{1,2} = \pm i\omega_n$, where $i = \sqrt{-1}$. The general equation of 3-2 is 3-7, which after substituting with the roots becomes equation 3-8, a form of solution of linear differential equation with constant coefficients.

$$u(t) = a_1 e^{\lambda_1 t} + a_2 e^{\lambda_2 t} \quad 3-7$$

$$u(t) = a_1 e^{i\omega_n t} + a_2 e^{-i\omega_n t} \quad 3-8$$

where a_1 and a_2 are undetermined values. By using the Euler's formula, given in equation 3-9, that establishes the relation between trigonometric functions and exponential functions, equation 3-8 can be rewritten as equation 3-10. Equation 3-10 is further differentiated to equation 3-11.

$$e^{\pm ix} = \cos x \pm i \sin x \quad 3-9$$

$$u(t) = A \cos \omega_n t + B \sin \omega_n t \quad 3-10$$

$$\dot{u}(t) = -\omega_n A \sin \omega_n t + \omega_n B \cos \omega_n t \quad 3-11$$

where A and B are undetermined real-value constants. Constants can be found at initial conditions $t = 0$ by evaluating equations 3-10 and 3-11, which gives displacement $u = u(0) = A$ and velocity $\dot{u} = \dot{u}(0) = \omega_n B$. Substituting A and B into equation 3-10 leads to the solution of undamped free vibration:

$$u(t) = u(0) \cos \omega_n t + \frac{\dot{u}(0)}{\omega_n} \sin \omega_n t \quad 3-12$$

where $u(0)$ is initial displacement, $\dot{u}(0)$ is initial velocity and ω_n as shown in equation 3-13, is the natural circular frequency of vibration.

$$\omega_n = \sqrt{\frac{k}{m}} \quad 3-13$$

3.1.2.2 UNDAMPED FORCED VIBRATION

When externally applied harmonic force $p(t)$ is continuously acting on the structure, as in contrast to 3.1.2.1, the system is in an undamped forced vibration. The equation of motion for an undamped forced vibration in absence of damping is

$$m\ddot{u}(t) + ku(t) = p_0 \sin \omega t \quad 3-14$$

where the excitation sinusoidal force which is in form of $p(t) = p_0 \sin \omega t$ by p_0 being amplitude and ω being exciting or forcing frequency.

Equation 3-14 can be solved by for dividing all the terms by mass, which results in a non-homogeneous differential equation 3-15, with a two-parted solution shown in equation 3-16.

$$\ddot{u} + \omega_n^2 u = \frac{p_0}{m} \sin \omega t \quad 3-15$$

$$u(t) = u_c(t) + u_p(t) \quad 3-16$$

where $u_c(t)$ is complimentary and $u_p(t)$ is particular integral. Complimentary component depends on the natural properties of the system and particular integral component depends on force being applied. The particular integral component has its solution shown in 3-17.

$$u = C \sin \omega t \quad \text{Displacement } u$$

$$\ddot{u} = -\omega^2 C \sin \omega t \quad \leftarrow \text{Derivation of } u$$

$$(-\omega^2 C \sin \omega t) + \frac{k}{m} C \sin \omega t = \frac{p_0}{m} \sin \omega t \quad \leftarrow \text{Inserting in equation 3-14}$$

$$(-\omega^2 + \omega_n^2) C \sin \omega t = \frac{p_0}{m} \sin \omega t \quad \leftarrow \text{Rearranging the last one}$$

$$C = \frac{p_0}{m} \frac{1}{(-\omega^2 + \omega_n^2)} \quad \leftarrow \text{Taking out } C$$

$$\beta_n = \frac{\omega}{\omega_n} \quad \leftarrow \text{Introducing frequency ratio}$$

$$C = \frac{p_0}{m \omega_n^2 |1 - \beta_n^2|} \quad \leftarrow \text{Adding } r \text{ to } C \text{ equation and getting}$$

$$u_p = \frac{p_0}{k} \frac{1}{|1 - r^2|} \sin \omega t \quad 3-17$$

The complementary solution has already been calculated in equation 3-10. The complete solution of the complementary and particular component is

$$u(t) = A \cos \omega_n t + B \sin \omega_n t + \frac{p_0}{k} \frac{1}{|1 - \beta_n^2|} \sin \omega t \quad 3-18$$

By imposing the initial condition where $u = u(0) = A$ and $\dot{u} = \dot{u}(0) = B \omega_n + \frac{p_0}{k} \frac{\omega}{1 - \beta_n^2}$, constants A and B can be determined. The solution of undamped forced vibration with transient and steady state components as shown in Figure 3-2, is:

$$u(t) = \underbrace{u(0)\cos\omega_n t + \left[\frac{\dot{u}(0)}{\omega_n} - \frac{p_0}{k} \frac{r}{1 - \beta_n^2} \right] \sin\omega t}_{\text{transient}} + \underbrace{\frac{p_0}{k} \frac{1}{1 - \beta_n^2} \sin\omega t}_{\text{steady-state}} \quad 3-19$$

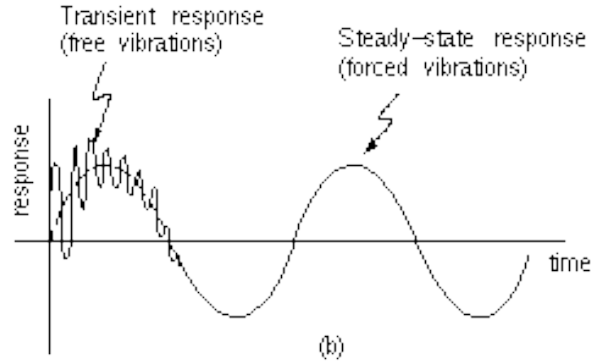


Figure 3-2 Transient and steady-state dynamic response of a system (Ansys.stuba.sk 2016).

Steady-state response as a response to forced vibrations continues as long the force is applied as transient response does if damping is not present. Figure 3-2 shows that transient response fades out and becomes as one with steady-state since damping is introduced to the system.

3.1.2.3 DAMPED FREE VIBRATION

As mentioned in 3.1.2.1, free vibration occurs when there is no external force $p(t) = 0$ applied to the system. But when the energy is dissipated through a viscously damper and the free vibration stops, the system suddenly becomes damped. Adding damping c to equation 3-2, gives the differential equation for a “damped free vibration system” :

$$m\ddot{u}(t) + c\dot{u}(t) + ku(t) = 0 \quad 3-20$$

The solution of damped free vibration is described as;

$$\ddot{u} + \frac{c}{m}\dot{u} + \frac{k}{m}u = 0 \quad \leftarrow \text{Dividing equation 3-20 by mass}$$

$$\ddot{u} + 2\xi\omega_n\dot{u} + \omega_n^2u = 0 \quad \leftarrow \text{Replacing with equivalent equations}$$

where the damping ratio is given by equation 3-21 and critically damping coefficient, which is the damping required to remove energy from system, by equation 3-22.

$$\xi = \frac{c}{2m\omega_n} = \frac{c}{c_{cr}} \quad 3-21$$

$$c_{cr} = 2m\omega_n = 2\sqrt{km} = \frac{2k}{\omega_n} \quad 3-22$$

By assuming $u = e^{\lambda t}$ like in the undamped free vibration system, we get acceleration and velocity terms $\dot{u} = \lambda e^{\lambda t}$ and $\ddot{u} = \lambda^2 e^{\lambda t}$. Adding these terms in equation 3-20 and rearranging the terms gives equation 3-23.

$$(\lambda^2 + 2\xi\omega_n\lambda + \omega_n^2)e^{\lambda t} = 0 \quad 3-23$$

Equation 3-23 is satisfied for all values of t if

$$\lambda^2 + 2\xi\omega_n\lambda + \omega_n^2 = 0 \quad 3-24$$

Equation 3-24 has two roots:

$$\lambda_{1,2} = \omega_n(-\xi \pm i\sqrt{1 - \xi^2}) \quad 3-25$$

By further simplification $\lambda_{1,2}$ can be expressed as

$$\lambda_{1,2} = -\omega_n\xi \pm i\omega_D \quad 3-26$$

where ω_D is the natural frequency of damped structure given by equation 3-27.

$$\omega_D = \omega_n\sqrt{1 - \xi^2} \quad 3-27$$

Based on equation 3-27 will the natural frequency of damped structure be equal the natural frequency if the damping ratio ξ is set to zero. Upon substituting equation 3-26 in 3-23, it can be rewritten as equation 3-28.

$$u(t) = e^{-\omega_n\xi t}(A \cos\omega_D t + B \sin\omega_D t) \quad 3-28$$

By introducing equation 3-28 to initial conditions, constant A and B becomes $A = u(0)$ and $B = \frac{\dot{u}(0) + \omega_n\xi u(0)}{\omega_D}$. Substituting for A and B in equation 3-28 gives:

$$u(t) = e^{-\omega_n\xi t}\left(u(0) \cos\omega_D t + \frac{\dot{u}(0) + \omega_n\xi u(0)}{\omega_D} \sin\omega_D t\right) \quad 3-29$$

which can be illustrated with different damping ratio, as shown in Figure 3-3.

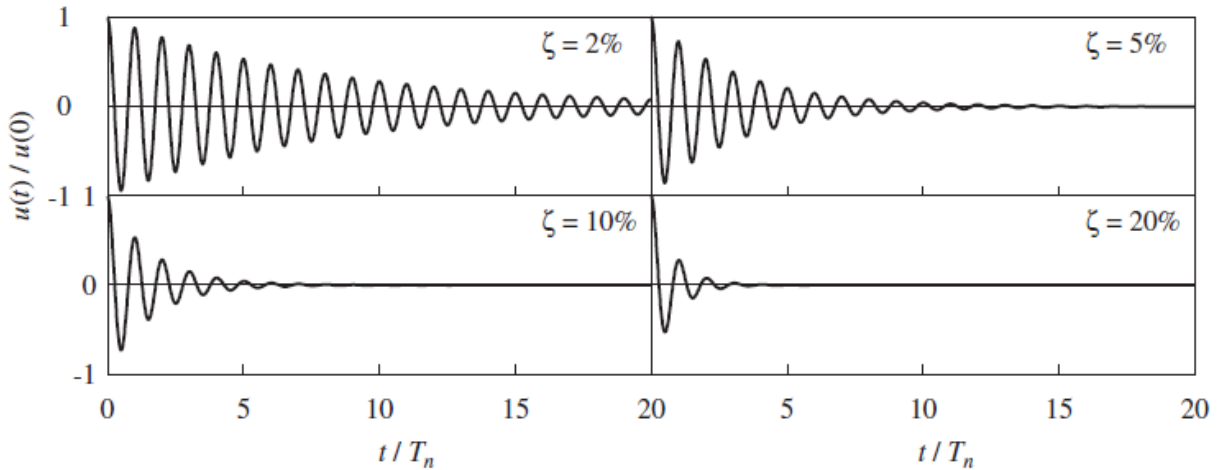


Figure 3-3 Free vibration of systems with four levels of damping (Chopra 2012).

Damping is an influence in system that effects it by reducing its oscillation/vibration. Friction at connections, micro cracks in concrete and friction in between the parts are some of known damping types in constructions that influence within the oscillatory/vibratory system.

System which is in free vibration can react to damping in three different situations, *Underdamped*, *Critically damped* and *Overdamped*, based on the ratio of damping being $\xi < 1$, $\xi = 1$ or $\xi > 1$. The vibrating will system lose its energy, which dissipates by these damping value and returns to the equilibrium position. Figure 3-4 shows a plot of the motion for three values of ξ .

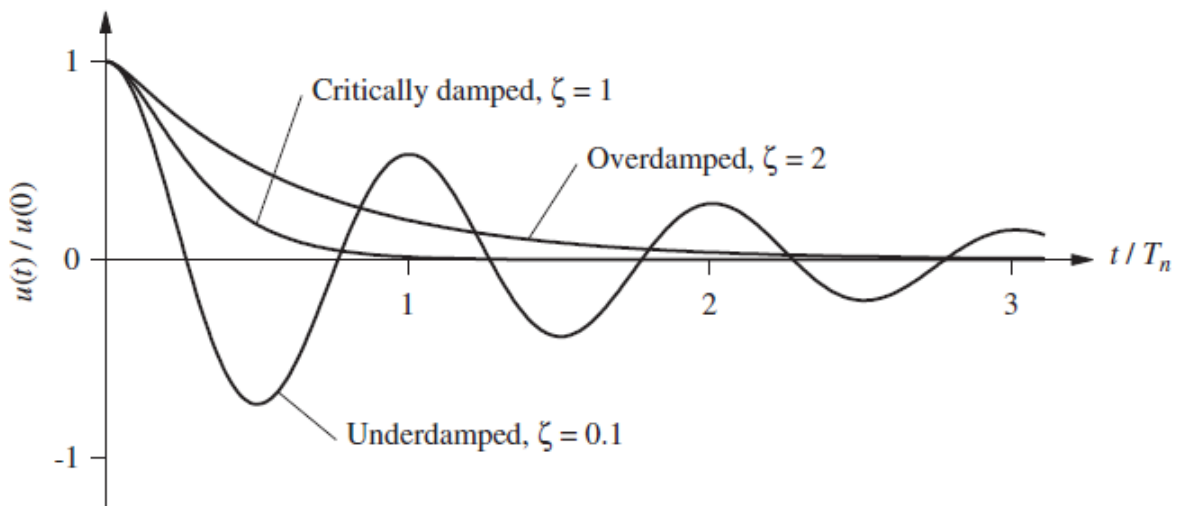


Figure 3-4 Free vibration of critically damped, under- and overdamped systems (Chopra 2012).

3.1.2.4 DAMPED FORCED VIBRATION

If the system is vibrating because of the applied externally force and damping is introduced to it, the vibration governing the system is called damped forced vibration.

EOM of 3-14 with damping subjected to initial conditions $u = u(0)$ and $\dot{u} = \dot{u}(0)$ is given in equation 3-30.

$$m\ddot{u}(t) + c\dot{u}(t) + ku(t) = p_0 \sin \omega t \quad 3-30$$

The equation of motion for a damped forced vibration has complementary and particular integral solution as shown in equation 3-31 and 3-32.

$$\ddot{u} + 2\xi\omega_n\dot{u} + \omega_n^2 u = \frac{p_0}{m} \sin \omega t \quad \leftarrow \text{Dividing equation 3-30 by mass}$$

$$u_p = C \cos \omega t + D \sin \omega t \quad 3-31$$

$$\dot{u}_p = -\omega_D C \sin \omega t + \omega_D D \cos \omega t \quad \leftarrow \text{Differentiating } u_p \text{ gives}$$

$$\ddot{u}_p = -\omega_D^2 C \cos \omega t + \omega_D^2 D \sin \omega t \quad \leftarrow \text{Differentiating } \dot{u}_p \text{ gives}$$

$$C = \frac{p_0}{k} \frac{2\xi\beta_n}{(1 - \beta_n^2)^2 + (2\xi\beta_n)^2}$$

$$D = \frac{p_0}{k} \frac{1 - (\beta_n)^2}{(1 - \beta_n^2)^2 + (2\xi\beta_n)^2}$$

\leftarrow Substituting in EOM gives

$$u_c = e^{-\xi\omega_n t} (A \cos \omega_D t + B \sin \omega_D t) \quad 3-32$$

where the damped natural frequency ω_D is given by equation 3-27. The complete solution with transient and steady-state response is given by

$$u(t) = \underbrace{e^{-\xi\omega_n t} (A \cos \omega_D t + B \sin \omega_D t)}_{\text{transient}} + \underbrace{C \cos \omega t + D \sin \omega t}_{\text{steady-state}} \quad 3-33$$

3.1.3 SINGLE-DEGREE-OF-FREEDOM SYSTEMS

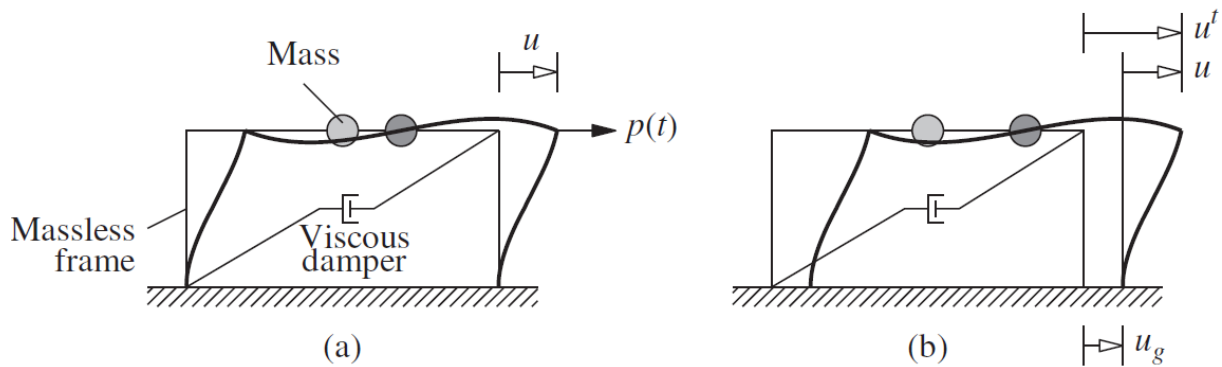


Figure 3-5 Single-degree-of-freedom system: (a) applied force $p(t)$; (b) earthquake-induced ground motion (Chopra 2012).

The system shown in Figure 3-5 illustrates a massless frame with stiffness k , a mass m concentrated at the roof level and a viscous damper c that dissipates the vibration of the system. This system can be considered as a linear and idealized one-storey building where all parts can be determined at any time. Acceleration and velocity are both acting in the same direction as the structure is displaced. Each structural member contributes to inertial, elastic and energy dissipation and these properties can be separated in three different components: mass, stiffness and damping. In structural analysis in order to formulate the problem we look at the independent co-ordinates (e.g. displacements) required to define the displaced position of all the masses that corresponds to their initial stand point, as known as *degrees of freedom* (DOF). In Figure 3-5 we see a system with a concentrated mass at one location, two joints and is displaced laterally. These are the main information we need to find the lateral stiffness of the system which we call a single-degree-of-freedom (SDOF) system. Since we live in a three dimensional world, a SDOF system where the mass is excited by horizontal force and displaced in one direction does not really exist. Although, it helps though the understanding of how a structure, like a water tower with tank as a point mass and column with negligible mass, vibrates when induced to an external force $p(t)$ in lateral direction and ground motion excitation $u_g(t)$ (Chopra 2012).

Dynamic calculation is based on equation of motion, as described in equation 3-1, and can be illustrated by looking at the SDOF system in Figure 3-5a. The system's total displacement of the lumped mass $u^t(t)$ is given by summing the relative displacement u and the displacement of the ground u_g due to seismic waves, as shown in the Figure 3-5b and described in equation 3-34.

$$u^t(t) = u_g(t) + u(t) \quad 3-34$$

By assuming that the system which shows the externally applied force $p(t)$ is a linear system, the resisting forces in the system can be defined as

$$\text{Elastic forces} \rightarrow f_S(t) = \left(\frac{k}{2} + \frac{k}{2}\right) u(t) \quad 3-35$$

$$\text{Damping forces} \rightarrow f_D(t) = c\dot{u}(t) \quad 3-36$$

$$\text{Inertia forces} \rightarrow f_I(t) = m\ddot{u}^t(t) \quad 3-37$$

Equilibrium of the system in [Figure 3-5](#), which shows two frames each exposed to $p(t)$ and $u_g(t)$ gives us dynamic equilibrium of forces as equation [3-38](#) presents.

$$f_S + f_D + f_I = 0 \quad 3-38$$

By using equations [3-35](#), [3-36](#) and [3-37](#) we can express the EOM for structure subjected to earthquake-induced ground motion \ddot{u}_g , as shown in [3-39](#).

$$\begin{aligned} m\ddot{u}^t + c\dot{u} + ku &= 0 \\ m(\ddot{u}_g + \ddot{u}) + c\dot{u} + ku &= 0 \\ m\ddot{u} + c\dot{u} + ku &= -m\ddot{u}_g(t) \end{aligned} \quad 3-39$$

where it relates to \ddot{u} acceleration, \dot{u} velocity and u the relative displacement between the base of the structure and the mass as shown in [Figure 3-5b](#).

By comparing equation [3-39](#) and [3-1](#), which results in equation [3-40](#), the term of *effective earthquake force* appears on the right-hand side. Since this force is proportional to the mass of structure, if mass is increased the effective earthquake force will increase.

$$p(t) = p_{eff}(t) = -m\ddot{u}_g(t) \quad 3-40$$

The equation of motion for a SDOF system with damping ratio ξ subjected to seismic motion, as illustrated in [Figure 3-5b](#), is described by its the natural vibration frequency ω_n as in equation [3-42](#) (Javed 2015).

$$c = c_{cr}\xi = \xi(2m\omega_n) \quad 3-41$$

$$\ddot{u} + 2\omega_n \xi \dot{u} + \omega_n^2 u = -\ddot{u}_g(t) \quad 3-42$$

Elements of structure subjected to earthquake-induced ground acceleration that stops shaking after the seismic load dissipates, have different displacements $u^t(t)$ than the initial displacement caused by ground acceleration $u_g(t)$. The difference between displacements causes that forces to act on columns and the damping element, as shown in Figure 3-5b. This can be described in a linear elastic system where forces in columns and the displacement of beams on top of them are proportional (Øystad-Larsen 2010).

3.1.4 GENERALIZED SDOF SYSTEMS

In section 3.1.3, we looked at one-storey building and described it as a single degree of freedom system with a lumped mass where the shape mode is constant in case of earthquake.

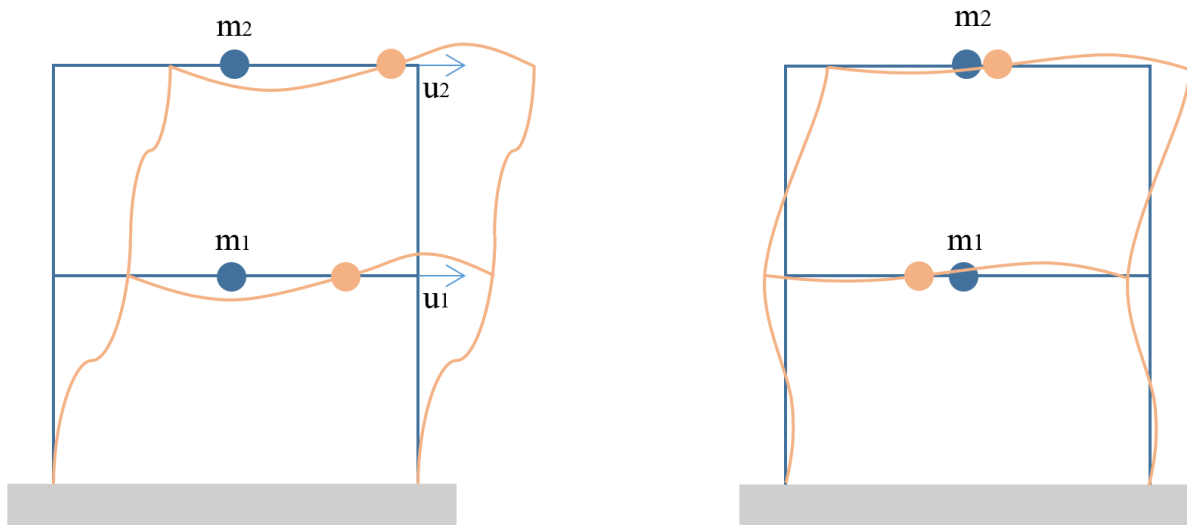


Figure 3-6 System with the mass distributed over two storey and two possible mode shapes.

When added more mass, system gets more complex and behaves differently. Figure 3-6 shows the possible mode shapes of a two-storey structure reacting to ground motion and that the relation between relative displacement in first u_1 and second u_2 storey is not constant. One of the mode shapes will sometimes dominate the response of the system. If the masses follow that one mode shape, the approach used to find the response is called *Generalized SDOF system approximation*, which is applicable for all systems. The accuracy of this analysis procedure is depended on how dominated the mode shape is. Since this is based on an assumed shape function, when a mode shape

is known and we have a generalized displacement, the equation of floor displacement $u(t)$ relative to the ground can be written in vector form as shown in equation 3-43, where ψ is the assumed shape vector that defines deflected shape and $z(t)$, generalized coordinate response. The total displacement for j th floor by can be expressed as presented in equation 3-44 (Chopra 2012). When the displacement of a point in a system is known, we can find the response of the entire system.

$$u(t) = \psi z(t) \tag{3-43}$$

$$u_j^t(t) = u_j(t) + u_g(t) \tag{3-44}$$

3.1.5 MULTI-DEGREE-OF-FREEDOM SYSTEMS

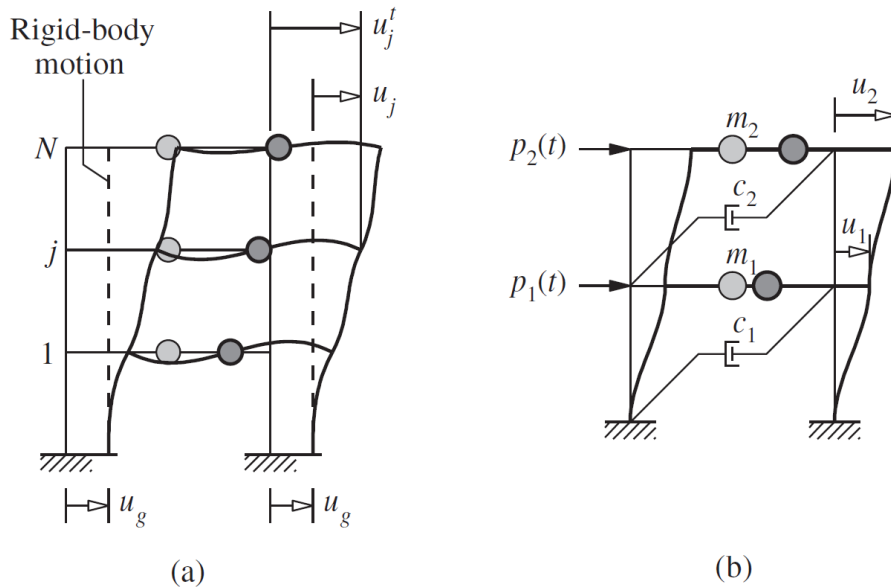


Figure 3-7 Multi-degree-of-freedom system: (a) earthquake induced ground motion and (b) external forces (Chopra 2012).

A multi-degree-of-freedom system with a rigid body in contrast with SDOF system and generalized SDOF system cannot be determined by a single mode shape because of its complexity and configuration of the structure. Figure 3-7a illustrates a three-storey frame exposed to ground motion u_g . Its dynamic equation of equilibrium is described in equation 3-45, where the load vector $-m \iota \ddot{u}_g(t)$, according to D'Alembert's principle, is an influence vector.

$$m\ddot{u} + c\dot{u} + ku = -m \iota \ddot{u}_g(t) \tag{3-45}$$

The influence vector is often described as

“Displacement transformation vector that expresses the displacement of each structure degree of freedom due to static application of a unit support displacement” (Taushanov 2012)

and because of equation 3-46, which means that total amount of acceleration is equal to sum of the relative acceleration of the system and the ground motion, the value of influence vector is set to $\iota = 1$ when the system is subjected to earthquake-induced motion in one given direction.

$$\ddot{u}_j^t = \ddot{u}_j(t) + \ddot{u}_g(t) \quad 3-46$$

If the degree of freedom of a system with structural axes x , y or z is not defined in same direction as ground acceleration, which has principal axes 1, 2 and 3, the difference between these two sets of axes is defined by an angle θ and can be describe as presented in equation 3-47 (Chopra 2012). Usually most structures are simplified and calculated for displacement in the same direction as the ground motion and therefore the influence vector becomes $\iota = 1$.

$$\ddot{u}_j^t = \cos\theta (\ddot{u}_j(t) + \ddot{u}_g(t)) \quad 3-47$$

where the influence vector is $\cos\theta$.

MDOF systems are described with more than one mode shape. By assuming the system illustrated in Figure 3-7b being linear elastic, undamped with two translational DOFs, its necessary to find the all values in order to determine the structure's response.

The equation of motion for this system is described back in section 3.1.2.1. The structure has two possible mode shapes with different properties that are time dependent. At the state of free oscillation, the displacement of DOFs will vary with time and the mode shape remains constant. In addition, the displacement vector can be described as a linear combination of mode shapes. For a system that matches the properties in equation 3-1, we can write the equation 3-48.

$$u(t) = \sum_{i=1}^n u_i(t) = \sum_{i=1}^n \phi_i q_i(t) = \mathbf{\Phi} \mathbf{q}(t) \quad 3-48$$

where $\mathbf{\Phi}$ consists of *the natural vibration mode* ϕ_i , n is the amount of DOFs and $\mathbf{q}(t)$ consists of $q_i(t)$ which is the amount of contribution from mode shape i of displacement

vector $u_i(t)$. Since we assumed that our system is linear, undamped and is in a free oscillation state, every displacement function $u_i(t)$ should satisfy the equation 3-1.

This requirement gives the equation 3-49 where the time dependent function $q_i(t)$ is as a sinus wave and $\ddot{q}_i(t) = -\omega_i^2 q_i(t)$ (Øystad-Larsen 2010).

$$m \phi_k \ddot{q}_k(t) + k \phi_k q_k(t) = 0 \quad 3-49$$

Equation 3-49 introduces the so-called trivial solution if it's satisfied by $q_i(t) = 0$, which implies that the structure stands still, and that is not of interest. We need to see the equation 3-49 equal to zero and not a system that do not have any motion. Therefore, by introducing matrix eigenvalue problem presented in equation 3-50, and rewriting it to equation 3-51, we can come to the nontrivial equation 3-52, based on that 3-50 is an equation for i -elements ϕ_{in} ($k = 1, 2, \dots, k$) with a trivial solution $\phi_i = 0$, and that the stiffness and mass matrix is known for the system.

$$k \phi_i = m \phi_i \omega_i^2 \quad 3-50$$

$$[k - m \omega_i^2] \phi_i = 0 \quad 3-51$$

$$\det[k - m \omega_i^2] = 0 \quad 3-52$$

Equation 3-52 gives, for a system with n-DOF, n-solutions based on value of ω . The natural vibration frequency can be set up after quantity as $\omega_1 \leq \omega_2 \leq \dots \leq \omega_k \leq \dots \leq \omega_n$. By adding the value of ω_k in equation 3-51 we can find the natural mode of vibration ϕ_k . For a multistorey structure, equation 3-50 can be expressed as equation 3-53, since a linear combination of natural modes has the property of being expressed for displacement of degrees of freedom

$$\phi_i^T m \phi_j = 0 \quad \phi_i^T k \phi_j = 0 \quad \text{when } i \neq j \quad 3-53$$

The dynamic equilibrium for a damped, linear elastic system with n-DOF can be expressed by using equation 3-45 and 3-48 as:

$$\begin{aligned} m \Phi \ddot{q}(t) + c \Phi \dot{q}(t) + k \Phi q(t) &= -m \iota \ddot{u}_g(t) \\ \Leftrightarrow \Phi^T m \Phi \ddot{q}(t) + \Phi^T c \Phi \dot{q}(t) + \Phi^T k \Phi q(t) & \\ &= -\Phi^T m \iota \ddot{u}_g(t) \end{aligned} \quad 3-54$$

$$\Leftrightarrow M \ddot{q}(t) + C \dot{q}(t) + Kq(t) = -\Phi^T m \iota \ddot{u}_g(t)$$

$$M = \Phi^T m \Phi$$

$$C = \Phi^T c \Phi$$

$$K = \Phi^T k \Phi$$

where M and K are the diagonal modal mass matrix and modal stiffness matrix since their modes are diagonally set up. Parameters on the diagonal are respectively $M_k = \Phi_k^T m \phi_k$ and $K_k = \Phi_k^T k \phi_k$. C is the modal damping matrix, which also is diagonal since there is much uncertainty in damping of a system (Øystad-Larsen 2010).

3.1.6 RESPONSE OF A MDOF SYSTEM

In this section we develop the effective modal mass to determine the response of a structure to earthquake induced ground motion. Ground motion tends to transfer force to the structure which reacts in terms of displacement and can be presented as:

$$M_k \ddot{q}_k(t) + C_k \dot{q}_k(t) + K_k q_k(t) = -L_k \ddot{u}_g(t) \quad 3-55$$

$$M_k = \Phi_k^T m \phi_k \quad C_k = \Phi_k^T c \phi_k \quad 3-56$$

$$K_k = \Phi_k^T k \phi_k \quad L_k = \Phi_k^T m \iota$$

By dividing the equation 3-55 with M_k we achieve the equation 3-57, which gives the damping ratio for all the mode shapes $\xi_k = \frac{C_k}{2M_k\omega_k}$.

$$\ddot{q}_k(t) + 2\xi_k\omega_k \dot{q}_k(t) + \omega_k^2 q_k(t) = -\frac{L_k}{M_k} \ddot{u}_g(t) \quad 3-57$$

The solution of modal equation can be obtained by comparing 3-57 to the EOM for the nth mode SDOF system, expressed as the equation 3-58.

$$\ddot{D}_n(t) + 2\xi_k\omega_k \dot{D}_n(t) + \omega_k^2 D_n(t) = -\ddot{u}_g(t) \quad 3-58$$

Which gives the time dependent function $q_k(t)$:

$$q_k(t) = \frac{L_k}{M_k} D_k(t) \quad 3-59$$

The displacement due to the n th mode is given by:

$$u(t) = \sum_{k=1}^n u_k(t) = \sum_{k=1}^n \phi_k q_k(t) = \sum_{k=1}^n \frac{L_k}{M_k} \phi_k D_k(t) \quad 3-60$$

The equivalent static force is

$$f_k(t) = k u_k(t) = k \phi_k q_k(t) = \omega_k^2 m \phi_k q_k(t) \quad 3-61$$

By using the equation 3-59, equation 3-61 can be rewritten as

$$f_k(t) = \omega_k^2 \frac{L_k}{M_k} m \phi_k D_k(t) = s_k \omega_k^2 D_k(t) = \sum_{k=1}^n s_k \omega_k^2 D_k(t) \quad 3-62$$

where vector $s_k = \frac{L_k}{M_k} m \phi_k$ is the contribution from the k -mode to the load vector $m \iota$, represented by combining the response contributions of all the modes as described in 3-63 (Chopra 2012):

$$m \iota = \sum_{k=1}^n s_k = \sum_{k=1}^n \frac{L_k}{M_k} m D_k(t) \quad 3-63$$

The response contribution r_k from the n th mode is combined to the response from a static force s_k and can be expressed by a combination of a static and dynamic solution for any response quantity as presented below:

$$r(t) = \sum_{k=1}^n r_k(t) = \sum_{k=1}^n r_k^{st} \omega_k^2 D_k(t) \quad 3-64$$

The effective modal mass, which is the mass for a given mode shape that contributes in calculation of structure's total base shear in the same direction as the induced ground acceleration, can be expressed for a k -mode by the equation 3-65 and summed up as in 3-66.

$$m_k = \iota^T s_k = \iota^T \frac{L_k}{M_k} m \phi_k \quad 3-65$$

$$\sum_{k=1}^n m_k = \iota^T \sum_{k=1}^n s_k = \iota^T m \iota \quad 3-66$$

Effective mass has an impact in calculating base shear. EC8-1 requires that there are enough modes included in a modal analysis that sum of the effective modal masses are

higher than 90% of the structure's total mass. This is important in case of calculating the base shear of each storey or the total of the building. Based on the equation 3-64, we can find the shear force using the equation

$$V(t) = \sum_{k=1}^n V_k^{st} D_k(t) \quad 3-67$$

The shear force value of equation 3-67 in order to be denoted, must be a quantity of mass. The mass of each mode gives the total shear force. This provides the effective modal mass expression given in equation 3-68 (Øystad-Larsen 2010)

$$m_k = V_{k,b}^{st} \quad 3-68$$

where $V_{k,b}^{st}$ is the shear force at the ground level. We can further by considering the modal mass m_k , which corresponds to the mass of the structure, the natural circular frequency of vibration ω_k^2 and the damping ratio ξ in combination with equation 3-67, write the formula for the base shear:

$$V_b = m_k \omega_k^2 D_k(t) \quad 3-69$$

3.1.7 DUCTILITY OF STRUCTURE

Ductility is defined as the ability to deform beyond the elastic zone without fracturing. This is an important concept in engineering, and even more of importance in hybrid structure with different materials and yielding strength exposed to earthquake-induced forces. It is here that the mass and stiffness of the structure plays a vital part in how the structure reacts to these forces, and how badly the structure is displaced. The ground motion and the energy it sends through the structure is dynamic. To retain the strength and function of a structure these requirements should be satisfied (Løset et al. 2011):

1. Building materials must have sufficient deformability.
2. Components such as columns and beams should be able to withstand high repeated deformations, strains and bending.
3. The substructure is composed of the ductile structural parts to a deformable mechanism.

In this thesis, we look at three different materials where each behave differently in terms of tension and compression. Steel and concrete are more ductile and able to

deform into the elastic zone. Timber as a brittle material is weaker in tension and has its best performance in compression, as shown in Figure 3-8. This is because timber as an anisotropic material, has different mechanical characteristics along x, y and z axes. In case of an earthquake, the ground motion will affect the structure and displace it repeatedly in different directions.

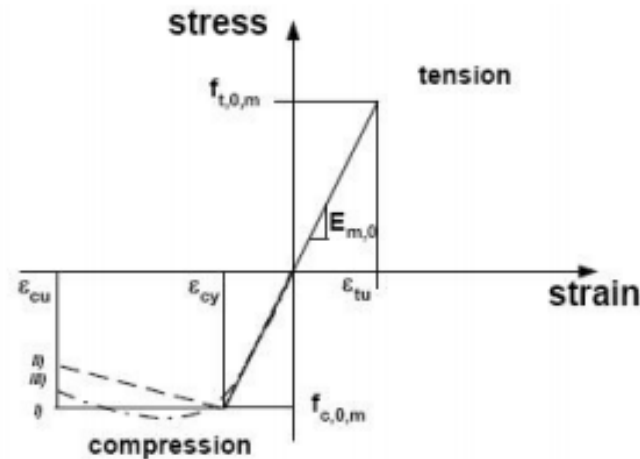


Figure 3-8 Typical stress-strain curve of timber (Kirkegaard et al. 2010).

By choosing ductile elements that can mostly stand in elastic zone when these forces accrue (and does not collapse in plastic zone if they reach their yield point), and structural system that absorbs the energy and distributes it to the supporting soil, can we ensure that the designed structure has seismic withstand capability.

In seismic deign of a structure we categorize the ductility of a structure according to Eurocode 8 guidelines in three levels of absorbing energy, which are based on plastic deformation capacity of the structure and the behavior factor q .

DCL: Low ductility – $q \leq 1,5$

DCM: Medium ductility – $1,5 < q \leq 4$

DCH: High ductility – Values according to *EC8-1 Table 6.2*

In section 3.3.2.4, we will look deeper at what behavior factor q stands for and the influence it has in seismic design and the elastic spectrum.

The dimensionless ratio of ductility factor with its reducing impact on the system can be expressed by equation 3-70. It is the relation between the maximum displacement u_m and the displacement in transition from the elastic to plastic behavior, also called yield deformation point u_y . Figure 3-9 illustrates that occurs when yielding begins.

$$\mu = \frac{u_m}{u_y} \quad 3-70$$

Ductility factor $\mu = 1$ for linear system. The ratio between peak deformation of an inelastic and elastic system can be found by its ductility factor μ and yield strength reduction factor R_y , given in 3-71. Yield strength reduction factor is equal to 1 for linear system and defined by equation 3-72. For a system that remains elastic $\bar{f}_y = 1$, which is defined as the normalized yield strength and expressed as equation 3-73.

$$\frac{u_m}{u_0} = \mu \bar{f}_y = \frac{\mu}{R_y} \tag{3-71}$$

$$R_y = \frac{f_y}{f_0} = \frac{u_0}{u_y} = \frac{1}{\bar{f}_y} \tag{3-72}$$

$$\bar{f}_y = \frac{f_y}{f_0} = \frac{u_y}{u_0} \tag{3-73}$$

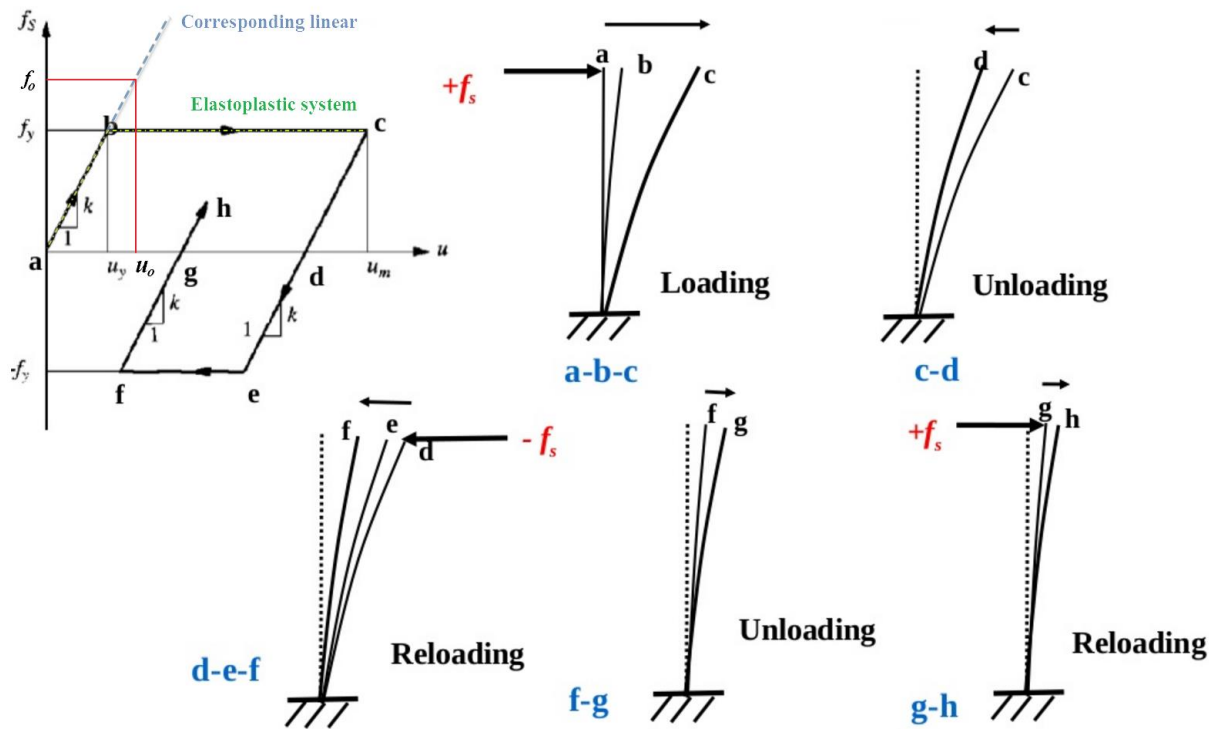


Figure 3-9 Elastoplastic and its corresponding linear system (Chopra 2012) & (Javed 2015).

3.1.8 FREQUENCY AND PERIOD

Frequency and period are two different time related properties. Period T refers to the time needed for a cycle of vibration to complete its journey from a specific position (a) and back to that same position (c) as shown in Figure 3-10. In case of earthquakes, the

ground motion can often be periodical and give huge amount of loads with the natural circular frequency ω_n at a specific position. This frequency is a vital part of the equation 3-74, which gives us the natural period for an undamped system.

$$T_n = \frac{2\pi}{\omega_n} \tag{3-74}$$

Frequency is the amount of periods that occurs in cycle of vibration per unit of time, usually known by unit Hertz and founded by equation 3-75.

$$f_n = \frac{1}{T_n} = \frac{\omega_n}{2\pi} \tag{3-75}$$

The relation between stiffness and mass gives the natural circular frequency ω_n of the system, as presented in equation 3-13, which is further used in finding both period and frequency of the system.

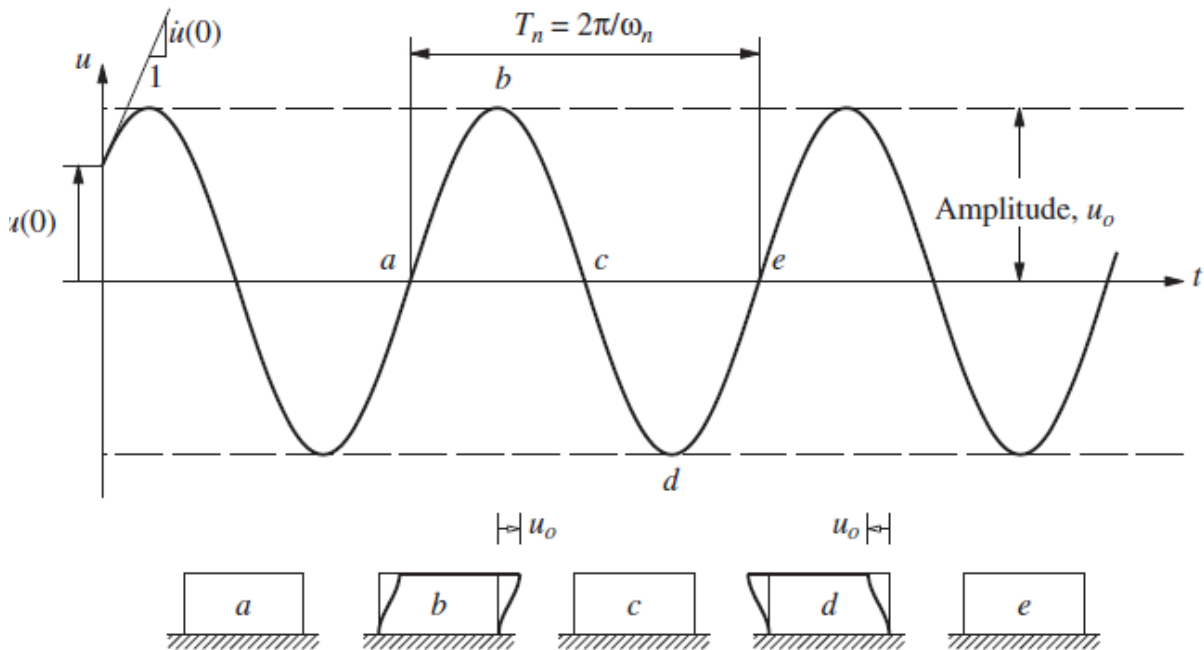


Figure 3-10 Free vibration of a system without damping with natural period T_n (Chopra 2012).

3.1.9 MASS AND STIFFNESS MATRIX

Mass and stiffness are two main variables that influences a building’s response to dynamic forces. If we have two water towers with different height, where the mass is concentrated at the top of the tower, the one with more stiffness has a quicker response and tends to resist displacement. Therefore, geometry and the elasticity of the system

are two main factors in finding stiffness that result in determining the systems response to external forces. One way of achieving this is by using unit load method. Mass and stiffness matrix for a four storey building can be set up as;

$$m = \begin{bmatrix} m_1 & 0 & 0 & 0 \\ 0 & m_2 & 0 & 0 \\ 0 & 0 & m_3 & 0 \\ 0 & 0 & 0 & m_4 \end{bmatrix} \quad k = \begin{bmatrix} k_1 + k_2 & -k_2 & 0 & 0 \\ -k_2 & k_2 + k_3 & -k_3 & 0 \\ 0 & -k_3 & k_3 + k_4 & -k_4 \\ 0 & 0 & -k_4 & k_4 \end{bmatrix}$$

3.1.10 SECOND-ORDER EFFECTS

3.1.10.1 P – Δ EFFECT

For multistorey buildings, transverse displacement and deformation in addition to affecting the normal condition, have an impact in structural safety through P – Δ effect. Unlike the single-storey building where the vertical deformation of load bearing elements are of concerns, in high-rise buildings, horizontal deflection are more of interest. Column in Figure 3-11a is subjected to lateral force F causing a large displacement Δ and moment M_{tot}. The total moment is a product of a primary moment M_{pri} = F · h and secondary moment M_{sec} = P · Δ. The increase of force \tilde{F} , as shown in Figure 3-11b, acting at a given height, can be presented as mentioned in equation 3-76,

$$\tilde{F} = \frac{P\Delta}{h} \tag{3-76}$$

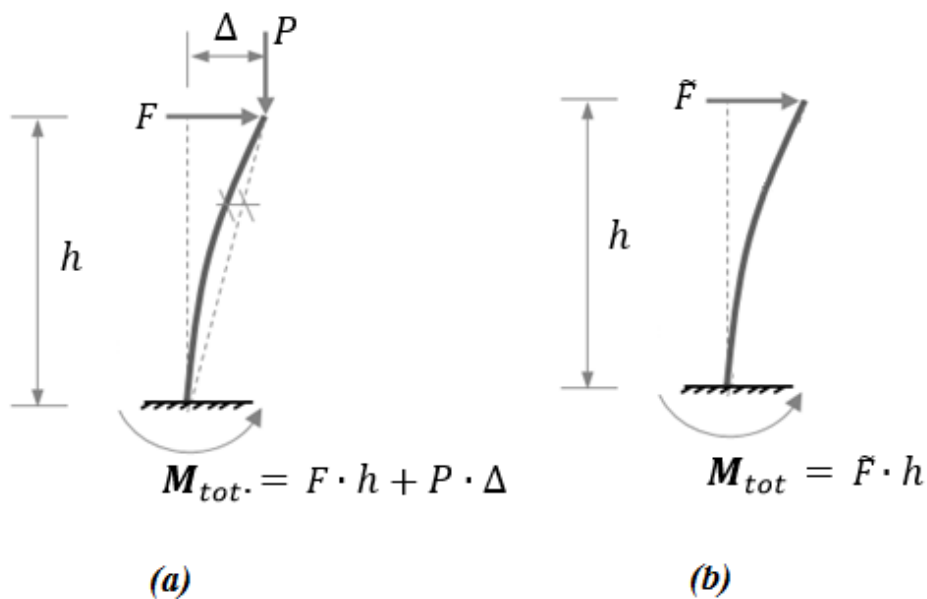


Figure 3-11 Column with horizontal displacement.

By comparing the lateral displacement given by forces F and \tilde{F} , as given by equation 3-77, an additional displacement will take place as a result of the $P - \Delta$ effect. Furthermore by normalizing this relation, as showed in equation 3-80, the displacement ratio based on secondary moment and primary moment that determines how large the displacement can be presented.

$$\frac{\tilde{F}}{F} = 1 + \frac{P\Delta}{h} \quad 3-77$$

$$\theta = \frac{P\Delta}{h} \quad 3-78$$

Equation 3-78 is given in EC8-1 as the sensitivity coefficient. The total shear force that the column presented in Figure 3-11a needs to resist is calculated based on equation 3-79.

$$V_{tot} = F + \tilde{F} = F + \frac{P\Delta}{h} \quad 3-79$$

EC8-1 requires that $P - \Delta$ (second-order effect) is considered under the seismic design situation to ensure the resistance of the building, if following condition is not fulfilled:

$$\theta = \frac{P_{tot} \cdot d_r}{V_{tot} \cdot h} > 0,10 \quad 3-80$$

where θ is the interstorey drift sensitivity coefficient, P_{tot} is the total gravity load, V_{tot} the total seismic storey shear and h and d_r explained earlier. It further adds that sensitivity coefficient shall not exceed the value of 0,3.

As mentioned in equation 3-80, if the incensement of shear force, because of large displacement of a column, does not extends 10% of the total shear force, then there is no need to calculate in accordance to second-order effect

Second-order effects, like $P - \Delta$, when added to non-linear analysis tends to decrease the stiffness of system, which further reduces the capacity of it.

3.1.10.2 GEOMETRIC-STIFFNESS MATRIX

As (Clough & Penzien) discuss the stiffness of SDOF and MDOF systems in a non-linear analyses, it was observed that axial forces or any other loads that can cause buckling of a structure, may have an appreciable effect on the stiffness. The force component acting parallel to the original axis of the element leads to additional load,

which is expressed by *geometric-stiffness coefficient* f_G , as showed in Figure 3-12. Taking into account the negative effect of this load, influences the dynamic equilibrium of forces as mentioned in equation 3-38, as presented in 3-81.

$$f_S + f_D + f_I - f_G = 0 \tag{3-81}$$

When the beam of Figure 3-12 is deflected, the auxiliary link is forced to deflect equality. And this will result in development of force in the main beam, which it must resist in order to maintain the stability of the system.

These forces may be expressed by f_G in matrix form, as presented below:

$$\begin{Bmatrix} f_{G1} \\ f_{G2} \\ \vdots \\ f_{Gi} \\ \vdots \end{Bmatrix} = \begin{bmatrix} k_{G11} & k_{G12} & k_{G13} & \cdots & k_{G1i} & \cdots & k_{G1N} \\ k_{G21} & k_{G22} & k_{G23} & \cdots & k_{G2i} & \cdots & k_{G2N} \\ \cdots & \cdots & \cdots & \cdots & \cdots & \cdots & \cdots \\ k_{Gi1} & k_{Gi2} & k_{Gi3} & \cdots & k_{Gii} & \cdots & k_{GiN} \\ \cdots & \cdots & \cdots & \cdots & \cdots & \cdots & \cdots \end{bmatrix} = \begin{Bmatrix} v_1 \\ v_2 \\ \vdots \\ v_i \\ \vdots \end{Bmatrix} \tag{3-82}$$

where k_G is the *geometric-stiffness matrix* of force corresponding to i due to unit displacement of coordinate j , and \mathbf{u} , the displacement vector, representing the displaced shape of the structure. k_G acts as an adjustment to the conventional stiffness matrix. Geometric-stiffness coefficient factor as an influenced deformation that takes into account the effect of loads, may symbolically be written as

$$f_G = k_G \mathbf{u} \tag{3-83}$$

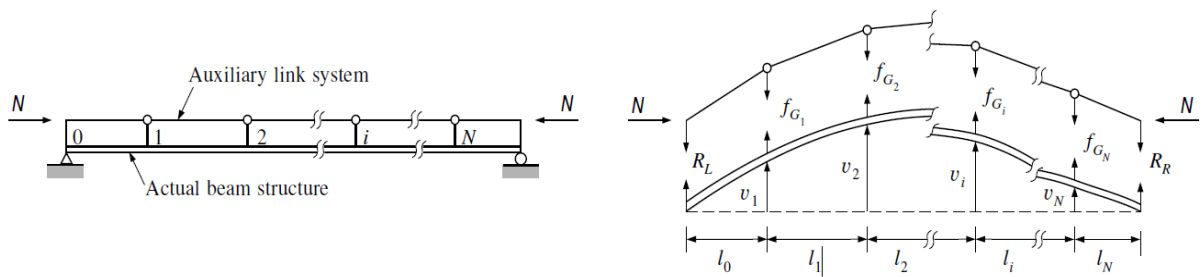


Figure 3-12 Idealization of axial-load mechanism in beam (Clough & Penzien).

Furthermore by considering the impact of geometric-stiffness coefficient, the equation of dynamic equilibrium of a “ damped free vibration system” becomes

$$m\ddot{\mathbf{u}}(t) + c\dot{\mathbf{u}}(t) + k\mathbf{u}(t) - k_G \mathbf{u}(t) = 0 \tag{3-84}$$

in which the combined stiffness that includes both elastic and plastic geometric effects can be expressed by

$$\mathbf{k}_c = k\mathbf{u}(t) - \mathbf{k}_G \mathbf{u}(t) \quad 3-85$$

In terms of a structural elements such as bracing or column, if subjected axial load, lateral stiffness can be decreased. This loss of capacity caused by \mathbf{k}_G can be damaging, and even result in buckling if exposed to extended lateral load. Considering the horizontal rod shown in Figure 3-13 with the length L and a lateral load acting on. If the element is subjected to lateral displacement, v_1 and v_2 , then additional forces F_1 and F_2 must be developed to maintain the equilibrium of the element.

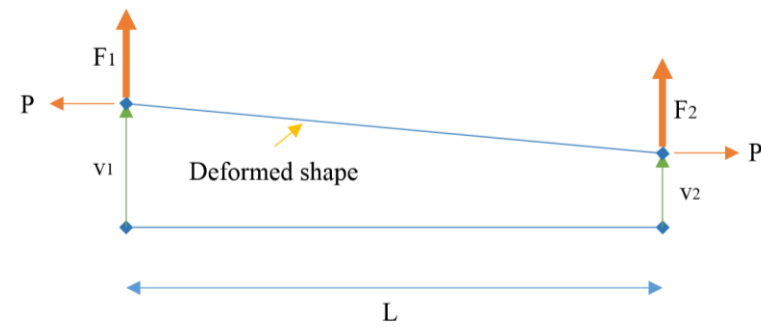


Figure 3-13 Force acting on a rod element.

Taking the moment about point 2 and 1 in deformed shape of Figure 3-13, gives the following equilibrium equation of forces acting on it:

$$F_1 = \frac{P}{L}(v_1 - v_2) \quad 3-86$$

$$F_2 = -\frac{P}{L}(v_1 - v_2) \quad 3-87$$

Combination of equation 3-86 and 3-87 can be presented in the following matrix equation:

$$\begin{Bmatrix} F_1 \\ F_2 \end{Bmatrix} = \frac{P}{L} \begin{bmatrix} 1 & -1 \\ -1 & -1 \end{bmatrix} \begin{Bmatrix} v_1 \\ v_2 \end{Bmatrix} \quad 3-88$$

If the forces acting on an element have been reduced by ductility factor μ , the $P - \Delta$ shall be intensified by μ to reflect ultimate load behavior, as showed in the equation 3-87.

$$k_G = \mu \frac{P}{L} \begin{bmatrix} 1 & -1 \\ -1 & -1 \end{bmatrix} \quad 3-89$$

3.2 RESPONDS AND DESIGN SPECTRA

3.2.1 INTRODUCTION

Earthquake engineering, as a scientific field based on research, practical experience and collected data, gives the necessary tools to prevent and limit damages by designing structures with high earthquake resistance. To achieve a seismic design that provides efficient parameters, understanding the more detailed concepts of earthquake and interpreting the ground motion is essential. Using instruments (see [APPENDIX E](#)) like gravimeter, accelerometers or geophones (loose spring device that measures the velocity), and observing the motion data, verifying peak ground acceleration, effects of magnitude and different characteristics properties of quake are achievable. In case of design, it is important to have procedures which makes it possible to characterize the ground motions in a way that is useful and not time consuming for engineers. Concept of response spectrum is a result of this requirement, which has significant place in this field. Most of the theory and figures in this chapter are from (Chopra 2012).

3.2.2 DEFINITION OF RESPONSE SPECTRUM

The main challenge with earthquakes is that acceleration of ground varies a lot with time and is quite sporadic. [Figure 3-14](#) illustrates some of the recorded incidents from Managua (Nicaragua), El Centro (CA, USA), Chile and Mexico City.

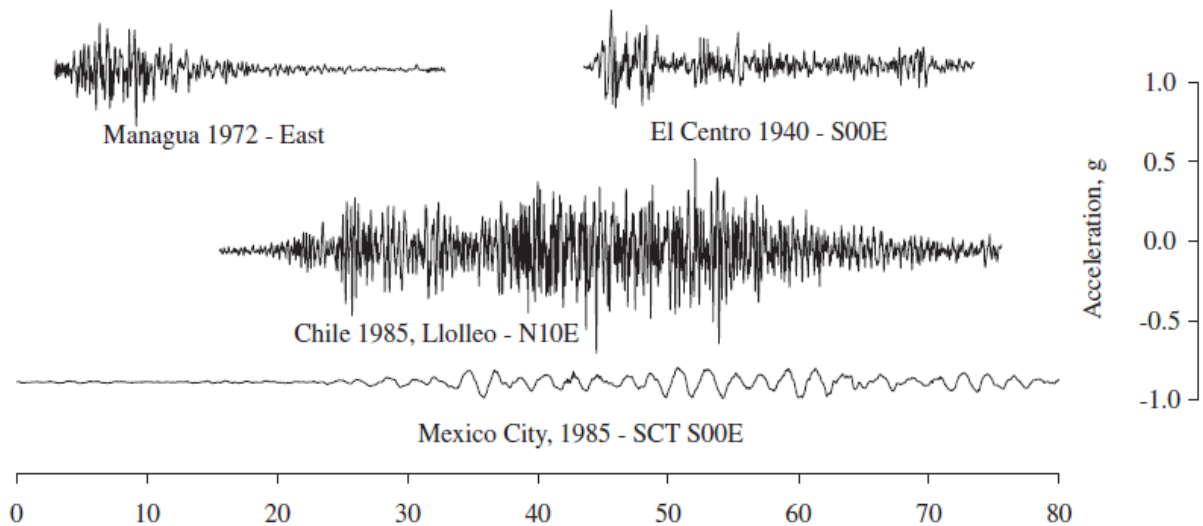


Figure 3-14 Recorded ground motion based on 1979 Hudson (Chopra 2012).

Duhamel's integral can be used in order to find the response of a time dependent system that is induced by an external force. This numerical method gives us the displacement, velocity and acceleration of a system. By comparing equation [3-39](#) and a corresponding

system with a force $p(t)$ applied to, we can observe that the displacement of structure caused by ground acceleration $\ddot{u}_g(t)$ is the same as in case of structure not being in motion when induced by an external force, which gives $p(t) = -m \ddot{u}_g(t)$. By inserting this into equation 3-90, the Duhamel's integral, equation for relative displacement of an undamped SDOF system induced by dynamic excitation of the ground is expressed, as showed in equation 3-91 (Chopra 2012).

$$u(t) = \frac{1}{m\omega_n} \int_0^t p(\tau) \sin[\omega_n(t - \tau)] d\tau \quad 3-90$$

$$u(t) = -\frac{1}{\omega_n} \int_0^t \ddot{u}_g(\tau) \sin[\omega_n(t - \tau)] d\tau \quad 3-91$$

However, in case of design of a structure, it is sufficient to know the peak value of earthquake response, deformation of the system being one of the important part, and necessary to compute the internal forces. A plot of response quantity as a function of the natural period T_n , the natural circular frequency ω_n or the natural cyclic frequency f_n of a system with a fixed damping ratio ζ is called *response spectrum* for that quantity. Equations 3-92, 3-93 and 3-94 show a variety of response spectra depending on response quantity that is plotted (Chopra 2012).

$$u_o(T_n, \zeta) \equiv \max_t |u(t, T_n, \zeta)| \quad 3-92$$

$$\dot{u}_o(T_n, \zeta) \equiv \max_t |\dot{u}(t, T_n, \zeta)| \quad 3-93$$

$$\ddot{u}_o(T_n, \zeta) \equiv \max_t |\ddot{u}(t, T_n, \zeta)| \quad 3-94$$

For the horizontal components of the seismic action, the elastic response spectrum $S_e(T)$ is defined by the following expressions:

$$0 \leq T \leq T_B \quad S_e(T) = a_g \times S \times \left[1 + \frac{T}{T_B} \times (\eta \times 2,5 - 1) \right]$$

$$T_B \leq T \leq T_C \quad S_e(T) = a_g \times S \times \eta \times 2,5$$

$$T_C \leq T \leq T_D \quad S_e(T) = a_g \times S \times \eta \times 2,5 \left[\frac{T_C}{T} \right]$$

$$T \leq T_D \quad S_e(T) = a_g \times S \times \eta \times 2,5 \left[\frac{T_C T_D}{T^2} \right]$$

where

a_g = design ground acceleration

T = vibration period of a linear single-degree-of-freedom system

T_B = lower limit of the period of the constant spectral acceleration branch

T_C = upper limit of the period of the constant spectral acceleration branch

T_D = value defining the beginning of the constant displacement response range of the spectrum depends on the magnitude of an earthquake $T_D = 10 \frac{M-5}{2}$

S = soil factor

η = damping correction factor

Horizontal elastic response spectra for use in Norway are presented in [Figure 3-15](#). These are calculated using critical damping ratio $\xi = 5\%$ which refers to the damping correction factor of $\eta = 1$.

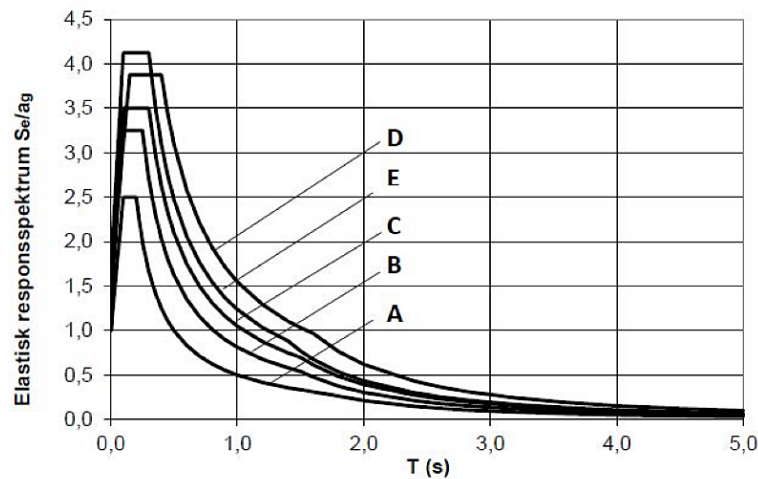


Figure 3-15 Horizontal elastic response spectra for use in Norway (EC8 2014).

3.2.3 DIFFERENT RESPONSE SPECTRUM

3.2.3.1 Deformation Response Spectrum

Deformation response spectrum is a function of the natural period T_n and the damping ratio ζ . The procedure of determining it can be found in [Figure 3-16](#). The ground motion of El Centro, shown in [Figure 3-16a](#), is presented for three different single-degree-of-freedom systems. For each system, the time variation of the deformation determines the peak value of deformation, as showed in equation 3-95.

$$D \equiv u_0$$

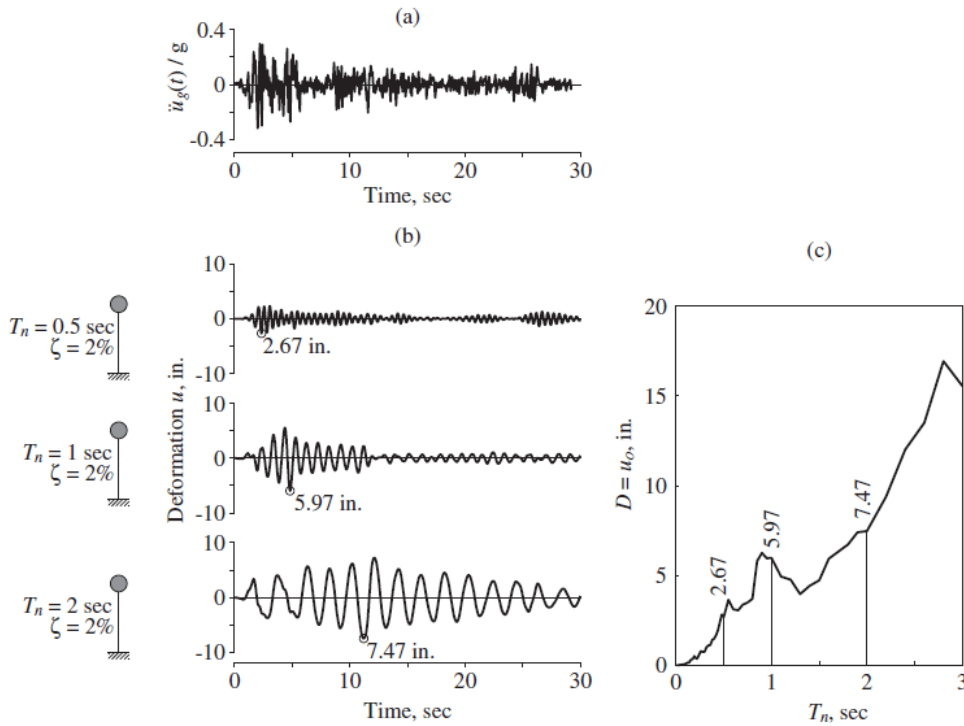


Figure 3-16 (a) Ground acceleration; (b) deformation response of three SDF systems with $\zeta = 2\%$ and $T_n = 0.5, 1,$ and 2 sec; (c) deformation response spectrum for $\zeta = 2\%$ (Chopra 2012).

3.2.3.2 Pseudo-velocity Response Spectrum

Pseudo-velocity response spectrum for SDOF system is a function of T_n and the natural frequency ω_n of the system related to its peak deformation D , and can be expressed as equation 3-96 with quantity V being velocity.

$$V = \omega_n D = \frac{2\pi}{T_n} D \tag{3-96}$$

The value of V , with unit meters per second, relates to system's stored maximum strain energy E_{S0} and is expressed as equation 3-97 during an earthquake. The right side of equation 3-97 is kinetic energy of the structural mass with velocity V , called *pseudo-velocity*, which further is derived into a new equation, 3-98, using equation 3-96. The pseudo-velocity can be calculated in the same method as the deformation response spectrum by repeating the calculation for different systems with various T_n as illustrated in Figure 3-17.

$$E_{So} = \frac{mV^2}{2} \quad 3-97$$

$$E_{So} = \frac{1}{2}ku_o^2 = \frac{1}{2}kD^2 = \frac{1}{2}k\left(\frac{V}{\omega_n}\right)^2 = \frac{mV^2}{2} \quad 3-98$$

3.2.3.3 Pseudo-acceleration Response Spectrum

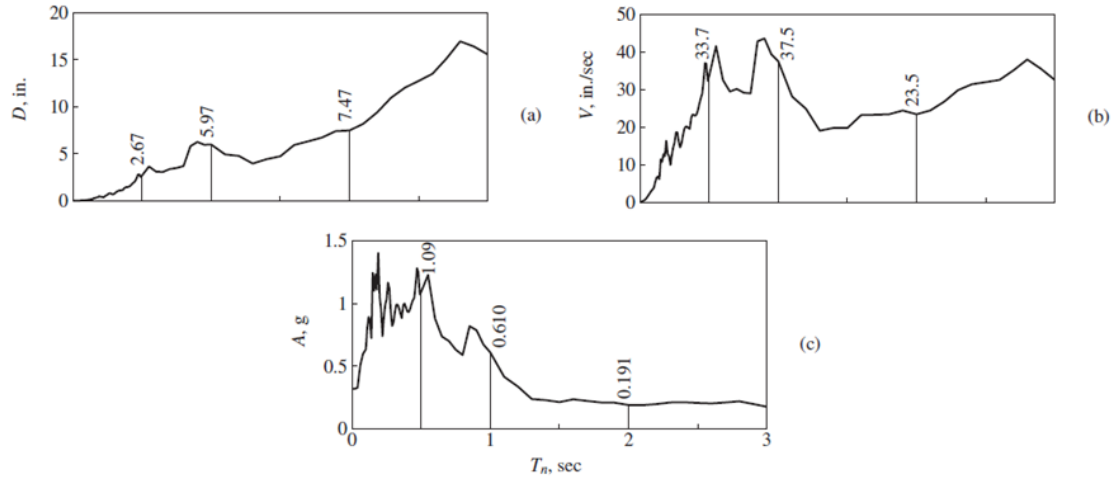


Figure 3-17 Graph that shows different response spectrum based on El Centro ground motion with damping ratio 0.02. (a) Deformation response spectrum; (b) pseudo-velocity response spectrum; (c) pseudo-acceleration response spectrum (Chopra 2012).

The pseudo-acceleration response spectrum for a SDOF system is a function of T_n and the natural frequency ω_n of the system related to its peak deformation D , and can be expressed as equation 3-99 with quantity A being acceleration.

$$A = \omega_n^2 D = \left(\frac{2\pi}{T_n}\right)^2 D \quad 3-99$$

The value of A with unit meters per second squared relates to base shear's or equivalent static force's peak value (V_{bo} or f_{So}) and expressed as equation 3-100.

$$V_{bo} = f_{So} = mA \quad 3-100$$

Maximum base shear can be calculated using the equation 3-101, by w being weight of the system.

$$V_{bo} = \frac{A}{g}w \quad 3-101$$

3.2.3.4 Combined D-V-A Response Spectrum

Since these three spectrums are related through equation 3-102 or 3-103, and are just different way of presenting same information regarding the system’s response, using combined response spectrum (combined in one plot) called *D-V-A Response Spectrum* can be reasonable to use. Figure 3-18 illustrates combined D-V-A response spectra for EL Centro in a four-way plot in logarithmic scale with different damping ratio and replaces the three plots of Figure 3-17.

$$\frac{A}{\omega_n} = V = \omega_n D \tag{3-102}$$

$$\frac{T_n}{2\pi} A = V = \frac{2\pi}{T_n} D \tag{3-103}$$

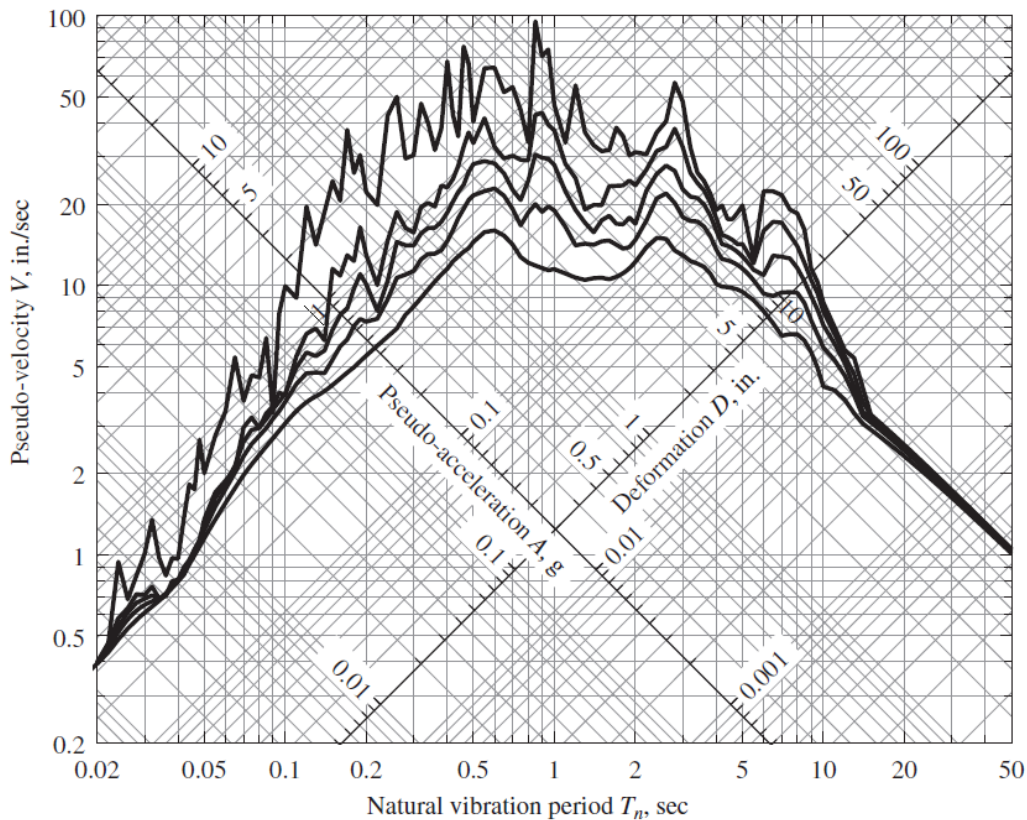


Figure 3-18 D-V-A plot for El Centro ground motion (Chopra 2012).

3.2.4 DEFINITION OF DESIGN SPECTRUM

When it comes to designing a structure and finding the response of that structure to a ground acceleration, having the peak ground acceleration or velocity is not sufficient. Time history that represent acceleration and its spectrum varies very much for different

earthquakes at the same location. This introduces an uncertainty around the collected information, and whether the data can provide useful basis for future earthquakes response spectrums. Based on the weakness just mentioned, it is necessary to develop a design spectrum (a smooth average curve) that consists of average value of several spectrums with eliminated maximum and minimum values.

George W. Housner, often considered the father of earthquake, first introduced the concept of design spectrum based on the response spectrum. The main different between design spectrum and response spectrum is that the one called *design*, is developed on averaging spectra from past earthquakes, while response spectra is a representation of the influence of a given quake. Design spectrum is presented after the same principles as response spectrum, but with reduction based on the ductile behavior of structure's elements which is introduced by behavior factor q . The design value of design spectrum $S_d(T)$ for the horizontal components are described in section 3.2.2.5 of *EN 1998-1:2004* and is as followed:

$$0 \leq T \leq T_B : S_d(T) = a_g \cdot S \cdot \left[\frac{2}{3} + \frac{T}{T_B} \cdot \left(\frac{2,5}{q} - \frac{2}{3} \right) \right] \quad 3-104$$

$$T_B \leq T \leq T_C : S_d(T) = a_g \cdot S \cdot \frac{2,5}{q} \quad 3-105$$

$$T_C \leq T \leq T_D : S_d(T) \begin{cases} = a_g \cdot S \cdot \frac{2,5}{q} \left[\frac{T_C}{T} \right] \\ \geq \beta \cdot a_g \end{cases} \quad 3-106$$

$$T_D \leq T : S_d(T) \begin{cases} = a_g \cdot S \cdot \frac{2,5}{q} \left[\frac{T_C T_D}{T} \right] \\ \geq \beta \cdot a_g \end{cases} \quad 3-107$$

where a_g, S, T_B, T_C, T_D are as defined in section 3.2.2, and other parameters are as following;

q = behavior factor

β = lower bound factor for the horizontal design spectrum (*Norwegian National Annex NA 3.2.2.5(4)* gives 0.2)

Values that describe the recommended elastic response spectrum are as shown over, listed in [Table 1](#) and illustrated in [Figure 3-19](#). In section 3.3.2, we will look more into these values.

Ground types	S	T_B	T_C	T_D
A	1,0	0,10	0,25	1,50
B	1,25	0,10	0,30	1,50
C	1,40	0,15	0,35	1,50
D	1,60	0,15	0,45	1,50
E	1,70	0,10	0,35	1,50

Table 1 Elastic response spectrum values (EC8 2014).

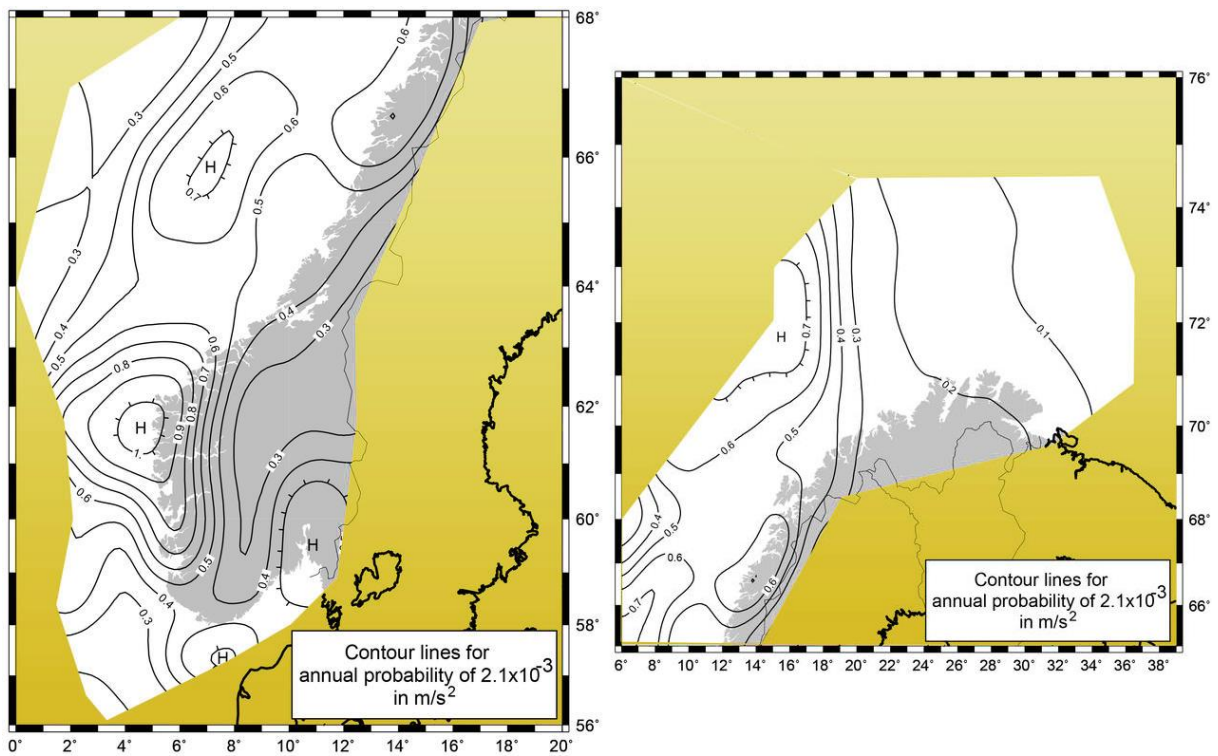


Figure 3-19 Norwegian Seismic zoning maps (Jordskjelv.no).

3.3 DESIGN GUIDELINES AND BUILDING CODES

3.3.1 INTRODUCTION

Design of land based structures, as mentioned back in 2.4, have been subjected to guidelines from *NS 3419-12* from year 2004. Seismic design procedures after 2010 followed *Eurocode 8 (EC8)* with an additional document accounting for the local conditions and regulations. Purpose of these codes and guidelines as mentioned in *NS-EN 1998 1.1.1* in event of earthquakes is that:

“ Human lives are protected,
 damage is limited and
 structures important for civil protection remain operational ”

It is in everyone’s benefit to have and respect certain rules. [Table 2](#) lists the different parts of NS-EN series that gives the necessary values and equations for civil engineering works in Norway. EC1 and EC8 are the two main parts that engineers working with seismic related project need to base their calculation on.

NS-EN 1990	Eurocode 0: Basis of structural design
NS-EN 1991	Eurocode 1: Actions on structures
NS-EN 1992	Eurocode 2: Design of concrete structures
NS-EN 1993	Eurocode 3: Design of steel structures
NS-EN 1994	Eurocode 4: Design of composite steel and concrete structures
NS-EN 1995	Eurocode 5: Design of timber structures
NS-EN 1996	Eurocode 6: Design of masonry structures
NS-EN 1997	Eurocode 7: Geotechnical design
NS-EN 1998	Eurocode 8: Design of structures for earthquake resistance
	Part 1: General rules, seismic actions and rules for buildings
	Part 2: Bridges
	Part 3: Assessment and retrofitting of buildings
	Part 4: Silos, tanks and pipelines
	Part 5: Foundations, retaining structures and geotechnical aspects
	Part 6: Towers, masts and chimneys
NS-EN 1999	Eurocode 9: Design of aluminum structures

Table 2 Summary of design guidelines used in Norway (EC8 2014).

In the remaining parts of this chapter, we look at main aspect of EC8 regarding seismic design of a new structure in Norway. Most information will be provided from the *NS-EN 1998*; other sources will be mentioned upon their use.

3.3.2 FUNDAMENTAL CRITERIA, FACTORS AND PARAMETERS

3.3.2.1 Importance classes

EC8-1, as shown in [Table 3](#), divides structures in four different importance classes based on of what Eurocode stands for (as described in section [3.3.1](#)). This lays the ground criteria and parameters used for seismic design of buildings, and makes it possible to differentiate between structures with various importance and reliability. *NA table.4 (902)* gives a more indicative table for choice of importance class.

Importance class	Buildings	γ_1
I	Buildings of minor importance for public safety, e.g. agricultural buildings, etc.	0,7
II	Ordinary buildings, not belonging in the other categories.	1,0
III	Buildings whose seismic resistance is of importance in view of the consequences associated with a collapse, e.g. schools, assembly halls, cultural institutions, etc.	1,4
IV	Buildings whose integrity during earthquake is of vital importance for civil protection, e.g. hospitals, fire stations, power plants, etc.	2,0

Table 3 Values for importance factor γ_1 and type of structures it applies to (EC8 2014).

3.3.2.2 Ground condition

Identification of ground type is one of the first actions at a construction site. It is vital to investigate and classify the bedrock for ground improvement. Building foundation with bedrock support is in most cases a better approach. Soft ground condition can cause the seismic waves to decay because of their non-linear behavior and intensify waves with low frequency. This can result in resonance if the structure's frequency is in the same range, which will increase the vibration and the seismic load that structure shall resist. *EC8-1 Table 3.1* and *NA:2014 Table NA.3.3* gives the necessary description

of ground types based on stratigraphic profiles and soil factor S . In this thesis, ground type **A** for the plot of horizontal spectra is selected as described in Table 1 and Table 4, based of the location of office building in Bergen, Hordaland.

Ground type	Description of stratigraphic profile	Parameters		
		$V_{s,30}(\frac{m}{s})$	N_{SPT}	$c_u(kPa)$
A	Rock or other rock-like geological formation, including at most 5m of weaker material at the surface.	> 800	-	-
B	Deposits of very dense sand, gravel, or very stiff clay, at least several tens of meters in thickness, characterized by a gradual increase of mechanical properties with depth.	360 - 800	> 50	> 250
C	Deep deposits of dense or medium-dense sand, gravel or stiff clay with thickness from several tens to many hundreds of meters.	180 - 360	15 – 50	70 – 250
D	Deposits of loose-to-medium cohesionless soil (with or without some soft cohesive layers), or of predominantly soft-to-firm cohesive soil.	< 180	< 15	< 70
E	A soil profile consisting of surface alluvium layer with $v_s > 800 \frac{m}{s}$	-	-	-

Table 4 Ground types (EC8 2014).

Bedrock is classified by using the average shear-wave velocity between 0 and 30-meters depth with equation 3-108, where h_i and V_i are respectively thickness and shear wave velocity. If the $v_{s,30}$ is not accessible, N_{SPT} , which is the standard penetration test with “N” values, can be used (Løset & Rif 2010).

$$V_{s,30} = \frac{30}{\sum_{i=1,N} \frac{h_i}{V_i}} \quad 3-108$$

3.3.2.3 Ground acceleration

The first value needed in order to create the curve of design spectrum after choosing the ground type, is *Peak Ground Acceleration (PGA)*. PGA is adjusted with respect to the area's ground conditions and seismicity. Figure 3-19 shows the map of Norway divided in zones with ground at an acceleration of 40 hertz of the elastic response spectrum for ground type A, based on a return period of 475 years. That is higher than a_{gR} , the reference ground acceleration of frequency $f \rightarrow \infty$ that is EC1's designation value. The reference peak ground acceleration is therefore set to $0.8 \cdot a_{g40Hz}$ as the characteristic value.

$$a_g = a_{gR} \cdot \gamma_1 \quad 3-109$$

The characteristic value is, in order to convert to a design value a_g , multiplied with importance class factor γ_1 for different seismic classifications, as showed in equation 3-109, based on different consequences of collapse listed in the Table 3. For locations between two different a_{g40Hz} interpolation is recommended. It is important to notice that a_{g40Hz} is only meant for mainland Norway and do not cover continental shelf, Svalbard, Jan Mayen and Bear Island.

3.3.2.4 Seismic behavior factor q

Seismic behavior factor q is an expression of structure's ability to absorb and distribute earthquake energy, mainly through the ductile behavior. It depends on several parameters including structural material and the selected system. By the EC8-1 definition, a structure can be divided in three different ductility classes (DCL, DCM and DCH), whereas each of them refers to a q value, as described in section 3.1.7.

Design concept	Structural ductility class	Range of the reference values of the behaviour factor, q
Concept a) Low dissipative structural behaviour	DCL (Low)	$\leq 1,5$
Concept b) Dissipative structural behaviour	DCM (Medium)	≤ 4 also limited by the values for DCM in Table 6.2
	DCH (High)	Same as for DCM

Figure 3-20 List of current behavior factor (EC8 2014).

In Norway as the National annex implies, only recommended classes are DCL and DCM. However, since the tradition of designing indeterminate structures with more strength is not common in Norway (because of Norway being a low to intermediate seismicity area), most new buildings are designed according to DCL with value $q \leq 1,5$, shown in Figure 3-20. By introducing this type of practice structures are mostly non-dissipative rather fully dissipative (A. Rønquist et al. 2012).

3.3.2.5 Combination of loads

Earthquake is considered as an accidental load and should be combined with other accidental loads based on *NS-EN 1990 Table A1.3*.

Following table gives the load factors for seismic action used in creating load combination in ultimate limit state (Løset et al. 2011).

Permanent load	Seismic load Variable load	Design load	Other variables	
1,0	1,0	0,0 – 0,8	0,0 – 0,8	For forces In structure
1,0	1,0	1,0 or 0,0	1,0 or 0,0	For forces in ground

Table 5 Load factor for seismic action (Løset et al. 2011).

NS-EN 1990 criteria for combinations of actions (accidental and seismic design situations) is to be satisfied in terms of ultimate limit state as given in *NS-EN 1990 6.4.3.4, A1.3.2* and *Table NA.A.1.3*. Basic load combination as given in *NS-EN 1990* for design and seismic load are as follows (Elghazouli 2009)

$$\begin{aligned}
 E_d \\
 \text{Design action effect} &= \sum_{\text{Permaent}} G_{kj} + E_{Ed} + \sum_{\text{Permaent}} \psi_{2i} Q_{kj}
 \end{aligned}
 \tag{3-110}$$

To define the capacity in ultimate limit state, it is recommended to use different partial safety factors for different materials. Figure 3-21 gives the values based on EC8 and EC5.

Direction of earthquakes are random and will not be as identical as the structures coordinate system. To calculate seismic load, having an orthogonally system with x and y axis in the same direction primary length and width of the building, makes the calculation smoother, therefore to consider earthquakes direction, load effects in

primary direction of building are combined with (“+”) a factor of 1,0, and the secondary with 0,3, as showed in equation 3-111 and 3-112.

	DCL	DCM	DCH
γ_c	1,2	1,5	1,5
γ_s	1,0	1,15	1,15

Materials and products	γ_m
Solid timber	1,25
Glued laminated timber	1,15
Laminated veneer lumber (LVL),plywood	1,15
OSB	1,3
Particle board	1,3
Fibreboard	1,3
Connections	1,3
Punched timber plate	1,25
Punched metal plate	1,0
SLS and ULS load combinations	1,0

Figure 3-21 Recommended partial factors (EC8 2014) & (EC5 1994).

If the structure satisfies the requirement of regularity in plan according to *EC8-1* 4.3.3.5.1, the value of 0,3 can be reduced to zero, since rotations that occurs are not of importance (Løset et al. 2011).

$$E_{dx} + 0,3 \cdot E_{dy} \quad 3-111$$

$$0,3 \cdot E_{dx} + E_{dy} \quad 3-112$$

3.3.2.6 Mass conversion

It is necessary to determine the mass distribution of the building before performing seismic calculation. It influences the value for vibration shapes, corresponding periods and the earthquake forces that occurs from the ground level and across the building. *NS-EN 1990 Table NA.A1.1* gives the recommended value for imposed and snow load. As illustrated in [Figure 3-22](#), for office areas ψ_2 is set to 0,3 of imposed load's permanent part, 0,2 for snow load and 1 for structural and non-structural dead load. Wind load is not a part of seismic calculation.

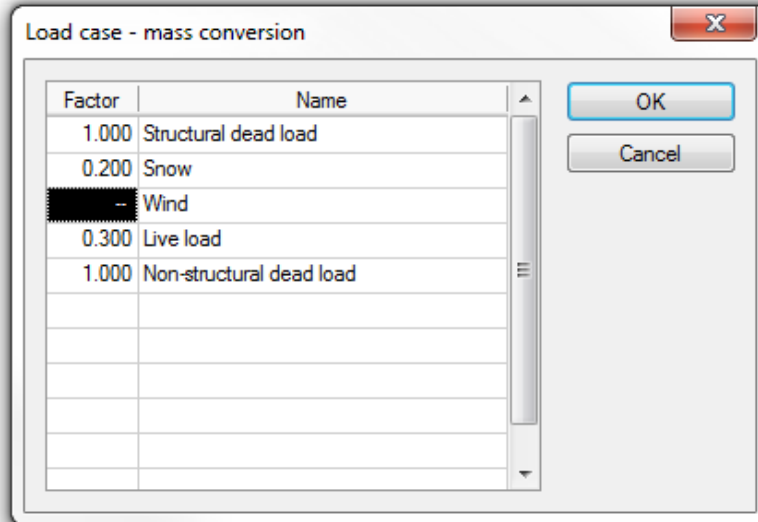


Figure 3-22 Load cases and their conversion of mass (FEM-DESIGN).

3.3.2.7 Horizontal design spectrum $S_d(T)$ and parameters (T_B, T_C, T_D)

$S_d(T)$ is defined in EC8-1 3.2.2.5 with a shape like response spectrum shown in EC8-1 figure NA.3(903). The plotted graph, as illustrated in Figure 3-15, shows how the values T_B, T_C, T_D , as described earlier in this chapter, defines the corner periods of the design spectrum curve. It is important to notice the effect that behavior factor q has on the graph. Higher q -value gives lower $S_d(T)$ and seismic load. EC8-1 gives four different type of response spectrum. Horizontally $S_e(T)$ and vertically $S_{ve}(T)$ elastic response spectrum, elastic response spectrum for displacement $S_{De}(T)$ and design spectrum for elastic analysis $S_d(T)$.

3.3.2.8 INTERSTORY DRIFT

Ground motion induced floor displacement or interstorey drift of inelastic or elastic systems are important part of a displacement-based design and seismic evaluation of a structure. This is a very useful quantity to determine structures, especially multistorey, performance and response subjected to an earthquake excitation and in case of high torsional effect, that should be taken into account in a very early stages of design. Drift and lateral stability rises concern and plays a vital role in design of a proper structural system. These concerns have resulted in requirements for limiting the lateral displacement. EC8-1 4.4.3.2 provides limits for buildings that shall be observed to

minimize the damage caused by displacement. The limitation of interstorey drift are as followed in Table 6.

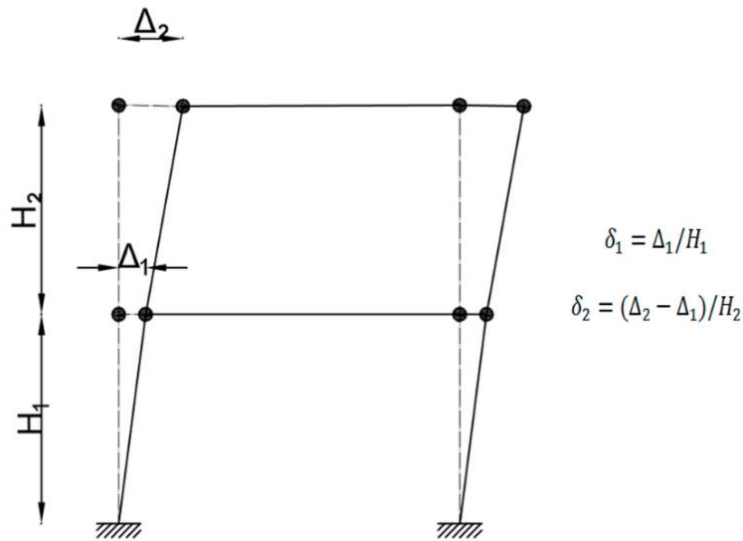


Figure 3-23 Presentation of interstorey drift (Seo et al. 2015).

Figure 3-23 shows the relative horizontal displacement between two floors in a multistorey building induced by the design seismic action. Design interstorey drift d_r is calculated based on equation 3-113, as described in EC8-1 4.3.4. Reduction factor v is 0,5 for importance class I and II and 0,4 for III and IV, as given by National Annex

$d_r v \leq 0,0050 h$	Buildings with non-structural elements of brittle materials attached to the structure.
$d_r v \leq 0,0075 h$	Buildings having ductile non-structural elements
$d_r v \leq 0,010 h$	Buildings having non-structural elements fixed in a way so as not to interface with structural deformations, or without non-structural elements.

Table 6 Limitation of interstorey drift (EC8 2014).

$$d_s = q_d \cdot d_r \quad 3-113$$

3.3.2.9 ELIMINATION CRITERIA

EC8-1 NA.3.2.1 gives five elimination criteria that in case of building in low seismic areas, results in leaving out seismic design, and leaves verifying the structures safety

on wind load as the main design load. If one of these five criteria, as listed below, are met, then we do not need to include seismic calculation in our design.

- I. If $a_g S < 0,05g = 0,49 \frac{m}{s^2}$
- II. If $S_d(T) < 0,05g = 0,49 \frac{m}{s^2}$ calculated with $q \leq 1,5$
- III. If constructions is seismic class 1
- IV. If it is a lightweight structure
- V. If shear force at foundation level due to earthquakes is less than the forces calculated for the other combinations of actions.

Figure 3-24 shows the impact of fifth criteria from the list above, which by satisfying the regularity criteria results in elimination of earthquake calculation and can be rewritten as

$$1,0 \cdot F_b < (1,5 \cdot wind + 1,05 \cdot skew) \cdot \left(\frac{\gamma_{c,ultimate\ limit}}{\gamma_{c,DCL}} \right)$$

with F_b being horizontal force on the ground level and EC providing the rest of values for different materials.

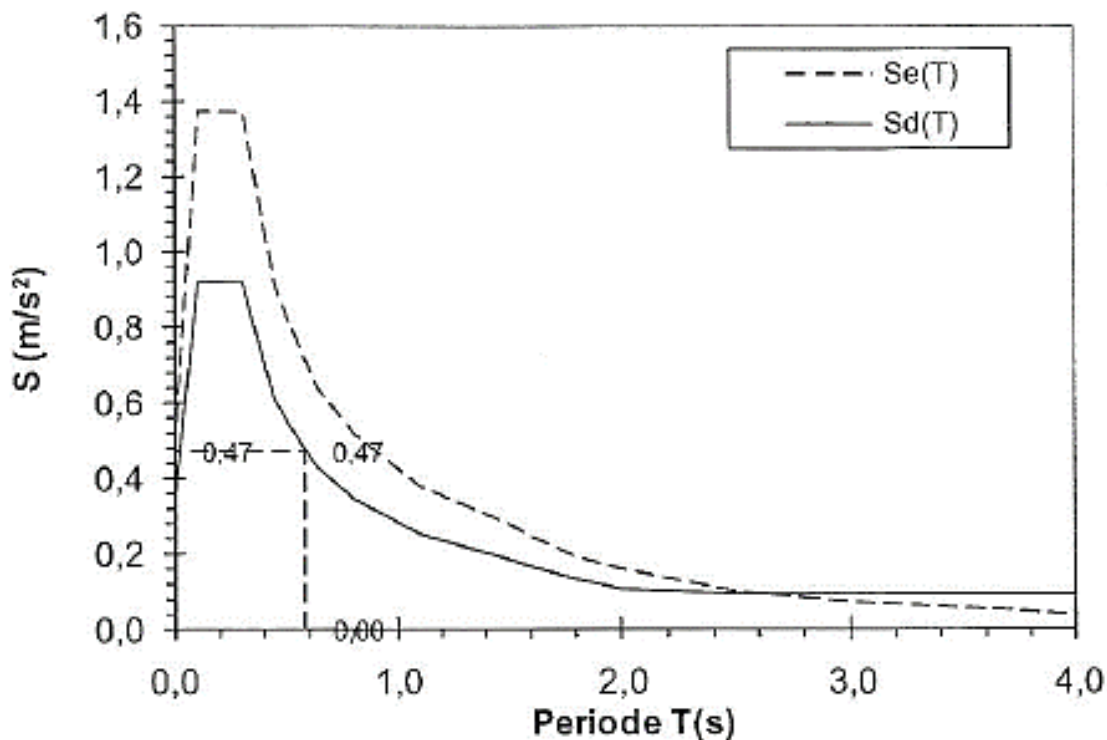


Figure 3-24 Example of how criteria “V” works. $S_d(T) \leq 0,49$ leads to elimination of earthquake calculation. The regularity criteria is fulfilled and the building only have one dominant natural period T (Løset & Rif 2010).

3.3.3 EARTHQUAKE CALCULATION ACCORDING TO EC8

3.3.4 DESIGN OF STRUCTURE

There are principles for design of structures with great decisive role in how natural forces reacts on them. EC8's "no collapse" and "damage limitation" requirements, which are not mandatory, gives an indication on what they are and why they should be included in conceptual design stage (Elghazouli 2009).

EC 8 4.2.1(2) lists these six basic guiding principles as it followed here:

I. Structural simplicity

Establishing a system with clear and direct load path for seismic forces from top of the building to the foundations. This critical objective will help reduction of uncertainty in evaluating the structure's dynamic response, strength and ductility.

II. Uniformity, symmetry and redundancy

Having uniformity and symmetry will affect the distribution of mass, strength and stiffness in plan and elevation, and will result in a better behavior of structure in case of earthquake. It also eliminates the torsional response in plane and sensitive zones with large stress or ductility demands in elevation.

Redundancy of a structure means that it has a better distribution system using the whole structure as load path to absorb the earthquake energy in a more efficient way.

III. Bi-directional resistance and stiffness

Based on the understanding that seismic loads are bi-directional along x- and y-axes. Structures by having an orthogonal plan structural pattern are able to resist these type of loads in every directions.

IV. Torsional resistance and stiffness

Rotary movement occurs when there is an eccentricity in buildings between center of mass and stiffness, which can result in increased damage in earthquakes. To avoid this effect it is necessary to design a building with sufficient torsional resistance and stiffness by minimizing the eccentricity of mass and stiffness.

V. Diaphragmatic behavior at storey level

The transmission of seismic inertia loads at each storey level depends on floor diaphragms such as shear walls and rooftops. In order to provide lateral stability and be able to distribute lateral load to the vertical resisting elements, structures must have diaphragms with sufficient in-plane stiffness, and minor openings.

VI. Adequate foundation

EC8-1 4.2.1.6 states that design and construction of foundations shall ensure a uniform seismic excitation throughout the building. The interaction of structure with foundation and foundation with ground is an important part of the design and vital to seismic performance (Elghazouli 2009).

3.3.5 REGULARITY

EC8 categorizes and defines criteria for each type of building structures with individual dynamically independent unit into being regular or non-regular. It also describes the consequences of structures regularity on design and seismic analysis, as shown in [Figure 3-25](#).

The regularity criteria for both in plan and elevation are respectively found in *EC8-1 4.2.3.2* and *4.2.3.3* and described in section [3.3.5.1](#) and [3.3.5.2](#).

Regularity		Allowed Simplification		Behaviour factor
Plan	Elevation	Model	Linear-elastic Analysis	(for linear analysis)
Yes	Yes	Planar	Lateral force ^a	Reference value
Yes	No	Planar	Modal	Decreased value
No	Yes	Spatial ^b	Lateral force ^a	Reference value
No	No	Spatial	Modal	Decreased value

Figure 3-25 Consequences of structural regularity on seismic analysis and design (EC8 2014)

3.3.5.1 REGULARITY IN PLAN

Buildings with non-symmetrical structural systems tends to act weaker in case of an earthquake. This is based on experience and fatal outcome of these types of structures. To avoid any torsional effect on the construction, which occurs when center of mass

and stiffness are widely away from each other, having a regular building in plan is preferred. Regularity in plan is applicable when;

- Conditions like having an approximately symmetrical plan with respect to x and y-axes.
- The slenderness ratio $\lambda = \frac{L_{max}}{L_{min}}$ does not exceed value of 4.
- The structural eccentricity e_o and the torsional radius r satisfies these conditions: $e_{ox,y} \leq 0,3 r_{x,y}$ and $r_{x,y} \geq I_s$ where $I_s = \sqrt{\frac{l^2+b^2}{12}}$ is the radius of gyration of the floor mass in plan.
- Plan should have a compact shape with a convex perimeter line and not more than 5% re-entrant area as illustrated in Figure 3-26.
- The in-plane stiffness of a diaphragm floor compared to the lateral stiffness of vertical elements shall be sufficient.

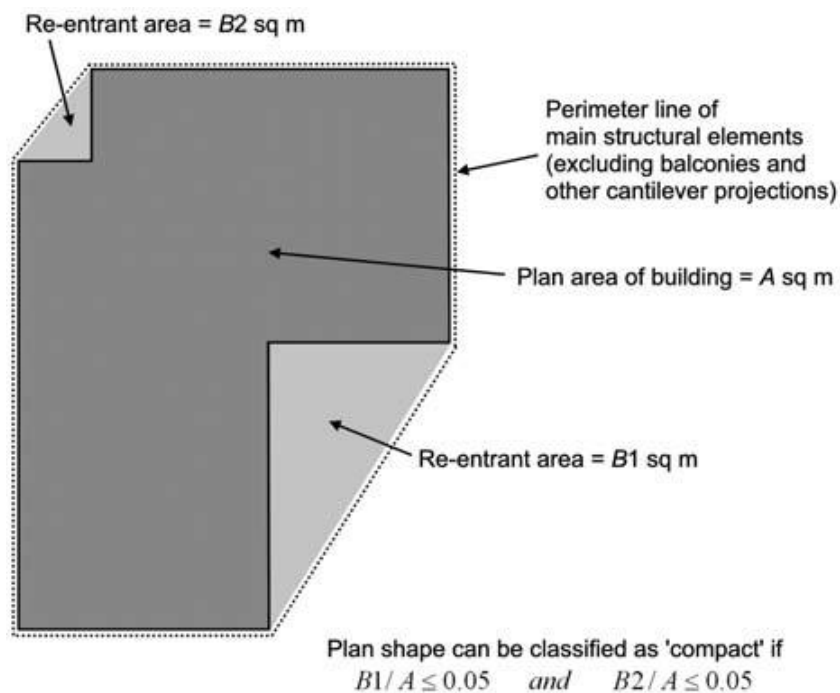


Figure 3-26 Definition of compact shape (Elghazouli 2009).

Majority of constructions built before the regulation took place in Norway have complicated geometry. This is due to the absent of seismic calculation and criteria of regularity. Figure 3-27 illustrates and describes the examples of complicated geometry and preferred solutions (Løset & Rif 2010)

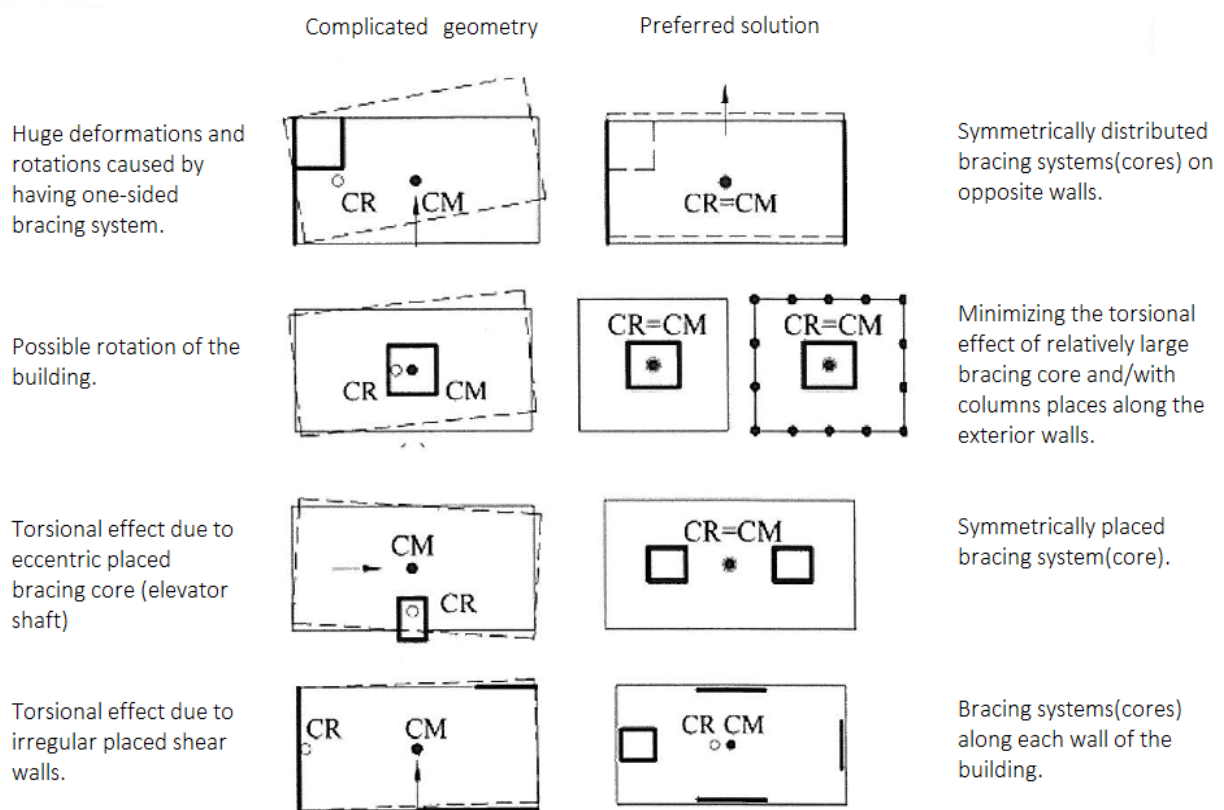


Figure 3-27 Example of different solutions of bracing systems (Løset & Rif 2010).
Translated by the author.

3.3.5.2 REGULARITY IN ELEVATION

As for regularity in plan, there are conditions a building needs to fulfil in terms of being classified as regular in elevation. Vertical regularity has more severe effects, if not equal part, in constructions behavior and seismic design. Criteria in *NS-EN 1998-1 4.2.3.3* for buildings being regular in elevation and *4.2.3.3 figure 4.1* for buildings with setbacks are to be followed.

STRUCTURAL TYPE	DCM	DCH
Frame system, dual system, coupled wall system	$3,0 \alpha_u / \alpha_1$	$4,5 \alpha_u / \alpha_1$
Uncoupled wall system	3,0	$4,0 \alpha_u / \alpha_1$
Torsionally flexible system	2,0	3,0
Inverted pendulum system	1,5	2,0

Figure 3-28 Basic values for behavior factor for systems regular in elevation (EC8 2014).

EC8 also provides basic values for behavior factor q_o for systems regular in elevation, as shown in Figure 3-28, where $\frac{\alpha_u}{\alpha_1} = 1,1$ for one-storey, 1,2 for multistorey one-bay

frames and 1,3 for multistorey, multibay or frame-equivalent dual structures. Behavior factor for irregular buildings in elevation as specified in *NS-EN 1998-1 4.2.3.1(7)* should be multiplied by 0,8.

Huge variation of height and structural system between levels in a building can result in increased load and loss of stiffness, which in case of seismic action can end in collapse. [Figure 3-29](#) provides examples of complicated and preferred solutions, whereas for the complicated case, sudden change in distribution of stiffness results in concentration of inelastic deformation of structure. Soft storey presents this sudden change of stiffness, which is a common issue for multistorey buildings in Norway. Preferred solution on the other hand, show that constant distribution or gradual reduction gives uniformly distributed deformation.

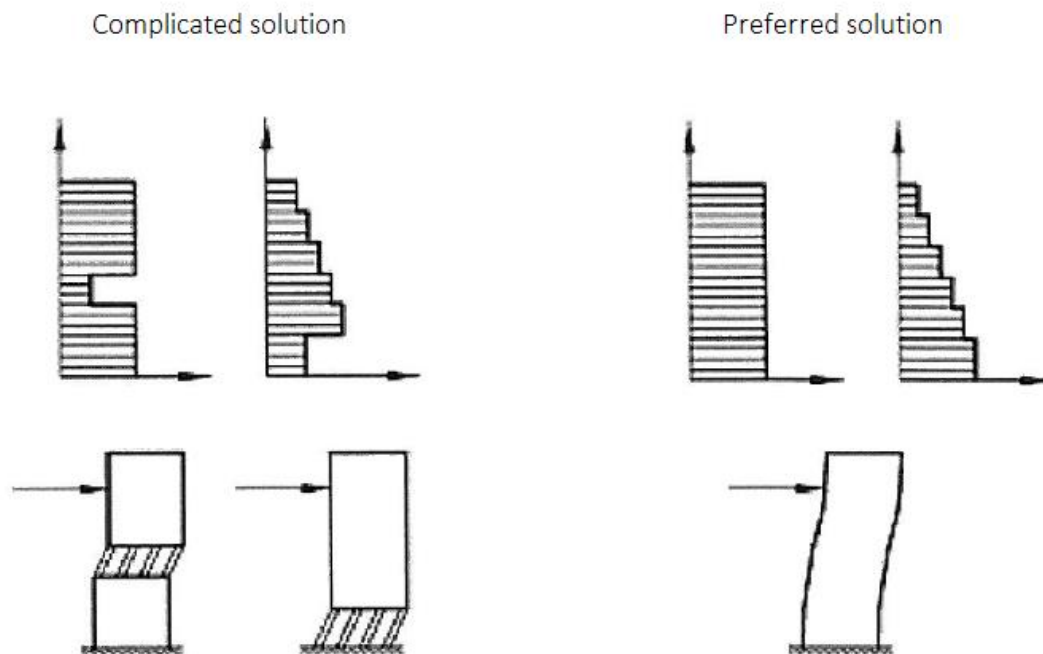


Figure 3-29 Example of stiffness distribution (Løset & Rif 2010)

3.3.6 TORSIONAL EFFECT

Collapse of a building due to its weak torsional response is one of the fatal error of poor design and not satisfying the criteria of EC8. Under seismic load, structures can be subjected to two types of torsional influences: inherent torsion and accidental torsion (Jarrett et al. 2014). Minimizing the torsional effect by adopting a preferred solution, as shown in [Figure 3-27](#), is one way to solve this issue. But uncertainties in the location of center of mass in each storey and asymmetric changes in strength and stiffness requires a better way of calculation. In order to address this issue, accidental

eccentricity e_{ai} and torsional effect factor δ are introduced. Accidental eccentricity, as shown in equation 3-114 is issued as an extra eccentricity to the center of mass by 5% of the diaphragm dimension in each direction, which creates an additional moment of inertia. The torsional effects factor, calculated by equation 3-115 deals with unaccounted effects of this phenomenon and increases forces in the floor diaphragm proportional to the center of mass, when the lateral stiffness and mass are symmetrically distributed (EC8 2014). Torsional effect criteria applies to both DCL and DCM.

$$e_{ai} = \pm 0,05 \cdot L_i \quad 3-114$$

$$\delta = 1 + 0,6 \cdot \frac{x}{L_e} \quad 3-115$$

whereas described in *EC8-1 4.3.2 and 4.3.3.2.4*, e_{ai} is the accidental eccentricity of storey mass, L_i is the floor-dimension perpendicular to the direction of seismic action, x is the distance of the elements and L_e is the distance between the two outermost lateral load resisting elements.

3.3.7 PRIMARY AND SECONDARY ELEMENTS

Constructions are based on two type of load carrying elements, primary and secondary. In terms of earthquake, primary seismic elements, are those contributing to the seismic resistance and the structures shall rely on them for their earthquake resistance. As far as the role of secondary elements, in the calculation of building's response, their strength and stiffness are neglected and ability to support gravity loads under the maximum deformations due to the seismic design situation is their main purpose.

EC8-1 4.2.2 requires that strength and stiffens of these elements shall be neglected and that the total contribution of them to lateral stiffness not exceed 15% of all primary seismic elements. (EC8 2014; Elghazouli 2009)

3.4 HYBRID BUILDING

3.4.1 INTRODUCTION

Hybrid or, as the Eurocode defines them composite, buildings, combines the benefits of different materials and their properties. As shown in [Figure 3-30](#), this is with respect to achieving good performance and overcoming the limitation each material type has.

Most of the structures around the world have a combination of steel and concrete because of the performance of these materials. However, due to the urgent need for building with respect to global environmental issues, timber has also taking a more leading role in this area. Hybrid materials are integrated in two levels as described here(Khorasani 2011):

- Component level: Hybrid beams and columns and bracings, hybrid posttension connection and hybrid slabs and walls
- System level: Vertically mixed system with hybrid bracings, steel frames and timber slabs and hybrid frames.

Approximate Material Properties for Steel, Wood and Concrete						
Material	Yield Strength (MPa)	Density (kg/m ³)	Poisson Ratio	Modulus Elasticity (MPa)	Compressive Strength (MPa)	Tensile Strength (MPa)
Steel	350	7800	0.3-0.31	200000	400-1000	400-1000
Concrete	N/A	2300	0.20-0.21	20000	20-40	2.0-5.0
Structural Timber	N/A	400-600		8000-11000	Parallel 30 Perpendicular 8	Parallel 6 Perpendicular 1

Material	Density (kg/m ³)	Strength (MPa)	Strength/Density (10 ⁻³ MPa.m ³ /kg)
Structural Steel	7800	400-1000	50-130
Aluminium	2700	100-300	40-110
Concrete,compression	2300	30-120	13-50
Clear softwood, tension	400-600	40-200	100-300
Clear softwood, compression	400-600	30-90	70-150
Structural timber, tension	400-600	15-40	30-80

Figure 3-30 Material properties for steel, concrete and timber (Khorasani 2011).

3.4.2 STEEL-CONCRETE

Choosing materials and structural systems that can perform satisfactorily are at the core of a new construction project. Steel and concrete have several advantages in term of stiffness, strength and energy dissipation. These materials when combined produces a fully composite building that can overcome the disadvantages of a homogenous concrete or steel structure. This is why steel-concrete structures, as schematically

shown in Figure 3-31, are the first choice construction materials for mid and high-rise buildings. However, requirements such as having minimum connection stiffness and strength to satisfy the seismic loads and parameters can restrict amount of levels in the building, and should be considered in design process since they can influence the seismic behavior of structure (Wang et al. 2013).

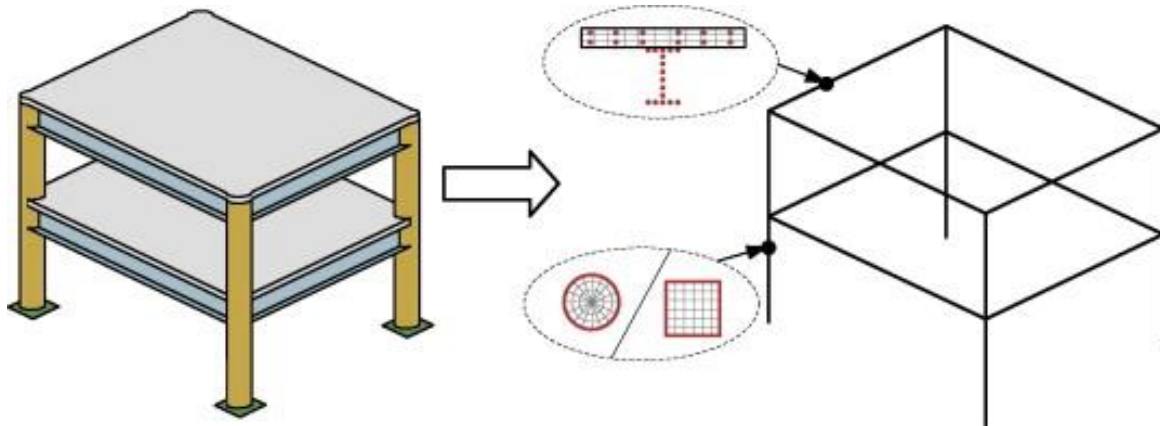


Figure 3-31 Steel-concrete composite beam-column model (Wang et al. 2013).

3.4.3 STEEL-TIMBER

Hybrid timber-steel construction is the combination of prefabricated timber elements such as CLT floors and steel or glued laminated columns and beams. Steel as an isotropic and timber as an orthotropic materials introduce various advantages, challenges and limitations. The most obvious difference is in properties such as young's modulus. Steel has the same value in any directions, while timber with its three, radial, longitudinal and tangential directions has different value for each direction along the object. Timber has its highest value of stress reached when compression is applied parallel to grain of the wood. Differing properties and the effect of temperature and humidity are some of the limitations. Although these materials seem far removed from each other, if used correctly, the benefits of a steel-timber structure include the loadbearing, strength, and lightness of timber plus the high specific strength, ductility and rigidity of steel. This can be very useful in an earthquake scenario (since forces in an earthquake are proportional to the weight).

One aspect of using timber and steel is with regards to the environmental aspect of a project, but there are also performance requirements (Fujita et al. 2014) for a building system of steel-timber that needs to be fulfilled. These are as follows:

- Safety performance (high load-bearing capacity)
- Functionality (securing effective space)

- Environmental friendliness (able to be recycled)
- Design characteristics (balance between size and visuality)
- Processability (easy to facilitate)
- Constructability (easy to assemble)
- Economic performance (based on previous parts)

3.4.4 EUROCODE 5

Eurocode is based on ultimate limit state, which defines what limit state structure shall not exceed. This state is further classified as ULS – ultimate state and SLS – serviceability limit state, which in case of timber have its design calculation done in accordance to *NS-EN 1990* and *EC5 (NS-EN 1995-1-1,-1-2 and 2)*. There are also only a few national applications like DIN EN 1995-1-1/NA (2010) and ÖNORM B 1995-1-1 (2014) for EC5. Guidelines and design regulations for timber in Norway, in addition to EC5, are mainly based on design guides from SINTEF Building Research Center and “*LIMTREBOKA*” published by Norwegian Glued laminated Timber Committee. These documents provide sufficient guidance which engineers can base their calculations on.

Following the Eurocode design concept requires that design values, e.g. the *partial safety factor* (see [Figure 3-21](#)) and *modification factor* are determined. In the remaining pages of this section we look at proposed values for CLT and GLT.

Meanwhile timber is quite different in term of being hygroscopic and orthotropic, and has requirements based on these properties in addition to the general set of rules, additional conditions should be satisfied in design of timber structures (Bell et al. 2015). These are as followed:

- Moisture variations – Service class ([Figure 3-34](#))
- Load duration – Load-duration classes. ([Figure 3-33](#))
- Modification factor
- Variation in flexural and tensile strength
- Different properties perpendicular or parallel to the grains

Timber is, relative to its weight, one of the strongest building material in the world, but has lower capacity over time. *EC 5* introduced five load-duration classes that should be considered in design. The influence of load-duration classes are based on modifications factor k_{mod} , which is a reduction factor for timber’s characteristic’s yield

strength. k_{mod} values for different type of timber is given in *EC5 Table 3.1* and *Figure 3-32*. For timber structures with different k_{mod} values equation 3-116 is introduced.

$$k_{mod} = \sqrt{k_{mod,1} \cdot k_{mod,2}} \quad 3-116$$

Material	Standard	Service class	Load-duration class				
			Permanent action	Long term action	Medium term action	Short term action	Instantaneous action
Solid timber	EN 14081-1	1	0,60	0,70	0,80	0,90	1,10
		2	0,60	0,70	0,80	0,90	1,10
		3	0,50	0,55	0,65	0,70	0,90
Glued laminated timber	EN 14080	1	0,60	0,70	0,80	0,90	1,10
		2	0,60	0,70	0,80	0,90	1,10
		3	0,50	0,55	0,65	0,70	0,90
LVL	EN 14374, EN 14279	1	0,60	0,70	0,80	0,90	1,10
		2	0,60	0,70	0,80	0,90	1,10
		3	0,50	0,55	0,65	0,70	0,90

Figure 3-32 Values of k_{mod} (EC5 1994).

Design value in ULS is calculated based on equation 3-117, where k_h , a height factor, is calculated based on the type of timber (Solid timber, equation 3-118 and Glued laminated timber, equation 3-119), $f_{m,k}$ is based on strength classes (GL28, 30c, etc.), γ_M is partial factor for given by *EC5 Table NA.2.3* and *Figure 3-21*.

$$f_{m,d} = k_{mod} k_h \frac{f_{m,k}}{\gamma_M} \quad 3-117$$

$$k_h = \min \left\{ \left(\frac{150}{h} \right)^{0,2} \right. \\ \left. 1,3 \right. \quad 3-118$$

$$k_h = \min \left\{ \left(\frac{600}{h} \right)^{0,1} \right. \\ \left. 1,1 \right. \quad 3-119$$

Design value in SLS, where the timber structure should have sufficient stiffness to avoid vibration and deformation that can result in discomfort, are calculated based a factor that takes the creep effect into account. Creep is determined by using k_{def} factors given in *EC5 Table 3.2* (showed in *Figure 3-34*).

For timber structures with different k_{def} values equation 3-120 is introduced.

$$k_{def} = 2 \sqrt{k_{def,1} \cdot k_{def,2}} \quad 3-120$$

Load-duration classes	Order of accumulated duration of characteristic load	Example of loading
Permanent	More than 10 years	Self-weight (dead load)
Long-term	6 months – 10 years	Storage loading (including in lofts), water tanks
Medium-term	1 week – 6 months	Imposed floor loading
Short-term	Less than one week	Snow, maintenance or man loading on roofs, residual structure after accidental event
Instantaneous	Immediate	Wind, impact loading, explosion

Figure 3-33 Load-duration classes (EC5 1994).

Service class	Definitions	Typical moisture content (m.c.)	Type of construction
1	Moisture content (m.c.) resulting from 20°C and Relative Humidity (RH) of surrounding air only exceeding 65% for a few weeks per year.	<ul style="list-style-type: none"> • Timber ≤ 12%. • Panels ≤ 8% 	Warm roofs, intermediate floors, timber frame walls (internal and party walls).
2	Moisture content (m.c.) resulting from 20°C and Relative Humidity (RH) of surrounding air only exceeding 85% for a few weeks per year.	<ul style="list-style-type: none"> • Timber ≤ 20%. • Panels ≤ 15% 	Cold roofs, ground floors, timber frame walls (external walls), external uses where member is protected from direct wetting. It is worth noting that this service class is the usual and safe choice for the UK unless you can guarantee that Service Class 1 is applicable during the life of the structure.
3	Conditions leading to higher moisture content than 1 and 2 above.	<ul style="list-style-type: none"> • Timber > 20%. • Panels > 15% 	External uses, fully exposed, outdoor structures or situations with constant high humidity and moisture content environment.

Figure 3-34 Service classes (EC5 1994).

Material	Standard	Service class		
		1	2	3
Solid timber	EN 14081-1	0,60	0,80	2,00
Glued Laminated timber	EN 14080	0,60	0,80	2,00
LVL	EN 14374, EN 14279	0,60	0,80	2,00
Plywood	EN 636			
	Part 1	0,80	–	–
	Part 2	0,80	1,00	–
	Part 3	0,80	1,00	2,50

Figure 3-35 Values of k_{def} (EC5 1994).

3.4.5 CROSS LAMINATED TIMBER (CLT)

CLT panels, as a part of mass timber family also known as Cross-laminated timber, are wood panels made from several layers of lamella jointed with glue, timber dowels, fasteners and/or nails. CLT, as an engineered timber product, has a large range of uses e.g. panels, walls, rooftops and balconies with many advantages. Significant improvements have been made in dimensional stability and an increased in- and out-of-plane strength and stiffness in both directions. CLT panels as illustrated in Figure 3-36, are put together in such a way that they allow the possibility of spanning in two direction without any additional structural framing supporting it, and can be produced with a length up to 12m, a width up to 3m and thickness up to 240mm (Byggforskserien 2001). In terms of strength and stiffness, the major axis (long direction) is stronger, stiffer and minor axis (short direction) has less strength and stiffness.

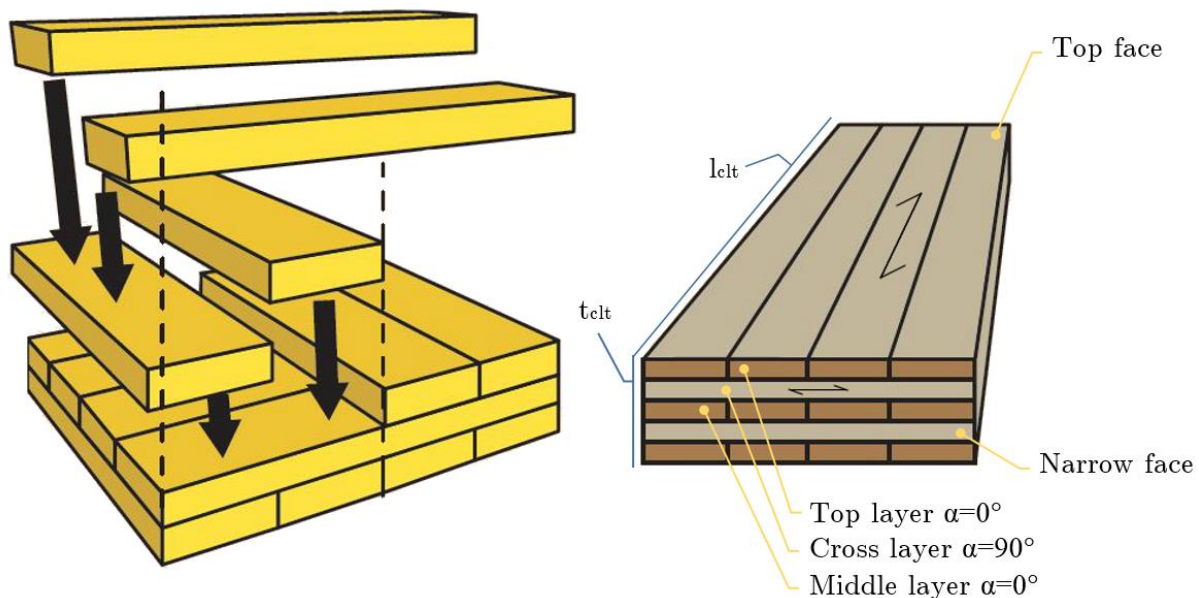


Figure 3-36 CLT element (BCA.GOV.SG 2017).

CLT is a technology that has been around for over 50 years, starting with initial development in Austria and Germany. Manufacturing and usage of massive timber in Norway first started in 1970s (Byggforskserien 2001) and mainly for wooden bridges, but with time and increased experience of building with this material, house developers, engineers and architectures started seeing the benefits as it can easily replace the old method of building with heavy timber elements. CLT is still a new material in Norway with no major domestic production. These types of panels are added as an additional part of a larger timber project that involves glue laminated timber and/or other materials.

	Class	C14	C16	C18	C20	C22	C24	C27	C30	C35	C40	C45	C50
Strength properties in N/mm²													
Bending	$f_{m,k}$	14	16	18	20	22	24	27	30	35	40	45	50
Tension parallel	$f_{t,0,k}$	7,2	8,5	10	11,5	13	14,5	16,5	19	22,5	26	30	33,5
Tension perpendicular	$f_{t,90,k}$	0,4	0,4	0,4	0,4	0,4	0,4	0,4	0,4	0,4	0,4	0,4	0,4
Compression parallel	$f_{c,0,k}$	16	17	18	19	20	21	22	24	25	27	29	30
Compression perpendicular	$f_{c,90,k}$	2,0	2,2	2,2	2,3	2,4	2,5	2,5	2,7	2,7	2,8	2,9	3,0
Shear	$f_{v,k}$	3,0	3,2	3,4	3,6	3,8	4,0	4,0	4,0	4,0	4,0	4,0	4,0
Stiffness properties in kN/mm²													
Mean modulus of elasticity parallel bending	$E_{m,0,mean}$	7,0	8,0	9,0	9,5	10,0	11,0	11,5	12,0	13,0	14,0	15,0	16,0
5 percentile modulus of elasticity parallel bending	$E_{m,0,k}$	4,7	5,4	6,0	6,4	6,7	7,4	7,7	8,0	8,7	9,4	10,1	10,7
Mean modulus of elasticity perpendicular	$E_{m,90,mean}$	0,23	0,27	0,30	0,32	0,33	0,37	0,38	0,40	0,43	0,47	0,50	0,53
Mean shear modulus	G_{mean}	0,44	0,50	0,56	0,59	0,63	0,69	0,72	0,75	0,81	0,88	0,94	1,00
Density in kg/m³													
5 percentile density	ρ_k	290	310	320	330	340	350	360	380	390	400	410	430
Mean density	ρ_{mean}	350	370	380	400	410	420	430	460	470	480	490	520

Figure 3-37 Strength classes for softwood (NS-EN338 2016)

But to ensure that the consistency of this material is kept, different standards have been developed by experts to help Figure 3-37 shows the strength classes used for CLT panels based on edgewise bending tests. NS-EN 388 gives a complete list of common used strength classes in Europe for both hardwood and softwood species. Strength class C24 is the recommended value for the central lamella, and for outer lamella is C14 is sufficient (Byggforskserien 2001).

There are several methods of analysis that are valid in design of CLT elements, such as the Modified Gamma Theory, the Shear Analogy, the Timoshenko Theory and Finite Element Analysis. Each of these method are to be used based on the configuration of the timber structure (StoraEnso 2016). For example if the design of CLT elements that are glued together (rigid connection) is considered, then there is no flexibility in the connection itself, and the Timoshenko method can be considered. Or if CLT elements are nailed together, taking into account the shear flexibility from the rolling shear in the cross layers and the flexibility of connections results in Timoshenko theory no longer be accurate. Characteristics of CLT in the design process are generally restricted to a homogenous layup. In addition, classification of elements exposed to loads in-plane and out-of-plane in different limit states has a significant impact in CLT design. These are briefly described here (Brandner et al. 2016):

1. ULS design of CLT elements

a. Loads out-of-plane

- i. Mandatory to consider the influence of shear of the transverse layers because of high shear flexibility.
- ii. Layer orientation and parameters of each material shall be taken into account when calculating stresses and stiffness.

- iii. The influence of layers with $\alpha = 90^\circ$ is insignificant because of the high ratio $E_0/E_{90} \approx 30$.
- iv. Normal stress ($\sigma_{max,d}$) in span direction $\alpha = 0^\circ$, shear stress (τ_d) in neutral axis and compression perpendicular to grain ($k_{c,90,CLT}$) must be verified.

b. Loads in-plane

- i. Tension, compression, bending and shear are to be considered in terms of calculating stresses in CLT.
- ii. Lateral buckling of members stressed in-plane has to be measured.
- iii. Three different failure mechanisms have to be taken into account for CLT:
 1. Gross-shear failure in all layer by longitudinal shear failures
 2. Net-shear (transverse) failure by exceedance of the shear resistance in-plane in layers oriented in weak direction.
 3. Torsional failure in the gluing-interface between orthogonal layers.

2. SLS design of CLT elements out-of-plane

a. Deformations

- i. Shear stiffness S_{CLT} , loaded out of plane, shall be calculated based on the following expression:

$S_{CLT} = \kappa \sum (G_{lay,i}, w_{lay,i}, t_{lay,i})$, with $G_{lay,i}$ as shear modulus, and $w_{lay,i}, t_{lay,i}$ as width and thickness for the i th layer. κ is the shear correction coefficient factor with value of $\kappa = 0,83$ for a unidirectional rectangular cross section.

$G_{0,lay,i}$ is defined for $\alpha = 0^\circ$ and $G_{r,lay,i}$ for $\alpha = 90^\circ$

- ii. Long-term effect due to creep are to be taken into account by deformation factor k_{def} (see equation 3-120).

b. Vibrations

- i. Design of CLT panels with spans over 4m are highly to be governed by vibration criteria.

- ii. Influence of support conditions and upper loads transmitted through walls may have impact on amount of vibration.
- iii. Verification can be neglected if isolation introduced.

It is suggested that, whether the design is for floor or wall, preventing any load situations where tension is applied perpendicular to the timber grain, is more suitable for this type of material. Since both the timber and binding material show poor resistance in this situation (Shrestha et al. 2014).

3.4.6 GLUED LAMINATED TIMBER (GLT)

Glued laminated timber or glulam, is a structural element with great stiffness and strength compared to for instance solid timber, and has range of applications from beams with large span to columns for high open areas. This type of structural element is very suitable as an additional part for applications that use concrete or steel. Glulam grades are performance-based. In Norway, glulam is produced according to *NS-EN 386* with the common strength class of GL32c, and the recommended partial factor γ_M of 1,15 for material properties and resistances (Byggforskserien 2011).

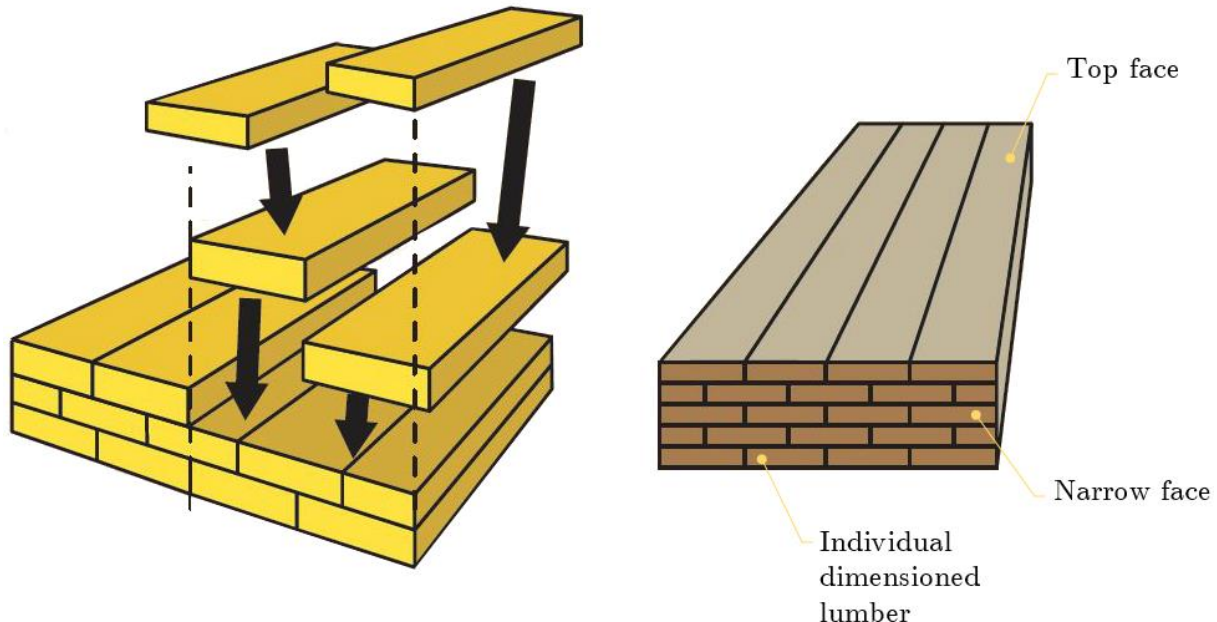


Figure 3-38 Glued laminated timber (BCA.GOV.SG 2017).

The stiffness of GLT structures is not only defined based on the geometry of elements, but on moisture content, load-duration and temperature. In a design process it is important to control the capacity of beams and columns in term of deflection and shear.

Components of deflection shown in Figure 3-39 results from a combination of actions, where w_{inst} is the instantaneous value of deformation and should be calculated using a value of slip moduli per fastener per shear plane (K_{ser}), modulus of elasticity (E_{mean}) and modulus of rigidity (shear modulus G_{mean}) for a combination of loads. w_{fin} is the final deformation based on calculations according to quasi-permanent combination. w_{fin} for a structure with same type of elements and is calculated in accordance to equation 3-121.

$$\begin{aligned}
 w_{fin} &= w_{fin,G} + w_{fin,Q1} + w_{fin,Qi} \\
 w_{fin,G} &= w_{inst,G}(1 + k_{def}) \\
 w_{fin,Q1} &= w_{inst,Q1}(1 + \psi_{2,1}k_{def}) \\
 w_{fin,Qi} &= w_{inst,Qi}(1 + \psi_{2,i}k_{def})
 \end{aligned}
 \tag{3-121}$$

where ψ_2 is given by *NS-EN 1990*, k_{def} from Figure 3-35. EC5 provides permissible deflection values for deflection of beams, as shown in Figure 3-40, and summarized in an overall deflection given by equation 3-122, where $w_{creep} = k_{def} w_{inst}$ and w_c the upward deflection.

$$w_{net,fin} = w_{inst} + w_{creep} - w_c = w_{fin} - w_c
 \tag{3-122}$$

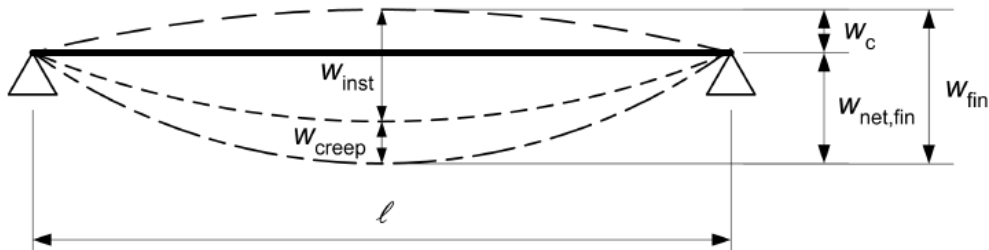


Figure 3-39 Deflection components (EC5 1994).

Eurocode 5

	w_{inst}	$w_{net,fin}$	w_{fin}
Beam Simply Supported at two ends	$l/300$ to $l/500$	$l/250$ to $l/350$	$l/150$ to $l/300$
Cantilever beam	$l/150$ to $l/250$	$l/125$ to $l/175$	$l/75$ to $l/150$

Experience based

	w_{inst}	$w_{net,fin}$	w_{fin}
Roof beams	$l/300$ to $l/375$	$l/160$ to $l/200$	$l/250$ to $l/300$
Floor beams	$l/400$ to $l/600$	$l/200$ to $l/250$	$l/300$

Figure 3-40 Example of possible beam deflection (EC5 1994) and (Bell et al. 2015).

Shear deformation is highly dependent on the relation between height and length of the beam. GLT has usually greater height ratio in proportion to length, and therefore lower shear modulus than elasticity modulus. Shear deformation, can be neglected if the relation between length of the beam and height of the cross-section is $\frac{L}{h} > 10$ (Bell et al. 2015).

In terms of columns, subjected to axial compression, following criteria from EC5 for verification of failure condition, that takes second order effect in consideration by introducing buckling factor k_c , should be satisfied:

$$\frac{\sigma_{c,0,d}}{k_c f_{c,d}} \leq 1 \quad 3-123$$

where k_c is defined with relation to relative slenderness λ_{rel} given by equation 3-124 and found as the minimum value of equation 3-125, A being the total cross sectional area and $f_{c,d}$ the design compressive strength.

$$\lambda_{rel} = \sqrt{\frac{P_c}{P_{cr}}} = \sqrt{\frac{f_{c,0,k} A}{\pi^2 \frac{E_{0,05} I}{(\beta L)^2}}} = \frac{\lambda}{\pi} \sqrt{\frac{f_{c,0,k}}{E_{0,05}}} \quad 3-124$$

where $f_{c,0,k}$ and $E_{0,05}$ are characteristics value that are different for each timber strength class. λ is determined by $\lambda = \frac{l_{ef}}{i}$.

$$\left. \begin{aligned} k_{c,y} &= \frac{1}{k_y + \sqrt{k_y^2 - \lambda_{rel,y}^2}} \\ k_{c,z} &= \frac{1}{k_z + \sqrt{k_z^2 - \lambda_{rel,z}^2}} \end{aligned} \right\} \min \quad 3-125$$

with k_y and k_z being

$$k_y = 0,5(1 + \beta_c(\lambda_{rel,y} - 0,3) + \lambda_{rel,y}^2)$$

$$k_z = 0,5(1 + \beta_c(\lambda_{rel,z} - 0,3) + \lambda_{rel,z}^2)$$

and $\beta_c = 0,2$ for solid timber and $\beta_c = 0,1$ for glue laminated/LVL. Value of λ_{rel} is not recommended to exceed 2,0 (Bell et al. 2015).

3.4.7 TIMBER BUILDINGS IN NORWAY

In the recent years, building smart and environmentally friendly constructions has been on the agenda with housing developers mainly due to the benefits of using a material that gives less carbon footprint, better internal climate, in some cases cheaper production (when made and put together as modules). It is also beneficial for the developer when customer relations are considered. Building an Eco-lighthouse also known as. *Miljøfyrtårn* construction shows that you consider the environmental impact of what you construct and in doing so show social responsibility.

Design and developing high timber buildings, which is for a key factor in sustainable and future-oriented development, has been greatly welcomed in Norway. As of April 2017, the world's highest timber building standing at eighty-meters high is under construction in Brumunddal, Ringsaker municipality. This building will go even further than "Treet", an existing thirty-meter high building in Bergen, Hordaland, in surmounting the structural and design challenges high timber buildings face.

It worth mentioning that student housing project, "Palisaden" in Ås, was the first of its kind in Norway back in 2013 and was used as a pilot project for future buildings (Ås-Kommune 2013). The success story of Palisaden has been in its impact on student housing projects, and through changing attitudes with an industry that has been characterized by reluctance in conversion and development. It is assumed that by 2017, almost 4100 student housing units will have been constructed using CLT elements.

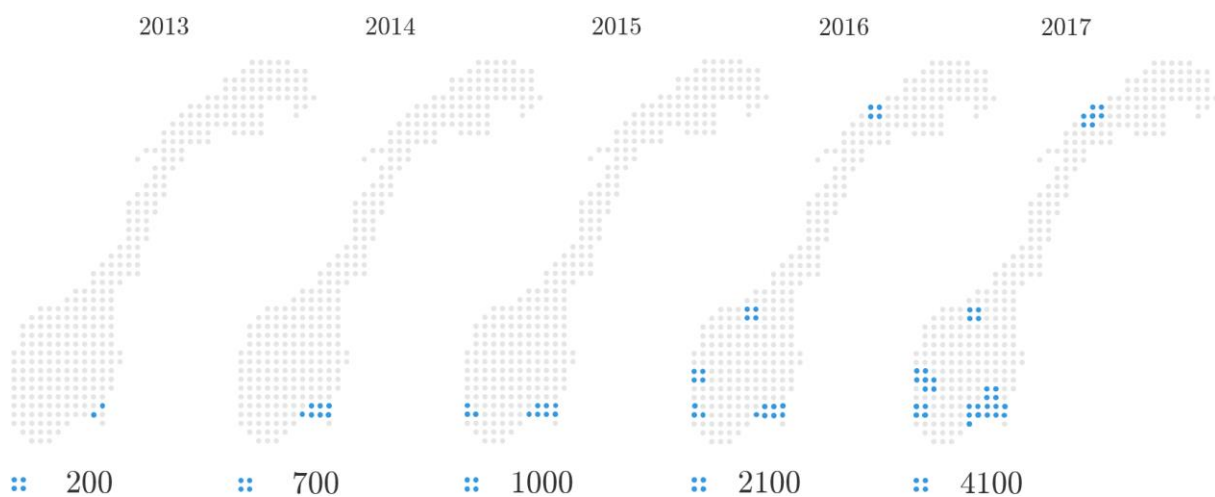


Figure 3-41 Increase in number of student housing units in Norway. Data from [Arkitektur-n.no](http://arkitektur-n.no)

Elements including columns, beams, prefabricated roof bracings and lattice beams with punched metal plate fasteners are some of the loadbearing structures that are traditionally used in timber buildings. In models of this thesis it is mainly CLT floors

and GLT beams and columns that have being analyzed. These are some of the most common types of prefabricated loadbearing elements with less degrees of freedom (Koyluoglu et al.).

CHAPTER 4 METHOD

4.1 ANALYSING METHODS

4.1.1 INTRODUCTION

Good design requires precise modelling of both the global model and local elements. EC8 provides different approaches of analyzing models and categorized them into linear-elastic and non-linear method. In order to perform the earthquake analysis of a building, one can chose between these approaches based on the level of detailing, difficulty of model and the need and time the engineer has. Methods are as followed:

- Linear-elastic methods
 - Lateral force method
 - Modal reposes spectrum analysis
- Non-linear methods
 - Non-linear time history analysis
 - Non-linear static pushover analysis

EC8 requires that in term of choosing an appropriate analyzing method, criteria showed in [Figure 3-25](#) and [4.2.3.1-Table 4.1](#) is fulfilled.

4.1.2 LATERAL FORCE METHOD

In case of investigating the structure using lateral force method, regularity in elevation given by *EC8-1 4.2.3.3*, and the period of the fundamental mode criteria in both directions, as mentioned in equation [4-1](#), needs to be satisfied. This method can be used for structures where the response in main directions is not under such influence from higher mode shapes than the first one.

$$T_1 \leq \begin{cases} 4 \cdot T_c \\ 2,0 \text{ seconds} \end{cases} \quad 4-1$$

The fundamental period can be calculated in several ways. Empirical formula of [4-2](#) for buildings up to 40 m based on *EC8-1 4.3.3.2.2(3)* is the readiliest approach. Simplified method given in equation [4-3](#), based on lateral elastic displacement of the top of the building, due to the gravity load in horizontal direction. The iterative Rayleigh method which assumes that the system is conservative, as mentioned by equation [4-4](#) , where n is amount of storeys, m_i is storey mass and f_i the horizontal forces. C_t value is different based on the structural system (Steel = 0,085, Concrete = 0,075 and 0,05 for all other structures). And Dunkerley's equation which is based on a theoretical formula

to estimate base shear conservatively in equation 4-5, where ρ is building's total mass per volume of it, κ is shape factor ($\kappa = 1,5$ for a rectangular plate), G is shear modulus and $\bar{A}_e = 100 \frac{A_e}{A_b}$ with A_b being the area of building and A_e the total plate area as mentioned in equation 4-6.

$$T_1 = C_t \cdot H^{\frac{3}{4}} \quad 4-2$$

$$T_1 = 2\pi \sqrt{\frac{M}{K}} = 2\pi \sqrt{\frac{F_h}{g \cdot K}} = 2\pi \sqrt{\frac{d}{g}} \cong 2 \cdot \sqrt{d} \quad 4-3$$

$$T_1 = 2\pi \sqrt{\frac{\sum_{i=1}^n (m_i \cdot s_i^2)}{\sum_{i=1}^n (f_i \cdot s_i)}} \quad 4-4$$

$$T_1 = 40 \sqrt{\frac{\rho}{\kappa \cdot G}} \frac{1}{\sqrt{\bar{A}_e}} H \quad 4-5$$

$$A_e = \sum_i \left(\frac{H}{H_i}\right)^2 \frac{A_i}{[1 + 0,83 \left(\frac{H_i}{D_i}\right)^2]} \quad 4-6$$

Equation 4-6 applies to all plates in a given orthogonal direction with H being buildings total height, H_i plate's height from the ground level, A_i the area of plate and D_i the dimension on the direction (Chopra & Goel 2000).

By defining the fundamental period and finding the design spectrum, seismic base shear for each horizontal direction at foundation level/on top of a rigid basement can be determined by expression 4-7

$$F_b = S_d(T_1) \cdot m \cdot \lambda \quad 4-7$$

where m is the mass above the basement level, $T_1 \leq 2 \cdot T_c$ and factor λ is set to 0,85 for buildings over to storeys. Shear force calculated in equation 4-7 is then distributed throughout the building in each direction as a horizontal force. *EC8-1 4.3.3.2.3* presents calculating the total horizontal force at each level by two equations based on the displacements s_i of masses in the fundamental mode shape (Equation 4-8), and height z_i of the masses above the level of foundation or top of a rigid basement (Equation 4-9). Distribution of the horizontal forces in a structure is illustrated in Figure 4-1. If the stiffness of storeys are the same, than a linear approach like equation 4-8 is sufficient,

but if the stiffness varies, then calculation based on displacement gives a more accurate result.

$$F_i = F_b \frac{s_i \cdot m_i}{\sum_{j=n} s_j \cdot m_j} \tag{4-8}$$

$$F_i = F_b \frac{z_i \cdot m_i}{\sum_{j=n} z_j \cdot m_j} \tag{4-9}$$

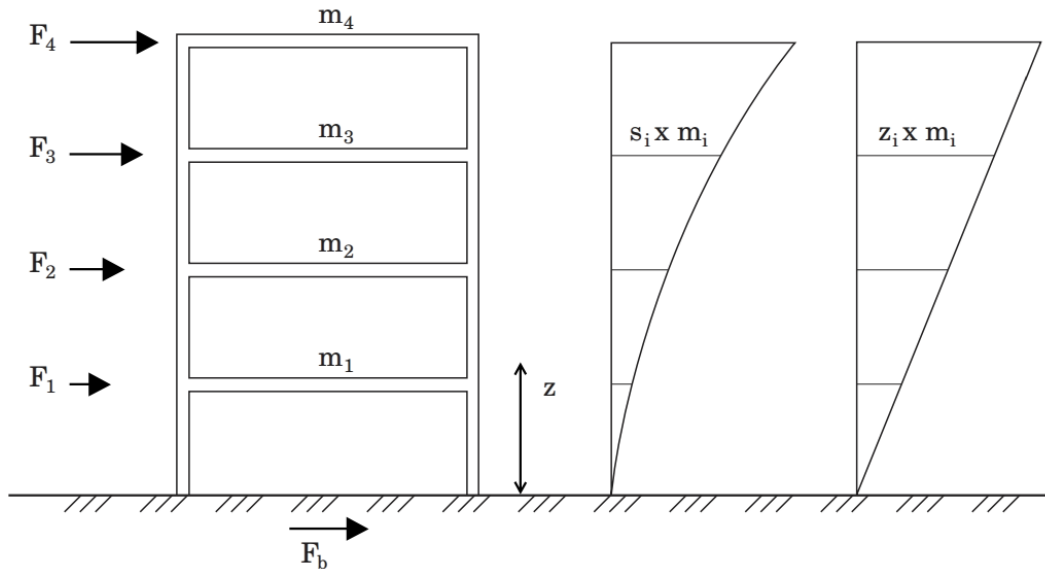


Figure 4-1 Distribution of horizontal force (Løset et al. 2011).

4.1.3 MODAL RESPONSE SPECTRUM

Modal response spectrum analysis, also known as RSA, is the reference method in Eurocode 8 and considered as a more accurate method than the lateral force method, since all modes and their masses are contributing to a global response of the structure. Irregularity of the structure in elevation, which results in increased number of mode shapes needed in terms of calculating seismic forces, as described in Figure 4-2, is why this method is used.

As EC8 requires, structure's total seismic mass $m = \sum M_i^{eff}$, as shown in Figure 4-2, and response from different independent mode shapes shall being taken into account. It also adds in 4.3.3.3.1(3) that there is a limit for how many modes and how much modal mass can be included in the calculation, when using a spatial model. Criteria are;

$$\sum M_i^{eff} > 0,9 \cdot m - \text{Sum of the effective modal mass shall be at least 90\%}$$

$M_i^{eff} > 0,05 \cdot m$ – Modes with more that 5% of the total mass can be included

If these criteria are not fulfilled, as it may be when tremendous amount of torsional effect is acting on the structures, then condition (1) and (2), as mentioned below, needs to be satisfied.

(1) $k \leq 3 \cdot \sqrt{n}$ and (2) $T_k \leq 0,20s$

where k is the amount of mode shapes considered, n is number of storeys and T_k is the vibration period of k . In terms of independency of modes (i and j) from each other, EC8-1 4.3.3.3.2(4.15) introduces following condition $T_j \leq 0,9 \cdot T_i$.

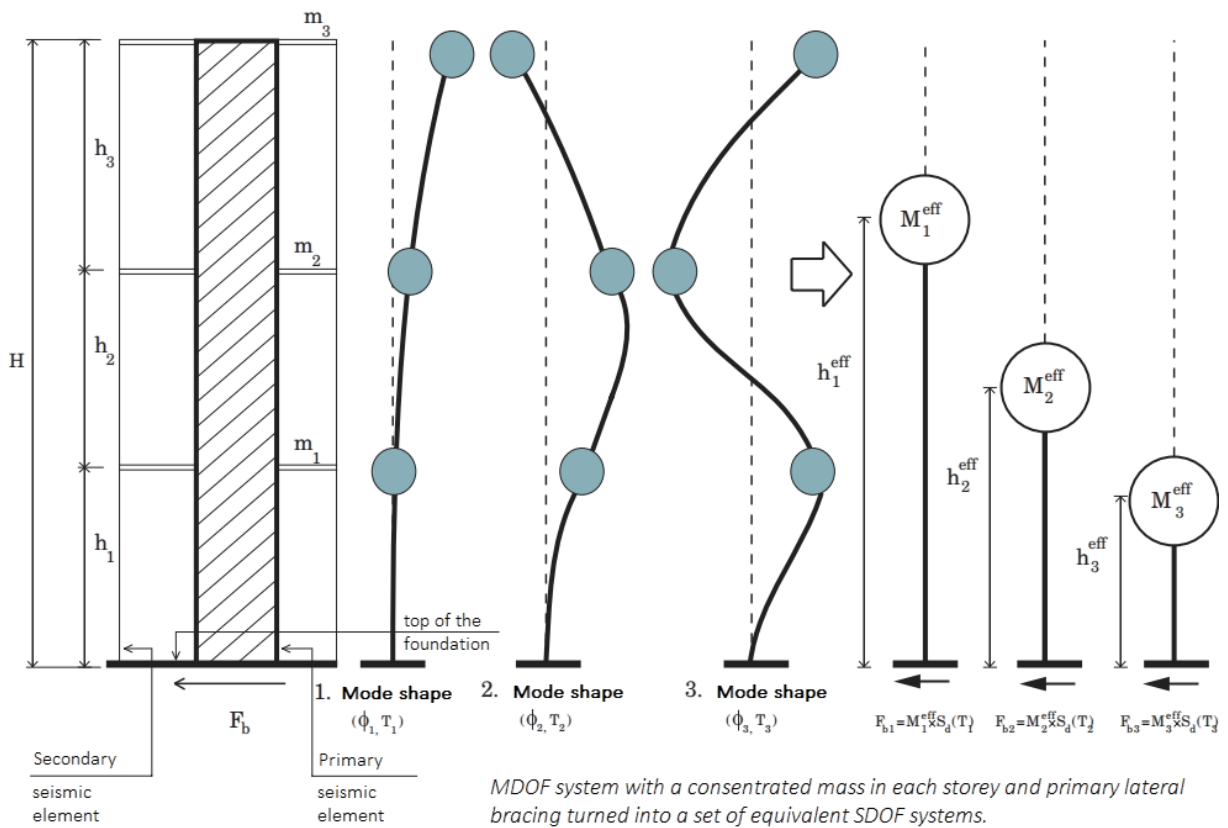


Figure 4-2 Modal response analysis described (Løset et al. 2011).
Translated by the author.

By fulfilling all the criteria mentioned, the maximum seismic action effect under consideration can be calculated using *Square root of Sum of Square* as known as SRSS method, and shown in expression below:

$$E_E = \sqrt{E_{Ex}^2 + E_{Ey}^2 + E_{Ez}^2}$$

Taking into account the maximum response from each mode shape can be very conservative, and sometimes criteria of EC8 cannot be met. Therefore by using

Complete Quadratic Combination (CQC), mentioned in *EC8-1 4.3.3.3.2(3)P*, combination of modal maxima can be more accurately found, as presented in the following expression:

$$E_E = \begin{cases} E_{Ex} + 0,3E_{Ey} + 0,3E_{Ez} \\ 0,3E_{Ex} + E_{Ey} + 0,3E_{Ez} \\ 0,3E_{Ex} + 0,3E_{Ey} + E_{Ez} \end{cases}$$

4.1.4 NONLINEAR ANALYSIS

Elastic analysis is usually used to design buildings for seismic resistance. But to determine the realistic behavior of structure beyond the elastic range in case of large earthquakes that most of the time results in inelastic deformations, nonlinear analysis are preferred. Advancements in today's technology and available test data provides necessary tools to perform this type of analysis.

Nonlinear analysis in structural earthquake engineering is applied in these occasions (Deierlein et al. 2010):

- To assess and design seismic retrofit solutions for existing buildings.
- In design of new buildings that do not conform to current building code requirements.
- To assess the performance of buildings for specific requirements.

CHAPTER 5 ANALYSIS

5.1 MODELLING

5.1.1 INTRODUCTION

Learning and using analyzing software has been a key parameter for engineers in terms of reducing time spent on heavy calculations. In recent years there has been significant progress in developing finite element software such as FEM-DESIGN developed by Strusoft, ROBOT by Autodesk and SAP2000 by Computers and Structures, Inc. The level of complexity, detailing and whether they can implement international design codes differs slightly. Choosing the correct tool is determined by the task's magnitude and the available resources. However EC8 requires that a proper software package is used in order to undertake the analysis described, even though the lateral force method can be calculated using software such as Excel or Mathcad. Software packages should be able to give a percentage of seismic mass for each mode shape, control effect of the seismic action in accordance to EC8 and present the seismic force on each storey in terms that can directly be used in design (Løset et al. 2011). Analysis in this thesis is based mainly on calculations made by FEM-DESIGN, one of the most used software packages in Norway. It satisfies the requirements of Eurocode and is fit to be used in the seismic calculation of structures in steel, concrete and timber. Although the timber part, like with most of the aforementioned software packages is not fully developed, it does produce results that can be used in design process.

5.1.2 PRESENTATION OF 3D MODELS

Four models with tree different materials are compared in this thesis. Models are based on a fictional office building first modeled by a thesis from 2010 (Øystad-Larsen 2010). This office is a four-storey building with an elevation shaft going from first to third floor. As the model in [Figure 5-1](#) shows, shaft is neglected in the calculation. Structural systems are as followed:

Model	Beam	Column	Floor panel	Bracing/Wall
#1	Steel	Steel	Concrete	Steel
#2	Steel	Steel	CLT	Steel
#3	GLT	GLT	CLT	Steel
#4	GLT	GLT	CLT	CLT

Table 7 Overview of models different configuration.

These models are fully presented both in plan and elevation in [APPENDIX B](#) and can be summed up with these key information:

- Total building height: 12 m, length: 24 m and width: 15,6 m
- Storey height of 3 m (including floor)
- S355 quality for steel
- Concrete quality of C30/37
- Timber floor is 7 layered CLT
- Non-structural dead load = 1 kN/m²
- Live load = 2 kN/m²
- Snow load = 0,56 kN/m²
- Location: **Bergen**

Since all of these models are different from each other, to be able to compare them, a main basic principle should be taken in consideration. In this case we optimize these models to have a ratio of utilization above 70% for their critical primary elements, and then change other elements of same kind, in regard to that. Also the deflection criteria of $L/250$ for the beams and $H/300$ for columns is added to the rang of criteria in the software. These optimizations are presented here:

Model #1 – STEEL-STEEL-CONCRETE-STEEL is optimized to have steel beams $HE - B 200$, columns $200 \times 200 \times 12.5$, concrete slab 200 mm with double layer reinforcement $\emptyset 16 C C 200$ and bracings $120 \times 120 \times 6,3$. Shrinkage 0,49 and Creep factor 2,58 for SLS and ULS is also added to this model based on the concrete type $B30$.

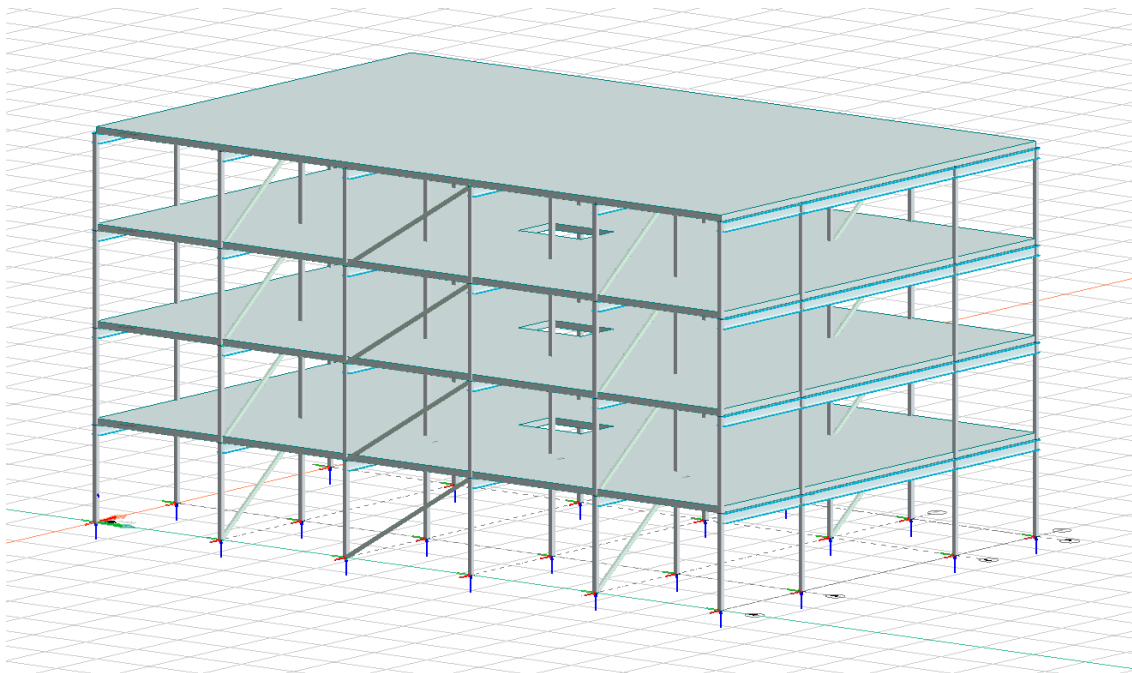


Figure 5-1 Model #1 as modeled in FEM-DESIGN version 16.

Model #2 – STEEL-STEEL-CLT-STEEL is optimized to have steel beams $HE - B 180$, columns $120 \times 120 \times 8$, CLT panel 240mm and bracings $80 \times 80 \times 6,3$.

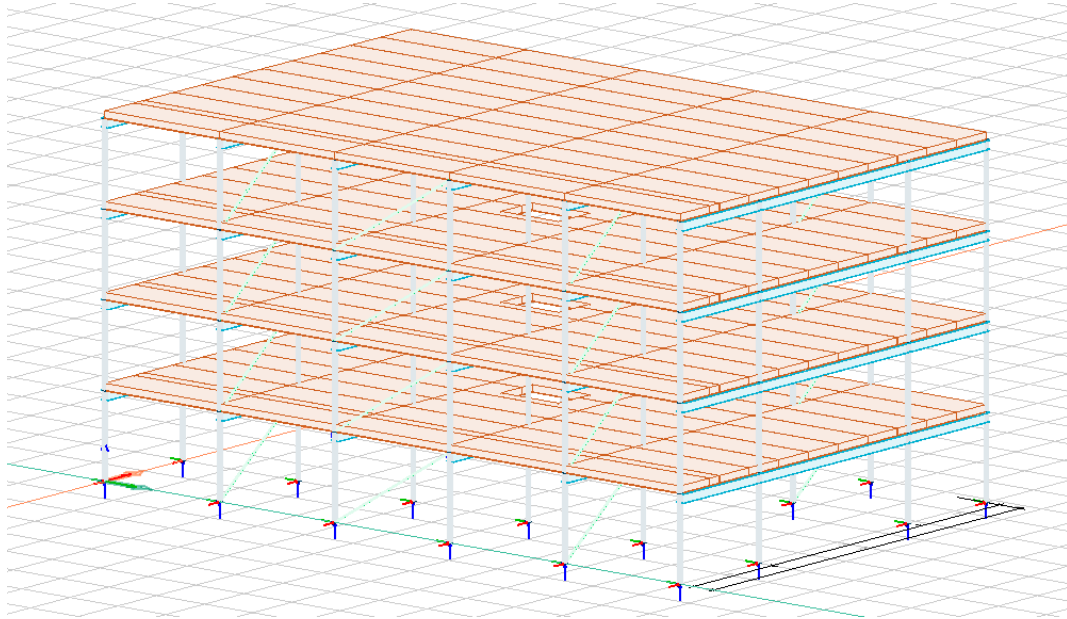


Figure 5-2 Model #2 as modeled in FEM-DESIGN version 16.

Model #3 – GLT-GLT-CLT-STEEL is optimized to have glulam beams 215×405 , glulam columns 215×225 , CLT panel 240mm with seven layer and steel bracings $80 \times 80 \times 6,3$. The same type of timber panel is kept in model #2 - #4 since loads given in these models are the same, and based on vibration criteria, 240mm fulfills the requirements. Material C24 is chosen as suggested in 3.4.5.

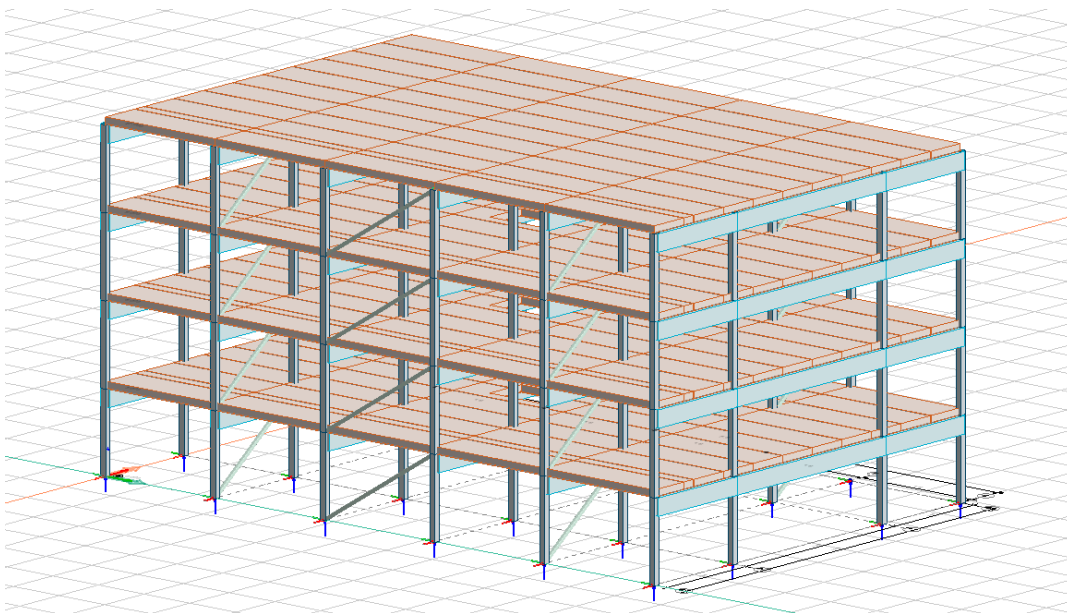


Figure 5-3 Model #3 as modeled in FEM-DESIGN version 16.

Model #4 – GLT-GLT-CLT-CLT is optimized to have glulam beam 215x405, glulam columns 215x225 and CLT panel (as floor and wall) 240mm with seven layer. This model is 100% timber and stands out from other models in terms of load bearing system.

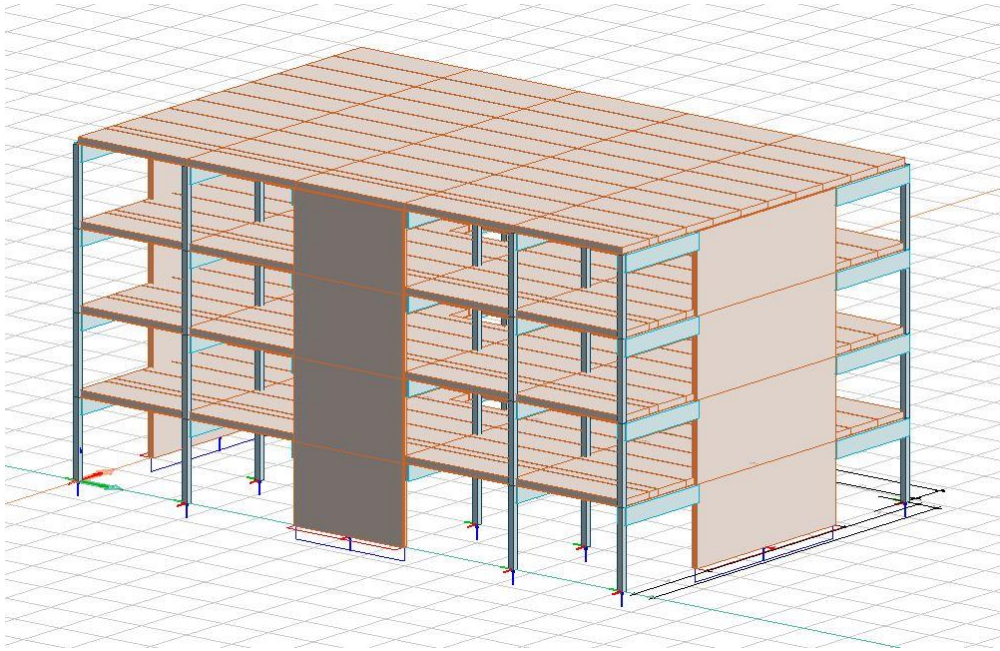


Figure 5-4 Model #4 as modeled in FEM-DESIGN version 16.

With regards to the modeling work completed in relation to this thesis, the CLT element was the most difficult to compose. This was due FEM-DESIGN's outdated values and the difficulty associated with adding new element procedures. By contacting the manufacture of CLT used in the software, Martinsson in Sweden, who provided Strusoft the previous values, I was able to update the timber library with the values presented in [APPENDIX E](#). Vibration has also been calculated in accordance to *EC5 7.3*. Criteria for vibration has been fulfilled in CLTdesigner calculation software. Reports are available in [APPENDIX D](#). Timoshenko method of analysis is used for calculating the CLT panel.

Office buildings are categorized under importance class II as *NS-EN 1998-1 Table NA.4(902)* indicates, which characterize it as a building with low consequences of collapse with importance factor $\gamma_1 = 1,0$, as listed in [Table 3](#). Reference peak ground acceleration $a_{gR} = 0,8 \cdot a_{g40Hz}$ is based on geographical position of the building. For seismic class I, II and III a return period of 475 years is used, which for Bergen gives $a_g = a_{gR} \cdot \gamma_1 = 0,8 \cdot 0,93 \frac{m}{s^2} \cdot 1,0 = 0,744 \frac{m}{s^2}$, with a correction factor of $k_{f,peak} = 0,8$. The chosen behavior factor q is 1,5 for structure with low ductility, since most of the new structures in Norway have design concept that put them in DCL category.

Ground conditions influence the amount of ground acceleration a structure is being designed for. For an office building in this thesis ground type A with the value presented in Table 1 is selected. Figure 5-5 illustrates the horizontal spectrum used in all four models.

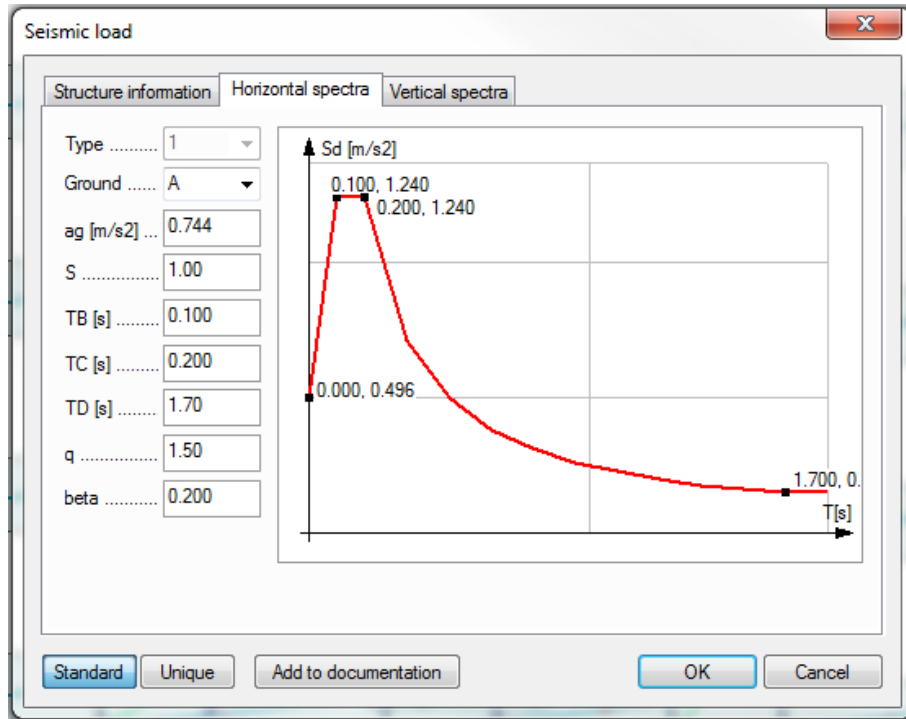


Figure 5-5 Horizontal spectrum created in FEM-DESIGN version 16.

5.2 ANALYTICAL ANALYSIS OF 3D MODEL

In this section we calculate the natural period T_n , mode shape ϕ , the effective modal mass and base shear of the **model #1** using modal analysis. Since the building is double symmetrical, modes will give displacement in either x- or y-axes. It is assumed that the slabs are rigid and vertical displacement is neglected.

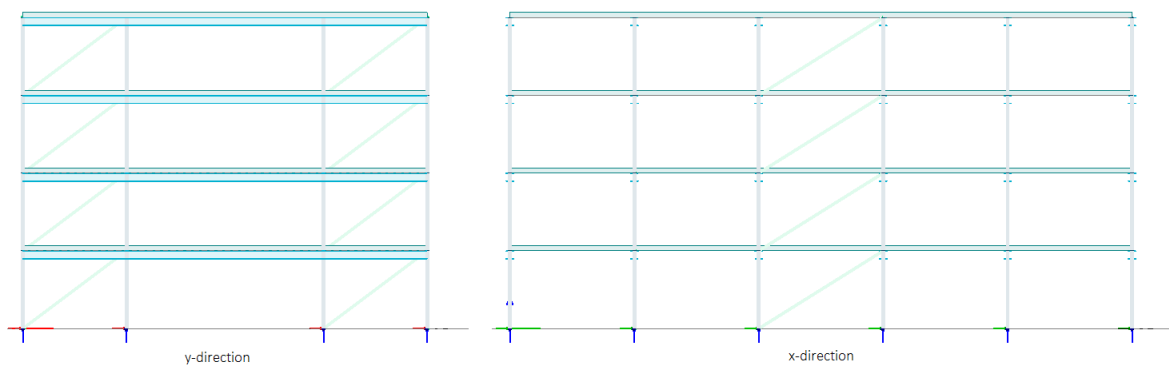


Figure 5-6 Model that hand calculation is based on in this section.

The mass matrix for the both x- and y-direction in the system is diagonal, since the mass is concentrated in the DOFs and is set-up as shown below.

$$m := \begin{bmatrix} m_4 & 0 & 0 & 0 \\ 0 & m_3 & 0 & 0 \\ 0 & 0 & m_2 & 0 \\ 0 & 0 & 0 & m_1 \end{bmatrix} \quad 5-1$$

The mass from each floor can be calculated based on the density of concrete $2.4 \cdot 10^3 \frac{kg}{m^3}$ (HiØF 2016) and the non-structural dead load ($1000 \frac{N}{m^2}$). This gives a concrete slab weight of:

$$m_{g,d} := \left(\frac{\rho_c}{g} \cdot t_c + \frac{Q_{nonstructure}}{g} \right) \cdot (5 \cdot L_1) \cdot (2 \cdot W_1 + W_2) = (229 \cdot 10^3) \text{ kg} \quad 5-2$$

Since the shaft area is not considered in the process of seismic design, it is considered negligible in further calculations. The moment of inertia and the dead load of bracings and columns are also neglected, which results in a diagonal mass matrix with a marginal error when the vertical components represent a small part of the structure's total mass.

The total mass of steel in each floor is then calculated based on the density of steel ($7850 \frac{kg}{m^3}$) and the area of each elements: *Column* $200 \times 200 \times 12,5 = 9208 mm^2$, *Beam HE – B 200* = $7808 mm^2$ and *Bracing/trusses* $120 \times 120 \times 6,3$, as shown in equation 5-3, where $H = 3000 \text{ mm}$, $L_1 = 4800 \text{ mm}$ and $W_1 = 4000 \text{ mm}$.

$$m_{g,s} := \rho_s \left((4 \sqrt{L_1^2 + H^2} + 8 \sqrt{W_1^2 + H^2}) \cdot A_{Truss} + 6 \cdot 4 \cdot H \cdot A_{RHS} + 6 \cdot L_2 \cdot A_{HEB} \right) \quad 5-3$$

$$m_{g,s} = (12.3 \cdot 10^3) \text{ kg}$$

Weight of the snow load ($560 \frac{N}{m^2}$) on 4th floor is

$$m_{p,4} := \frac{Q_{snow}}{g} (5 \cdot L_1) (2 \cdot W_1 + W_2) = (21.4 \cdot 10^3) \text{ kg} \quad 5-4$$

And live load on rest of the floors gives

$$m_{p,1} := \frac{Q_{liveload}}{g} (5 \cdot L_1) (2 \cdot W_1 + W_2) = (76.3 \cdot 10^3) \text{ kg} \quad 5-5$$

$$m_{p,2} := m_{p,1} \quad m_{p,3} := m_{p,1}$$

By combining equations 5-1 - 5-5, we can find the mass affiliated with each DOF;

$$m_1 := m_{g,d} + m_{g,s} + m_{p,1} = (318 \cdot 10^3) \text{ kg}$$

$$m_4 := m_{g,d} + \frac{1}{2} m_{g,s} + m_{p,4} = (257 \cdot 10^3) \text{ kg} \quad 5-6$$

$$m_2 := m_1 \quad m_3 := m_1$$

The mass matrix of equation 5-1 can then be rewritten as:

$$m := \begin{bmatrix} m_4 & 0 & 0 & 0 \\ 0 & m_3 & 0 & 0 \\ 0 & 0 & m_2 & 0 \\ 0 & 0 & 0 & m_1 \end{bmatrix} = \begin{bmatrix} 257 \cdot 10^3 & 0 & 0 & 0 \\ 0 & 318 \cdot 10^3 & 0 & 0 \\ 0 & 0 & 318 \cdot 10^3 & 0 \\ 0 & 0 & 0 & 318 \cdot 10^3 \end{bmatrix} \text{ kg} \quad 5-7$$

Now we look at the stiffness matrix in each direction, which is dependent on bracings in that direction. Stiffness of bracings are to be found using unit load method.

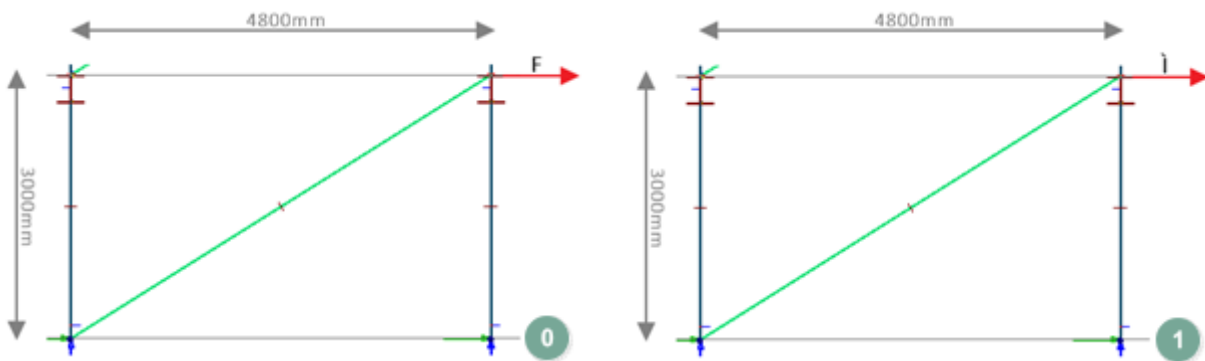


Figure 5-7 Bracing in x-direction.

Steel quality of both columns and bracings is S355, which gives an Elastic modulus of 210000 MPa. Length of column is 3000mm and bracing can be found by Pythagoras:

$$l_{truss} := \sqrt{H^2 + L_3^2} = 5000 \text{ mm} \quad 5-8$$

$$l_{column} := 3000 \text{ mm}$$

Axial forces in bracings are calculated based on equilibrium in each node. “1” represents the virtual load due to the system 1, illustrated in Figure 5-7, and “0” the real load.

$$S_{1.Truss} := \frac{1}{\cos\left(\text{atan}\left(\frac{H}{L_3}\right)\right)} = 1.25$$

$$S_{1.RHS} := -S_{1.Truss} \cdot \sin\left(\text{atan}\left(\frac{H}{L_3}\right)\right) = -0.75$$

5-9

$$S_{0.Truss} := \frac{1}{\cos\left(\text{atan}\left(\frac{H}{L_3}\right)\right)} = 1.25$$

$$S_{0.RHS} := -S_{1.Truss} \cdot \sin\left(\text{atan}\left(\frac{H}{L_3}\right)\right) = -0.75$$

The stiffness k_x for each bracing can be found by equation 5-11, where δ is founded according to section 3.3.6 and Figure 5-8, and calculated with factor 1,2. Factor 0,6, which EC8 represents, is for modal analysis in three dimensions. By doubling this factor we take into account any eccentricity of mass and stiffness between storeys that are neglected because of two dimensional analyzing method (Fardis 2005), as shown in equation 5-10.

$$\delta := 1 + 1.2 \frac{x}{L_e} = 1.6$$

5-10

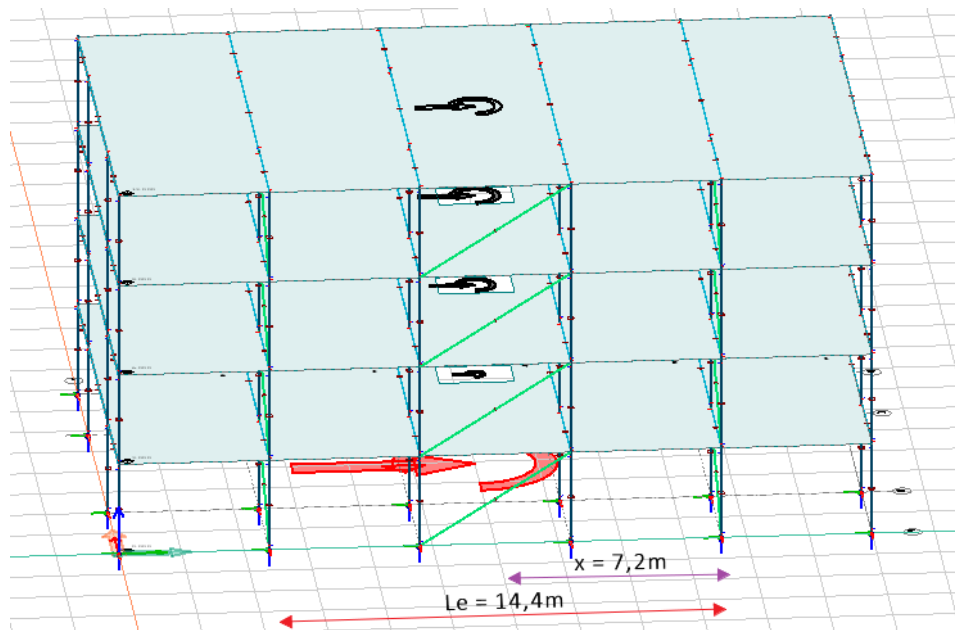


Figure 5-8 Factor δ is found by measuring the distance of the element under consideration from COM perpendicular to the direction of seismic action, in this case x-direction. And distance between two outermost lateral load resisting elements. (EC5 1994)

$$F := \frac{\delta}{\left(S_{1,Truss}^2 \cdot \frac{l_{truss}}{A_{Truss} \cdot E_s} + S_{1,RHS}^2 \cdot \frac{l_{column}}{A_{RHS} \cdot E_s} \right)} \quad 5-11$$

$$k_x := \frac{F}{\delta} = (71.2 \cdot 10^6) \frac{N}{m}$$

By setting up the stiffness matrix k_x for those two bracings in x-direction, we can get the stiffness matrix showed below.

$$K_x := 2 \begin{bmatrix} k_x & -k_x & 0 & 0 \\ -k_x & 2 \cdot k_x & -k_x & 0 \\ 0 & -k_x & 2 \cdot k_x & -k_x \\ 0 & 0 & -k_x & 2 \cdot k_x \end{bmatrix} = \begin{bmatrix} 142 & -142 & 0 & 0 \\ -142 & 285 & -142 & 0 \\ 0 & -142 & 285 & -142 \\ 0 & 0 & -142 & 285 \end{bmatrix} 10^6 \frac{N}{m} \quad 5-12$$

As mentioned 3.1.10.2, second order effect of geometric-stiffness must be considered. The geometric-stiffness matrix k_G in a rod as given in equation 3-89 with regard to equilibrium when the plastic deformation is considered gives the result presented in equation 5-13.

The ductility factor μ is set to 1,5. Axial force changes from segment to segment, which means that columns that hold the slabs, also hold the weight that should be taken into account. The total load in top columns is $m_4 \cdot g$, in the floor under $m_3 + m_4 \cdot g$ and so on. In the first floor is $m_{tot} \cdot g$. This gives the geometric stiffness matrix described under:

$$k_G := \mu \cdot \frac{g}{H} \begin{bmatrix} m_4 & -m_4 & 0 & 0 \\ -m_4 & m_3 + 2 m_4 & -m_3 - m_4 & 0 \\ 0 & -m_3 - m_4 & m_2 + 2 \cdot m_3 + 2 \cdot m_4 & -m_2 - m_3 - m_4 \\ 0 & 0 & -m_2 - m_3 - m_4 & m_1 + 2 \cdot m_2 + 2 \cdot m_3 + 2 \cdot m_4 \end{bmatrix} \quad 5-13$$

The combined stiffness matrix, can be determined as the subtraction of the geometric stiffness matrix from the elastic stiffness, as shown in equation 3-85.

$$K_{cx} := K_x - k_G = \begin{bmatrix} 141 & -141 & 0 & 0 \\ -141 & 281 & -140 & 0 \\ 0 & -140 & 277 & -138 \\ 0 & 0 & -138 & 274 \end{bmatrix} 10^6 \frac{N}{m} \quad 5-14$$

The natural frequency can be found by equation 3-52, which is presented here:

$$\omega_n := \sqrt{\lambda} = \begin{bmatrix} 7.49 \\ 21.63 \\ 32.73 \\ 39.62 \end{bmatrix}$$

This gives us the natural period for the four first frequencies:

$$T_x := \frac{2\pi}{\omega_n} = \begin{bmatrix} 0.838 \\ 0.291 \\ 0.192 \\ 0.159 \end{bmatrix} \quad 5-15$$

Mode shapes are found by using the combined stiffness matrix in and the equation 3-52.

$$U_x = \begin{bmatrix} 1 & 1 & 1 & 1 \\ 0.898 & 0.147 & -0.953 & -1.861 \\ 0.68 & -0.868 & -0.601 & 1.893 \\ 0.366 & -0.956 & 1.244 & -1.16 \end{bmatrix} \quad 5-16$$

Mode shapes from equation 5-16 are illustrated by Figure 5-9, Figure 5-10, Figure 5-11, and Figure 5-12. These figures give an indication of how the building is displaced over the height of it

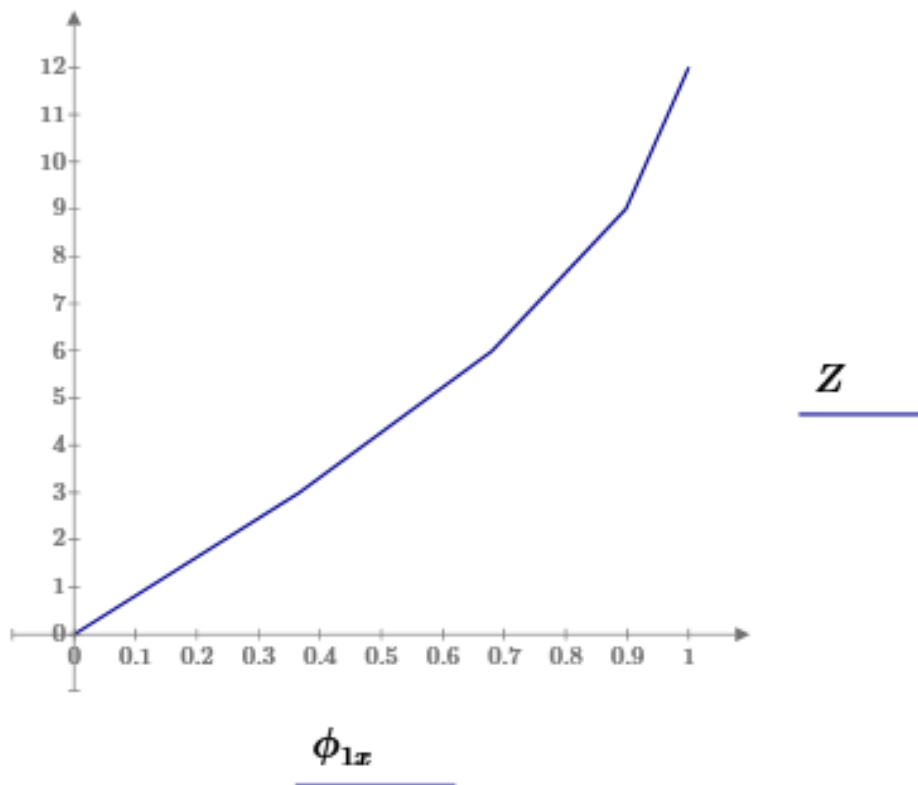


Figure 5-9 First mode shape in x-direction.

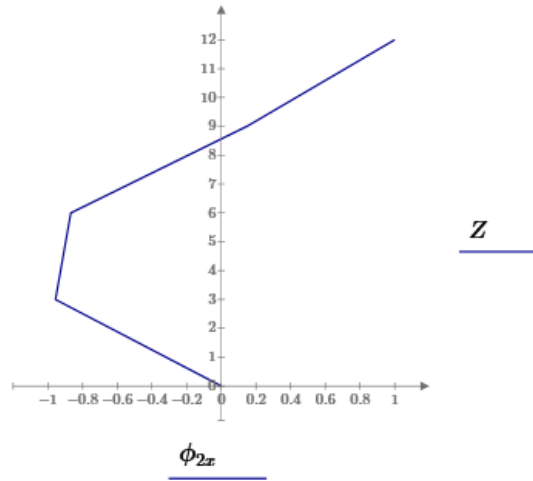


Figure 5-10 Second mode shape in x-direction.

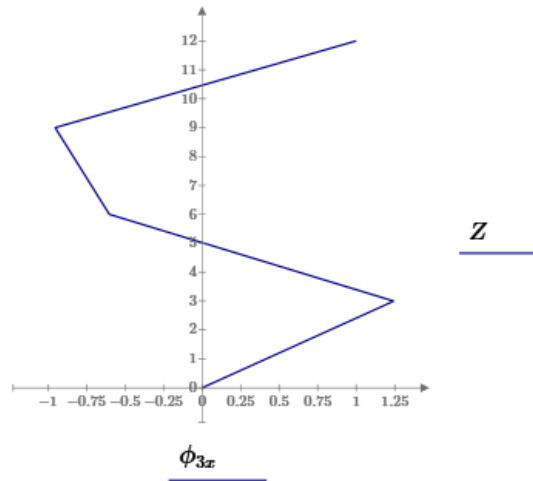


Figure 5-11 Third mode shape in x-direction.

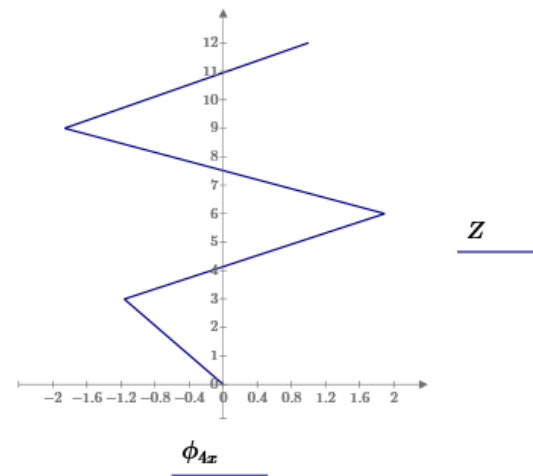


Figure 5-12 Fourth mode shape in x-direction.

Now we can look at the modal mass in each mode. This is given by equation 3-65. Since all the DOFs have affect in the same direction, the influence vector can be written as:

$$\iota := [1 \ 1 \ 1 \ 1]^T \quad 5-17$$

Equation 3-56 gives M_k and L_k values needed in order to find the effective modal mass, as presented below for each mode:

$$\begin{aligned} L_{1x} &= \phi_{1x}^T m \iota & M_{1x} &= \phi_{1x}^T m \phi_{1x} = 7.03 \cdot 10^5 \\ m_{1x} &= \iota^T \frac{L_{1x}}{M_{1x}} m \phi_{1x} = 1.1 \cdot 10^6 \\ \\ L_{2x} &= \phi_{2x}^T m \iota & M_{2x} &= \phi_{2x}^T m \phi_{2x} = 7.942 \cdot 10^5 \\ m_{2x} &= \iota^T \frac{L_{2x}}{M_{2x}} m \phi_{2x} = 964.6 \cdot 10^3 \\ \\ L_{3x} &= \phi_{3x}^T m \iota & M_{3x} &= \phi_{3x}^T m \phi_{3x} = 1.152 \cdot 10^6 \\ m_{3x} &= \iota^T \frac{L_{3x}}{M_{3x}} m \phi_{3x} = 22 \cdot 10^3 \\ \\ L_{4x} &= \phi_{4x}^T m \iota & M_{4x} &= \phi_{4x}^T m \phi_{4x} = 2.927 \cdot 10^6 \\ m_{4x} &= \iota^T \frac{L_{4x}}{M_{4x}} m \phi_{4x} = 3.5 \cdot 10^3 \end{aligned} \quad 5-18$$

The total modal mass is then found as shown below:

$$m_{tot} := \iota^T m \cdot \iota = 1.211 \cdot 10^6 \quad 5-19$$

The relation between modal mass for each mode to the total mass is given by

$$\begin{aligned} m_{1x} &= \frac{m_{1x}}{m_{tot}} = 0.900 & m_{2x} &= \frac{m_{2x}}{m_{tot}} = 0.797 \\ m_{3x} &= \frac{m_{3x}}{m_{tot}} = 0.018 & m_{4x} &= \frac{m_{4x}}{m_{tot}} = 0.003 \end{aligned}$$

We now calculate the natural period, natural mode shape and effective modal mass in y-direction.

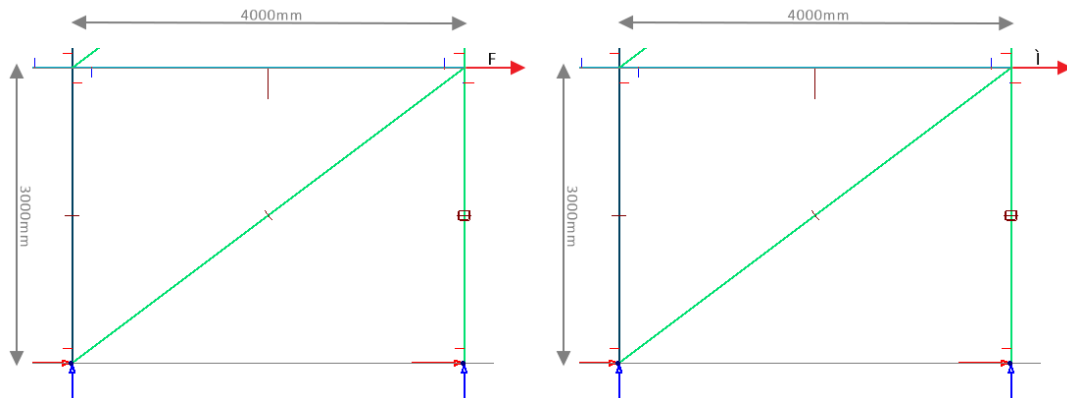


Figure 5-13 Bracing in y-direction

First we find the length of bracings by using Pythagoras formula as showed below.

$$l_{truss} = \sqrt{H^2 + L_1^2} = 5660.39 \text{ mm} \quad H = 3 \text{ m}$$

$$l_{column} = 3000 \text{ mm}$$

Axial Forces in bracings is calculated in the same way as for the x-direction. These values and the change in length gives us k_y , which is represented in the stiffness matrix below for four bracings in y-direction:

$$K_y := 4 \begin{bmatrix} k_y & -k_y & 0 & 0 \\ -k_y & 2 \cdot k_y & -k_y & 0 \\ 0 & -k_y & 2 \cdot k_y & -k_y \\ 0 & 0 & -k_y & 2 \cdot k_y \end{bmatrix} = \begin{bmatrix} 288 & -288 & 0 & 0 \\ -288 & 576 & -288 & 0 \\ 0 & -288 & 576 & -288 \\ 0 & 0 & -288 & 576 \end{bmatrix} 10^6 \frac{N}{m} \quad 5-20$$

By using equation 5-20 and 5-13 we can find the combined stiffness matrix, as presented below:

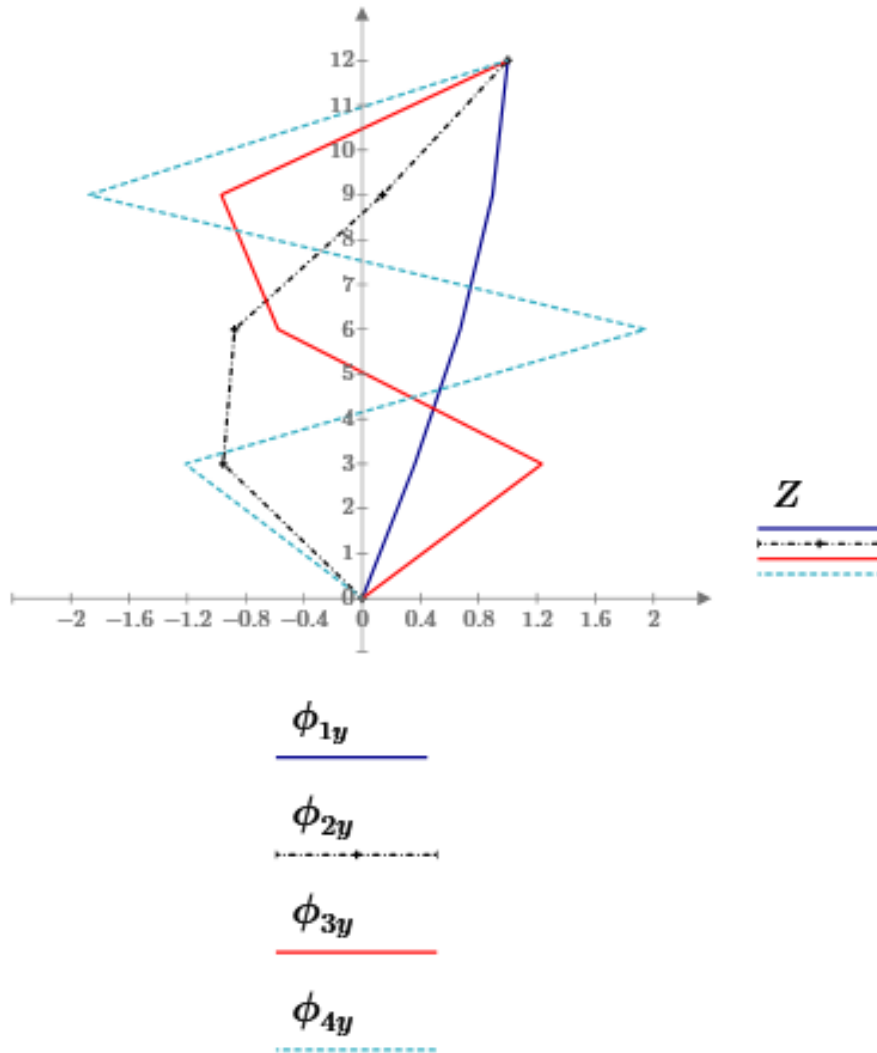
$$K_{cy} := K_y - k_G = \begin{bmatrix} 287 & -287 & 0 & 0 \\ -287 & 572 & -285 & 0 \\ 0 & -285 & 569 & -284 \\ 0 & 0 & -284 & 566 \end{bmatrix} 10^6 \frac{N}{m} \quad 5-21$$

Further we can find the nature frequency and modes in same way as for the x-direction:

$$T_y := \frac{2 \pi}{\omega} = \begin{bmatrix} 0.581 \\ 0.203 \\ 0.134 \\ 0.111 \end{bmatrix} \quad 5-22$$

$$\omega := \sqrt{\lambda} = \begin{bmatrix} 10.82 \\ 30.98 \\ 46.87 \\ 56.66 \end{bmatrix} \quad U_y = \begin{bmatrix} 1 & 1 & 1 & 1 \\ 0.895 & 0.14 & -0.968 & -1.875 \\ 0.673 & -0.876 & -0.577 & 1.946 \\ 0.361 & -0.954 & 1.234 & -1.215 \end{bmatrix}$$

Shapes of modes presented by U_y is given in the figure below.



We now find M_k and L_k , both in kg.

$$M_{1y} := \phi_{1y}^T \cdot m \cdot \phi_{1y} = 6.973 \cdot 10^5 \quad M_{2y} := \phi_{2y}^T \cdot m \cdot \phi_{2y} = 7.965 \cdot 10^5 \quad M_{3y} := \phi_{3y}^T \cdot m \cdot \phi_{3y} = 1.145 \cdot 10^6$$

$$M_{4y} := \phi_{4y}^T \cdot m \cdot \phi_{4y} = 3.048 \cdot 10^6$$

$$L_{1y} := \phi_{1y}^T \cdot m \cdot \iota = 8.705 \cdot 10^5 \quad L_{2y} := \phi_{1y}^T \cdot m \cdot \iota = 8.705 \cdot 10^5 \quad L_{3y} := \phi_{3y}^T \cdot m \cdot \iota = 1.584 \cdot 10^5$$

$$L_{4y} := \phi_{4y}^T \cdot m \cdot \iota = -1.067 \cdot 10^5$$

The effective modal mass for each mode can then be found

$$m_{tot} := \iota^T m \cdot \iota = 1.211 \cdot 10^6 \quad 5-23$$

Results of modal effective mass in x- and y-direction shows that they are almost the same, and how little the effect of increased stiffness plays in. Y-direction has two times higher stiffness than x-direction and shorter periods. Relation between modes are almost 0,7 based on equation of the natural period of a system with one DOF, as shown below:

$$\frac{T_{y_{0,0}}}{T_{x_{0,0}}} = 0.693 \quad \frac{T_{y_{1,0}}}{T_{x_{1,0}}} = 0.698 \quad \frac{T_{y_{2,0}}}{T_{x_{2,0}}} = 0.698 \quad \frac{T_{y_{3,0}}}{T_{x_{3,0}}} = 0.699$$

The relation between two systems with the same mass when the other one has two times higher stiffness is $\sqrt{\frac{1}{2}} \approx 0,71$. Like the building just calculated with the y-direction having two times higher stiffness than the x-direction. The reason for having the ratio under 0,7 is mainly the second order effects. These effects implies that even if the stiffness is the same for each storey in x- and y-direction, the relation between vibration periods for each modes varies.

Modal masses are also similar in x- and y-direction. This is due to the natural modes being almost the same in these directions. This may be alarming since the stiffness is different in each direction, but natural modes are almost the same with their only difference being that x-direction multiplied with a constant, 0,71, is y-direction ($\omega_x \approx 0,71 \cdot \omega_y$). The reason because mode shapes are not exactly the same in these two directions lies in the geometrical effects. (Øystad-Larsen 2010).

We now look at the base share force these directions give, and compare it to the base share given by FEM-DESIGN software. We use the first period and the equation (4.5) from EC8-1 4.3.3.2.2. In x-direction it gives us

$$S_d T_{1x} := a_g \cdot S \cdot \frac{2.5}{q} \cdot \frac{T_c}{T_{1x}} = 0.296 \quad F_{bx} := \frac{S_d T_{1x} \cdot m_{tot} \cdot \lambda_{correction}}{1000} = 358.191$$

Compared to FEM-DESIGN which has the value of 314,934 kN with the period of 0,934s, the hand calculation gives a 12% increased value. This is because of the equation from EC8 is a more conservative approach in calculating base shear force.

The y-direction is calculated in the same way as the x-direction, and gives a difference of 22%.

$$S_d T_{1y} := a_g \cdot S \cdot \frac{2.5}{q} \cdot \frac{T_c}{T_{1y}} = 0.427 \quad F_{by} := \frac{S_d T_{1y} \cdot m_{tot} \cdot \lambda_{correction}}{1000} = 517.129$$

Results imply that lower natural period gives a higher base shear at the ground level. It is important to also compare the result from empirical formula for building period as described in section 4.1.2, to see if the mode shapes given by software have any consistent differences with the approach given by EC8. Equation 4-2, as presented below, is used to calculate the fundamental vibration period.

$$T_1 := C_t \cdot H^{0.75}$$

To find the fundamental vibration period of a building, we need to know what kind of structure we are dealing with. *EC8-1 4.3.3.2.2(4.6)* provides the value $C_t = 0,005$ for structures that are not moment resistant space steel/concrete frames. By adding the height of structure we get the period of

$$T_1 := C_t \cdot H^{0.75} = 0.322$$

For the horizontal components of the seismic action the design spectrum $S_d(T)$ (since T_1 is between $T_c = 0,2$ and $T_D = 1,7$) is defined.

$$S_{d,T} := a_g \cdot S \cdot \frac{2.5}{q} \cdot \frac{T_c}{T_1}$$

By using the modal mass in x-direction from equation 5-19, we can find the base share based on equation 4-7, as presented here:

$$F_{b,EC8,x} := S_{d,T} \cdot m_{modal} \cdot \lambda = 791.879 \cdot 10^3 \quad N \quad 5-24$$

where $\lambda = 0,85$ since $2T_c > T_1$. Base shear based on the EC8's empirical formula, and fundamental period for each floor with its modal mass, can be calculated according to equation 4-9. This is presented in the table below:

Floor	Height	Mass(kg)	HxM	(kN)
1	3	351166	1053498	91,51212
2	6	351166	2106996	183,0242

3	9	306424	2757816	239,5577
4	12	266491	3197892	277,7849
	Sum	1275247	9116202	

Using the same approach to find equation 5-24, by using the first mode from model #1 we now can calculate the base shear. The first mode, as shown in Table 9, gives a natural period of 0,934s. The calculated base share is as followed:

$$S_{d,T,model1} := a_g \cdot S \cdot \frac{2.5}{q} \frac{T_c}{T_1} = 0.266$$

$$F_{b,m1,x} := S_{d,T,model1} \cdot m_{modal} \cdot \lambda = 321.55 \cdot 10^3 \quad 5-25$$

where $\lambda = 1$ since $2T_c < T_1$. By comparing values from equation 5-24 and 5-25, we observe that the difference between base shear with fundamental period calculated by empirical value is 2,5 times higher than base share with fundamental period founded by FEM-DESIGN. We can draw this difference fundamental periods result in, by using the horizontal elastic response spectra graph for ground type A, as showed in Figure 5-14.

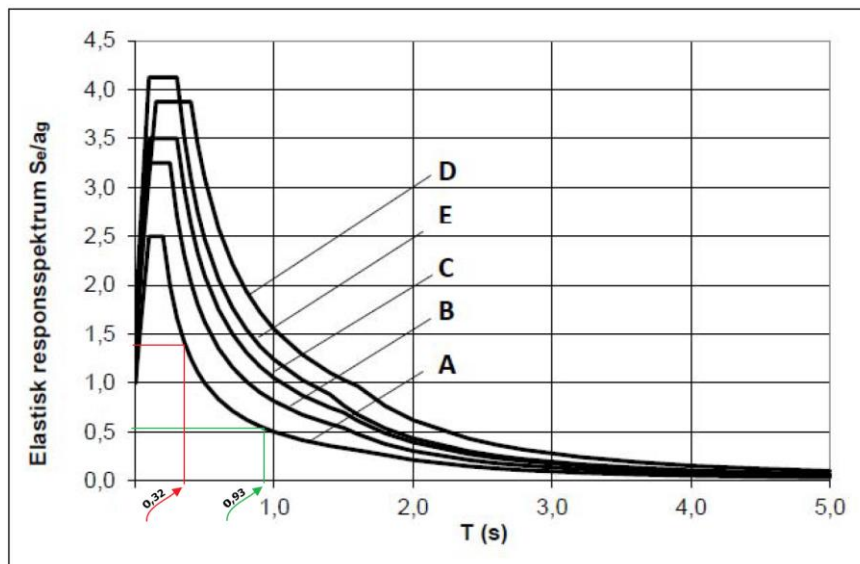


Figure 5-14 Difference in terms of elastic resposspektrum calculated periods give (EC8 2014).

The geometrical stiffness matrix was subtracted from the stiffness matrix shown in equation 5-14. We now look at the mode shapes when k_G is neglected. By doing this we can verify if this parameter has any significant effect on the result. In the first main direction results gives higher stiffness (equation 5-26), lower periods (equation 5-27),

very little difference in mode shapes (equation 5-28 and Figure 5-15) and 2% increase of base shear (equation 5-29).

$$K_x := \begin{bmatrix} 142 \cdot 10^6 & -142 \cdot 10^6 & 0 & 0 \\ -142 \cdot 10^6 & 285 \cdot 10^6 & -142 \cdot 10^6 & 0 \\ 0 & -142 \cdot 10^6 & 285 \cdot 10^6 & -142 \cdot 10^6 \\ 0 & 0 & -142 \cdot 10^6 & 285 \cdot 10^6 \end{bmatrix} \quad 5-26$$

$$T_x := \frac{2 \pi}{\omega_n} = \begin{bmatrix} 0.807 \\ 0.286 \\ 0.19 \\ 0.157 \end{bmatrix} \quad 5-27$$

$$U_x = \begin{bmatrix} 1 & 1 & 1 & 1 \\ 0.89 & 0.129 & -0.986 & -1.9 \\ 0.666 & -0.88 & -0.556 & 2.003 \\ 0.356 & -0.947 & 1.236 & -1.267 \end{bmatrix} \quad 5-28$$

$$F_{bx} := \frac{S_d T_{1x} \cdot m_{tot} \cdot \lambda_{correction}}{1000} = 372.181 \quad 5-29$$

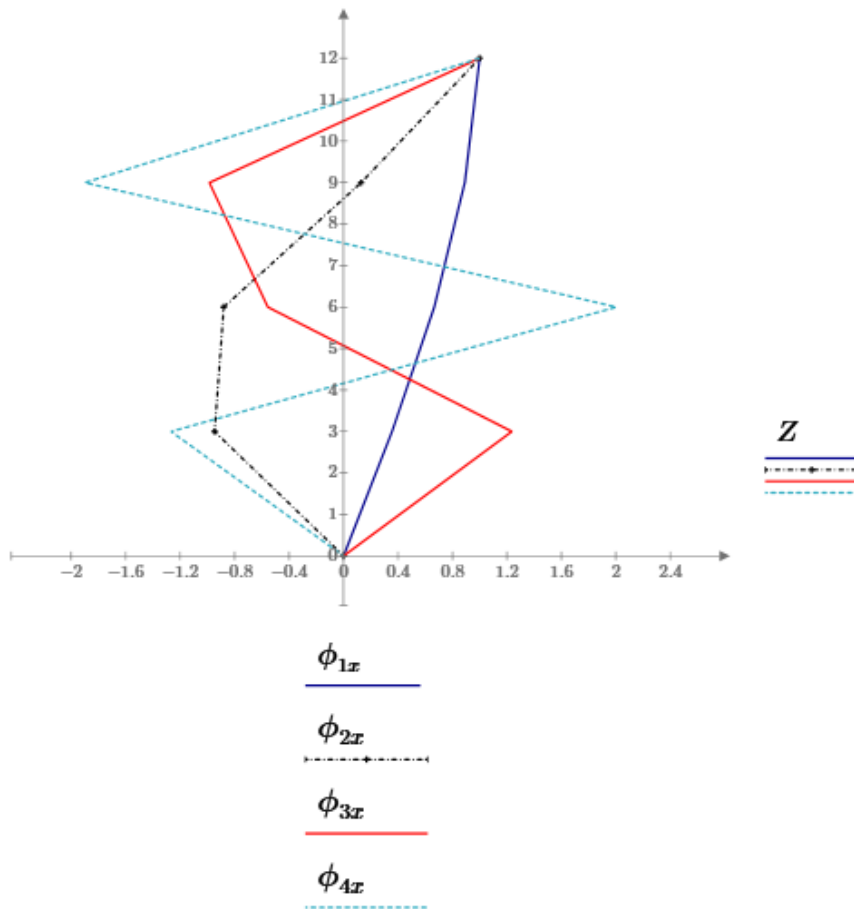


Figure 5-15 Mode shapes in absence of geometrical matrix.

Results of calculation for y-direction gives also higher stiffness (equation 5-265-30), lower periods (equation 5-31), very little difference in mode shapes (equation 5-32 and Figure 5-16) and 1% increase of base shear (equation 5-33).

$$K_y := \begin{bmatrix} 288 \cdot 10^6 & -288 \cdot 10^6 & 0 & 0 \\ -288 \cdot 10^6 & 576 \cdot 10^6 & -288 \cdot 10^6 & 0 \\ 0 & -288 \cdot 10^6 & 576 \cdot 10^6 & -288 \cdot 10^6 \\ 0 & 0 & -288 \cdot 10^6 & 576 \cdot 10^6 \end{bmatrix} \quad 5-30$$

$$T_y := \frac{2 \pi}{\omega} = \begin{bmatrix} 0.576 \\ 0.202 \\ 0.133 \\ 0.11 \end{bmatrix} \quad 5-31$$

$$U_y = \begin{bmatrix} 1 & 1 & 1 & 1 \\ 0.894 & 0.133 & -0.981 & -1.894 \\ 0.67 & -0.877 & -0.557 & 1.996 \\ 0.359 & -0.946 & 1.233 & -1.262 \end{bmatrix} \quad 5-32$$

$$F_{by} := \frac{S_d T_{1y} \cdot m_{tot} \cdot \lambda_{correction}}{1000} = 521.32 \quad 5-33$$

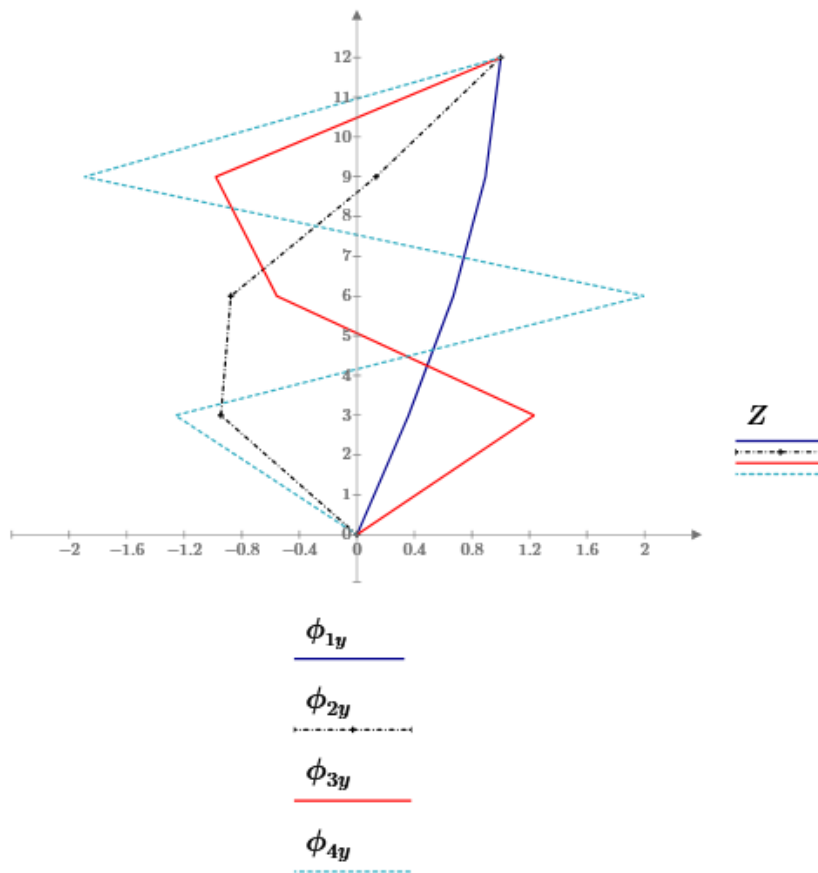


Figure 5-16 Mode shapes in absence of geometrical matrix.

5.3 MODAL ANALYSIS OF 3D MODELS

5.3.1 NATURAL FREQUENCY AND PERIOD

In this section we look at the different natural frequencies and periods between the models and empirical formula provided by EC8-1. To calculate the seismic effect on the structure knowing the period is necessary. [Table 8](#) shows ten different frequencies that represents ten different vibration shapes of the structure. Models have their masse distribution defined based on section [3.3.2.6](#).

Model #1	Model #2	Model #3	Model #4				
No.	Frequency [Hz]	No.	Frequency [Hz]	No.	Frequency [Hz]	No.	Frequency [Hz]
1.	1.070	1.	1.157	1.	1.133	1.	1.167
2.	1.487	2.	1.677	2.	1.638	2.	1.616
3.	1.633	3.	1.805	3.	1.768	3.	2.577
4.	3.064	4.	3.405	4.	3.368	4.	3.323
5.	4.300	5.	5.053	5.	5.013	5.	3.832
6.	4.698	6.	5.166	6.	5.141	6.	4.818
7.	5.000	7.	5.452	7.	5.413	7.	4.961
8.	6.139	8.	5.997	8.	5.979	8.	5.154
9.	7.119	9.	7.561	9.	7.560	9.	5.682
10.	7.715	10.	8.398	10.	8.398	10.	6.868

Table 8 Natural frequencies of different models from FEM-DESIGN.

We clearly see the pattern between stiffness and mass versus the frequency and period. Low mass, low stiffness gives higher frequency (light structure) and higher mass and stiffness gives lower frequency (heavy structure). And also by looking at the [Table 9](#) we see that lowest frequency results in highest period.

Model #1	Model #2	Model #3	Model #4	
No.	Period [s]	Period [s]	Period [s]	Period [s]
1.	0.934	0.864	0.883	0.857
2.	0.673	0.596	0.611	0.619
3.	0.612	0.554	0.565	0.388
4.	0.326	0.294	0.297	0.301
5.	0.233	0.198	0.199	0.261
6.	0.213	0.194	0.195	0.208
7.	0.200	0.183	0.185	0.202
8.	0.163	0.167	0.167	0.194
9.	0.140	0.132	0.132	0.176
10.	0.130	0.119	0.119	0.146

Table 9 Natural period of different models from FEM-DESIGN.

The natural period of vibration has a primary role depending on mass and stiffness of a MDOF system, and provides the time required for one cycle of harmonic motion in one of the natural modes, as presented in [Table 8](#).

The fundamental period can be calculated based on the different empirical formulas given in section [4.1.2](#), where coefficients are theoretically or experimentally derived. For the modeled building with the height of $12m$, the empirical formula [4-2](#) gives a fundamental value of $T_1 = 0,05 \cdot 12^{0,75} = 0,322 s$. The value of frequency can be calculated in Hertz as shown in the following formula: $f_1 = \frac{1}{T} = \frac{1}{0,322} = 3,1 Hz$. This is far from the calculated period and frequency presented in [Table 8](#) and [Table 9](#). The empirical formula is based on structure's material, type and overall dimension with the intension of underestimating the period in order to conservatively estimate the base shear (Chopra & Goel 2000).

[Table 10](#) to [Table 13](#) compares the different models with each other to give a better understanding of how the first, second and third modes that show displacement in x axis, y axis and torsional rotation increase and decrease.

Model 1 and 2		Model 1 and 3		Model 1 and 4	
Frequency	Period	Frequency	Period	Frequency	Period
8,13 %	-7,49 %	5,89 %	-5,46 %	9,07 %	-8,24 %
12,78 %	-11,44 %	10,15 %	-9,21 %	8,68 %	-8,02 %
10,53 %	-9,48 %	8,27 %	-7,68 %	57,81 %	-36,60 %

[Table 10](#) Frequency and period results from model #1 is compared to the rest.

Model 2 and 1		Model 2 and 3		Model 2 and 4	
Frequency	Period	Frequency	Period	Frequency	Period
-7,52 %	8,10 %	-2,07 %	2,20 %	0,86 %	-0,81 %
-11,33 %	12,92 %	-2,33 %	2,52 %	-3,64 %	3,86 %
-9,53 %	10,47 %	-2,05 %	1,99 %	42,77 %	-29,96 %

[Table 11](#) Frequency and period results from model #2 is compared to the rest.

Model 2 and 1		Model 2 and 3		Model 2 and 4	
Frequency	Period	Frequency	Period	Frequency	Period
-5,56 %	5,78 %	2,12 %	-2,15 %	3,00 %	-2,94 %
-9,22 %	10,15 %	2,38 %	-2,45 %	-1,34 %	1,31 %
-7,64 %	8,32 %	2,09 %	-1,95 %	45,76 %	-31,33 %

Table 12 Frequency and period results from model #3 is compared to the rest.

Model 2 and 1		Model 2 and 3		Model 2 and 4	
Frequency	Period	Frequency	Period	Frequency	Period
-8,31 %	8,98 %	-0,86 %	0,82 %	-2,91 %	3,03 %
-7,98 %	8,72 %	3,77 %	-3,72 %	1,36 %	-1,29 %
-36,63 %	57,73 %	-29,96 %	42,78 %	-31,39 %	45,62 %

Table 13 Frequency and period results from model #4 is compared to the rest.

The relations between natural periods in x- and y-direction, as mentioned in the 5.2, lies around the 0,71 ratio. These are presented in Table 14. The comparison shows that the effect of increased stiffness, which results in a lower natural period of y-direction, are in fact reasonable based on the ratio of relation between these periods.

Model nr.	x-direction		y-direction		Ratio
Hand calc.	T ₁	0,838	T ₁	0,581	0,693
	T ₂	0,291	T ₂	0,203	0,698
#1	T ₁	0,934	T ₁	0,612	0,655
	T ₂	0,326	T ₂	0,233	0,715
#2	T ₁	0,864	T ₁	0,596	0,690
	T ₂	0,294	T ₂	0,198	0,673

#3	T ₁	0,883	T ₁	0,611	0,692
	T ₂	0,297	T ₂	0,199	0,670

Table 14 Comparing the natural periods to see the effect of stiffness.

Table 14 indicates that model #1's first mode has a natural period of 0,934 in x-direction and 0,612 in y-direction. Equation 5-15 and 5-22 resulted in a natural period of 0,838 in x-direction and 0,581 in y-direction for the first mode, which is 10% shorter than FEM-DESIGN's value. Second order effect cannot be the cause of this difference as, it would give a much larger FEM-DESIGN value. It seems that the numerical value and different calculation methods are the cause of the variation in results.

Model#4 was further recalculated in a new software called *TimberTech* to verify the frequency and period of the building. This new software in contrast to FEM-DESIGN from Strusoft is developed by experts at Timber Research group of University of Trento (Italy). The results from TimberTech are presented Figure 5-17.

Name	Period [s]	Frequency [Hz]	Mx [%]	Sum Mx [%]	My [%]	Sum My [%]	Mz [%]	Sum Mz [%]
Mode 1	0,84	1,19	82,51	82,51	0,00	0,00	0,00	0,00
Mode 2	0,59	1,68	0,00	82,51	81,46	81,46	0,00	0,00
Mode 3	0,39	2,59	0,00	82,51	0,00	81,46	81,64	81,64
Mode 4	0,30	3,36	10,15	92,66	0,00	81,46	0,00	81,64
Mode 5	0,21	4,77	0,00	92,66	10,06	91,53	0,00	81,64

Figure 5-17 TimberTech modal analysis results.

Also the stiffness of shear walls from model #4 is calculated by hand to see if there is any difference between stiffness of bracings of model #1 and shear walls of model #4. These hand calculation are presented here without taking into account the connection forces.

$$G_{clt} := 690 \frac{N}{mm^2} \quad t_{clt} := 240 \text{ mm} \quad h_{clt} := 3000 \text{ mm}$$

$$l_{clt,y} := 7800 \text{ mm} \quad l_{clt,x} := 4800 \text{ mm}$$

$$k_x := \frac{G_{clt} \cdot t_{clt} \cdot l_{clt,x}}{h_{clt}} = (2.65 \cdot 10^8) \frac{N}{m} \quad 5-34$$

$$K_x := 2 \begin{bmatrix} k_x & -k_x & 0 & 0 \\ -k_x & 2 \cdot k_x & -k_x & 0 \\ 0 & -k_x & 2 \cdot k_x & -k_x \\ 0 & 0 & -k_x & 2 \cdot k_x \end{bmatrix} = \begin{bmatrix} 530 & -530 & 0 & 0 \\ -530 & 1 \cdot 10^3 & -530 & 0 \\ 0 & -530 & 1 \cdot 10^3 & -530 \\ 0 & 0 & -530 & 1 \cdot 10^3 \end{bmatrix} 10^6 \frac{N}{m} \quad 5-35$$

$$k_y := \frac{G_{clt} \cdot t_{clt} \cdot l_{clt,y}}{h_{clt}} = (4.306 \cdot 10^8) \frac{N}{m} \quad 5-36$$

$$K_y := 2 \begin{bmatrix} k_y & -k_y & 0 & 0 \\ -k_y & 2 \cdot k_y & -k_y & 0 \\ 0 & -k_y & 2 \cdot k_y & -k_y \\ 0 & 0 & -k_y & 2 \cdot k_y \end{bmatrix} = \begin{bmatrix} 861 & -861 & 0 & 0 \\ -861 & 2 \cdot 10^3 & -861 & 0 \\ 0 & -861 & 2 \cdot 10^3 & -861 \\ 0 & 0 & -861 & 2 \cdot 10^3 \end{bmatrix} 10^6 \frac{N}{m} \quad 5-37$$

The results from 5-12 and 5-20 and their comparison with 5-35 and 5-37 indicates that the stiffness of shear walls in model #4 are much higher than the bracings of model #1. Frequencies of the five first modes are, in other hand, quite similar.

5.3.2 MODE SHAPES AND MODAL MASS

A structure's response to ground motion can be calculated through a sufficient amount of vibration shapes. As with the modal analysis method, by investigating the different displacement in x-, y- and z-direction, and their effective mass, we can design a building and overcome the seismic and stability challenges.

Calculated effective modal mass, which fulfils the criteria from section 4.1.3 is presented in Table 15, as the percentage amount relative to the total mass of the building.

Shape no.	T	mx'	my'	mz'
[-]	[s]	[%]	[%]	[%]
1	0.934	85.3 (d)	-	-
2	0.673	-	84.6 (d)	-
4	0.326	12.0	-	-
5	0.233	-	12.8	-
Summa		97.3	97.3	0.0

Model #1

Shape no.	T	mx'	my'	mz'
[-]	[s]	[%]	[%]	[%]
1	0.864	82.6 (d)	-	-
2	0.596	-	81.1 (d)	-
4	0.294	13.5	-	-
5	0.198	-	15.4	-
Summa		96.0	96.5	0.0

Model #2

Model #3

Shape no.	T	mx'	my'	mz'
[-]	[s]	[%]	[%]	[%]
1	0.883	82.1 (d)	-	-
2	0.611	-	80.5 (d)	-
4	0.297	13.8	-	-
5	0.199	-	15.9	-
Summa		95.9	96.4	0.0

Model #4

Shape no.	T	mx'	my'	mz'
[-]	[s]	[%]	[%]	[%]
1	0.857	81.7 (d)	-	-
2	0.619	-	84.7 (d)	-
4	0.301	14.4	-	-
5	0.261	-	11.4	-
Summa		96.1	96.0	0.0

Table 15 Selected shapes and effective masses from FEM-DESIGN.

Modal mass, a constant that depends on mass distribution among the various floors in each mode shape, is the part of the structures total mass responding to earthquake. It gives an indication of the amount of response each modes have. In other words, the total mass is effective in producing base shear, and only a portion of each floor contributes to it, as in the case of a multistorey building (Chopra 2012).

By comparing the four models, we can tell that the heaviest model, model #1, has the most modal mass. Here the influence of the first modes are much higher than with the later ones. This can also indicate that as the models in this thesis follow regularity criteria, achieving 90% is possible within the second mode in each direction. Symmetrical buildings are not always the case. Buildings that are not regular in elevation are more dependent on higher modes than those with regular elevation and equally distributed stiffness between storeys.

EC8-1 criteria, as mentioned in section 4.1.3, allows a neglecting contribution from modes with modal mass less than 5%. Although this might be a good idea, neglecting modes with low mass that gives little base shear at the ground level can be vital for other response parameters such as axial forces in primary elements like a given column. Furthermore, buildings with more complicated geometry need every contribution of modes in order to reach the 90% limit (Øystad-Larsen 2010).

All the shell elements have been analyzed according to a very fine mesh. Mode shapes from the Table 15 are further presented in 3D, with elevation views given in x and y axis for each models.

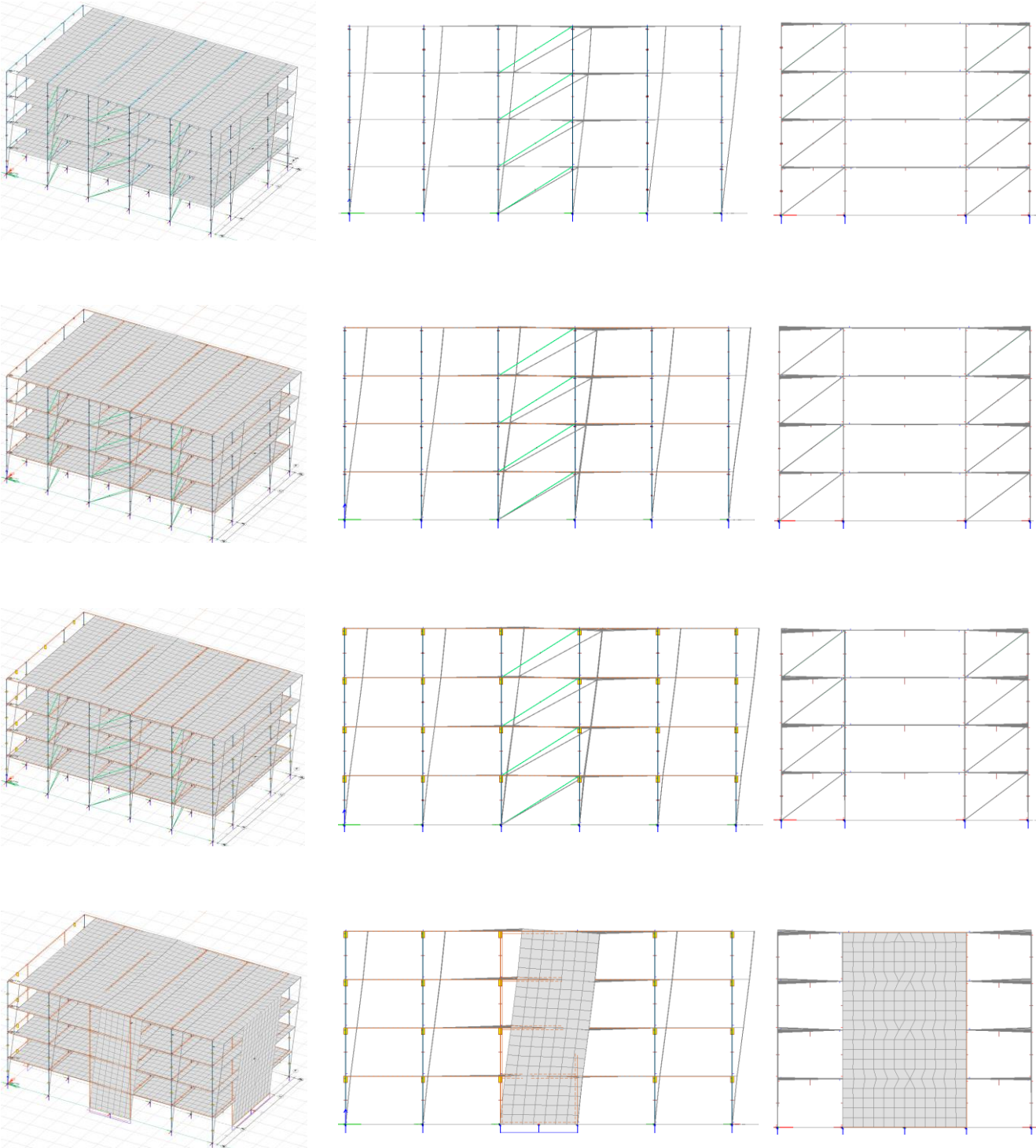


Table 16 Mode shape for the first mode according to FEM-DESIGN version 16. This mode indicates displacement in x-direction.

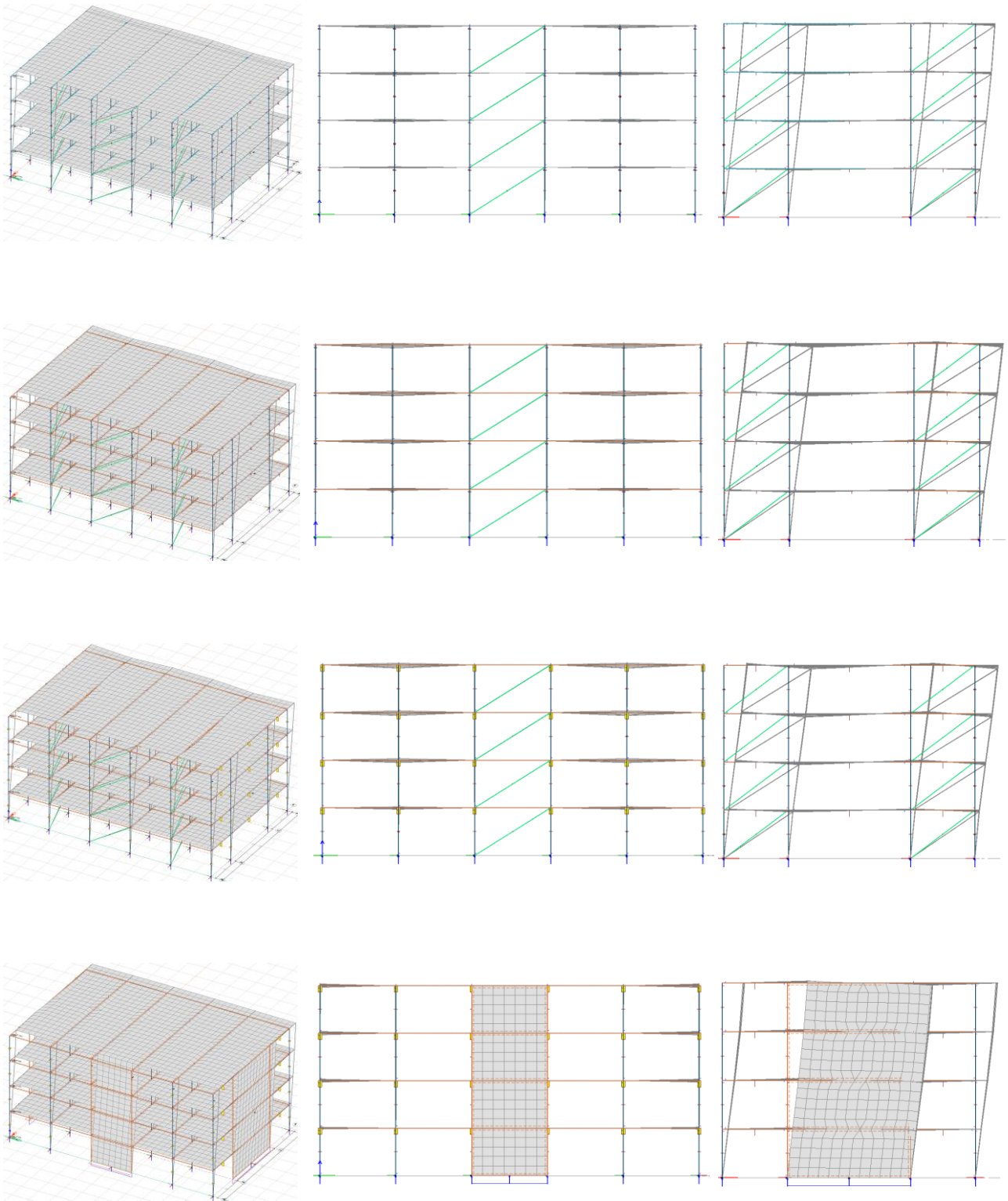
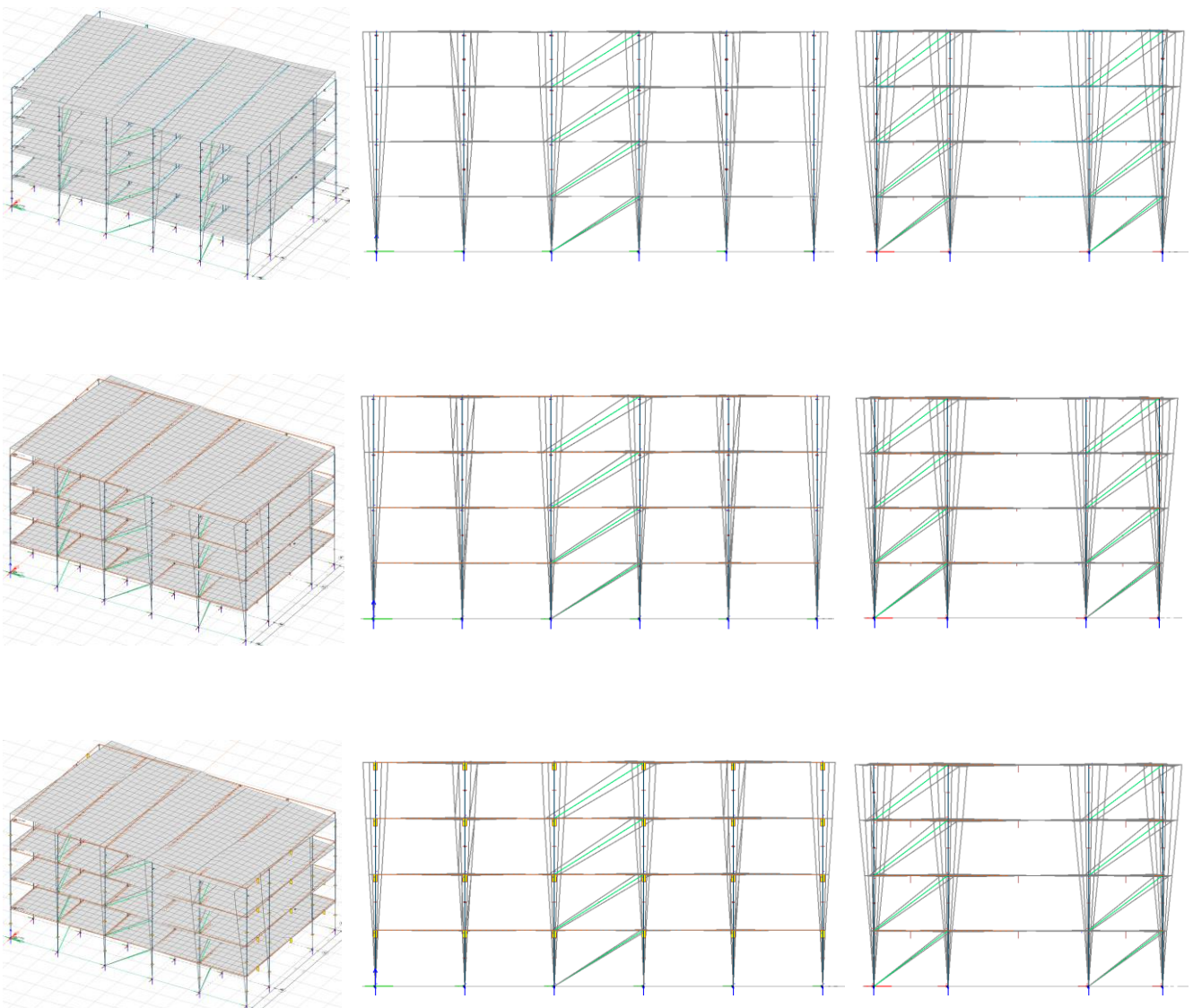


Table 17 Mode shape for the second mode according to FEM-DESIGN version 16. This mode indicates displacement in y-direction.

The third mode is neglected from all the models presented in [Table 15](#). This mode shape is illustrated in [Table 18](#), in accordance to the results of FEM-DESIGN models. The turning shape of this mode indicates the torsional mode. In terms of double symmetrical models, having torsional mode is not the case. The reason for presence of this mode, and not having any modal mass in any directions, is that the rotation around a vertical axes that goes through a double symmetrical structure's center of gravity, correspond to an antisymmetric turn. Torsional modes are a sign of numerical error. These type of modes have practically no influence on the results ([Øystad-Larsen 2010](#)).



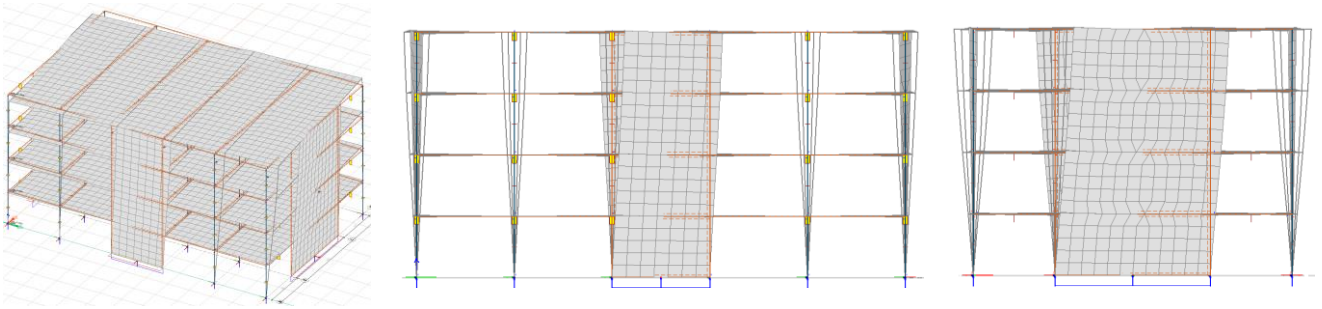
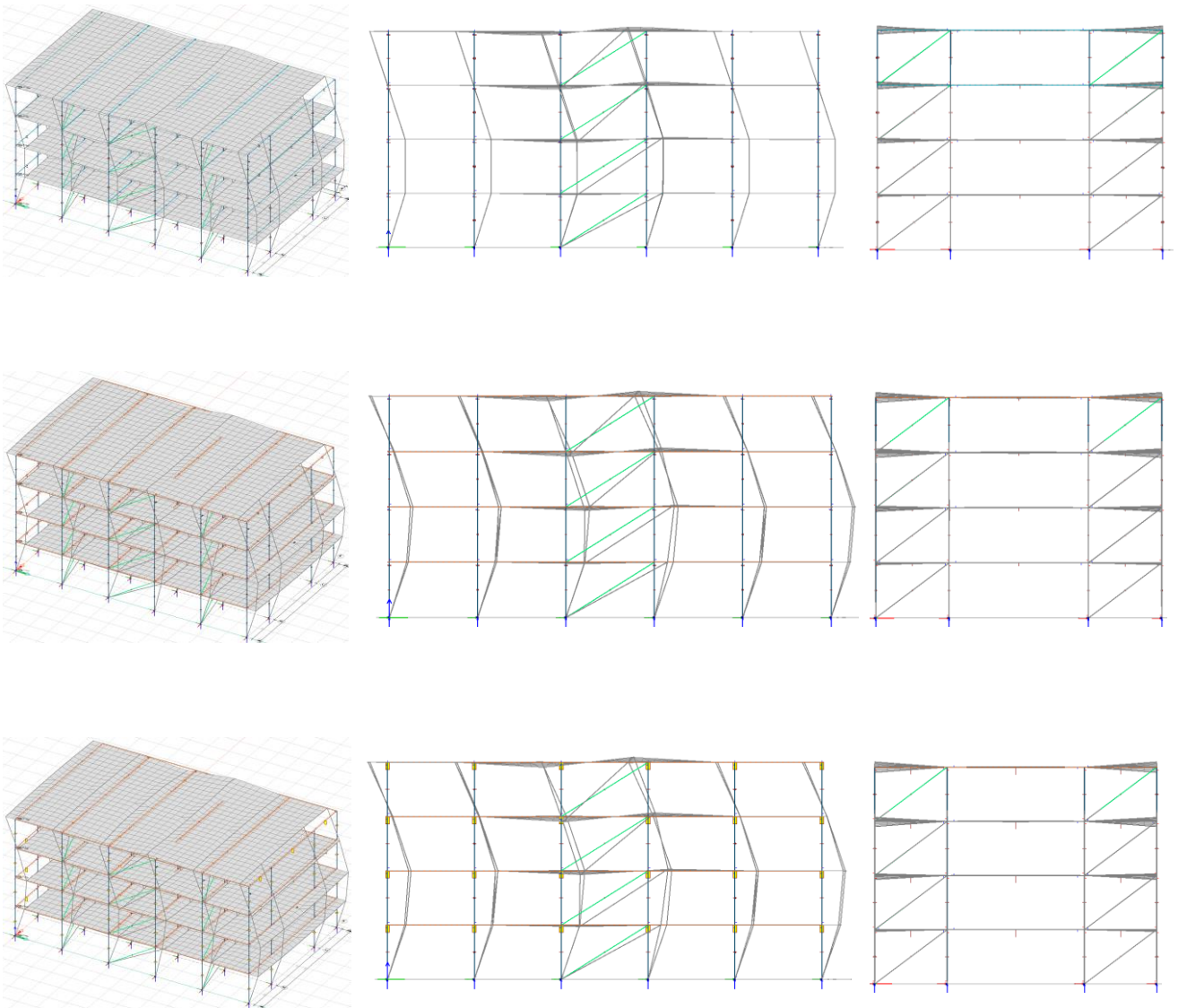


Table 18 Mode shape for the third mode according to FEM-DESIGN version 16. This mode indicates torsional effect.



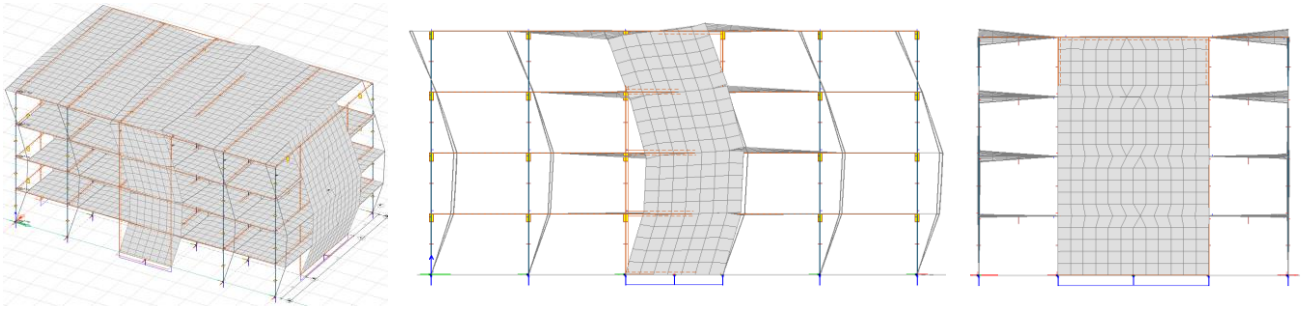
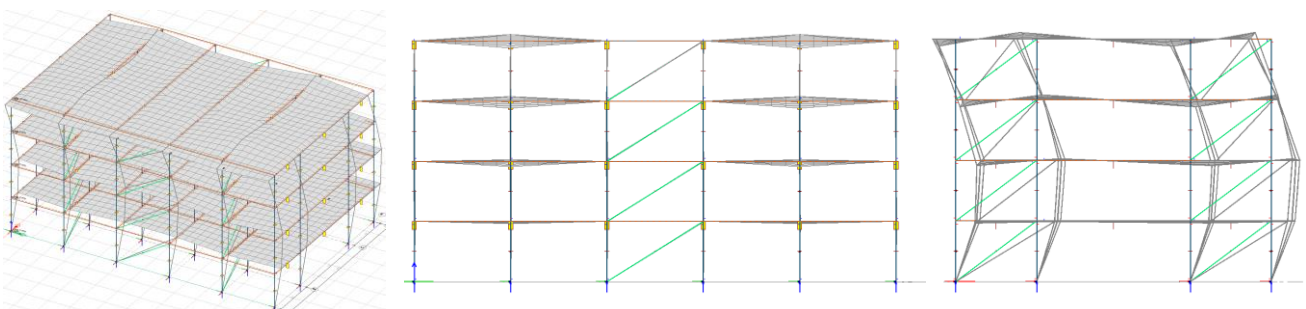
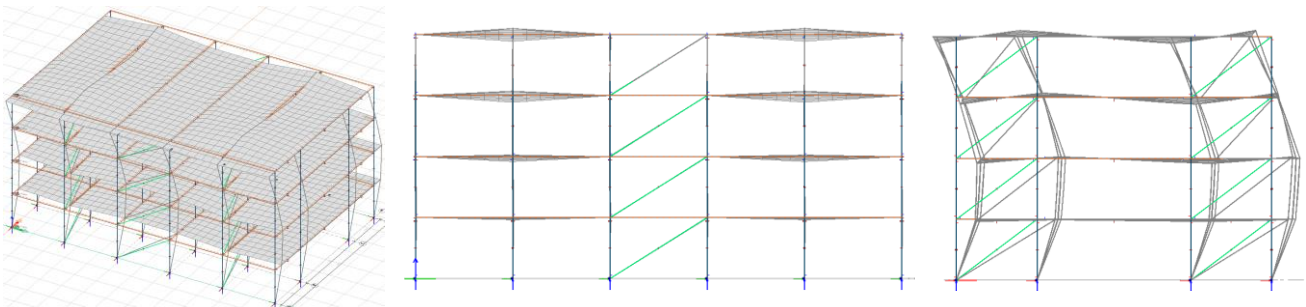
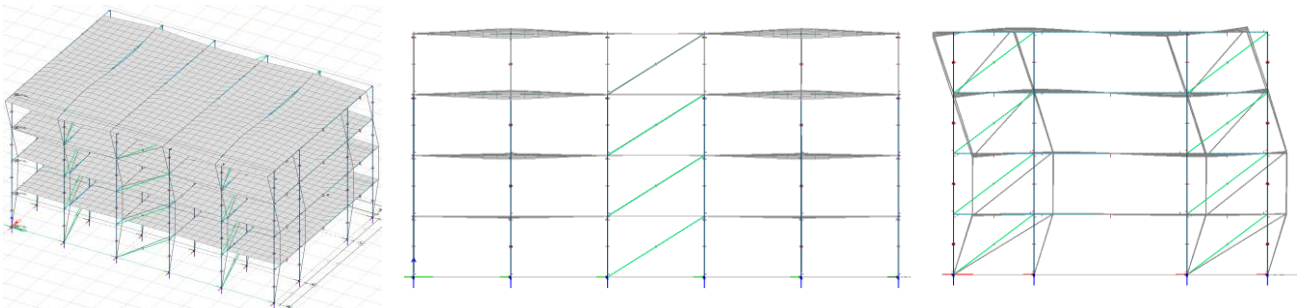


Table 19 Mode shape for the fourth mode according to FEM-DESIGN version 16. This mode indicates displacement in x-direction.



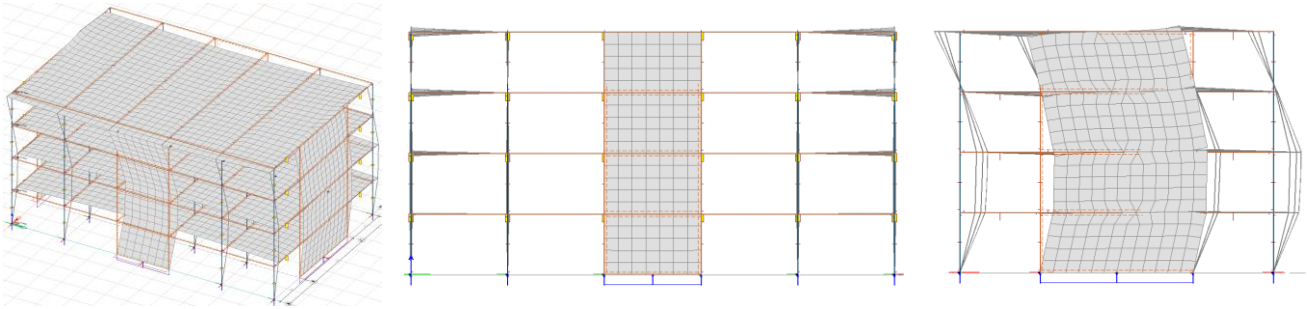


Table 20 Mode shape for the fifth mode according to FEM-DESIGN version 16. This mode indicates displacement in y-direction.

By comparing different mode shape figures given in Table 16, Table 17, Table 18, Table 19 and Table 20, we can verify that mode 1 and 4 corresponds to the displacement in x-direction. Mode 2 and 5 indicates the movement in y-direction, and in the same way mode 3 and 6(which is not included) display the torsional effect. We can also see that deflection increases as we ascend higher up the building.

We now look at the maximum horizontal load in bracings calculated by CQC for the modes and modal masses presented earlier. The maximum load in the x-direction is given by Table 21 and for the y-direction by Table 22.

Storey	Model #1	Model #2	Model #3	Model #4
Fourth	78,994	36,687	35,913	24,747
Third	125,098	49,462	47,876	55,184
Second	155,626	59,101	57,210	92,539
First	192,127	72,854	70,826	185,819

Table 21 Maximum horizontal force acted on bracings (kN) and shear wall (kN/m) in x-direction – FEM-DESIGN.

Storey	Model #1	Model #2	Model #3	Model #4
Fourth	63,726	28,616	27,980	13,898

Third	99,154	39,175	37,653	37,210
Second	122,525	47,596	45,724	66,475
First	153,788	62,069	59,244	153,084

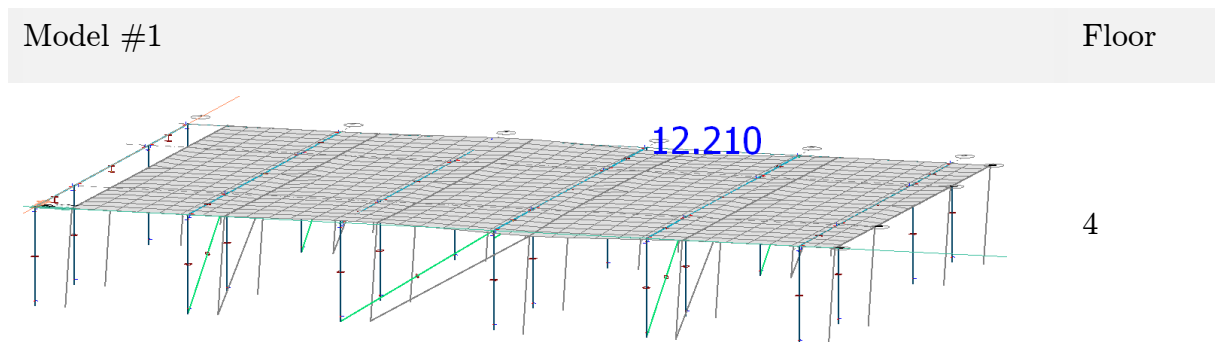
Table 22 Maximum horizontal force acted on bracings (kN) and shear wall (kN/m) in y-direction – FEM-DESIGN.

Since the y-direction has more bracings than the x-direction, the increase of stiffness reduces the maximum horizontal forces in that direction. As in x-direction, forces are decreased by 62% from model #1 to #2, and by 3% from #2 to #3. With model #4, the value of horizontal forces are almost the same. Difference between model #1 and #2 on the first storey in y-direction is 60%, whereas #1 and #4 have almost the same value. This shows the relative stiffness within the first storey of model #4 is, and that timber can have a significant impact in terms of load bearing when used correctly. Values from Table 21 and Table 22 for model #4 shows that the first storey shear walls have the most force acting upon them, and are basically displacing the rest of walls above, as shown in Table 17. In addition, values from y-direction in model #4 are less than x-direction because of distance between the elements.

5.3.3 INTERSTOREY DRIFT

EC8-1 4.3.4 introduces a simplified method of calculating the displacement based on a performed linear analysis. In this section we look at the different values from FEM-DESIGN models and evaluate them in regard to limitation from EC8-1 and equation 3-113.

We start investigating the interstorey drift in x-direction for all four models. Values for each model are presented in Table 23 to Table 26, and compared in Table 27.



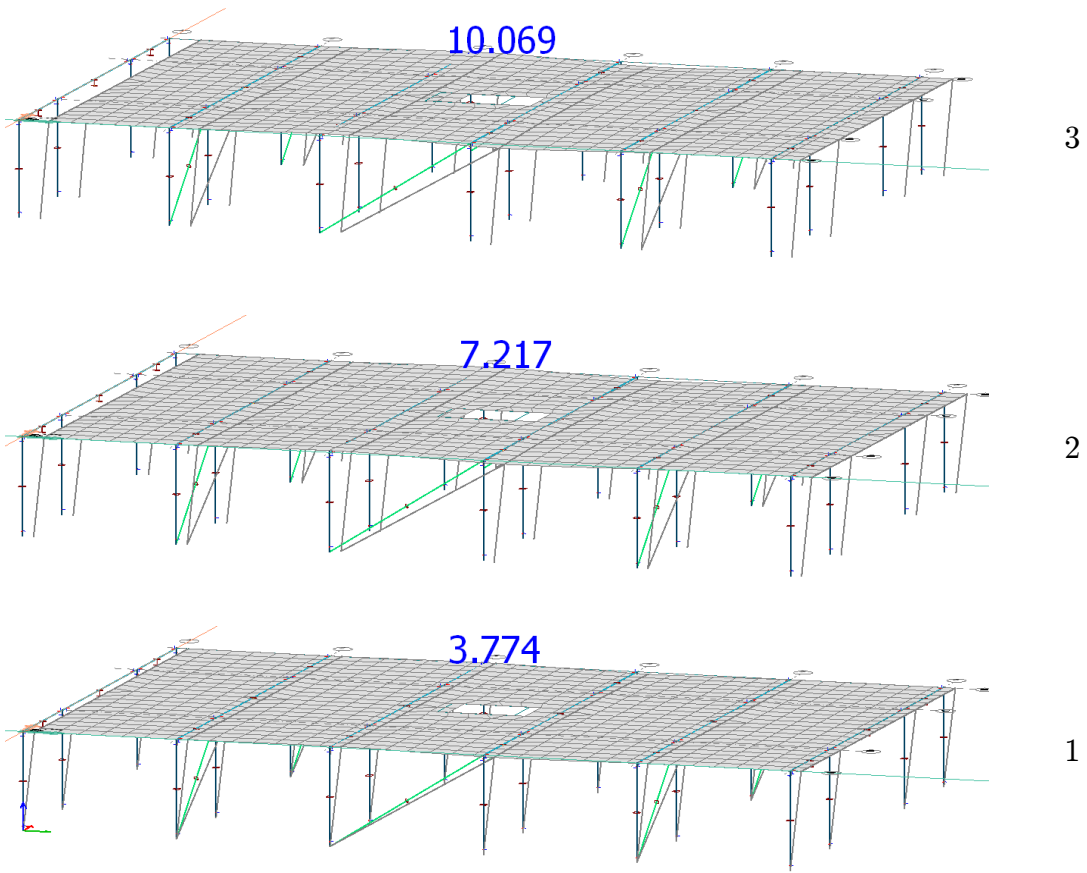
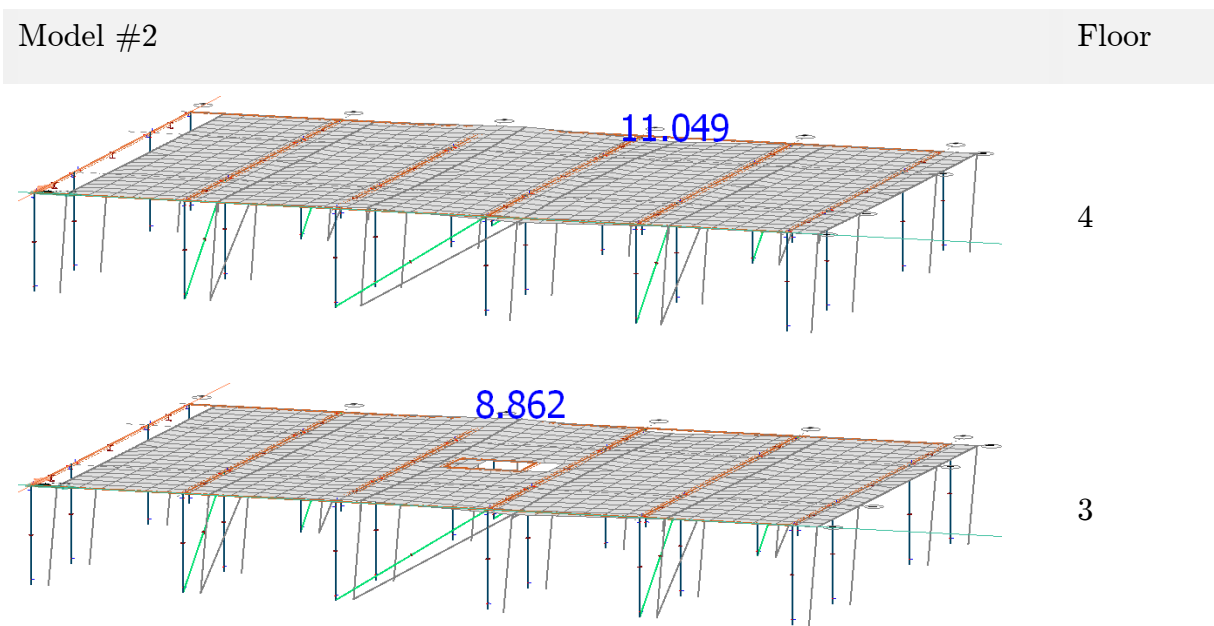


Table 23 Total displacement of model #1 in x-direction (mm) direction – FEM-DESIGN.



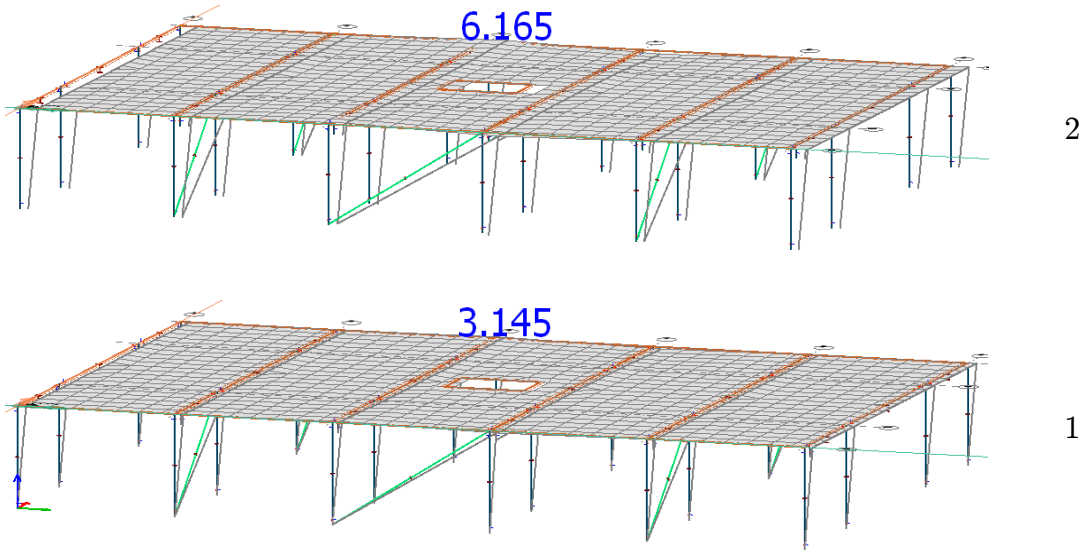


Table 24 Total displacement of model #2 in x-direction (mm) direction – FEM-DESIGN.

Model #3	Floor
	4
	3
	2

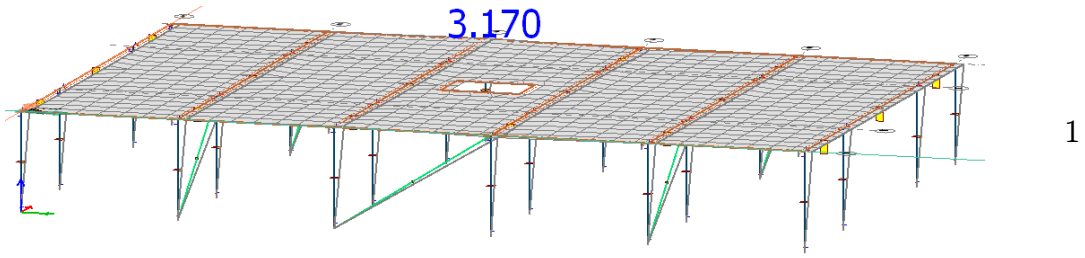


Table 25 Total displacement of model #3 in x-direction (mm) direction – FEM-DESIGN.

Model #4

Floor

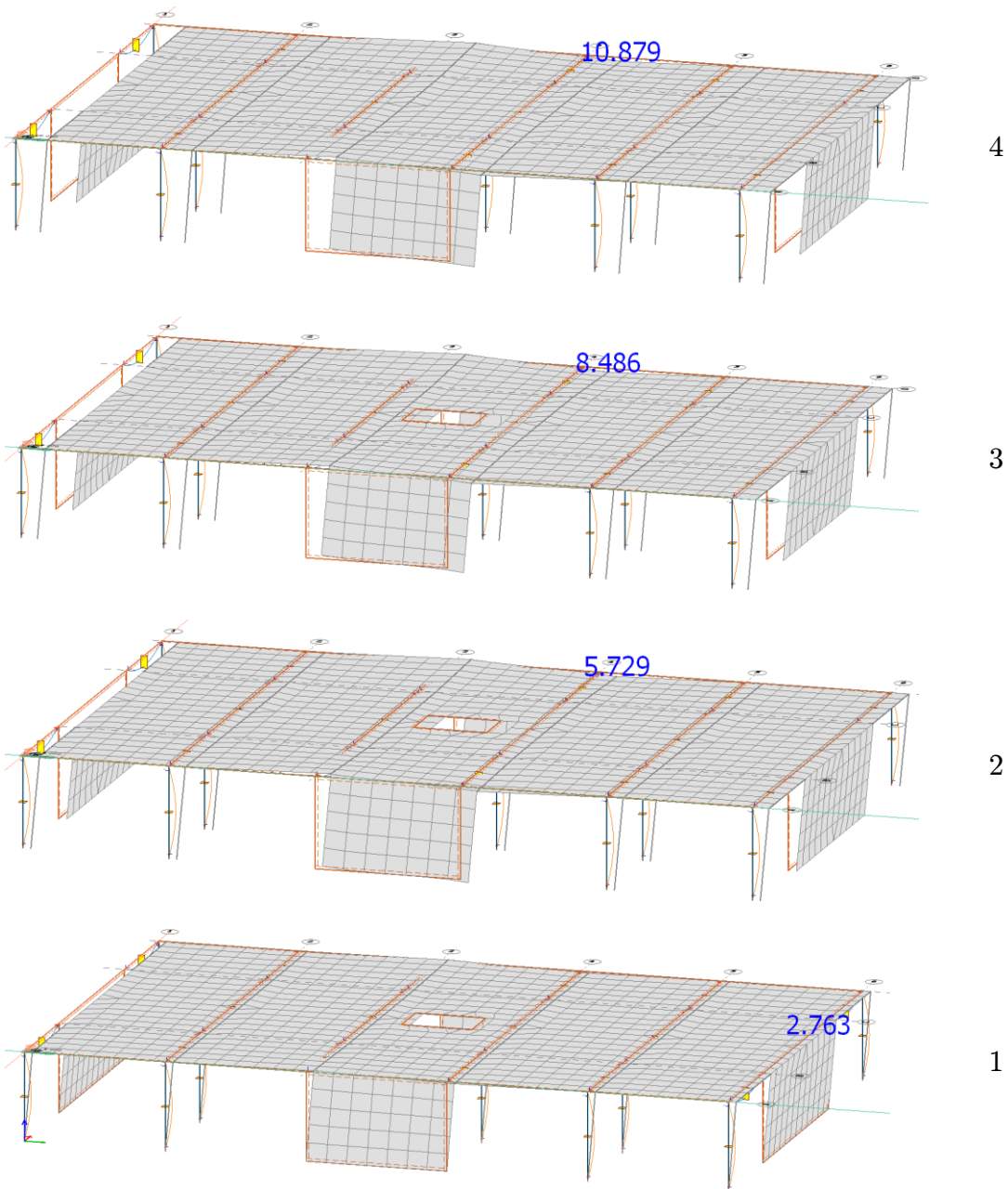


Table 26 Total displacement of model #4 in x-direction (mm) direction – FEM-DESIGN.

Storey	Model #1	Model #2	Model #3	Model #4
Fourth (roof)	12,210	11,049	11,322	10,879
Third	10,069	8,862	9,025	8,486
Second	7,217	6,165	6,245	5,729
First	3,774	3,145	3,170	2,763

Table 27 Displacements of different models in x-direction (mm) direction – FEM-DESIGN.

Criteria for building in this thesis is set to $d_r \cdot v \leq 0,005 \cdot h = 15\text{mm}$. The value of reduction factor is defined by EC8-1 and set to $v = 0,5$. This recommended value is for importance classes *I* and *II*. d_r is calculated based on equation 3-113 where $q_d = q = 1,5$ and d_e showed in Table 27.

Model	de1	de2	de3	de4	Storey
	12,210	11,049	11,322	10,879	4th
	10,069	8,862	9,025	8,486	3rd
	7,217	6,165	6,245	5,729	2nd
	3,774	3,145	3,170	2,763	1st
q	ds1	ds2	ds3	ds4	
1,5	18,315	16,574	16,983	16,319	4th
=	15,104	13,293	13,538	12,729	3rd
-	10,826	9,248	9,368	8,594	2nd
	5,661	4,718	4,755	4,145	1st
=	dr1	dr2	dr3	dr4	
	3,212	3,281	3,446	3,590	mm
	4,278	4,046	4,170	4,136	mm
	5,165	4,530	4,613	4,449	mm
	5,661	4,718	4,755	4,145	mm

Figure 5-18 Schematic calculation of interstorey drift in x-direction direction – FEM-DESIGN.

Displacement calculations for the main direction, x-axis, is presented in Figure 5-18. Results indicate that all of the models have much less drift than the criteria of 15mm. It also apparent that mode #1 has higher value than other models. The reason for this lies in the weight of this model, which is the largest among other models. Since forces acting on the building in model #1 is higher, even though it has more stiffness, drift is relatively large. Model #4, in contrast to #1, has lesser drift due to lightness of timber. This is relatively high, if the base shear of these two models are considered.

When interstorey drift is being observed, ensuring that the structural stability is preserved in both main directions is important. Therefore we look at the displacement of all four models in y-direction. These are presented in [Table 28](#) to [Table 31](#), and the compared in [Table 32](#).

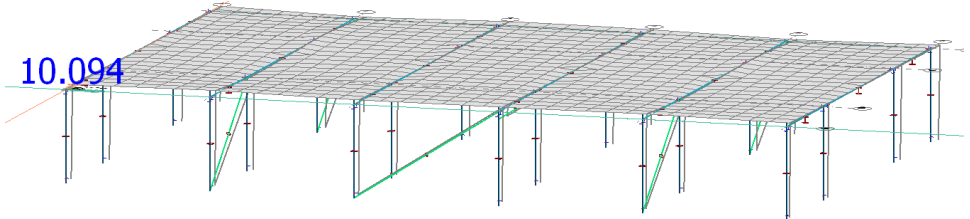
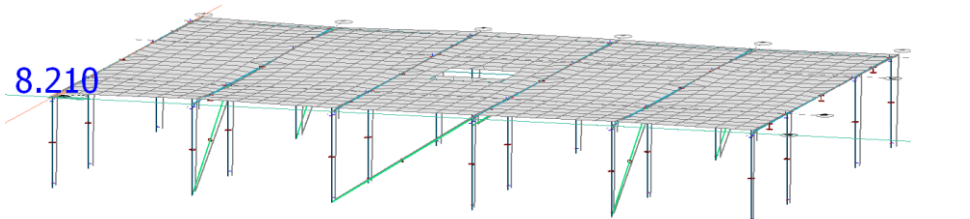
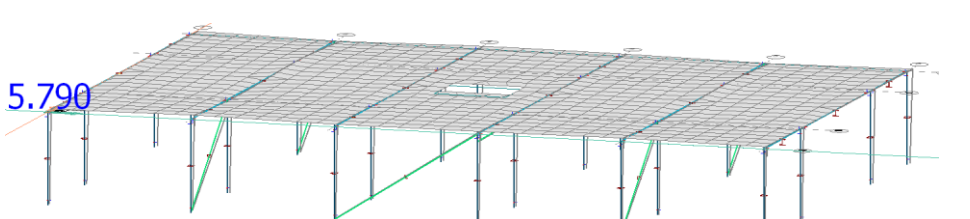
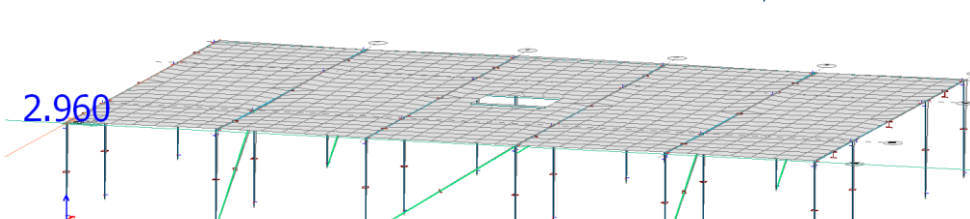
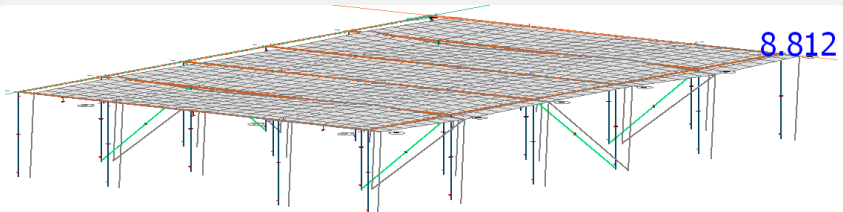
Model #1	Floor
	4
	3
	2
	1

Table 28 Total displacement of model #1 in y-direction (mm) direction – FEM-DESIGN.

Model #2	Floor
	4

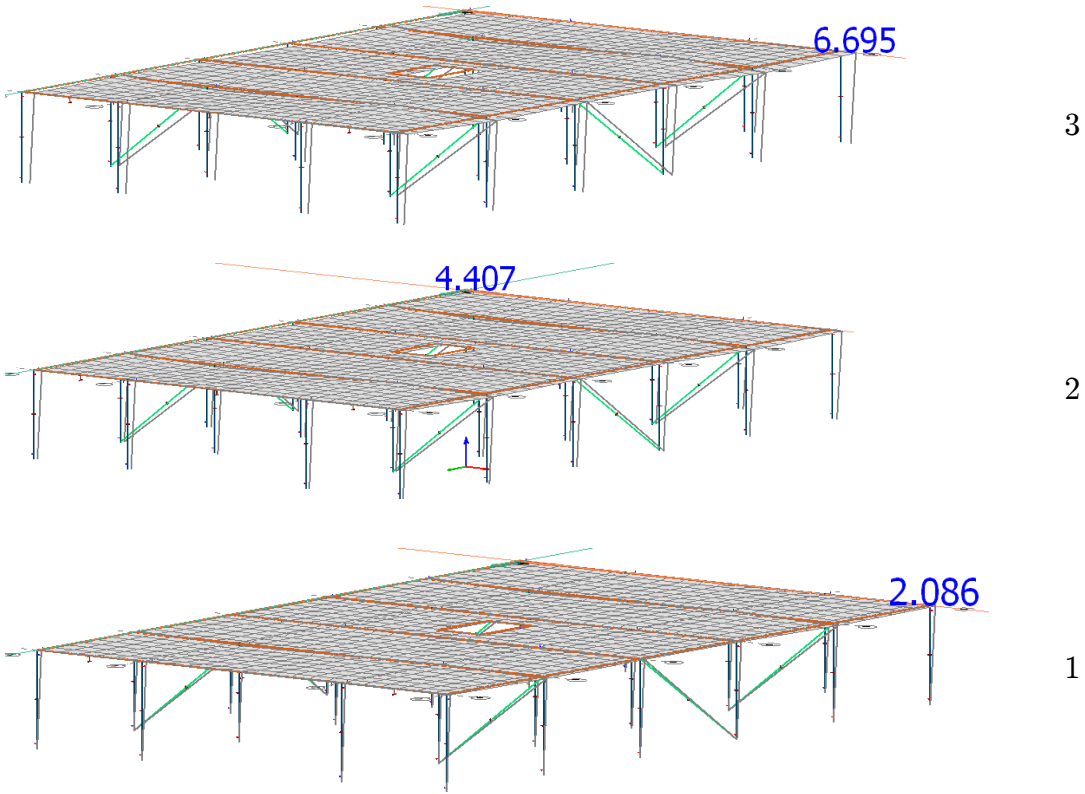
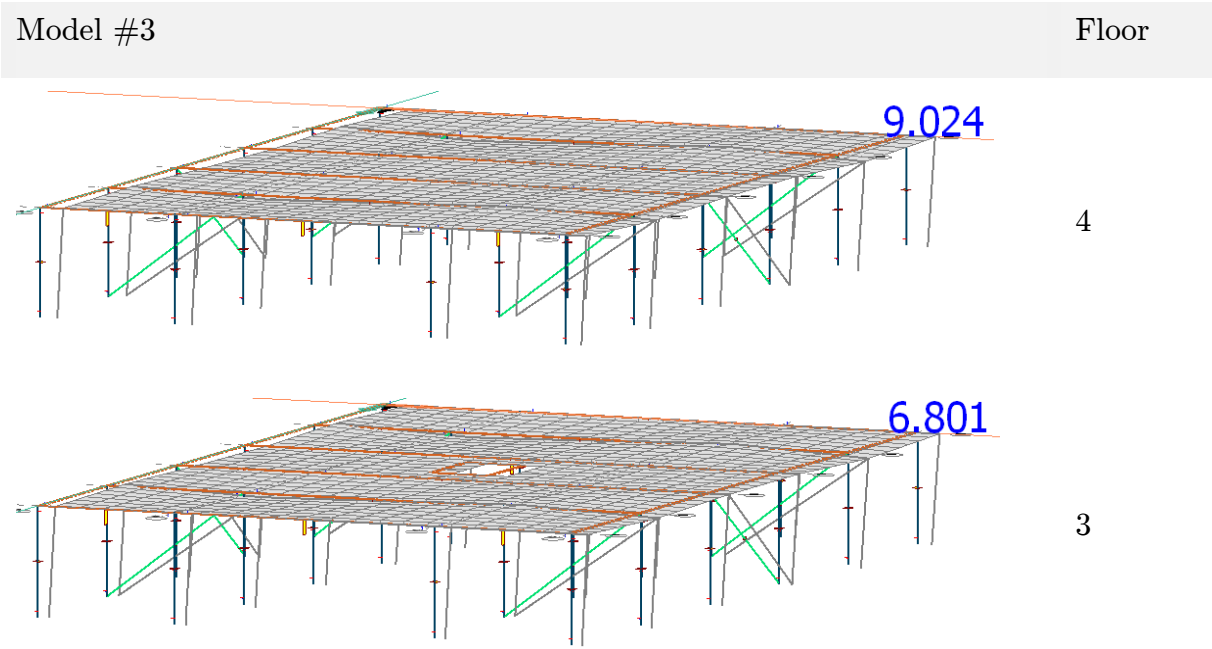


Table 29 Total displacement of model #2 in y-direction (mm) direction – FEM-DESIGN.



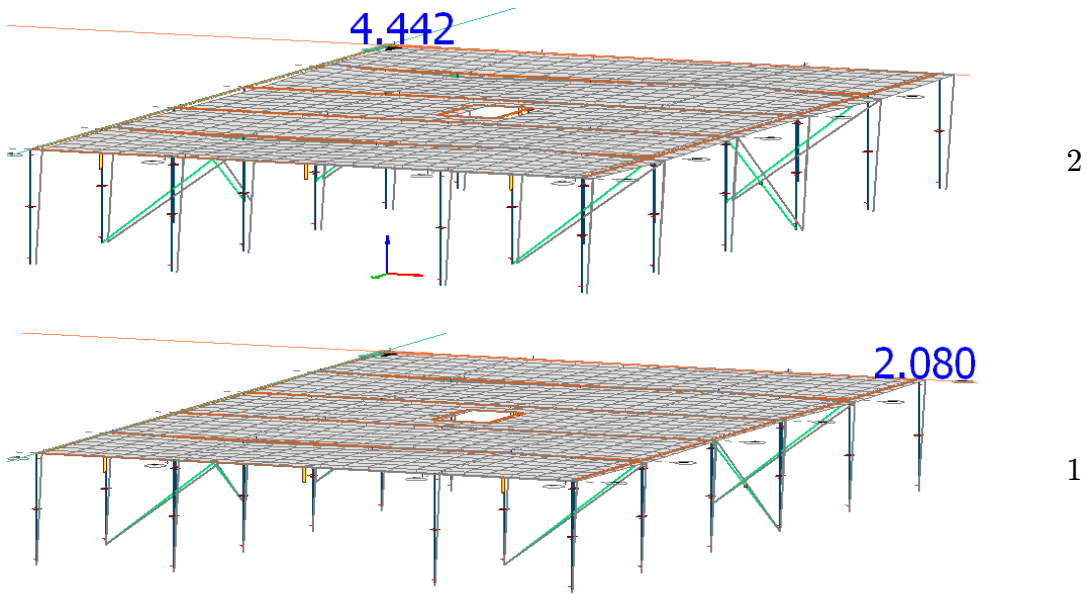


Table 30 Total displacement of model #3 in y-direction (mm) direction – FEM-DESIGN.

Model #4	Floor
	4
	3
	2

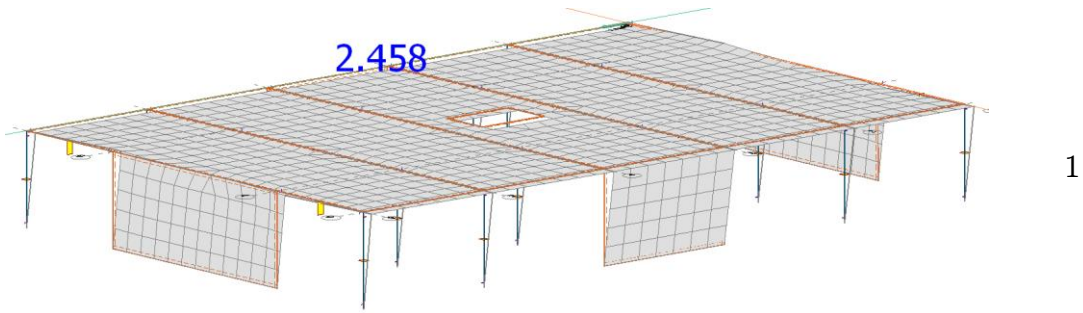


Table 31 Total displacement of model #4 in y-direction (mm) direction – FEM-DESIGN.

Displacement calculation for the second main direction, y-direction, is presented in Figure 5-19. Results indicate that all of the models have much less drift than the criteria of 15mm. It comes also to view that the displacement value for mode #1 is higher than other models. The reason for this result is the same as for the x-direction described earlier.

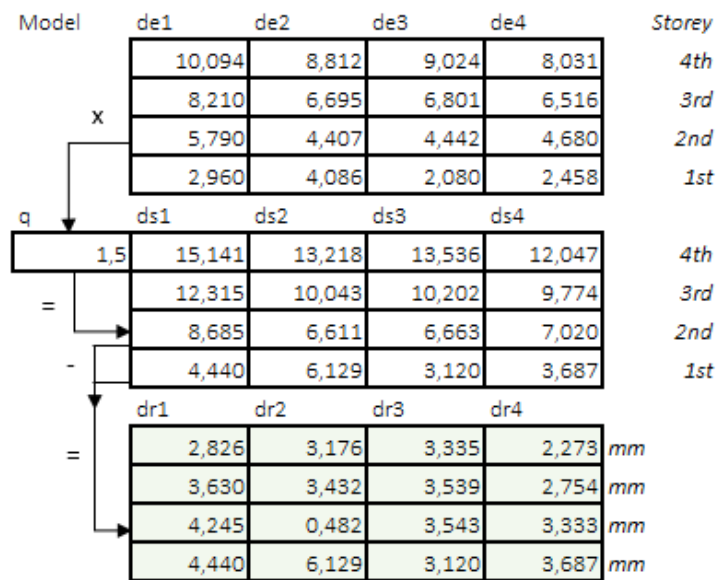


Figure 5-19 Schematic calculation of interstorey drift in y-direction

Storey	Model #1	Model #2	Model #3	Model #4
Fourth (roof)	10,094	8,812	9,024	8,031
Third	8,210	6,695	6,801	6,516
Second	5,790	4,407	4,442	4,680
First	2,960	4,086	2,080	2,458

Table 32 Displacements of different models in y-direction (mm).

By comparing forces in the bracings and the shear walls presented in [Table 21](#) and [Table 22](#) and the interstorey drift given in [Table 27](#) and [Table 32](#), we can verify what the mode shapes show. Forces acting on the first storey elements is the main cause of the deflection on top storey.

5.3.4 BASE SHEAR

Comparing the base shear from the dominant first mode and the sum in x- and y-direction provides an indication of how materials react under seismic excitation. Model #1 has the highest base shear value. Model #4 which is the full timber model has the second highest value. This is due to the level of stiffness shear walls introduce in seismic calculation. Model #2 and #3 display less shear than the others. From the calculations it looks like that introduction of timber is the main cause in the reduction of base shear. Base shear based on *EC8-1* calculation principles is also included in [Table 33](#).

[Figure 5-20](#) illustrates this change in a more visual way and gives an indication of how conservative the code provisions are. Values of the second mode that gives the displacement in y-direction, are presented in [Table 34](#) and illustrated in [Figure 5-21](#).

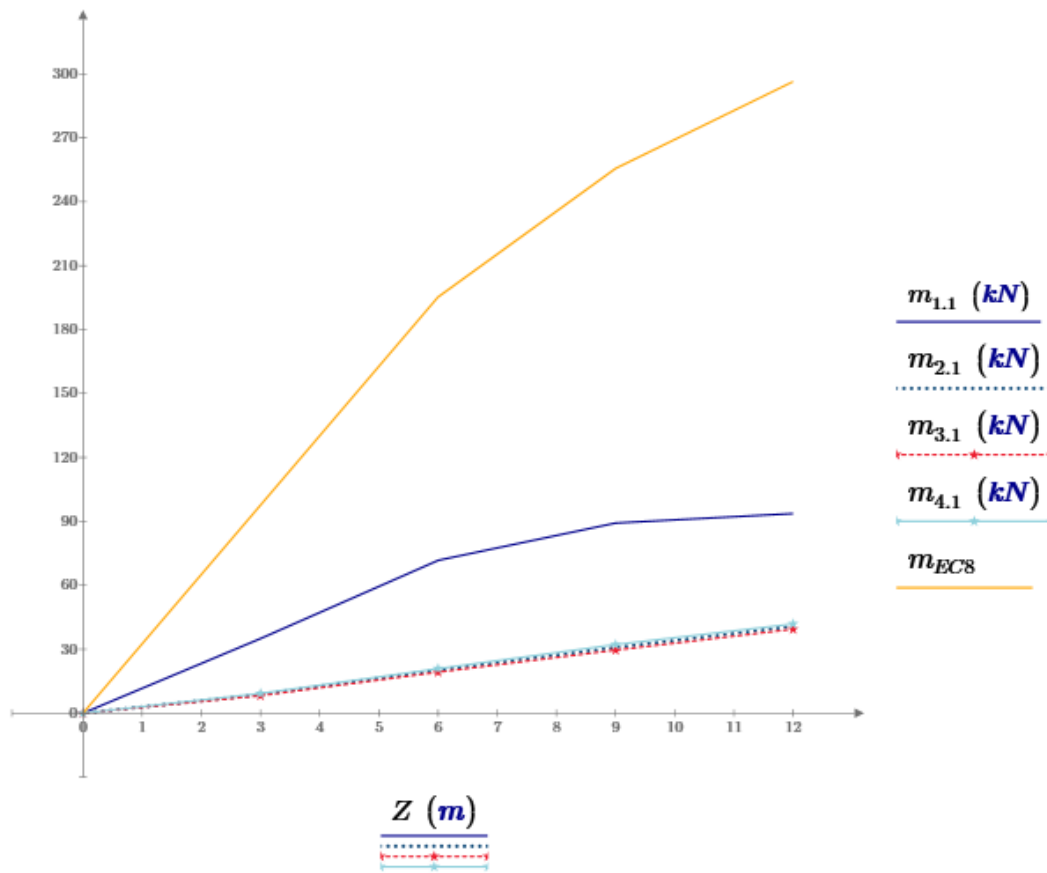


Figure 5-20 Graph showing the base shear difference between models in the first mode and the empirical formula given by EC8-1.

Storey	Model #1	Model #2	Model #3	Model #4	EC8
Fourth (roof)	93,664	40,719	39,383	41,866	277,785
Third	89,231	30,813	29,561	32,174	239,024
Second	71,693	20,194	19,226	20,892	183,024
First	35,025	8,730	8,204	9,241	91,512
Total base shear	289,613 kN	100,456 kN	96,374 kN	104,231 kN	791,879 kN

Table 33 Base shear of the first mode based on seismic calculation from FEM-DESIGN and hand calculation (kN).

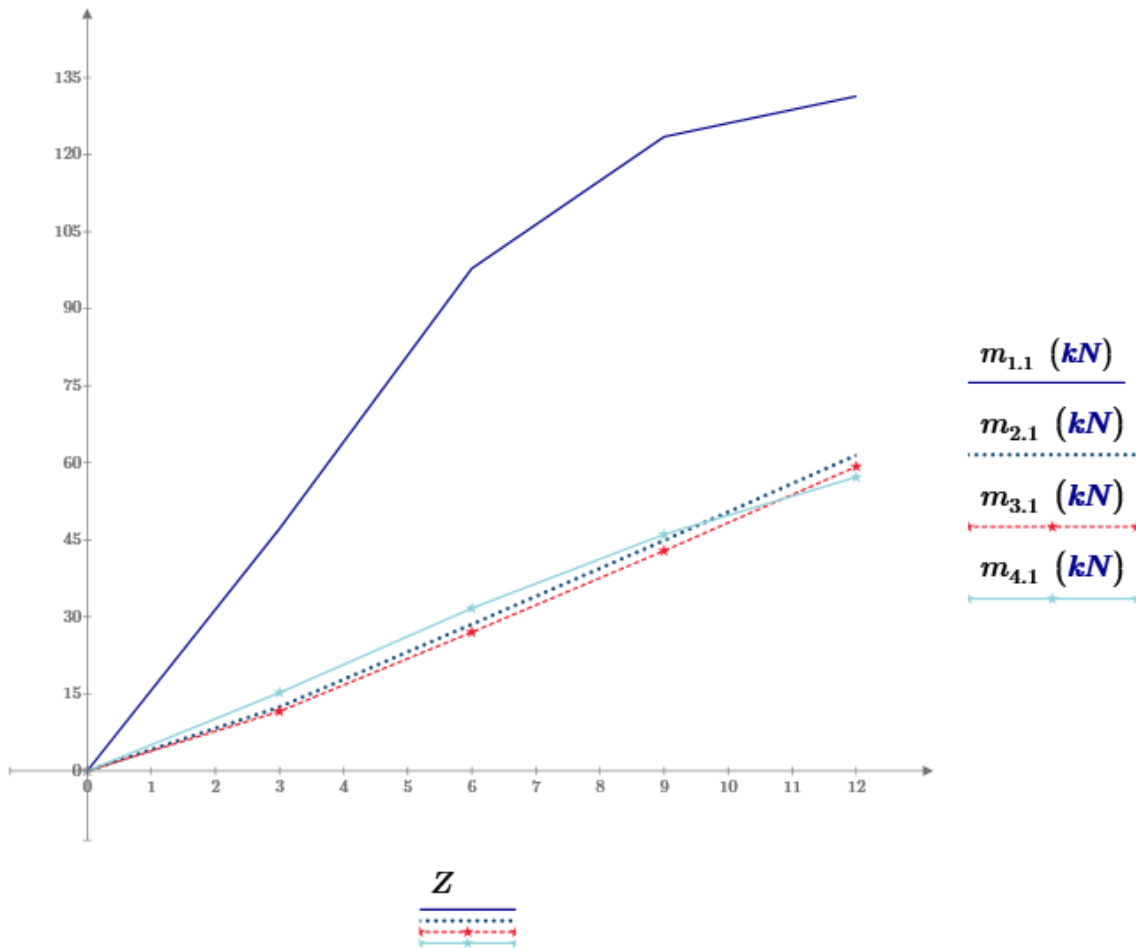


Figure 5-21 Graph showing the base shear difference between models in the second mode.

Storey	Model #1	Model #2	Model #3	Model #4
Fourth (roof)	131,391	61,488	59,271	57,200
Third	123,493	44,876	42,855	46,050
Second	97,839	28,542	26,999	31,670
First	47,166	12,430	11,584	15,229
Total base shear	399,889 kN	147,336 kN	140,709 kN	150,149 kN

Table 34 Base shear of the second mode based on seismic calculation (kN) – FEM-DESIGN.

The maximum expected seismic force acting between the ground and the structure are given in Table 35 and Table 36. These values are further presented visually in Figure 5-22 and Figure 5-23.

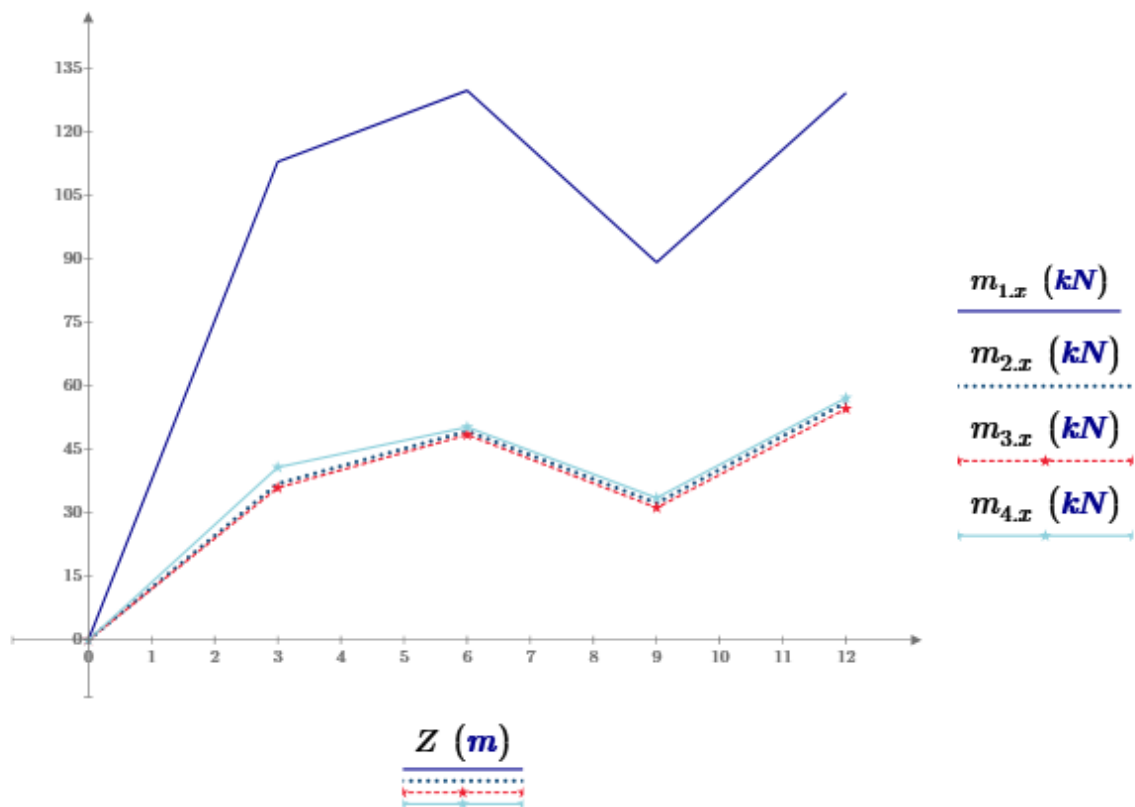


Figure 5-22 Graph showing the total base shear difference between models in x-direction.

Storey	Model #1	Model #2	Model #3	Model #4
Fourth (roof)	129,365	56,166	54,674	57,232
Third	89,275	32,378	31,293	33,607
Second	129,913	49,392	48,514	50,349
First	113,059	36,961	35,997	40,841
Total base shear	314,934 kN	113,231 kN	109,474 kN	118,575 kN

Table 35 Calculated maximum base shear force in x direction for all four models (kN) – FEM-DESIGN.

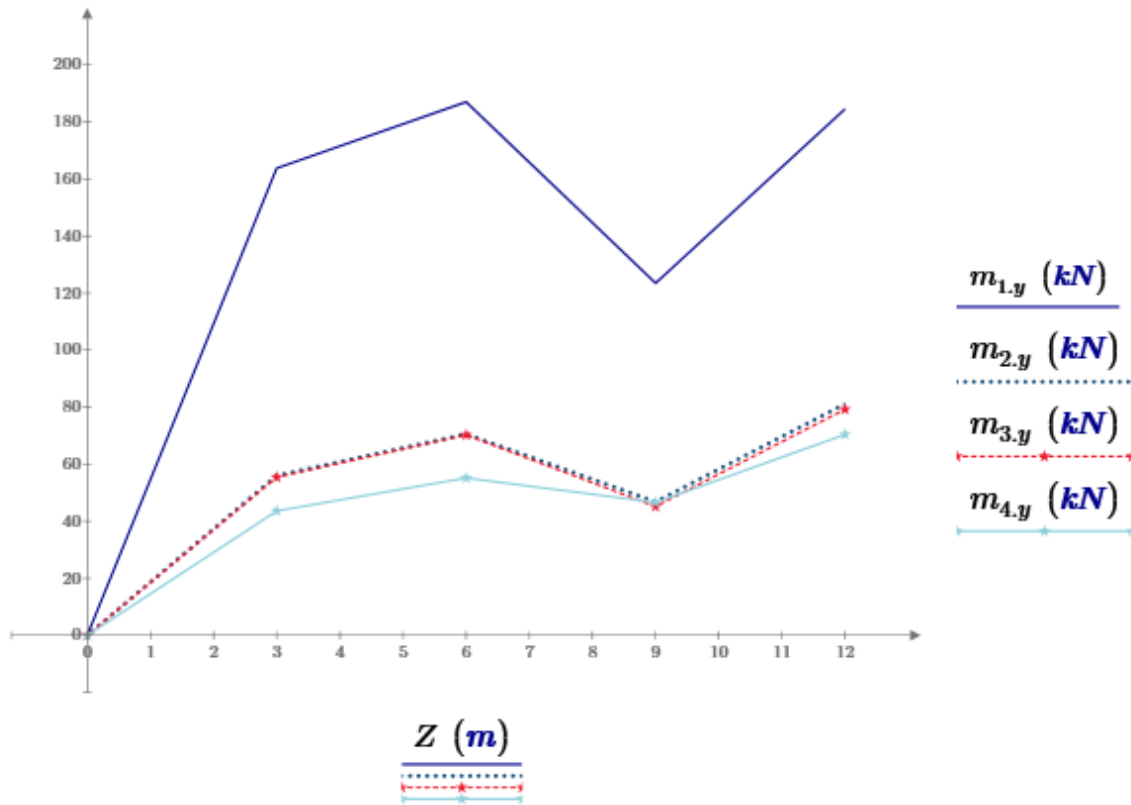


Figure 5-23 Graph showing the total base shear difference between models in y-direction.

Storey	Model #1	Model #2	Model #3	Model #4
Fourth (roof)	184,574	81,152	79,249	70,407

Third	123,493	46,819	45,179	46,627
Second	187,045	70,597	70,237	55,189
First	163,803	56,008	55,434	43,634
Total base shear	440,934 kN	165,666 kN	160,293 kN	159,174 kN

Table 36 Calculated maximum base shear force in y direction for all four models (kN) – FEM-DESIGN.

Comparing values from Table 33 and Table 34 with Table 35 and Table 36 indicates that higher modes have the bigger impact on the base shear experienced by the top storey and very little at the ground level.

Base shear of last model has been further investigated in TimberTech. Results from TimberTech are based on damage control (SLD) and life safety (SLV) performance levels. For the sake of comparison, the SLV values of 92,39 kN along the x-axis and 124,66 kN along the y-axis is used. It seems that the base shear from FEM-DESIGN mode #4 is higher than TimberTech in both directions, as presented in Table 37.

Base total shear			
Base shear - SLV seismic action along X		Base shear - SLV seismic action along Y	
$F_{h, SLV,x}$	$F_{h, SLV,y}$	$F_{h, SLV,x}$	$F_{h, SLV,y}$
[kN]	[kN]	[kN]	[kN]
92,39	1,30	1,30	124,66
Base shear - SLD seismic action along X		Base shear - SLD seismic action along Y	
$F_{h, SLD,x}$	$F_{h, SLD,y}$	$F_{h, SLD,x}$	$F_{h, SLD,y}$
[kN]	[kN]	[kN]	[kN]
69,29	0,97	0,97	93,49

Figure 5-24 Base shear results from TimberTech.

This is mainly because of how the connections are modelled in these two software. FEM-DESIGN is more rigid and therefore higher base shear.

FEM-DESIGN model #4		TIMBERTECH model #4	
x	y	x	y
118,575 kN	159,174 kN	92,39 kN	126,66 kN

Table 37 Comparing base shear of model #4 in FEM-DESIGN and TIMBERTECH.

5.4 SOFTWARE USAGE

Five different software packages were used to model and design the elements. Software packages are: **FEM-Design 16**, **CLTdesigner**, **PTC Mathcad prime 3.1** and **OVE SLETTEN** and **TimberTech**. A brief description of these software packages are presented here.

5.4.1 FEM-DESIGN

FEM-Design is a finite element software package with the ability to perform simple and extreme complicated static and dynamic analysis with materials such as concrete, steel and timber. Its simple interface and smart ability to link models from software packages such as Revit, Tekla, ArchiCAD, makes FEM-DESIGN a popular CAD tool in Norway, which is being used by the most top engineering companies.

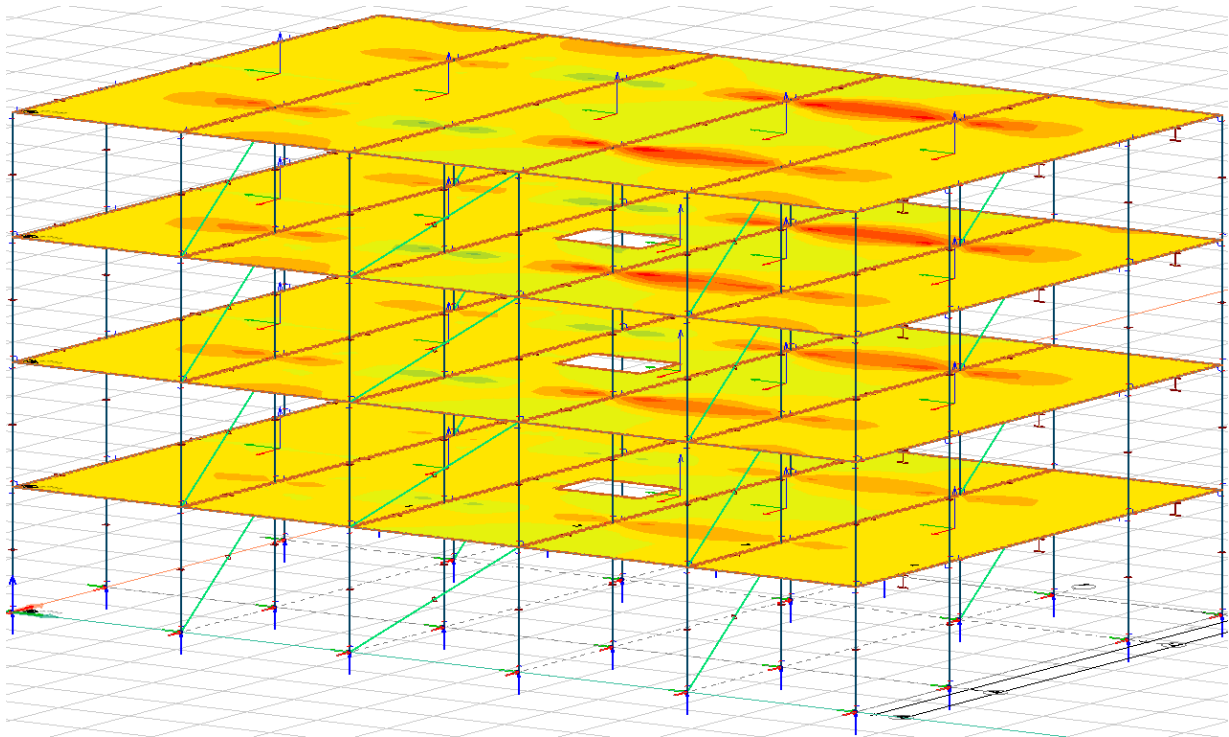


Figure 5-25 Different analysis and results in FEM-DESIGN.

Advantages of using FEM-DESIGN

- Simple interface
- Powerful in case of results with graphic and animation. Equilibrium of forces that lets users compare total horizontal forces from wind load and base shear from seismic analysis.
- Being able to add new Steel and Concrete profiles.

- Being able to produce professional reports and export to Excel.
- In addition to performing static calculations, the implementation of Eurocode in the software lets the user perform design calculations directly.
- Easy to generate surface wind loads on the entire structure, that are easily comparable with other software (like Ove Sletten)

Disadvantages of using FEM-DESING

- Timber library is far from up-to-date and lacks enough amount of profiles
- Difficult to add new profiles to CLT library without knowing how the earlier profiles were added.
- It is not possible to add deflection length for shell elements.
- The methodology of CLT calculation is accurate.

5.4.2 CLTDESIGNER

CLTdesigner is a free software based on JAVA environment, which can calculate continuous beam and plate. It verifies solid timber cross sections made of cross laminated timber in accordance to EN 1990, EN 1991-1-1, EN 1995-1-1 and the German National Annex. Methods used in this software are implemented from *CLT handbook* which is based on the new European concept for construction standards (available only in German), and are based on Timoshenko and Shear Analogy methods.

CLTdesigner is a very easy-to-use software with a simple interface. It manages to calculate the cross section with regard to fire and vibrations requirements.

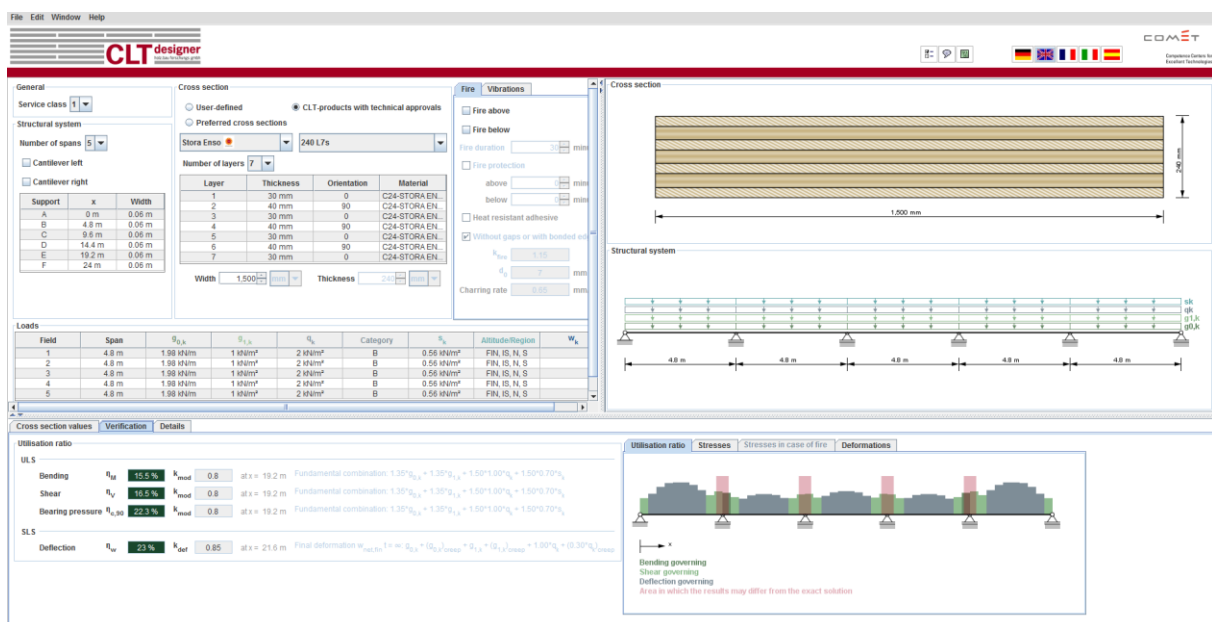


Figure 5-26 CLTdesigner environment.

5.4.3 OVE SLETTEN

OS is a series of engineering calculation applications used for calculation of concrete structures and load calculation of snow load and wind load with form factors as specified in NS-EN 1991-1-3 and NS-EN 1991-1-4.

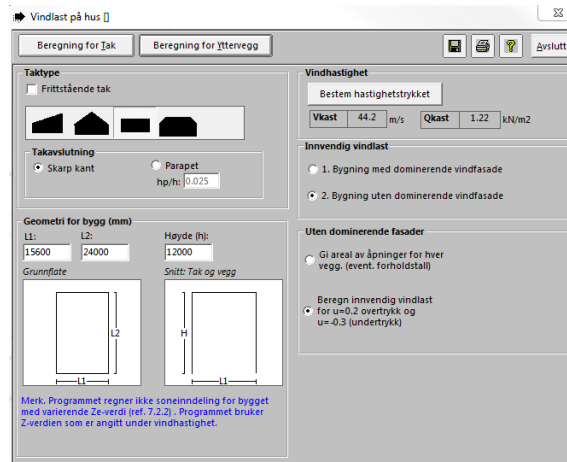


Figure 5-27 Ove Sletten snow load calculation modul.

5.4.4 MATHCAD PRIME

PTC Mathcad prime is one of most powerful engineering calculation software with its live mathematical notation, easy-to-use interface and unit intelligence. It increases the productivity and effectivity and reduces the miscalculation. In this thesis, hand calculation and graphs are created by this software. The only difficult issue is to learn the more complex formulas and using programs to define expressions that would either be impossible to construct using ranges, conditional functions and arrays.

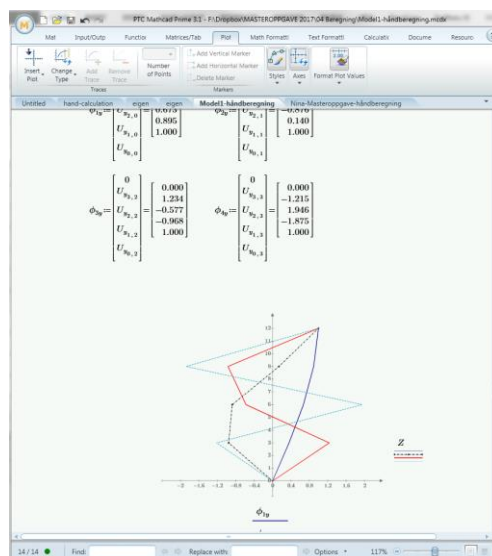


Figure 5-28 PTC Mathcad prime 3.0 envirement.

5.4.5 TIMBERTECH BUILDINGS

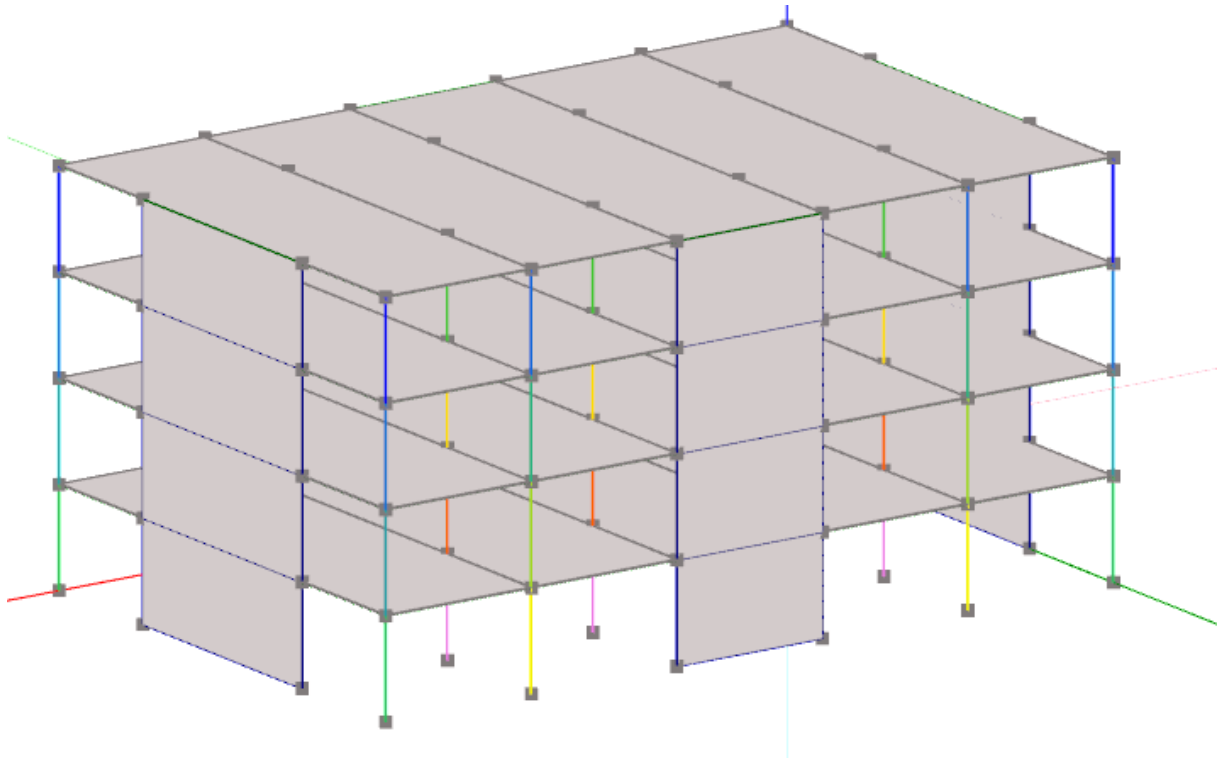


Figure 5-29 Model #4 as presented in TimberTech.

Timber Tech Buildings, developed by Timber Tech srl, startup of the University of Trento (Italy) is a structural design software for analysis of timber shear walls structures realized using both CLT and platform frame systems.

This state-of-the-art design software enables civil engineers to design and analysis the timber structure with its simple and user friendly interface, effective and powerful 3D tools, automatic generation of loads used in the analysis, ULS and SLS design check of walls, floors, beams, columns, metal fasteners and connections and seismic analysis. These advantages makes TimberTech Buildings a powerful software in the field of timber calculation.

CHAPTER 6 RESULTS, DISCUSSION AND CONCLUSION

6.1 ASSESSMENT OF ANALYSIS AND RESULTS

The **natural frequencies** presented for all four models are quite similar. Based on the similarity of the first three models in terms of bracing stiffness, it is logical to assume that the fundamental frequencies have barely any differences. For the fourth model, where the shear walls are introduced, hand calculation indicates a huge difference between stiffness of the first model and the last model. The reason for similar natural frequencies between the last model and the previous ones is that model #4 has lesser weight than model #1. Even though model #4 has higher stiffness in the shear walls than the bracing in model #1, the difference is justified by a high stiffness in model #4 and the high weight of model #1.

Modes presented in [Table 15](#) show that the *NS-EN 1998-1* criteria (see section [4.1.3](#)) are fulfilled within the fifth mode. These are the **mode shapes** with the lowest frequency and highest **effective mass**. Modes of this kind can easily be excited by ground excitation and contribute to the response of the system. [Table 15](#) also demonstrates that mode one and two are the dominant modes, and explains the most part of the system's response, as calculated by modal summation. Analyzing also indicates that the majority of mass of the structure moves in the direction these modes represent.

It is noted in model #1 that concrete slabs with high in-plane stiffness, and by acting as an infinitely rigid diaphragm, are able to carry their own weight, are able to carry their own weight and there is no need for beams in this model. Increasing a slab's thickness could eliminate use of beams. However, since the focus is the reaction of the structure when subjected to ground motion, by keeping the beams that increase the weight of structure and allowing for creep factor and shrinkage value, more realistic behavior is achieved. Timber is not as stiff as concrete and even though it can come in lengths of up to 15m, using the proposed system without beams can readily result in deformed panels. CLT panels, in contrast to traditional cast in-situ concrete slabs, are modelled with span of 4,8m. This method has caused the load transmission to the beams to be more noticeable and therefore the need for beams in the remainder of the models necessary.

The horizontal displacement in terms of **Interstorey drift**, can be determined by observing the result from both x- and y-direction, and highlights the influence of lateral forces on the columns. Drifts values are highest at the top storey, and logically decreases from fourth floor down to the foundation. Calculations and limits based on *EC8-1* indicate that interstorey drift is not a risk for structural stability. The displacements

presented in [Table 27](#) and [Table 32](#) demonstrates that the interstorey drift calculated by FEM-DESIGN is well below the drift limits set by EC8-1. Furthermore, model #1 has the highest value due to its high mass and base shear. [Table 16](#) and [Table 17](#) illustrates the first and second mode. These modes respectively indicate that the displacements in x- and y-directions are lowest in the first floor where the forces acting on them are highest, which results in top floor being displaced the most. Values for Model #4 are in the same range as the first three models. Using timber shear walls with given thickness has the same impact on the horizontal displacement as braces.

CLT floor calculation was done by experimenting with several thickness from 180mm to 240mm using Timoshenko method. Since the vibration verification had been taken into account, none of the cross sections under 240mm were satisfying the criteria according to *ON B 1995-1-1/NA:2014-11-15*, the Austrian Annex. According to the new rules in *EC5*, which will include the acceleration verification in addition to eigenfrequency and velocity, 240mm was chosen to meet the new and more demanding vibration criteria.

Parameters like dead load and stiffness are important in seismic design. By observing the natural period values of models, it seems that the stiffness has little influence. However, the change in mass from model #1 to model #4, due to the introduction of timber, has a more essential role and contribution. The influence of mass becomes apparent when comparing the ratio between 200mm concrete slab and 240mm CLT panel, which is $\frac{200mm \cdot \rho_{concrete}}{240mm \cdot \rho_{timber}} = \frac{0,2 \cdot 2,5}{0,24 \cdot 0,6} = 3,3$. **Base shear** results from [Table 35](#) and [Table 36](#) shows that the difference between model #1 and model #4 indicate an increase in base shear by a factor of three. And that the higher modes (mode with less than 5% modal mass) have relatively low impact on the total base shear.

Results from FEM-DESIGN and TIMBERTECH gives clear indication that model #4 is the second highest model in terms of base shear in x-direction. In y-direction, as the amount of bracings in model #2 and #3 have been doubled, while the amount of shear walls are the same, a marginal difference is observable.

Comparing the base shear calculated with the empirical formula and design spectrum to model #1 using same approach and fundamental period from FEM-DESIGN gives a $791,9kN/321kN = 2,5$ times difference. By looking at the [Figure 5-14](#), the same amount of difference is noticeable. The empirical equation is not based on direction (x or y), neither does it take into account the stiffness or mass of structure. Since the structure has different amount of bracings in each direction, using the empirical formula gives significantly different results.

6.2 ASSESSMENT OF WIND LOAD AND SEISMIC LOAD

This section will discuss the difference between wind load and seismic load in x and y direction for model #1 in order to determine the design load.

DCL is defined by choosing a behavior factor less or equal to 1,5, when calculating the seismic forces on a structure. Choosing this class offers a much less complicated approach. Even though DCL and DCM are those classes adopted in Norway, EC8-1 requires composite structures of steel and concrete to fulfil the criteria if they are to be designed in accordance with the requirements that apply to DCL. This criteria is given in *EC8-1 NA 3.2.1(4)* and presented below:

$$a_g S < 0,25g = 2,45 \frac{m}{s^2}$$

There are also other conditions beside the difference between wind load and base shear that affects elimination of seismic calculation, reference is made to section 03.3.2.9. Based on the calculation of base shear showed earlier in Table 35 and Table 36 and wind load in APPENDIX C, we can verify that wind load is the design load and should be calculated in combination with other loads, such as dead loads and permanent load. The difference between the values are given in Table 38.

Wind load (kN)		Seismic load (kN)		W _x vs S _x	W _y vs S _y
X	Y	X	Y		
385,39	650,95	314,93	440,93	-18 %	-32 %

Table 38 Comparison of loads in x and y direction.

This conclusion is not far from the reality of structural design in Norway. Most of the buildings which are in seismic class *I* and *II* are calculated in accordance to requirement for wind load. Ground conditions should always be a main parameter in choosing which design values to design the structure after. If a rectangular shaped building located in ground type B or C, as shown in Table 4, is designed with wind load and shear walls in the short direction, seismic load and bracings in the long direction, this approach can be formulated as an optimized case. In other cases, it is sufficient to consider the wind load in both directions. It is also worth mentioning that, in terms of foundation and stability of a building on a site with poor soil conditions, using timber offers more economically efficient solution. The weight of a timber building does not require soil stabilization measures such as lime cement piles.

6.3 CONCLUSION

Seismic load, in contrast to wind load, decreases with the height of the structure. It comes as a vibration force from ground and acts on the primary elements of the structure. How a multistorey building can survive this force transmission depends on its ductility and ability to dissipate the energy during earthquakes. Achieving an idealized design concept involves making crucial decisions about the materials and systems, bearing in mind the type of force acting on it.

In this thesis, it has been verified that experimenting with different materials in terms of stability and load bearing capacity is necessary for different scenarios. This thesis studies several types of multistorey building that are constructed in Norway, and through applying seismic analysis, has examined different materials and case studies. Based on comparison of the results from the four presented examples, the author can conclude the following;

- Using timber improves the seismic performance of a hybrid building. By changing the concrete slab to CLT panel and reducing weight, seismic load decreased by almost by three times. This also gives a structure the benefit of being more resistant to earthquake forces.
- Timber multistorey buildings have higher seismic deformations that increases linearly with their height. This represents a huge challenge in addition to fire-safety at a high level.
- Hybrid multistorey structures of steel-timber or concrete-timber are better replacements than traditionally concrete or steel structures in regions with seismic activity and poor soil conditions. A concrete-timber solution offers a much more suitable solution for floor structure. The weight of concrete reduces the problems with wind shear and vibrations that timber structures struggle with. It is, therefore, important to combine materials for each objective of construction.
- CLT panels are relatively new form of constructing elements in Norway. This is in spite of the fact that there is no domestic production of this type in the country. Due to having properties such as weight, being visually appealing and high load-bearing capacity, they have quickly become a popular construction material along with already established glulam.
- Higher mass and stiffness gives higher load effects from ground motion. Mass in contrast to stiffness gives higher natural periods.

It has also been acknowledged from research for this thesis that using timber introduces some advantages, challenges and solutions worth mentioning. These are listed below:

- Determining total stiffness in the building is very important in terms of finding the correct shear forces values. Timber to timber shear connection are usually performed by adding many angle brackets. This should be modelled and calculated correctly in terms getting the actual stiffness and base shear value of the timber building.
- Low weight, knowing the environmental aspects of the material and the visual quality, less waste at site and faster construction time (up to 30% faster than concrete structure) are some of benefits timber brings to the construction industry.
- Fire safety requirements for a timber building can be addressed by internally applying gypsum board and also by increasing the thickness of CLT elements.
- Acoustic challenges of timber structures are always demanding because of the weight of material. Noises at low frequency are very difficult to block. Adding a layer of sound insulation plate inside of the building, or increasing the mass of the floors by using a concrete cast on top of the surface may give a better sound insulation performance.
- Less work traffic to job site since all the elements are prefabricated and transported predominantly at the same time.
- Using prefabricated modules of cross-laminated timber in buildings in contrast to concrete that mainly is casted at the site gives the benefit of efficiency. Also by using timber as an all-weather material, constructing is possible any time of the year. Whereas with concrete, the weather and temperature can delay the project.

6.4 PROPOSED FURTHER WORK

The purpose of this thesis was to examine the benefits of adding various levels timber ratio added to different multistorey buildings. A significant amount of further work remains in terms of clarifying timber and its behavior when used in combination to other materials. The following themes are proposed based on outcome of this thesis:

- Several producers offer materials with different properties. Moelven in Norway produces GL30c, SINTEF recommends GL32c and other manufactories around the Europe like Eugen Decker, Binderholz, Derix, Hasslacher, HMS, KLH, MM Kaufmann and Stora Enso produce their technical approved CLT-products commonly with material type C24 $f_{m,k} = 24 \frac{N}{mm^2}$. We see that the Young modulus, measure of stiffness, varies differently from manufacturer to manufacturer. This makes it difficult to use a software like FEM-DESIGN where the timber module is very poor and misleading. For further studies, it is proposed to collect more data about behavior of CLT and GLT in a taller timber building. Changing the geometry and analyzing a new range of challenges that timber structures face, in addition to earthquakes.
- Addressing the challenges and limitation of software used for seismic analysis introduce, comparing ROBOT, FEM-DESING and TIMBERTECH will be very interesting. This will be of great advantage to engineers wishing to work effectively with timber.
- Analyzing timber structures with semi-rigid steel connectors, instead of bracing elements.
- Establish a better understanding of how effective seismic effect on structures can dissipate, use of seismic dampers and other isolators for reducing the effect of earthquake on buildings is proposed.

APPENDIX A HAND CALCULATION

Hand calculation documentation from MATHCAD for the first model is as followed:

Mass matrix

$$\rho_c = 25000 \frac{N}{m^3} \quad g = 9.81 \frac{m}{s^2} \quad Q_{nonstructure} = 1000 \frac{N}{m^2} \quad Q_{snow} = 560 \frac{N}{m^2}$$

$$Q_{liveload} = 2000 \frac{N}{m^2}$$

$$t_c = 0.20 \text{ m} \quad L_1 = 4.8 \text{ m} \quad W_1 = 4 \text{ m} \quad W_2 = 7.6 \text{ m}$$

$$L_2 = 15.6 \text{ m} \quad L_3 = 4 \text{ m} \quad H = 3 \text{ m}$$

Mass on each floor with 500N/m2 is then:

$$m_{g,d} = \frac{\rho_c}{g} t_c + \frac{Q_{nonstructure}}{g} 5 L_1 + 2 W_1 + W_2 = 229 \cdot 10^3 \text{ kg}$$

Shaf's area is not neglected since they are not considered in the process.

$$\rho_s = 7850 \frac{kg}{m^3} \quad \text{Column } 200 \times 200 \times 12,5 \quad A_{RHS} = 9208 \text{ mm}^2$$

$$\text{Truss } 120 \times 120 \times 6,3 \quad A_{TRUSS} = 2823 \text{ mm}^2$$

$$\text{Beam HE-B 200} \quad A_{HEB} = 7808 \text{ mm}^2$$

Mass of steel on each floor with is then:

$$m_{g,s} = \rho_s \left(4 \sqrt{L_1^2 + H^2} + 8 \sqrt{W_1^2 + H^2} \right) A_{TRUSS} + 6 \cdot 4 \cdot H \cdot A_{RHS} + 6 \cdot L_2 \cdot A_{HEB}$$

$$m_{g,s} = 12.3 \cdot 10^3 \text{ kg}$$

$$m_{p,4} = \frac{Q_{snow}}{g} 5 L_1 + 2 W_1 + W_2 = 21.4 \cdot 10^3 \text{ kg}$$

$$m_{p,1} = \frac{Q_{liveload}}{g} 5 L_1 + 2 W_1 + W_2 = 76.3 \cdot 10^3 \text{ kg}$$

$$m_{p,2} = m_{p,1} \quad m_{p,3} = m_{p,1}$$

$$m_1 = m_{g,d} + m_{g,s} + m_{p,1} = 318 \cdot 10^3 \text{ kg}$$

$$m_4 = m_{g,d} + \frac{1}{2} m_{g,s} + m_{p,4} = 257 \cdot 10^3 \text{ kg}$$

$$m_2 = m_1 \quad m_3 = m_1$$

Mass matrix is then

$$m := \begin{bmatrix} m_4 & 0 & 0 & 0 \\ 0 & m_3 & 0 & 0 \\ 0 & 0 & m_2 & 0 \\ 0 & 0 & 0 & m_1 \end{bmatrix} = \begin{bmatrix} 257 \cdot 10^3 & 0 & 0 & 0 \\ 0 & 318 \cdot 10^3 & 0 & 0 \\ 0 & 0 & 318 \cdot 10^3 & 0 \\ 0 & 0 & 0 & 318 \cdot 10^3 \end{bmatrix} \text{ kg}$$

Stiffness matrix in x-direction

$$E_s = 210000 \text{ MPa} \quad H = 3 \text{ m}$$

$$l_{\text{truss}} = \sqrt{H^2 + L_3^2} = 5000 \text{ mm} \quad l_{\text{column}} = 3000 \text{ mm}$$

Forces are calculated by criteria of equilibrium in each end

$$S_{1,\text{Truss}} = \frac{1}{\cos \operatorname{atan} \frac{H}{L_3}} = 1.25$$

$$S_{0,\text{Truss}} = \frac{1}{\cos \operatorname{atan} \frac{H}{L_3}} = 1.25$$

$$S_{1,\text{RHS}} = S_{1,\text{Truss}} \sin \operatorname{atan} \frac{H}{L_3} = 0.75$$

$$S_{0,\text{RHS}} = S_{1,\text{Truss}} \sin \operatorname{atan} \frac{H}{L_3} = 0.75$$

$$x = 7.2 \quad L_e = 14.4$$

$$\delta = 1 + 1.2 \frac{x}{L_e} = 1.6$$

$$F = \frac{\delta}{S_{1,\text{Truss}}^2 \frac{l_{\text{truss}}}{A_{\text{Truss}} E_s} + S_{1,\text{RHS}}^2 \frac{l_{\text{column}}}{A_{\text{RHS}} E_s}}$$

$$k_x = \frac{F}{\delta} = 71.2 \cdot 10^6 \frac{\text{N}}{\text{m}}$$

$$K_x := 2 \begin{bmatrix} k_x & -k_x & 0 & 0 \\ -k_x & 2 \cdot k_x & -k_x & 0 \\ 0 & -k_x & 2 \cdot k_x & -k_x \\ 0 & 0 & -k_x & 2 \cdot k_x \end{bmatrix} = \begin{bmatrix} 142 & -142 & 0 & 0 \\ -142 & 285 & -142 & 0 \\ 0 & -142 & 285 & -142 \\ 0 & 0 & -142 & 285 \end{bmatrix} 10^6 \frac{\text{N}}{\text{m}}$$

Geometrical stiffness matrix

$$\mu = 1.5$$

$$k_G := \mu \cdot \frac{g}{H} \begin{bmatrix} m_4 & -m_4 & 0 & 0 \\ -m_4 & m_3 + 2 \cdot m_4 & -m_3 - m_4 & 0 \\ 0 & -m_3 - m_4 & m_2 + 2 \cdot m_3 + 2 \cdot m_4 & -m_2 - m_3 - m_4 \\ 0 & 0 & -m_2 - m_3 - m_4 & m_1 + 2 \cdot m_2 + 2 \cdot m_3 + 2 \cdot m_4 \end{bmatrix}$$

$$k_G = \begin{bmatrix} 1 & -1 & 0 & 0 \\ -1 & 4 & -3 & 0 \\ 0 & -3 & 7 & -4 \\ 0 & 0 & -4 & 10 \end{bmatrix} 10^6 \frac{N}{m}$$

Combined matrix

		0
		3
Height of	Z	6
the building		9
		12

$$K_{cx} := K_x - k_G = \begin{bmatrix} 141 & -141 & 0 & 0 \\ -141 & 281 & -140 & 0 \\ 0 & -140 & 277 & -138 \\ 0 & 0 & -138 & 274 \end{bmatrix} 10^6 \frac{N}{m}$$

Eigenvalue

$$\lambda := \text{eigenvals}(m^{-1} \cdot K_x) = \begin{bmatrix} 1.57 \cdot 10^3 \\ 1.07 \cdot 10^3 \\ 468.07 \\ 54.42 \end{bmatrix}$$

$$\lambda = \begin{bmatrix} 54.422 \\ 468.069 \\ 1.070 \cdot 10^3 \\ 1.572 \cdot 10^3 \end{bmatrix} \quad \lambda := \text{sort}(\text{eigenvals}(m^{-1} \cdot K_x))$$

Natural frequency

$$\omega_n := \sqrt{\lambda} = \begin{bmatrix} 7.38 \\ 21.63 \\ 32.72 \\ 39.65 \end{bmatrix}$$

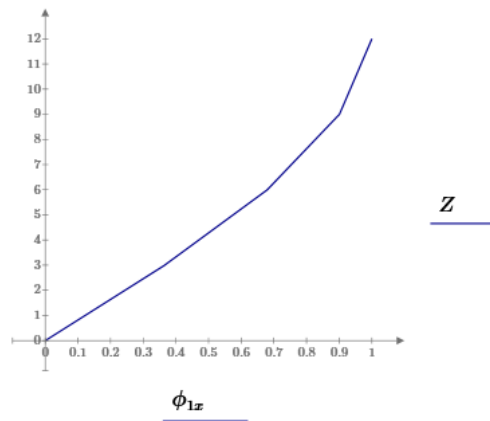
Natural period

$$T_x := \frac{2 \pi}{\omega_n} = \begin{bmatrix} 0.852 \\ 0.29 \\ 0.192 \\ 0.158 \end{bmatrix}$$

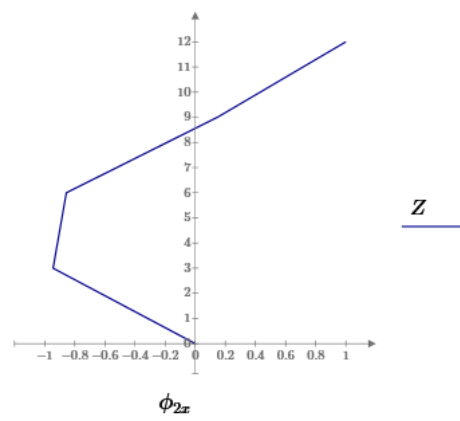
$$U_x^{(i)} := \frac{\text{eigenvec}(m^{-1} \cdot K_x, \lambda_i)}{\text{eigenvec}(m^{-1} \cdot K_x, \lambda_i)_{\text{ORIGIN}}}$$

$$U_x = \begin{bmatrix} 1 & 1 & 1 & 1 \\ 0.901 & 0.147 & -0.951 & -1.866 \\ 0.68 & -0.856 & -0.595 & 1.884 \\ 0.365 & -0.944 & 1.238 & -1.15 \end{bmatrix}$$

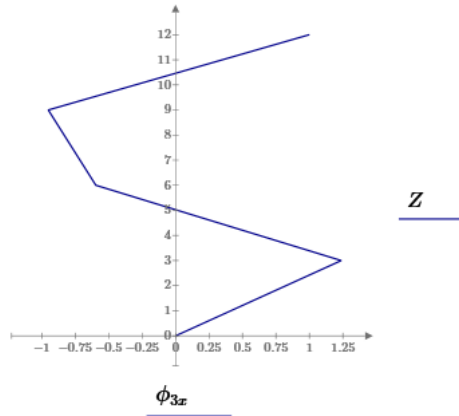
$$\phi_{1x} := \begin{bmatrix} 0 \\ U_{x_{3,0}} \\ U_{x_{2,0}} \\ U_{x_{1,0}} \\ U_{x_{0,0}} \end{bmatrix} = \begin{bmatrix} 0.000 \\ 0.365 \\ 0.680 \\ 0.901 \\ 1.000 \end{bmatrix}$$



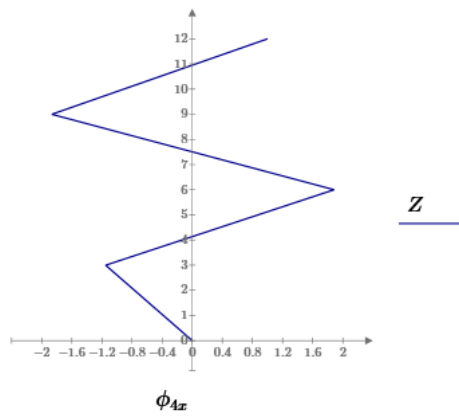
$$\phi_{2x} := \begin{bmatrix} 0 \\ U_{x_{3,1}} \\ U_{x_{2,1}} \\ U_{x_{1,1}} \\ U_{x_{0,1}} \end{bmatrix} = \begin{bmatrix} 0.000 \\ -0.944 \\ -0.856 \\ 0.147 \\ 1.000 \end{bmatrix}$$



$$\phi_{3x} := \begin{bmatrix} 0 \\ U_{x_{3,2}} \\ U_{x_{2,2}} \\ U_{x_{1,2}} \\ U_{x_{0,2}} \end{bmatrix} = \begin{bmatrix} 0.000 \\ 1.238 \\ -0.595 \\ -0.951 \\ 1.000 \end{bmatrix}$$



$$\phi_{4x} := \begin{bmatrix} 0 \\ U_{x_{3,3}} \\ U_{x_{2,3}} \\ U_{x_{1,3}} \\ U_{x_{0,3}} \end{bmatrix} = \begin{bmatrix} 0.000 \\ -1.150 \\ 1.884 \\ -1.866 \\ 1.000 \end{bmatrix}$$



Modal mass

$$L_{1x} \phi_{1x}^T m \iota \quad M_{1x} \phi_{1x}^T m \phi_{1x} = 7.045 \cdot 10^5$$

$$m_{1x} \iota^T \frac{L_{1x}}{M_{1x}} m \phi_{1x} = 1.1 \cdot 10^6$$

$$L_{2x} \phi_{2x}^T m \iota \quad M_{2x} \phi_{2x}^T m \phi_{2x} = 7.805 \cdot 10^5$$

$$m_{2x} \iota^T \frac{L_{2x}}{M_{2x}} m \phi_{2x} = 982.9 \cdot 10^3$$

$$L_{3x} \phi_{3x}^T m \iota \quad M_{3x} \phi_{3x}^T m \phi_{3x} = 1.145 \cdot 10^6$$

$$m_{3x} \iota^T \frac{L_{3x}}{M_{3x}} m \phi_{3x} = 22 \cdot 10^3$$

$$L_{4x} \phi_{4x}^T m \iota \quad M_{4x} \phi_{4x}^T m \phi_{4x} = 2.913 \cdot 10^6$$

$$m_{4x} \iota^T \frac{L_{4x}}{M_{4x}} m \phi_{4x} = 3.6 \cdot 10^3$$

$$m_{tot} \quad \ell^T m \quad \ell = 1.211 \cdot 10^6$$

We now find the relation between modal mass for each mode in relation to the total mass:

$$m_{1x} \quad \frac{m_{1x}}{m_{tot}} = 0.899 \quad m_{2x} \quad \frac{m_{2x}}{m_{tot}} = 0.812$$

$$m_{3x} \quad \frac{m_{3x}}{m_{tot}} = 0.018 \quad m_{4x} \quad \frac{m_{4x}}{m_{tot}} = 0.003$$

Stiffness matrix in y-direction

$$l_{truss} \quad \sqrt{H^2 + L_1^2} = 5660.39 \text{ mm} \quad H = 3 \text{ m}$$

$$l_{column} \quad 3000 \text{ mm}$$

Steel quality of both columns and trusses is S355 which gives a Elastic modulus

Forces are calculated by criteria of equilibrium in each end

$$S_{1,Truss} \quad \frac{1}{\cos \operatorname{atan} \frac{H}{L_1}} = 1.18 \quad S_{0,Truss} \quad \frac{1}{\cos \operatorname{atan} \frac{H}{L_1}} = 1.18$$

$$S_{1,RHS} \quad S_{1,Truss} \sin \operatorname{atan} \frac{H}{L_1} = 0.63 \quad S_{0,RHS} \quad S_{1,Truss} \sin \operatorname{atan} \frac{H}{L_1} = 0.63$$

δ 1.6 Torsional effect

$$F \quad \frac{\delta}{S_{1,Truss}^2 \frac{l_{truss}}{A_{Truss} E_s} + S_{1,RHS}^2 \frac{l_{column}}{A_{RHS} E_s}}$$

$$k_y \quad \frac{F}{\delta} = 72 \cdot 10^6 \frac{N}{m}$$

$$K_y := 4 \begin{bmatrix} k_y & -k_y & 0 & 0 \\ -k_y & 2 \cdot k_y & -k_y & 0 \\ 0 & -k_y & 2 \cdot k_y & -k_y \\ 0 & 0 & -k_y & 2 \cdot k_y \end{bmatrix} = \begin{bmatrix} 288 & -288 & 0 & 0 \\ -288 & 576 & -288 & 0 \\ 0 & -288 & 576 & -288 \\ 0 & 0 & -288 & 576 \end{bmatrix} 10^6 \frac{N}{m}$$

The combined stiffness matrix

$$K_{cy} := K_y - k_C = \begin{bmatrix} 287 & -287 & 0 & 0 \\ -287 & 572 & -285 & 0 \\ 0 & -285 & 569 & -284 \\ 0 & 0 & -284 & 566 \end{bmatrix} 10^6 \frac{N}{m}$$

Eigenvalue

$$\lambda := \text{eigenvals}(m^{-1} \cdot K_y) = \begin{bmatrix} 3.21 \cdot 10^3 \\ 2.2 \cdot 10^3 \\ 960.04 \\ 117.05 \end{bmatrix} \quad \lambda = \begin{bmatrix} 117.04849 \\ 960.03828 \\ 2.19721 \cdot 10^3 \\ 3.21036 \cdot 10^3 \end{bmatrix}$$

$$\lambda := \text{sort}(\text{eigenvals}(m^{-1} \cdot K_y))$$

Natural frequency

$$\omega := \sqrt{\lambda} = \begin{bmatrix} 10.82 \\ 30.98 \\ 46.87 \\ 56.66 \end{bmatrix}$$

Natural period

$$T_y := \frac{2 \pi}{\omega} = \begin{bmatrix} 0.581 \\ 0.203 \\ 0.134 \\ 0.111 \end{bmatrix}$$

$$i := 0..3$$

$$U_y^{(i)} := \frac{\text{eigenvec}(m^{-1} \cdot K_y, \lambda_i)}{\text{eigenvec}(m^{-1} \cdot K_y, \lambda_i)_{\text{ORIGIN}}}$$

$$U_y = \begin{bmatrix} 1 & 1 & 1 & 1 \\ 0.895 & 0.14 & -0.968 & -1.875 \\ 0.673 & -0.876 & -0.577 & 1.946 \\ 0.361 & -0.954 & 1.234 & -1.215 \end{bmatrix}$$

$$\phi_{1y} := \begin{bmatrix} 0 \\ U_{y_{3,0}} \\ U_{y_{2,0}} \\ U_{y_{1,0}} \\ U_{y_{0,0}} \end{bmatrix} = \begin{bmatrix} 0.000 \\ 0.361 \\ 0.673 \\ 0.895 \\ 1.000 \end{bmatrix} \quad \phi_{2y} := \begin{bmatrix} 0 \\ U_{y_{3,1}} \\ U_{y_{2,1}} \\ U_{y_{1,1}} \\ U_{y_{0,1}} \end{bmatrix} = \begin{bmatrix} 0.000 \\ -0.954 \\ -0.876 \\ 0.140 \\ 1.000 \end{bmatrix}$$

$$\phi_{3y} := \begin{bmatrix} 0 \\ U_{y_{3,2}} \\ U_{y_{2,2}} \\ U_{y_{1,2}} \\ U_{y_{0,2}} \end{bmatrix} = \begin{bmatrix} 0.000 \\ 1.234 \\ -0.577 \\ -0.968 \\ 1.000 \end{bmatrix} \quad \phi_{4y} := \begin{bmatrix} 0 \\ U_{y_{3,3}} \\ U_{y_{2,3}} \\ U_{y_{1,3}} \\ U_{y_{0,3}} \end{bmatrix} = \begin{bmatrix} 0.000 \\ -1.215 \\ 1.946 \\ -1.875 \\ 1.000 \end{bmatrix}$$

Modal mass

$$L_{1y} \phi_{1y}^T m \iota = 8.705 \cdot 10^5 \quad M_{1y} \phi_{1y}^T m \phi_{1y} = 6.973 \cdot 10^5$$

$$m_{1y} \iota^T \frac{L_{1y}}{M_{1y}} m \phi_{1y} = 1.1 \cdot 10^6$$

$$L_{2y} \phi_{2y}^T m \iota = 8.705 \cdot 10^5 \quad M_{2y} \phi_{2y}^T m \phi_{2y} = 7.965 \cdot 10^5$$

$$m_{2y} \iota^T \frac{L_{2y}}{M_{2y}} m \phi_{2y} = 951.3 \cdot 10^3$$

$$L_{3y} \phi_{3y}^T m \iota = 1.584 \cdot 10^5 \quad M_{3y} \phi_{3y}^T m \phi_{3y} = 1.145 \cdot 10^6$$

$$m_{3y} \iota^T \frac{L_{3y}}{M_{3y}} m \phi_{3y} = 22 \cdot 10^3$$

$$L_{4y} \phi_{4y}^T m \iota = 1.067 \cdot 10^5 \quad M_{4y} \phi_{4y}^T m \phi_{4y} = 3.048 \cdot 10^6$$

$$m_{4y} \iota^T \frac{L_{4y}}{M_{4y}} m \phi_{4y} = 3.7 \cdot 10^3$$

$$m_{tot} \iota^T m \iota = 1.211 \cdot 10^6$$

We now find the relation between modal mass for each mode in relation to the total mass:

$$m_{1y} \frac{m_{1y}}{m_{tot}} = 0.897 \quad m_{2y} \frac{m_{2y}}{m_{tot}} = 0.786$$

$$m_{3y} \frac{m_{3y}}{m_{tot}} = 0.018 \quad m_{4y} \frac{m_{4y}}{m_{tot}} = 0.003$$

Relation between modes

$$\frac{T_{y_{0,0}}}{T_{x_{0,0}}} = 0.682 \quad \frac{T_{y_{1,0}}}{T_{x_{1,0}}} = 0.698 \quad \frac{T_{y_{2,0}}}{T_{x_{2,0}}} = 0.698 \quad \frac{T_{y_{3,0}}}{T_{x_{3,0}}} = 0.7$$

Finding the base shear with formula from EC8 based on calculated fundamental period:

$$T_c := 0.2 \quad S := 1 \quad a_g := 0.744 \quad q := 1.5$$

$$T_{1x} := T_{x_{0,0}} = 0.852 \quad T_{1y} := T_{y_{0,0}} = 0.581$$

$$\lambda_{correction} := 1 \quad \text{Since the } T_1 > 2 \cdot T_c$$

$$S_d T_{1x} := a_g \cdot S \cdot \frac{2.5}{q} \cdot \frac{T_c}{T_{1x}} = 0.291$$

$$S_d T_{1y} := a_g \cdot S \cdot \frac{2.5}{q} \cdot \frac{T_c}{T_{1y}} = 0.427$$

$$F_{bx} := \frac{S_d T_{1x} \cdot m_{tot} \cdot \lambda_{correction}}{1000} = 352.616$$

$$F_{by} := \frac{S_d T_{1y} \cdot m_{tot} \cdot \lambda_{correction}}{1000} = 517.129$$

Base shear based on empirical formula for building period

$C_t := 0.05$ For all other types of structures based on EC8-1 4.3.3.2.2(4.6)

$H := 12$ $T_B := 0.1$ $T_c := 0.2$ $T_d := 1.7$

$T_1 := C_t \cdot H^{0.75} = 0.322$ $a_g := 0.744$ $S := 1$ $q := 1.5$ $\beta := 0.2$

$\beta \cdot a_g = 0.149$ OK!

$2 T_c = 0.4 > T_1$ gives $\lambda = 0,85$ $\lambda := 0.85$

$$S_{d.T} := a_g \cdot S \cdot \frac{2.5}{q} \frac{T_c}{T_1}$$

$$m_{modal} := 1.211 \cdot 10^6$$

$$F_{b.EC8.x} := S_{d.T} \cdot m_{modal} \cdot \lambda = 791.879 \cdot 10^3 \text{ N}$$

Base shear based EC8 empirical formula and fundamental period for each floor is as presented below

$$F_i = F_b \frac{z_i \cdot m_i}{\sum_{j=n} z_j \cdot m_j}$$

351,166 351,166 306,424 266,491 ton
 3 6 9 12 m

Fb 791,879 kN

Floor	Height	Mass(kg)	HxM	
1	3	351166	1053498	91,51212
2	6	351166	2106996	183,0242
3	9	306424	2757816	239,5577
4	12	266491	3197892	277,7849
sum		1275247	9116202	

Using the T1 from FEM-DESIGN to find the base shear based on design spectrum

$T_1 := 0.934$ $\lambda := 1$

$$S_{d.T.model1} := a_g \cdot S \cdot \frac{2.5}{q} \frac{T_c}{T_1} = 0.266$$

$$F_{b.m1.x} := S_{d.T.model1} \cdot m_{modal} \cdot \lambda = 321.55 \cdot 10^3$$

Results without geometrical matrix

$$K_x := \begin{bmatrix} 142 \cdot 10^6 & -142 \cdot 10^6 & 0 & 0 \\ -142 \cdot 10^6 & 285 \cdot 10^6 & -142 \cdot 10^6 & 0 \\ 0 & -142 \cdot 10^6 & 285 \cdot 10^6 & -142 \cdot 10^6 \\ 0 & 0 & -142 \cdot 10^6 & 285 \cdot 10^6 \end{bmatrix}$$

$$\text{Eigenvalue } \lambda := \text{eigenvals}(m^{-1} \cdot K_x) = \begin{bmatrix} 1.6 \cdot 10^3 \\ 1.1 \cdot 10^3 \\ 481.23 \\ 60.63 \end{bmatrix}$$

$$\lambda := \text{sort}(\text{eigenvals}(m^{-1} \cdot K_x)) \quad \lambda = \begin{bmatrix} 60.629 \\ 481.226 \\ 1.097 \cdot 10^3 \\ 1.602 \cdot 10^3 \end{bmatrix}$$

$$\text{Natural frequency } \omega_n := \sqrt{\lambda} = \begin{bmatrix} 7.79 \\ 21.94 \\ 33.12 \\ 40.03 \end{bmatrix} \quad \begin{array}{l} \text{1.st} \\ \text{2nd} \\ \text{3rd} \\ \text{4th} \end{array}$$

$$\text{Natural period } T_x := \frac{2 \pi}{\omega_n} = \begin{bmatrix} 0.807 \\ 0.286 \\ 0.19 \\ 0.157 \end{bmatrix}$$

$$i := 0..3$$

$$U_x^{(i)} := \frac{\text{eigenvec}(m^{-1} \cdot K_x, \lambda_i)}{\text{eigenvec}(m^{-1} \cdot K_x, \lambda_i)_{\text{ORIGIN}}} \quad \begin{array}{cccc} & \text{1st} & \text{2nd} & \text{3rd} & \text{4th} \end{array}$$

$$U_x = \begin{bmatrix} 1 & 1 & 1 & 1 \\ 0.89 & 0.129 & -0.986 & -1.9 \\ 0.666 & -0.88 & -0.556 & 2.003 \\ 0.356 & -0.947 & 1.236 & -1.267 \end{bmatrix}$$

$$\phi_{1x} := \begin{bmatrix} 0 \\ U_{x_{3,0}} \\ U_{x_{2,0}} \\ U_{x_{1,0}} \\ U_{x_{0,0}} \end{bmatrix} = \begin{bmatrix} 0.000 \\ 0.356 \\ 0.666 \\ 0.890 \\ 1.000 \end{bmatrix} \quad \phi_{2x} := \begin{bmatrix} 0 \\ U_{x_{3,1}} \\ U_{x_{2,1}} \\ U_{x_{1,1}} \\ U_{x_{0,1}} \end{bmatrix} = \begin{bmatrix} 0.000 \\ -0.947 \\ -0.880 \\ 0.129 \\ 1.000 \end{bmatrix}$$

$$\phi_{3x} := \begin{bmatrix} 0 \\ U_{x_{3,2}} \\ U_{x_{2,2}} \\ U_{x_{1,2}} \\ U_{x_{0,2}} \end{bmatrix} = \begin{bmatrix} 0.000 \\ 1.236 \\ -0.556 \\ -0.986 \\ 1.000 \end{bmatrix} \quad \phi_{4x} := \begin{bmatrix} 0 \\ U_{x_{3,3}} \\ U_{x_{2,3}} \\ U_{x_{1,3}} \\ U_{x_{0,3}} \end{bmatrix} = \begin{bmatrix} 0.000 \\ -1.267 \\ 2.003 \\ -1.900 \\ 1.000 \end{bmatrix}$$

$$K_y := \begin{bmatrix} 288 \cdot 10^6 & -288 \cdot 10^6 & 0 & 0 \\ -288 \cdot 10^6 & 576 \cdot 10^6 & -288 \cdot 10^6 & 0 \\ 0 & -288 \cdot 10^6 & 576 \cdot 10^6 & -288 \cdot 10^6 \\ 0 & 0 & -288 \cdot 10^6 & 576 \cdot 10^6 \end{bmatrix}$$

$$m := \begin{bmatrix} 257 \cdot 10^3 & 0 & 0 & 0 \\ 0 & 318 \cdot 10^3 & 0 & 0 \\ 0 & 0 & 318 \cdot 10^3 & 0 \\ 0 & 0 & 0 & 318 \cdot 10^3 \end{bmatrix}$$

Height of
the building

$$Z := \begin{bmatrix} 0 \\ 3 \\ 6 \\ 9 \\ 12 \end{bmatrix}$$

Eigenvalue $\lambda := \text{eigenvals}(m^{-1} \cdot K_y) = \begin{bmatrix} 3.24 \cdot 10^3 \\ 2.22 \cdot 10^3 \\ 971.7 \\ 118.95 \end{bmatrix}$ $\lambda := \text{sort}(\text{eigenvals}(m^{-1} \cdot K_y))$

Natural frequency $\omega := \sqrt{\lambda} = \begin{bmatrix} 10.91 \\ 31.17 \\ 47.12 \\ 56.95 \end{bmatrix}$ $\lambda = \begin{bmatrix} 118.95362 \\ 971.69808 \\ 2.22035 \cdot 10^3 \\ 3.24358 \cdot 10^3 \end{bmatrix}$

1.st
2nd
3rd
4th

Natural period $T_y := \frac{2 \pi}{\omega} = \begin{bmatrix} 0.576 \\ 0.202 \\ 0.133 \\ 0.11 \end{bmatrix}$ $\begin{matrix} 1.st \\ 2nd \\ 3rd \\ 4th \end{matrix}$

$$i := 0..3$$

$$U_y^{(i)} := \frac{\text{eigenvec}(m^{-1} \cdot K_y, \lambda_i)}{\text{eigenvec}(m^{-1} \cdot K_y, \lambda_i)_{\text{ORIGIN}}}$$

	1st	2nd	3rd	4th
$U_y =$	1	1	1	1
	0.894	0.133	-0.981	-1.894
	0.67	-0.877	-0.557	1.996
	0.359	-0.946	1.233	-1.262

$$\phi_{1y} := \begin{bmatrix} 0 \\ U_{y_{3,0}} \\ U_{y_{2,0}} \\ U_{y_{1,0}} \\ U_{y_{0,0}} \end{bmatrix} = \begin{bmatrix} 0.000 \\ 0.359 \\ 0.670 \\ 0.894 \\ 1.000 \end{bmatrix} \quad \phi_{2y} := \begin{bmatrix} 0 \\ U_{y_{3,1}} \\ U_{y_{2,1}} \\ U_{y_{1,1}} \\ U_{y_{0,1}} \end{bmatrix} = \begin{bmatrix} 0.000 \\ -0.946 \\ -0.877 \\ 0.133 \\ 1.000 \end{bmatrix}$$

$$\phi_{3y} := \begin{bmatrix} 0 \\ U_{y_{3,2}} \\ U_{y_{2,2}} \\ U_{y_{1,2}} \\ U_{y_{0,2}} \end{bmatrix} = \begin{bmatrix} 0.000 \\ 1.233 \\ -0.557 \\ -0.981 \\ 1.000 \end{bmatrix} \quad \phi_{4y} := \begin{bmatrix} 0 \\ U_{y_{3,3}} \\ U_{y_{2,3}} \\ U_{y_{1,3}} \\ U_{y_{0,3}} \end{bmatrix} = \begin{bmatrix} 0.000 \\ -1.262 \\ 1.996 \\ -1.894 \\ 1.000 \end{bmatrix}$$

$$T_c := 0.2 \quad S := 1 \quad a_g := 0.744 \quad q := 1.5$$

$$T_{1x} := T_{x_{0,0}} = 0.807 \quad T_{1y} := T_{y_{0,0}} = 0.576$$

$$\lambda_{correction} := 1 \quad \text{Since the } T1 > 2 * Tc$$

$$S_d T_{1x} := a_g \cdot S \cdot \frac{2.5}{q} \cdot \frac{T_c}{T_{1x}} = 0.307$$

$$S_d T_{1y} := a_g \cdot S \cdot \frac{2.5}{q} \cdot \frac{T_c}{T_{1y}} = 0.43$$

$$F_{bx} := \frac{S_d T_{1x} \cdot m_{tot} \cdot \lambda_{correction}}{1000} = 372.181 \quad 314.9 \text{ kN} \quad 0.934 \text{ s}$$

$$F_{by} := \frac{S_d T_{1y} \cdot m_{tot} \cdot \lambda_{correction}}{1000} = 521.32 \quad 440.9 \text{ kN} \quad 0.683 \text{ s}$$

Base shear

$$m_{1,1} := \begin{bmatrix} 93.664 \\ 89.231 \\ 71.693 \\ 35.025 \\ 0 \end{bmatrix} \text{ kN} \quad m_{2,1} := \begin{bmatrix} 40.719 \\ 30.813 \\ 20.194 \\ 8.730 \\ 0 \end{bmatrix} \text{ kN} \quad m_{3,1} := \begin{bmatrix} 39.383 \\ 29.561 \\ 19.226 \\ 8.204 \\ 0 \end{bmatrix} \text{ kN} \quad m_{4,1} := \begin{bmatrix} 41.866 \\ 32.174 \\ 20.892 \\ 9.241 \\ 0 \end{bmatrix} \text{ kN} \quad m_{ECS} := \begin{bmatrix} 296.415 \\ 255.624 \\ 195.299 \\ 97.650 \\ 0 \end{bmatrix}$$

Storey	Model #1	Model #2	Model #3	Model #4
Fourth (roof)	129,365 kN	56,166	54,674	57,232 kN
Third	89,275 kN	32,378	31,293	33,607 kN
Second	129,913 kN	49,392	48,514	50,349 kN
First	113,059 kN	36,961	35,997	40,841
Total base shear	314,934 kN	113,231	109,474	118,575

X-direction

$$m_{1,x} := \begin{bmatrix} 129.365 \\ 89.275 \\ 129.913 \\ 113.059 \\ 0 \end{bmatrix} \text{ kN} \quad m_{2,x} := \begin{bmatrix} 56.166 \\ 32.378 \\ 49.392 \\ 36.961 \\ 0 \end{bmatrix} \text{ kN} \quad m_{3,x} := \begin{bmatrix} 54.674 \\ 31.293 \\ 48.514 \\ 35.997 \\ 0 \end{bmatrix} \text{ kN} \quad m_{4,x} := \begin{bmatrix} 57.232 \\ 33.607 \\ 50.349 \\ 40.841 \\ 0 \end{bmatrix} \text{ kN}$$

Storey	Model #1	Model #2	Model #3	Model #4
Fourth (roof)	184,574 kN	81,152	79,249	70,407
Third	123,493 kN	46,819	45,179	46,627
Second	187,045 kN	70,597	70,237	55,189
First	163,803 kN	56,008	55,434	43,634
Total base shear	440,934 kN	165,666	160,293	159,174

Y-direction

$$m_{1,y} := \begin{bmatrix} 184.574 \\ 123.493 \\ 187.045 \\ 163.803 \\ 0 \end{bmatrix} \text{ kN} \quad m_{2,y} := \begin{bmatrix} 81.152 \\ 46.819 \\ 70.597 \\ 56.008 \\ 0 \end{bmatrix} \text{ kN} \quad m_{3,y} := \begin{bmatrix} 79.249 \\ 45.179 \\ 70.237 \\ 55.434 \\ 0 \end{bmatrix} \text{ kN} \quad m_{4,y} := \begin{bmatrix} 70.407 \\ 46.627 \\ 55.189 \\ 43.634 \\ 0 \end{bmatrix} \text{ kN}$$

Shear wall calculation of model #4

$$G_{ct} := 690 \frac{\text{N}}{\text{mm}^2} \quad t_{ct} := 240 \text{ mm} \quad l_{ct,y} := 7800 \text{ mm} \quad h_{ct} := 3000 \text{ mm}$$

$$l_{ct,x} := 4800 \text{ mm}$$

$$k_x := \frac{G_{ct} \cdot t_{ct} \cdot l_{ct,x}}{h_{ct}} = (2.65 \cdot 10^8) \frac{\text{N}}{\text{m}}$$

$$k_y := \frac{G_{ct} \cdot t_{ct} \cdot l_{ct,y}}{h_{ct}} = (4.306 \cdot 10^8) \frac{\text{N}}{\text{m}}$$

X-direction

$$K_x := 2 \begin{bmatrix} k_x & -k_x & 0 & 0 \\ -k_x & 2 \cdot k_x & -k_x & 0 \\ 0 & -k_x & 2 \cdot k_x & -k_x \\ 0 & 0 & -k_x & 2 \cdot k_x \end{bmatrix} = \begin{bmatrix} 530 & -530 & 0 & 0 \\ -530 & 1 \cdot 10^3 & -530 & 0 \\ 0 & -530 & 1 \cdot 10^3 & -530 \\ 0 & 0 & -530 & 1 \cdot 10^3 \end{bmatrix} 10^6 \frac{N}{m}$$

Stiffness matrix for x-direction (we have 2 in x-direction on each floor)

$$\begin{bmatrix} 142 & -142 & 0 & 0 \\ -142 & 285 & -142 & 0 \\ 0 & -142 & 285 & -142 \\ 0 & 0 & -142 & 285 \end{bmatrix} 10^6 \frac{N}{m}$$

Combined stiffness matrix in X direction

$$K_{cx} := K_x - k_G = \begin{bmatrix} 141 & -141 & 0 & 0 \\ -141 & 281 & -140 & 0 \\ 0 & -140 & 277 & -138 \\ 0 & 0 & -138 & 274 \end{bmatrix} 10^6 \frac{N}{m}$$

Y-direction

$$K_y := 2 \begin{bmatrix} k_y & -k_y & 0 & 0 \\ -k_y & 2 \cdot k_y & -k_y & 0 \\ 0 & -k_y & 2 \cdot k_y & -k_y \\ 0 & 0 & -k_y & 2 \cdot k_y \end{bmatrix} = \begin{bmatrix} 861 & -861 & 0 & 0 \\ -861 & 2 \cdot 10^3 & -861 & 0 \\ 0 & -861 & 2 \cdot 10^3 & -861 \\ 0 & 0 & -861 & 2 \cdot 10^3 \end{bmatrix} 10^6 \frac{N}{m}$$

Stiffness matrix for each braces in y-axes (we have 4 in y-direction on each floor)

$$\begin{bmatrix} 288 & -288 & 0 & 0 \\ -288 & 576 & -288 & 0 \\ 0 & -288 & 576 & -288 \\ 0 & 0 & -288 & 576 \end{bmatrix} 10^6 \frac{N}{m}$$

Combined stiffness matrix in Y direction

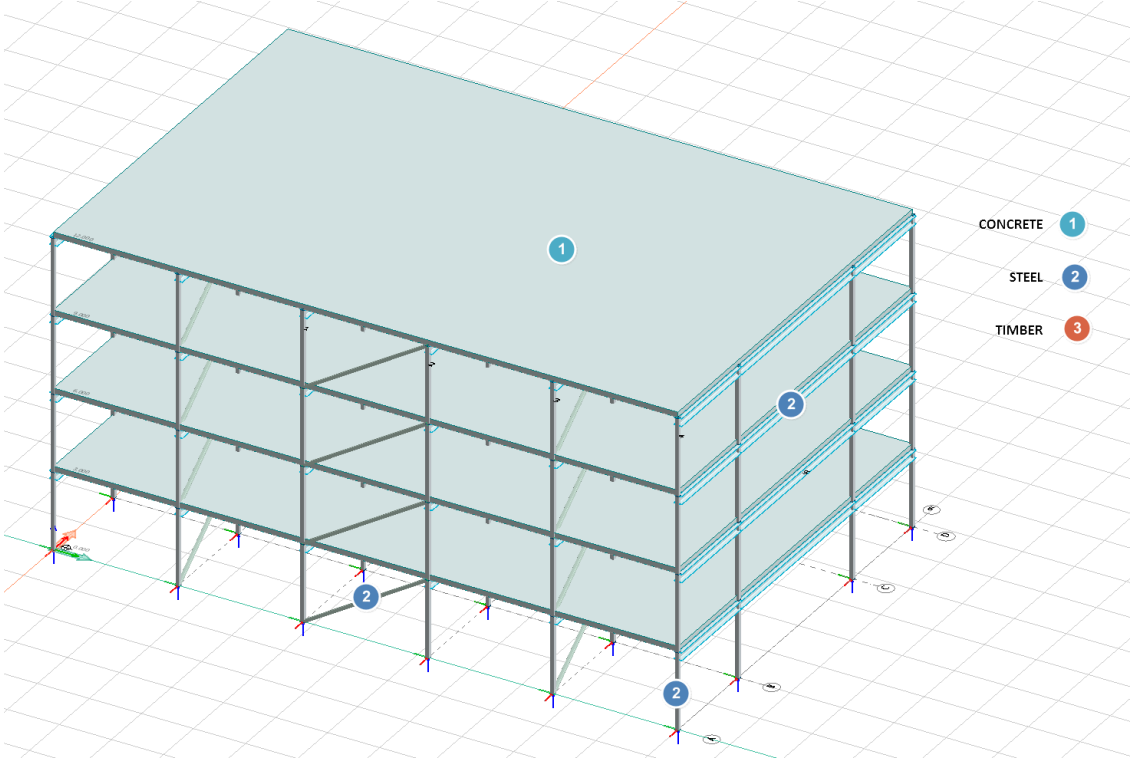
$$K_{cy} := K_y - k_G = \begin{bmatrix} 287 & -287 & 0 & 0 \\ -287 & 572 & -285 & 0 \\ 0 & -285 & 569 & -284 \\ 0 & 0 & -284 & 566 \end{bmatrix} 10^6 \frac{N}{m}$$

APPENDIX B PRESENTATION OF 3D MODELS

1 Geometri / Structure

1.1 Generell informasjon / General information

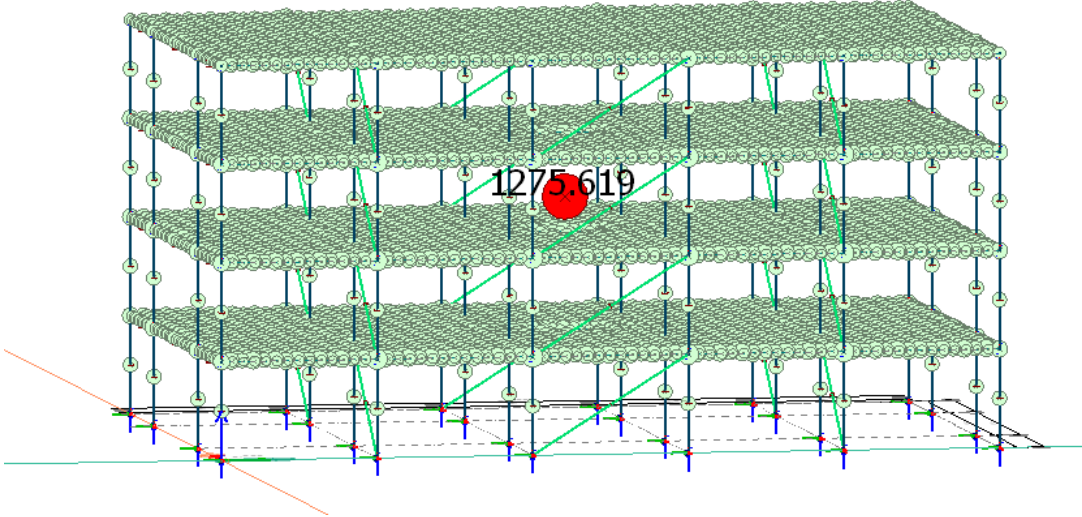
1.2 Grafisk presentasjon geometri / Graphic presentation geometry



Model #2 – Steel-CLT-Steel

The figure below shows modal mass of each element and the amount of total mass for this model.

Eurocode (NA: Norwegian) code: Eigenfrequencies - Converted masses - [t]



Storeys

No.	Name	Height	Level
[-]	[-]	[m]	[m]
1	Storey 1	3.000	3.000
2	Storey 2	3.000	6.000
3	Storey 3	3.000	9.000
4	Storey 4	3.000	12.000

1.3 Materiale / Material

Steel materials

No.	Name	Fyk(t <=16)	Fyk(16 <=t <=40)	Fyk(40 <=t <=63)	Fyk(63 <=t <=80)
[-]	[-]	[N/mm ²]	[N/mm ²]	[N/mm ²]	[N/mm ²]
1	S 355	355.000	355.000	335.000	335.000

Fyk(80 <=t <=100)	Fyk(100 <=t <=150)	Fyk(150 <=t <=200)	Fyk(200 <=t <=250)	Fyk(250 <=t <=400)
[N/mm ²]	[N/mm ²]	[N/mm ²]	[N/mm ²]	[N/mm ²]
335.000	335.000	335.000	335.000	335.000

fuk(t <=3)	fuk(3 <=t <=40)	fuk(40 <=t <=100)	fuk(100 <=t <=150)	fuk(150 <=t <=250)
[N/mm ²]	[N/mm ²]	[N/mm ²]	[N/mm ²]	[N/mm ²]
510.000	510.000	470.000	470.000	470.000

fuk(250 <=t <=400)	Gamma M0	Gamma M0, acc	Gamma M1	Gamma M1, acc	Gamma M2	Gamma M2, acc
[N/mm ²]	[-]	[-]	[-]	[-]	[-]	[-]
470.000	1.050	1.000	1.050	1.000	1.250	1.000

Gamma M5	Gamma M5, acc	Ek	Poisson's ratio	G	Therm. coeff.	Density
[-]	[-]	[N/mm ²]	[-]	[N/mm ²]	[1/°C]	[t/m ³]
1.000	1.000	210000.000	0.300	80769.000	1.2000e-05	7.850000

Concrete materials

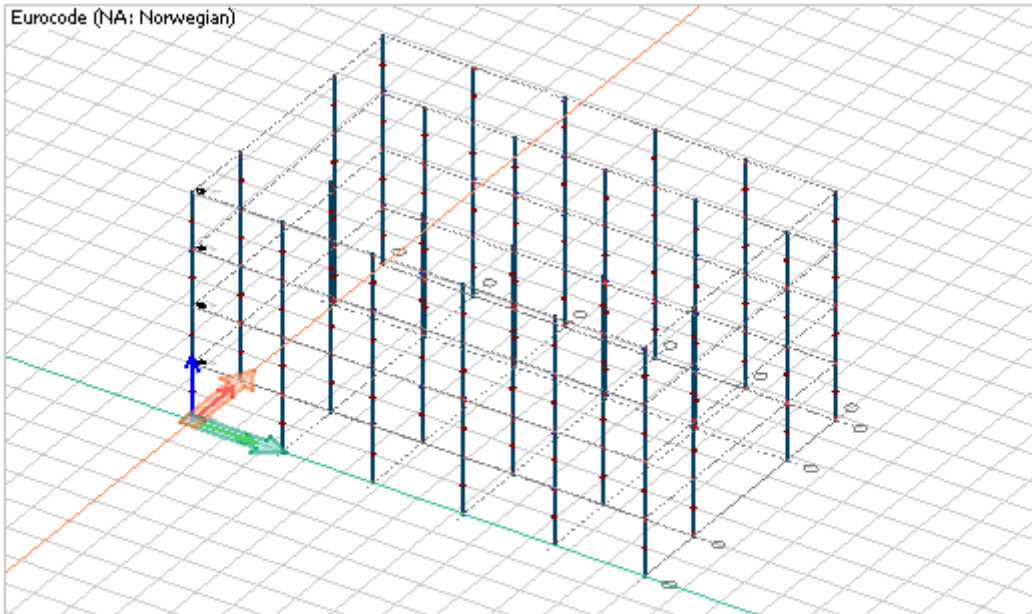
No.	Name	Fck	Fctm	Fctk	Ecm	Yield strain	Ultimate strain
[-]	[-]	[N/mm ²]	[N/mm ²]	[N/mm ²]	[N/mm ²]	[-]	[-]
1	C30/37	30.000	2.900	2.000	33000.000	0.00175	0.00350

Gamma c	Gamma c, acc	Gamma cE	Gamma s	Gamma s, acc	Alfa cc	Alfa ct
[-]	[-]	[-]	[-]	[-]	[-]	[-]
1.50	1.20	1.20	1.15	1.00	0.85	0.85

Density	Therm. coeff.	Poisson's ratio	Creep coefficient, SLS	Creep coefficient, ULS
[t/m ³]	[1/°C]	[-]	[-]	[-]
2.548	0.000010	0.200	2.580	2.580

Shrinkage	Dyna r.	Stab r.
[-]	[-]	[-]
0.490	1.000	1.000

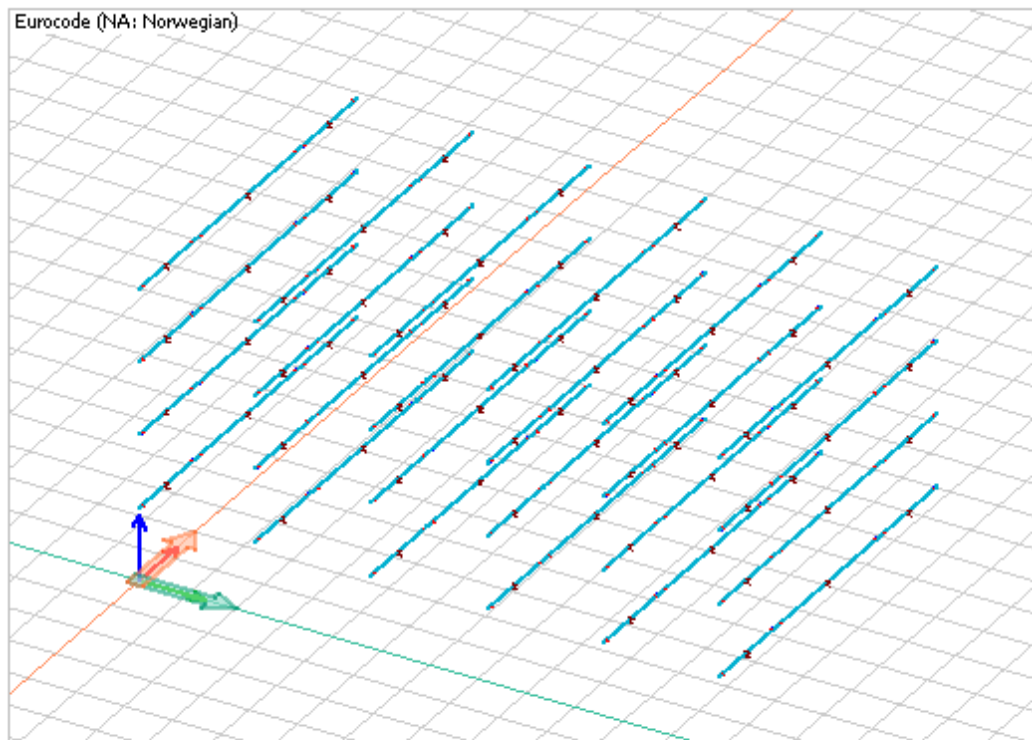
Columns



Columns

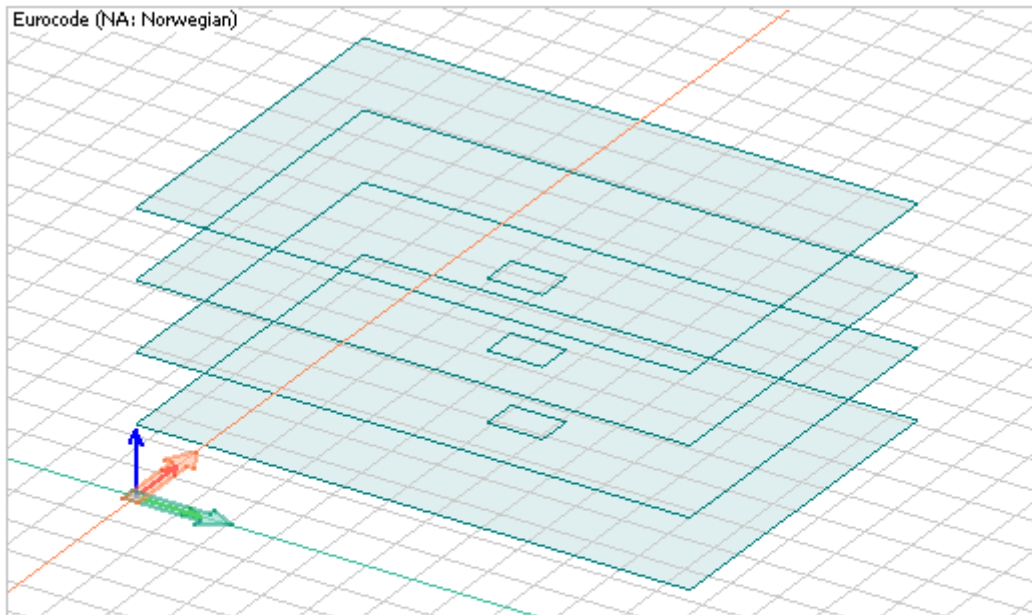
ID	Material	Section, start	Section, end	Ecc(y'), end	Ecc. crack.	Sp. cond.	Ep. cond.
[-]	[-]	[-]	[-]	[m]	[-]	[-]	[-]
1.eta...	S 355	VKR 200x200x12.5	VKR 200x200x12.5	0.000	No	FFFF--	FFFF--

Beams



Material	Section, start	Section, end	Ecc(x'), start	Ecc(y'), start	Ecc(z'), start	Ecc(x'), end	Ecc(y'), end
[-]	[-]	[-]	[m]	[m]	[m]	[m]	[m]
S 355	HE-B 200	HE-B 200	0.000	0.000	0.000	0.000	0.000

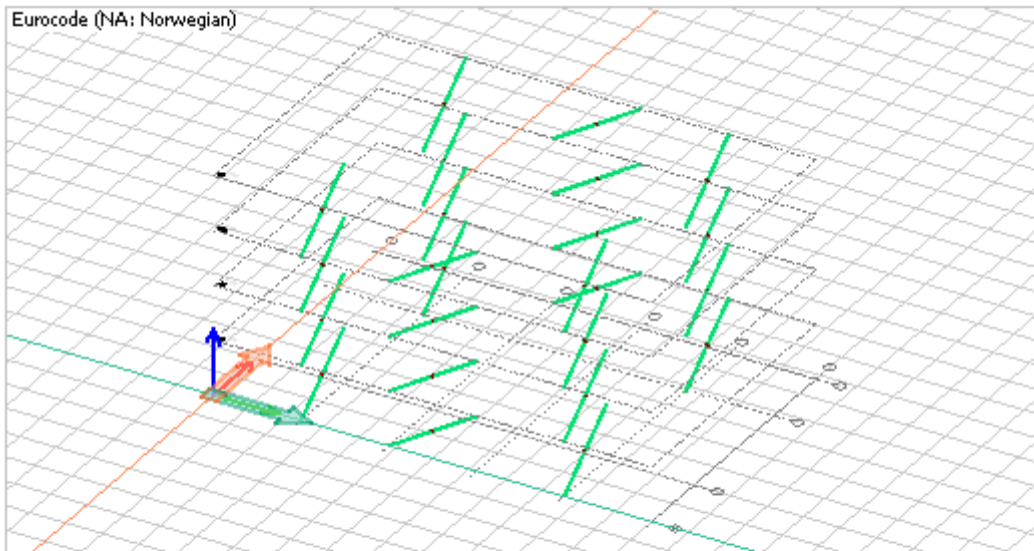
Plates



Plates

ID	Material	t1	t2	t3	E2 / E1	Alpha	Ecc.	Ecc. calc.	Ecc. crack.
[-]	[-]	[m]	[m]	[m]	[-]	[rad]	[m]	[-]	[-]
Plan ...	C30/37	0.200	0.200	0.200	1.000	0.000	0.000	No	No
Plan ...	C30/37	0.200	0.200	0.200	1.000	0.000	0.000	No	No
Plan ...	C30/37	0.200	0.200	0.200	1.000	0.000	0.000	No	No
Plan ...	C30/37	0.200	0.200	0.200	1.000	0.000	0.000	No	No

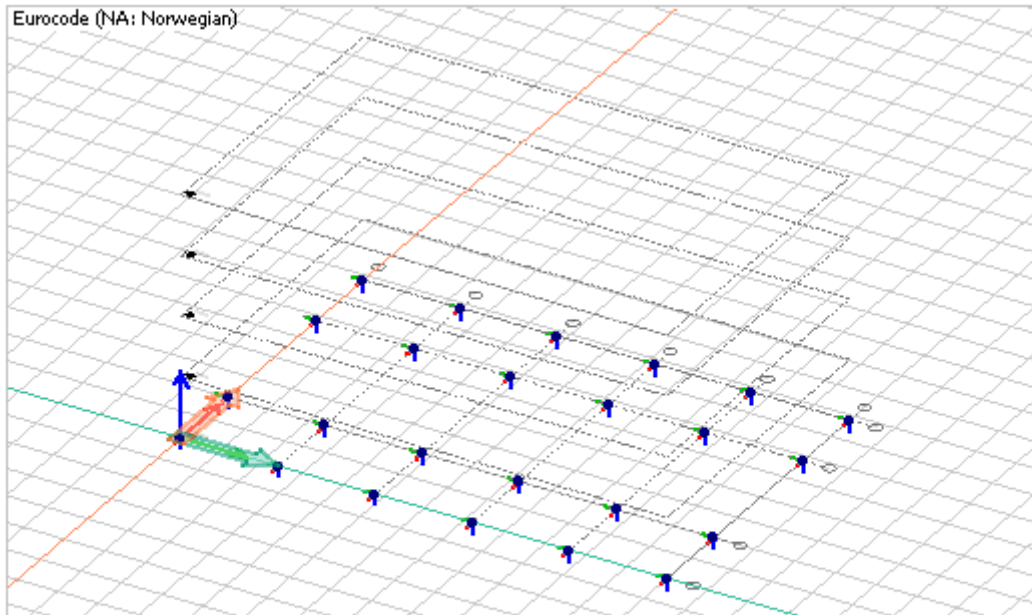
Trusses (Vindkryss)



Trusses

ID	Material	Section	Compression Capacity
[-]	[-]	[-]	[kN]
1.eta...	S 355	VKR 120x120x6.3	-

Supports



Point support groups

ID	x	y	z	Kx' comp.	Kx' tens.	Ky' comp.	Ky' tens.
[-]	[m]	[m]	[m]	[kN/m]	[kN/m]	[kN/m]	[kN/m]
Søyle opplegg ...	24.000	-0.001	0.000	1.00E+10	1.00E+10	1.00E+10	1.00E+10

2 Laster / Loads

2.1 Generell informasjon / General information

2.2 Grafisk presentasjon laster / Graphic presentation loads

2.3 Laster / Loads

Site and load information

Value	Quantity	Value	Quantity
Wind speed [m/s]	26	Building width x-dir [m]	24.00
Characteristic snow load [kN/m ²]	2.0	Building width y-dir [m]	15.60
Terrain type[-]	II	Ground level [m]	0.0
Extent [m]	24.00x15.60	Altitude	700.0
Building height [m]	12.00	Reigon	2

Load cases

No.	Name	Type	Duration class
1	Structural dead load	+Struc. dead load	Permanent
2	Snow	Ordinary	Short-term
3	Wind	Ordinary	Short-term
4	Live load	Ordinary	Medium-term
5	Non-structural dead load	Ordinary	Permanent

2.4 Last kombinasjoner / Load combinations

Load combinations

No.	Name	Type	Factor	Load cases
1	LC1ULS	Ultimate	1.350	Structural dead load+Struc. dea...
			1.350	Non-structural dead load
			1.050	Live load
			1.050	Snow
2	LC2ULS	Ultimate	1.202	Structural dead load+Struc. dea...
			1.202	Non-structural dead load
			1.500	Live load
			1.050	Snow
3	LC3ULS	Ultimate	1.202	Structural dead load+Struc. dea...
			1.202	Non-structural dead load
			1.050	Live load
			1.500	Snow
4	LC1SqLS	Quasi-permanent	1.000	Structural dead load+Struc. dea...
			1.000	Non-structural dead load
			0.200	Live load
			0.200	Snow
5	LC1SfLS	Frequent	1.000	Structural dead load+Struc. dea...
			1.000	Non-structural dead load
			0.500	Live load
			0.200	Snow
6	LC2SfLS	Frequent	1.000	Structural dead load+Struc. dea...
			1.000	Non-structural dead load
			0.200	Live load
			0.500	Snow
7	LC1ScLS	Characteristic	1.000	Structural dead load+Struc. dea...
			1.000	Non-structural dead load
			1.000	Live load
			0.700	Snow
8	LC2ScLS	Characteristic	1.000	Structural dead load+Struc. dea...
			1.000	Non-structural dead load
			0.700	Live load
			1.000	Snow
9	Dead load + Påført Egen...	Seismic	1.000	Structural dead load+Struc. dea...
			1.000	Non-structural dead load
			0.200	Live load
			0.200	Snow
10	Dead load + Påført Egen...	Seismic	1.000	Seis res, Fx+Mx
			0.300	Seis res, Fy+My
			1.000	Structural dead load+Struc. dea...
			1.000	Non-structural dead load
			0.200	Live load
			0.200	Snow
			1.000	Seis res, Fx+Mx
			-0.300	Seis res, Fy+My

No.	Name	Type	Factor	Load cases
27	Dead load + Påført Egen...	Seismic	0.300	Seis res, Fx+Mx
			-1.000	Seis res, Fy+My
			1.000	Structural dead load+Struc. dea...
			1.000	Non-structural dead load
			0.200	Live load
			0.200	Snow
			0.300	Seis res, Fx+Mx
28	Dead load + Påført Egen...	Seismic	1.000	Seis res, Fy-My
			1.000	Structural dead load+Struc. dea...
			1.000	Non-structural dead load
			0.200	Live load
			0.200	Snow
			0.300	Seis res, Fx+Mx
			1.000	Seis res, Fy-My
29	Dead load + Påført Egen...	Seismic	1.000	Structural dead load+Struc. dea...
			1.000	Non-structural dead load
			0.200	Live load
			0.200	Snow
			-0.300	Seis res, Fx+Mx
			1.000	Seis res, Fy+My
			1.000	Structural dead load+Struc. dea...
30	Dead load + Påført Egen...	Seismic	1.000	Non-structural dead load
			0.200	Live load
			0.200	Snow
			-0.300	Seis res, Fx+Mx
			-1.000	Seis res, Fy+My
			1.000	Structural dead load+Struc. dea...
			1.000	Non-structural dead load
31	Dead load + Påført Egen...	Seismic	0.200	Live load
			0.200	Snow
			-0.300	Seis res, Fx+Mx
			1.000	Seis res, Fy-My
			1.000	Structural dead load+Struc. dea...
			1.000	Non-structural dead load
			0.200	Live load
32	Dead load + Påført Egen...	Seismic	0.200	Snow
			-0.300	Seis res, Fx+Mx
			-1.000	Seis res, Fy-My
			1.000	Structural dead load+Struc. dea...
			1.000	Non-structural dead load
			0.200	Live load
			0.200	Snow
33	Dead load + Påført Egen...	Seismic	-0.300	Seis res, Fx+Mx
			-1.000	Seis res, Fy-My
			1.000	Structural dead load+Struc. dea...
			1.000	Non-structural dead load
			0.200	Live load
			0.200	Snow
			0.300	Seis res, Fx-Mx
34	Dead load + Påført Egen...	Seismic	1.000	Seis res, Fy+My
			1.000	Structural dead load+Struc. dea...
			0.200	Live load

No.	Name	Type	Factor	Load cases
35	Dead load + Påført Egen...	Seismic	0.200	Snow
			0.300	Seis res, Fx-Mx
			-1.000	Seis res, Fy+My
			1.000	Structural dead load+Struc. dea...
			1.000	Non-structural dead load
36	Dead load + Påført Egen...	Seismic	0.200	Live load
			0.200	Snow
			0.300	Seis res, Fx-Mx
			1.000	Seis res, Fy-My
			1.000	Structural dead load+Struc. dea...
37	Dead load + Påført Egen...	Seismic	1.000	Non-structural dead load
			0.200	Live load
			0.200	Snow
			0.300	Seis res, Fx-Mx
			-1.000	Seis res, Fy-My
38	Dead load + Påført Egen...	Seismic	1.000	Structural dead load+Struc. dea...
			1.000	Non-structural dead load
			0.200	Live load
			0.200	Snow
			-0.300	Seis res, Fx-Mx
39	Dead load + Påført Egen...	Seismic	1.000	Seis res, Fy+My
			1.000	Structural dead load+Struc. dea...
			1.000	Non-structural dead load
			0.200	Live load
			0.200	Snow
40	Dead load + Påført Egen...	Seismic	-0.300	Seis res, Fx-Mx
			1.000	Seis res, Fy-My
			1.000	Structural dead load+Struc. dea...
			1.000	Non-structural dead load
			0.200	Live load
			0.200	Snow
			-0.300	Seis res, Fx-Mx
			-1.000	Seis res, Fy-My

2.5 Last grupper / Load groups

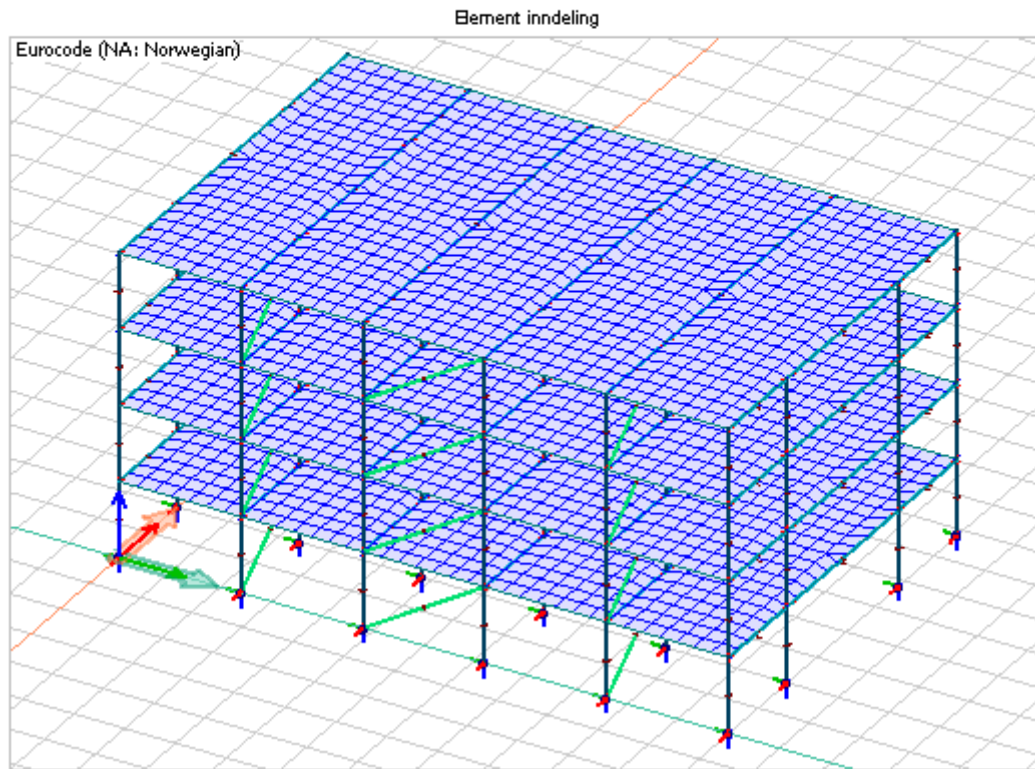
Load groups

No.	Load group	Included load cases
1	Dead load (Permanent, 1.00, 1.35, 1.00, 1.00, 0.89)	Structural dead load (+Dead l...
2	Påført egen (Permanent, 1.00, 1.35, 1.00, 1.00, 0.89)	Non-structural dead load
3	Nyttelast (Temporary, 1.50, 0.70, 0.50, 0.20, L)	Live load
4	Snø (Temporary, 1.50, 0.70, 0.50, 0.20, L)	Snow
5	Seismic load (Seismic, 1.00, Results)	(Automatic)

3 Elementnett / Finite elements

3.1 Generell informasjon / General information

3.2 Element inndeling / Mesh



4 Statikk / Analysis

4.1 Generell informasjon / General information

4.2 Likevekt / Equilibrium

Equilibrium, Load case

Load case	Component	Loads	Reactions	Error
[-]	[-]	kN(m)	kN(m)	[%]
Structural d...	Fx'	0.000	0.000	-
	Fy'	0.000	0.000	-
	Fz'	-7886.965	7886.965	0.00
	Mx'	-61513.792	61513.785	0.00
	My'	94643.585	-94643.577	0.00
	Mz'	0.000	0.001	-
Snow	Fx'	0.000	0.000	-
	Fy'	0.000	0.000	-
	Fz'	-209.664	209.664	0.00
	Mx'	-1635.258	1635.258	0.00
	My'	2515.968	-2515.968	0.00
Wind	Mz'	0.000	0.000	-
	Fx'	0.000	0.000	-
	Fy'	0.000	0.000	-
	Fz'	0.000	0.000	-
	Mx'	0.000	0.000	-
	My'	0.000	0.000	-
	Mz'	0.000	0.000	-

Live load	Fx'	0.000	0.000	-
	Fy'	0.000	0.000	-
	Fz'	-10383.360	10383.359	0.00
	Mx'	-80984.222	80984.214	0.00
	My'	124600.320	-124600.309	0.00
	Mz'	0.000	0.002	-
Non-structur...	Fx'	0.000	0.000	-
	Fy'	0.000	0.000	-
	Fz'	-1486.080	1486.080	0.00
	Mx'	-11590.567	11590.566	0.00
	My'	17832.960	-17832.958	0.00
	Mz'	0.000	0.000	-

4.4 Egenfrekvenser / Eigenfrequencies

4.4.1 Masser / Masses

Load case - mass conversions

No.	Factor	Load case
1	1.000	Structural dead...
2	0.200	Snow
3	0.000	Wind

No.	Factor	Load case
4	0.300	Live load
5	1.000	Non-structural ...

4.5 Jordskjelv analyse / Seismic analysis

4.5.1 Indata jordskjelv / Input data seismic

Seismic load, structure information

Value	Quantity
Structure type	Building structure
ξ (damping factor) [%]	5.000
q _d (behaviour factor for displacements)	1.500

Seismic load, horizontal sp., standard

Value	Quantity
Type	1
Ground	A
ag [m/s ²]	0.744
S	1.000
TB [s]	0.100

Value	Quantity
TC [s]	0.200
TD [s]	1.700
q	1.500
beta	0.200

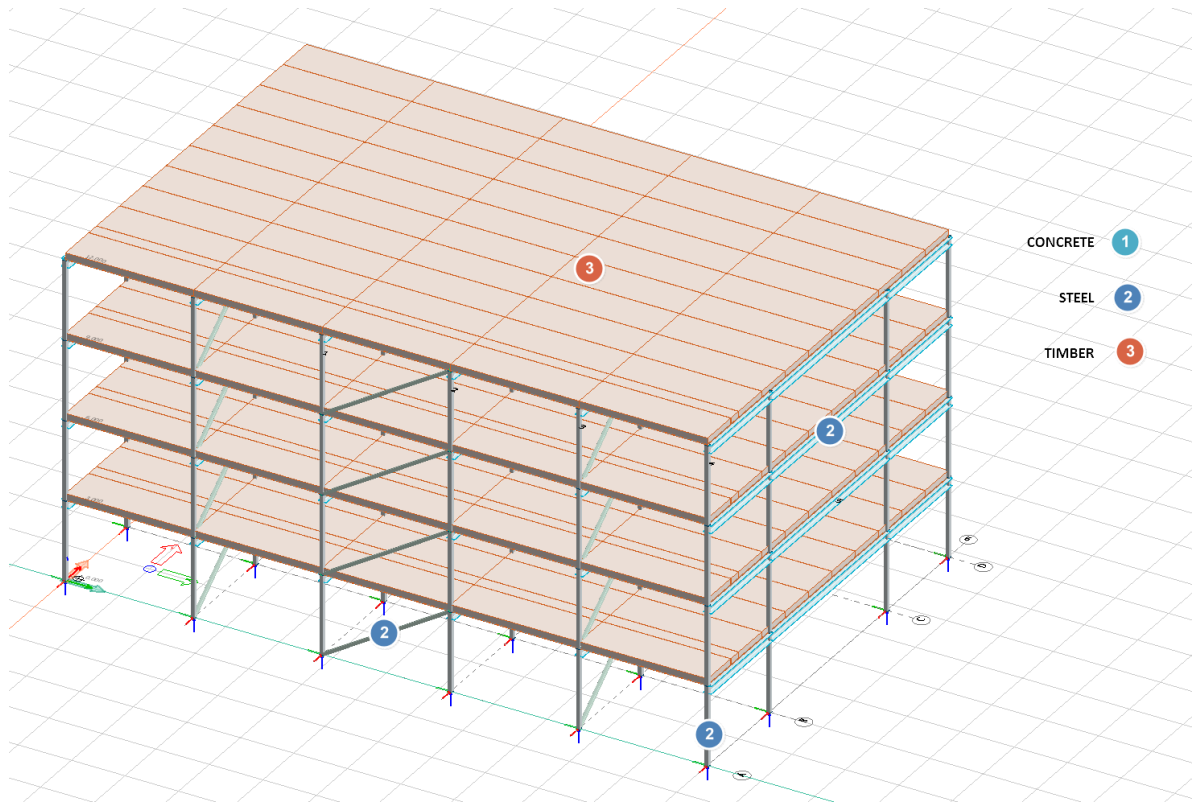
Seismic load, vertical sp., standard

Value	Quantity
Type	1
agv/ag [m/s ²]	0.446
S	1.000
TB [s]	0.050

Value	Quantity
TC [s]	0.200
TD [s]	1.200
q	1.000
beta	0.200

Seis. calc.: modal analysis

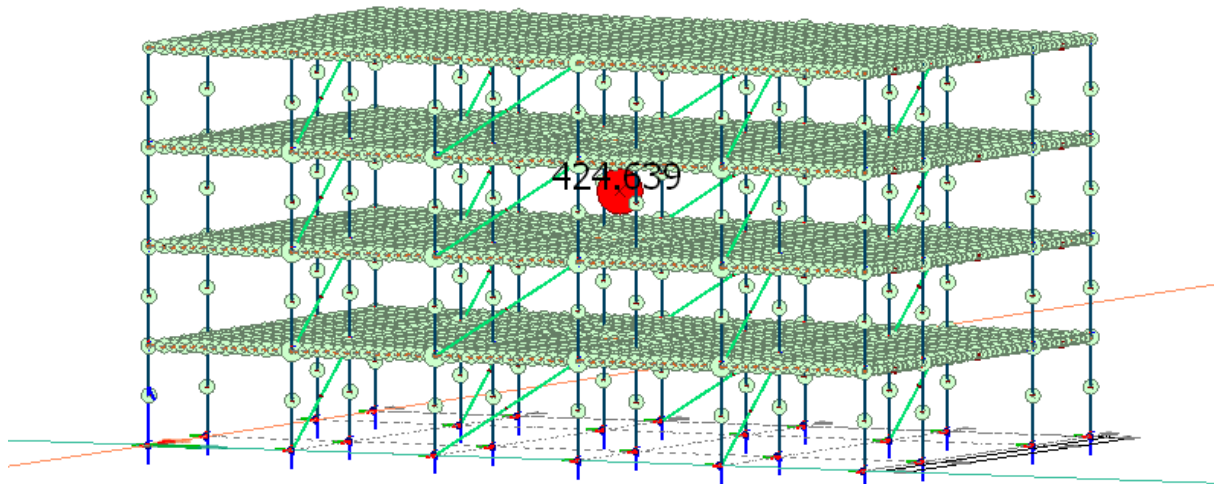
Value	Quantity
Alfa (angle of x-x')	0.000 [rad]
Summation rule	CQC
Combination rule	Ex "+" 0.3Ey "+" 0.3Ez...
Signed result	Yes
Torsional effect	5.0 [%]



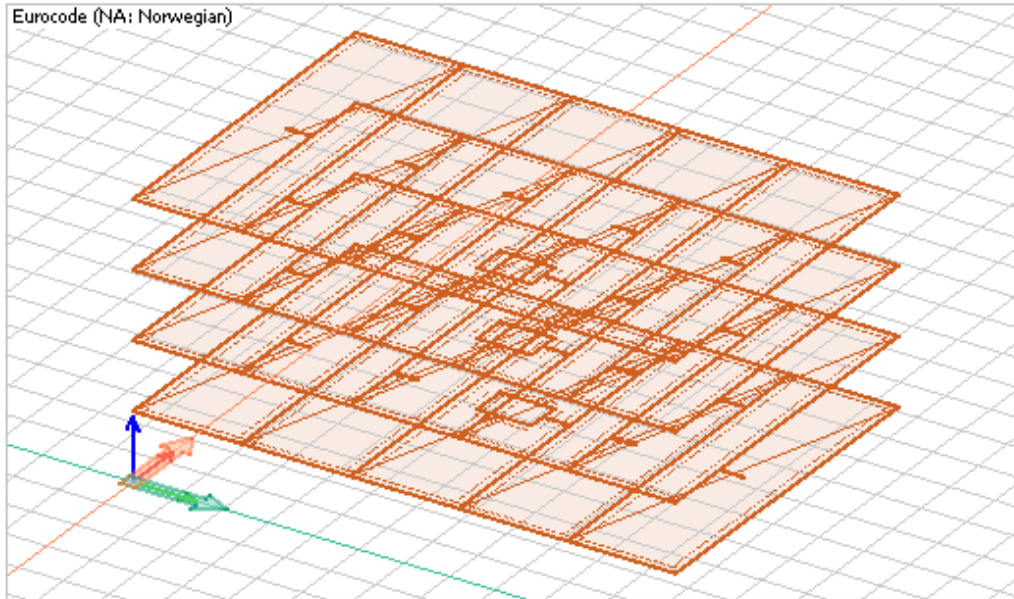
Model #3 – Steel-CLT-Steel

The figure below shows modal mass of each element and the amount of total mass for this model.

Eurocode (NA: Norwegian) code: Eigenfrequencies - Converted masses - [t]



Plates



Timber panels

ID	Panel type	Alignment	Eccentricity	Gamma M, ult	Gamma M, acc./seis.	Service class	System factor	Creep factor
[-]	[-]	[-]	[m]	[-]	[-]	[-]	[-]	[-]
TP.1	CLT 240 ...	Bottom	0.000	1.250	1.000	1	1.000	0.670

1.3 Materiale / Material

No.	Name	Thickness	Description	Em,k 0°	Em,k 90°	Et,k 0°
[-]	[-]	[mm]	[-]	[N/mm ²]	[N/mm ²]	[N/mm ²]
8	CLT 210	210.000	Cross laminated board	5500.000	4100.000	4100.000
9	CLT 240 C24	240.000	Cross laminated board	11000.000	370.000	8308.000

Et,k 90°	Ec,k 0°	Ec,k 90°	Gv,k 0°	Gr,k 0°	rho 0°	fm,k 0°	fm,k 90°
[N/mm ²]	[N/mm ²]	[N/mm ²]	[N/mm ²]	[N/mm ²]	[kg/m ³]	[N/mm ²]	[N/mm ²]
5500.000	4100.000	5500.000	110.000	110.000	430.000	14.000	10.300
2028.000	8308.000	2028.000	690.000	50.000	420.000	24.000	24.000

ft,k 0°	ft,k 90°	fc,k 0°	fc,k 90°	Fv,k 0°	Fv,k 90°	fr,k 0°	kdef 1 s. class
[N/mm ²]	[N/mm ²]	[N/mm ²]	[N/mm ²]	[N/mm ²]	[N/mm ²]	[N/mm ²]	[-]
9.800	13.200	9.800	13.200	2.000	2.000	2.000	0.600
14.500	0.400	21.000	2.500	4.000	4.000	1.250	0.600

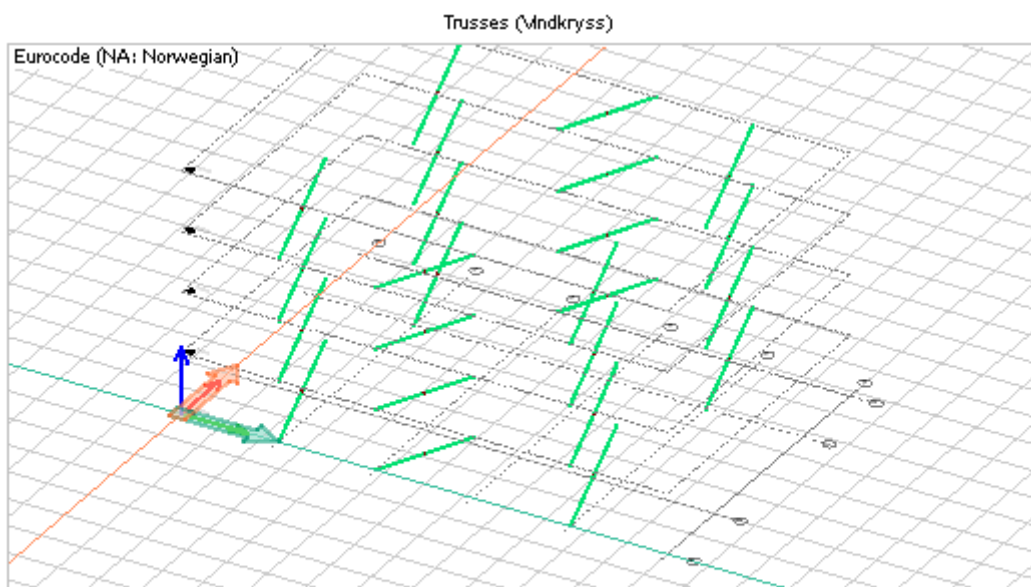
$f_{t,k}$	$f_{t,k}$	$f_{c,k}$	$f_{c,k}$	$f_{v,k}$	$f_{v,k}$	$f_{r,k}$	k_{def}
0°	90°	0°	90°	0°	90°	0°	1 s. class
[N/mm ²]	[N/mm ²]	[N/mm ²]	[N/mm ²]	[N/mm ²]	[N/mm ²]	[N/mm ²]	[-]
9.800	13.200	9.800	13.200	2.000	2.000	2.000	0.600
14.500	0.400	21.000	2.500	4.000	4.000	1.250	0.600

k_{def}	k_{def}	k_{mod} - Permanent	k_{mod} - Permanent	k_{mod} - Permanent
2 s. class	3 s. class	1. s. class	2. s. class	3. s. class
[-]	[-]	[-]	[-]	[-]
0.800	2.000	0.600	0.600	0.500
0.800	2.000	0.600	0.600	0.500

k_{mod} - Long term	k_{mod} - Long term	k_{mod} - Long term	k_{mod} - Medium term
1. s. class	2. s. class	3. s. class	1. s. class
[-]	[-]	[-]	[-]
0.700	0.700	0.550	0.800
0.700	0.700	0.550	0.800

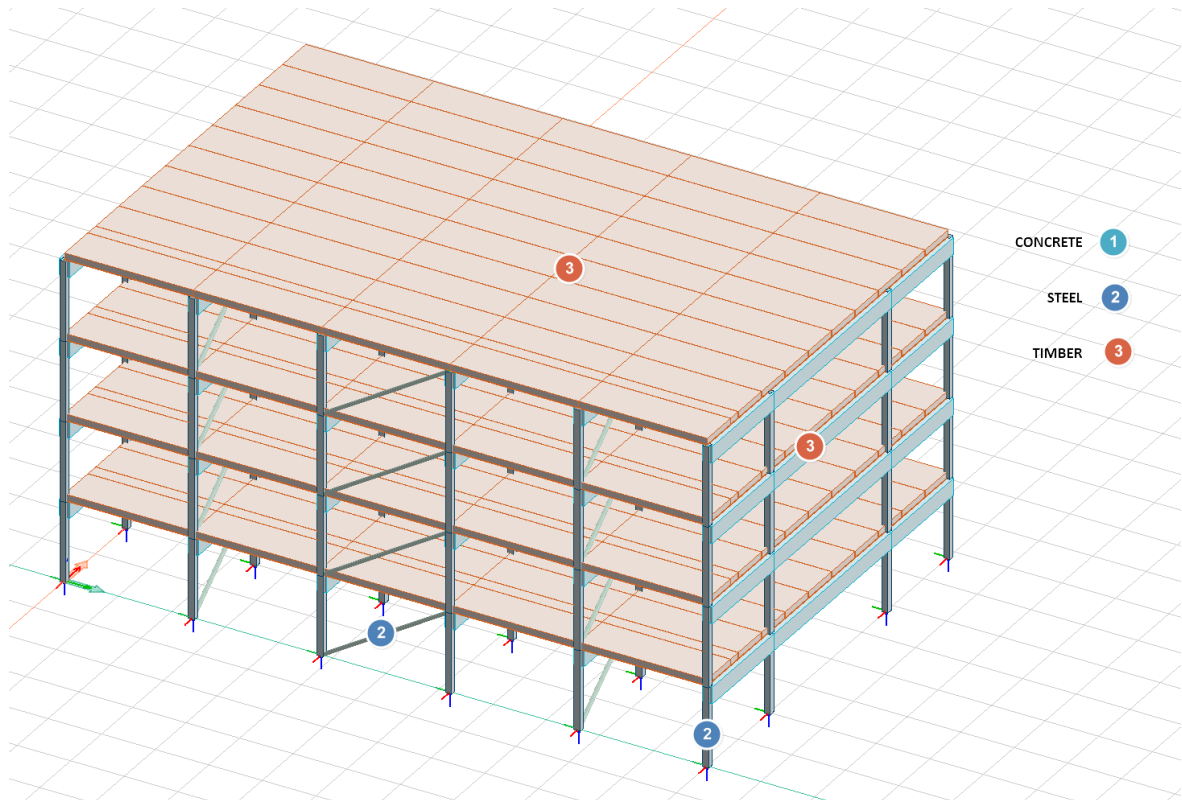
k_{mod} - Medium term	k_{mod} - Medium term	k_{mod} - Short term	k_{mod} - Short term
2. s. class	3. s. class	1. s. class	2. s. class
[-]	[-]	[-]	[-]
0.800	0.650	0.900	0.900
0.800	0.650	0.900	0.900

k_{mod} - Short term	k_{mod} - Instantaneous	k_{mod} - Instantaneous	k_{mod} - Instantaneous
3. s. class	1. s. class	2. s. class	3. s. class
[-]	[-]	[-]	[-]
0.700	1.100	1.100	0.900
0.700	1.100	1.100	0.900



Trusses

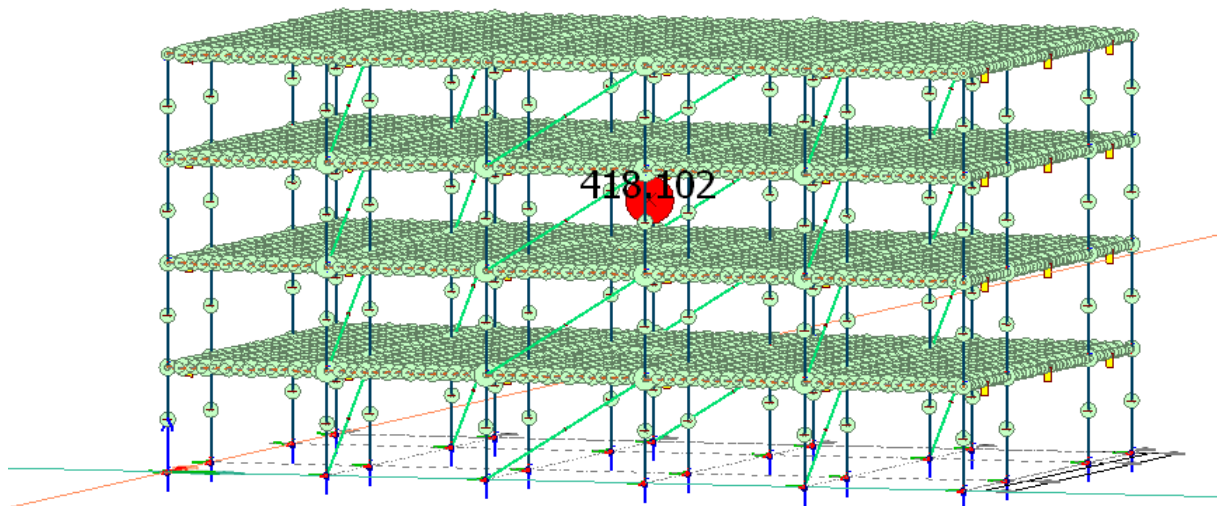
ID	Material	Section	Compression Capacity
[-]	[-]	[-]	[kN]
T.1.1	S 355	VKR 80x80x6.3	-



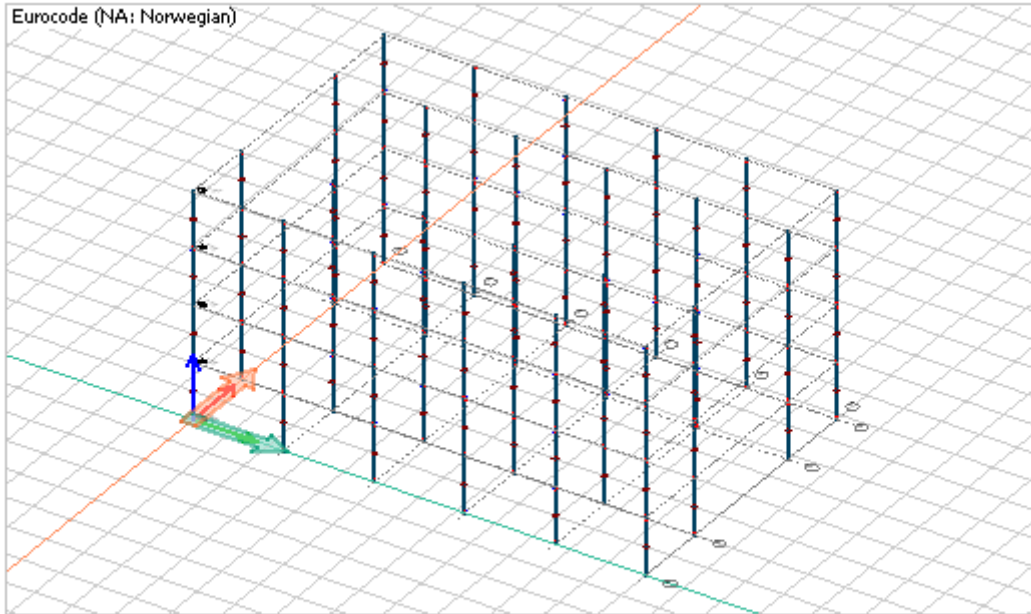
Model #3 – Glulam-CLT-Steel

The figure below shows modal mass of each element and the amount of total mass for this model.

Eurocode (NA: Norwegian) code: Eigenfrequencies - Converted masses - [t]



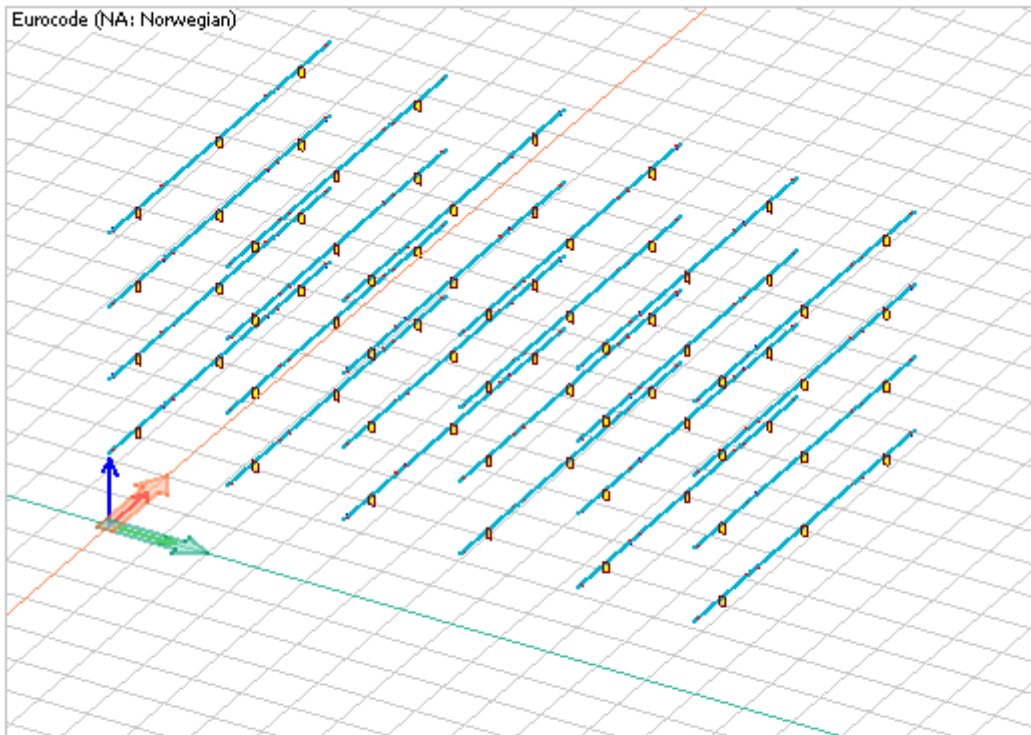
Columns



Columns

ID	Material	Section, start	Section, end	Ecc(y'), end	Ecc. crack.	Sp. cond.	Ep. cond.
[-]	[-]	[-]	[-]	[m]	[-]	[-]	[-]
C.1.1	GL 32c	Glulam 215x225	Glulam 215x225	0.000	No	FFFF--	FFFF--

Beams



Beams

Material	Section, start	Section, end	Ecc(x'), start	Ecc(y'), start	Ecc(z'), start	Ecc(x'), end	Ecc(y'), end
[-]	[-]	[-]	[m]	[m]	[m]	[m]	[m]
GL 32c	Glulam 215...	Glulam 215x405	0.000	0.000	0.000	0.000	0.000

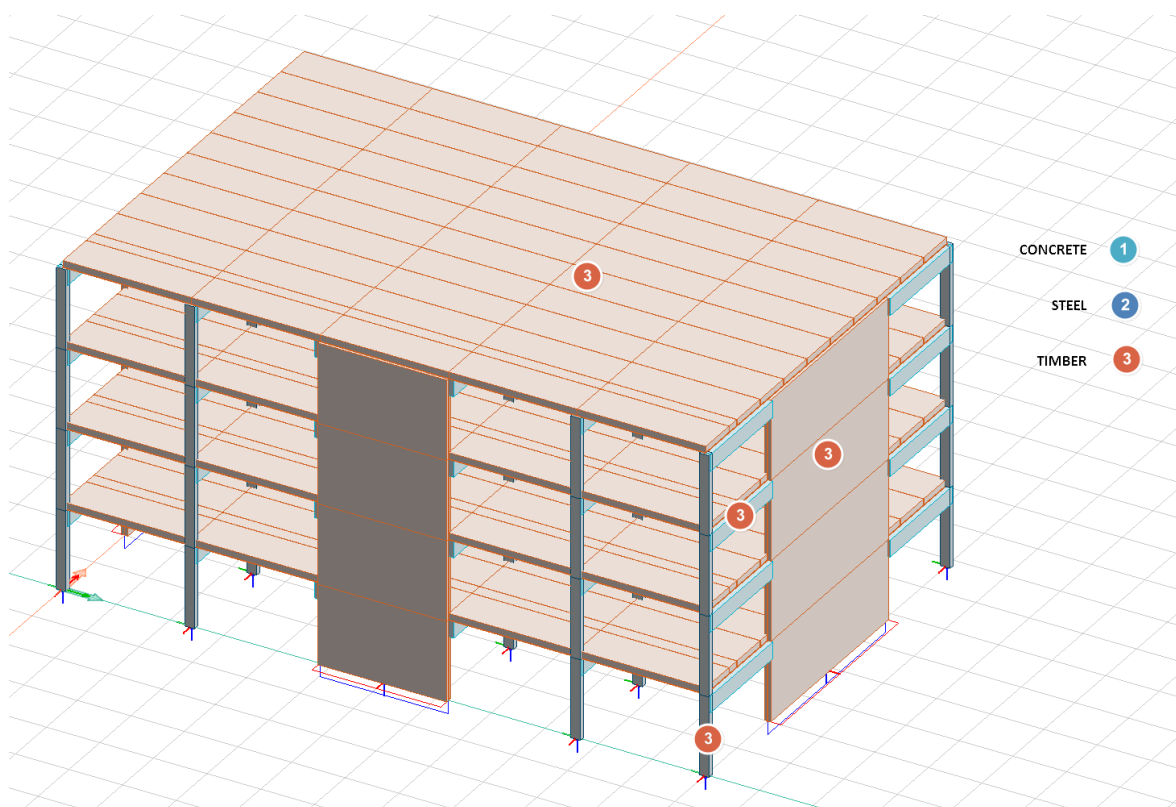
Timber materials

No.	Name	Type	Gamma M	Gamma M, ac	Service class	System factor	k cr factor
[-]	[-]	[-]	[-]	[-]	[-]	[-]	[-]
1	GL 32c	Glued lamin...	1.150	1.000	1	1.000	0.800

f _{m,0,k}	f _{m,90,k}	f _{t,0,k}	f _{t,90,k}	f _{c,0,k}	f _{c,90,k}	f _{v,k}	E _{0,mean}
[N/mm ²]	[N/mm ²]	[N/mm ²]	[N/mm ²]	[N/mm ²]	[N/mm ²]	[N/mm ²]	[N/mm ²]
32.000	32.000	19.500	0.500	24.500	2.500	3.500	13500.000

E _{90,mean}	E _{0,05}	G _{mean}	G _{0,05}	Rho _k	Rho _{mean}	Thermal coefficient x'
[N/mm ²]	[N/mm ²]	[N/mm ²]	[N/mm ²]	[kg/m ³]	[kg/m ³]	[-]
300.000	11200.000	650.000	540.000	400.000	440.000	0.000

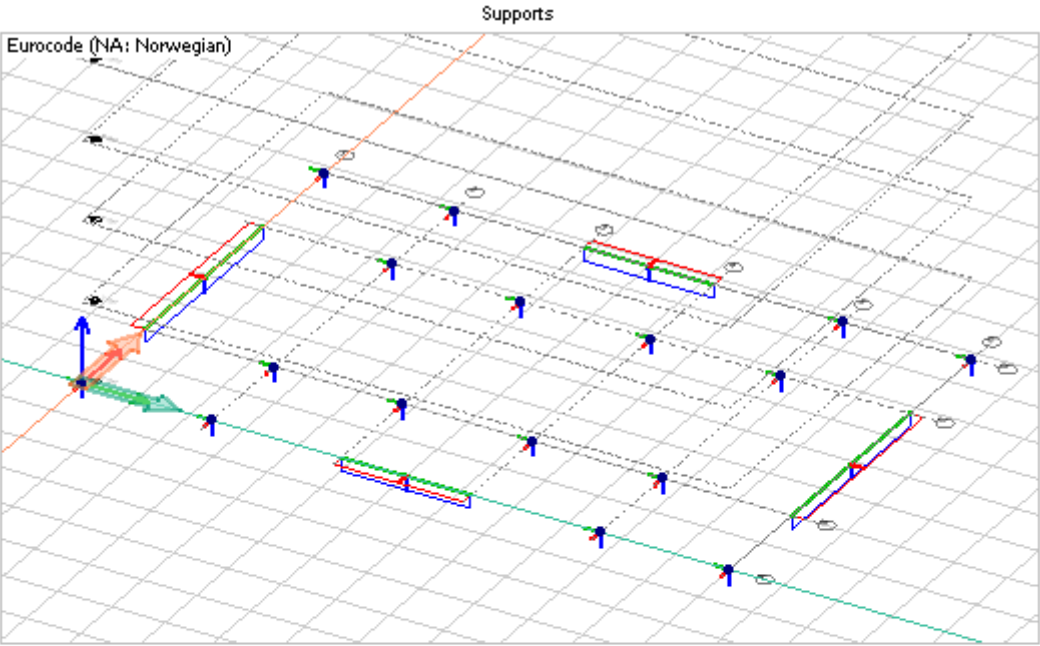
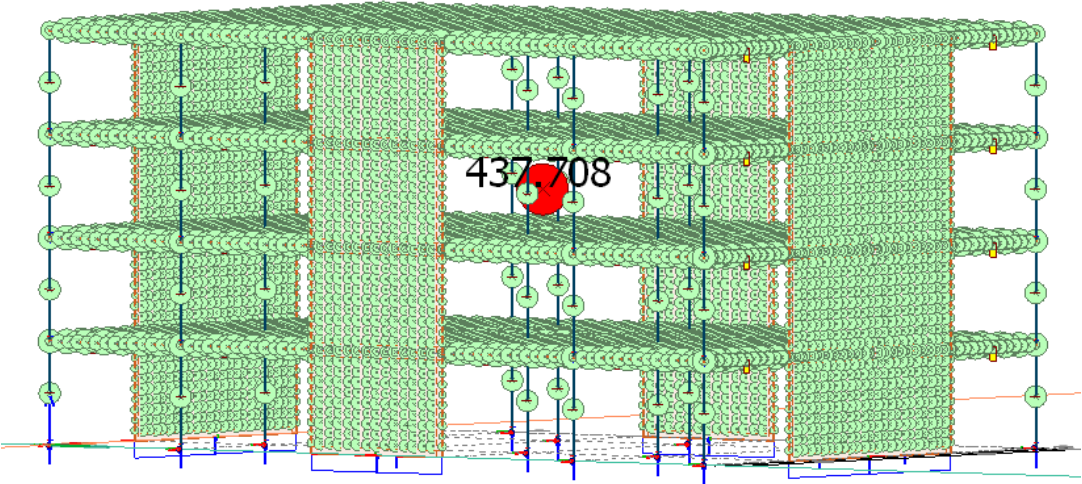
Thermal coefficient y'	Thermal coefficient z'
[-]	[-]
0.000	0.000



Model #4 – Glulam-CLT-Steel

The figure below shows modal mass of each element and the amount of total mass for this model.

Eurocode (NA: Norwegian) code: Eigenfrequencies - Converted masses - [t]



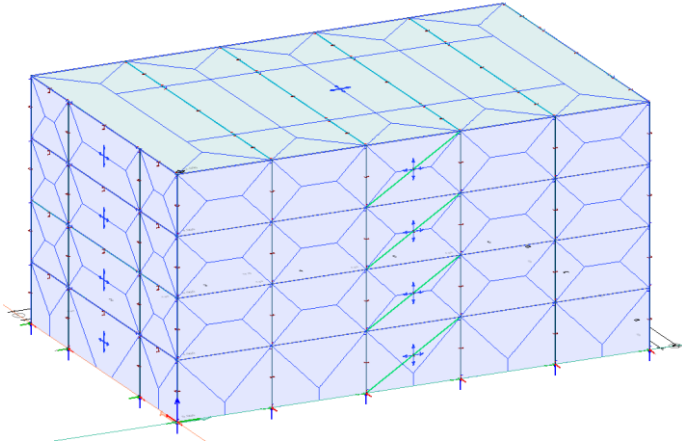
Point support groups

ID	x	y	z	Kx' comp.	Kx' tens.	Ky' comp.	Ky' tens.	Kz' comp.
[-]	[m]	[m]	[m]	[kN/m]	[kN/m]	[kN/m]	[kN/m]	[kN/m]
S.1	24.000	15.600	0.000	1.00E+10	1.00E+10	1.00E+10	1.00E+10	1.00E+10
S.2	24.000	0.000	0.000	1.00E+10	1.00E+10	1.00E+10	1.00E+10	1.00E+10
S.3	19.200	15.600	0.000	1.00E+10	1.00E+10	1.00E+10	1.00E+10	1.00E+10
S.4	19.200	11.600	0.000	1.00E+10	1.00E+10	1.00E+10	1.00E+10	1.00E+10
S.5	19.200	4.000	0.000	1.00E+10	1.00E+10	1.00E+10	1.00E+10	1.00E+10
S.6	19.200	0.000	0.000	1.00E+10	1.00E+10	1.00E+10	1.00E+10	1.00E+10
S.7	14.400	11.600	0.000	1.00E+10	1.00E+10	1.00E+10	1.00E+10	1.00E+10
S.8	14.400	4.000	0.000	1.00E+10	1.00E+10	1.00E+10	1.00E+10	1.00E+10
S.9	9.600	11.600	0.000	1.00E+10	1.00E+10	1.00E+10	1.00E+10	1.00E+10

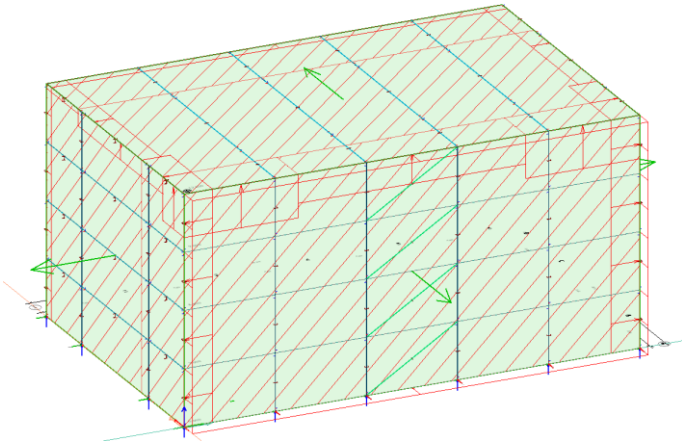
APPENDIX C WIND LOAD CALCULATION

Wind load

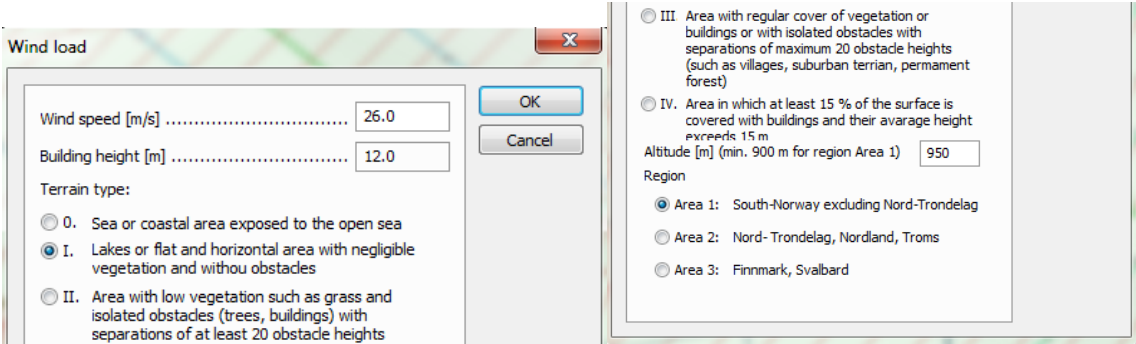
Before starting to calculate wind-load in FEM-DESIGN we need to cover up the structure, as showed in the figure below:



Then by defining the direction of force, with green arrows, for flat roof and external walls we can generate load. These arrows are in accordance to wind direction terminology of EC.



Then by classifying the building according to EC by giving it wind speed, building height, terrain type, altitude and region we can generate different load cases for x and y-direction.



Equilibrium				Equilibrium			
Check... Load combinations				Check... Load combinations			
Load cases / combinations				Load cases / combinations			
Wind (X-direction) Wind (Y-direction)				Wind (X-direction) Wind (Y-direction)			
Component	Loads	Reactions	Error [%]	Component	Loads	Reactions	Error [%]
Fx [kN]	385.39	-385.39	0.00	Fx [kN]	-1.725e-05	7.769e-05	77.80
Fy [kN]	4.559e-05	2.513e-04	118.14	Fy [kN]	650.95	-650.95	0.00
Fz [kN]	-20293	20293	0.00	Fz [kN]	-20091	20091	0.00
Mx [kNm] ...	-158275	158275	0.00	Mx [kNm] ...	-161766	161766	0.00
My [kNm] ...	247289	-247289	0.00	My [kNm] ...	241094	-241094	0.00
Mz [kNm] ...	-3005.8	3005.8	0.00	Mz [kNm] ...	7811.4	-7811.4	0.00

Wind loads have been checked with another software, OV-Sletten, to verify the values from FEM-DESING. The results are presented in Norwegian next pages:

Master thesis

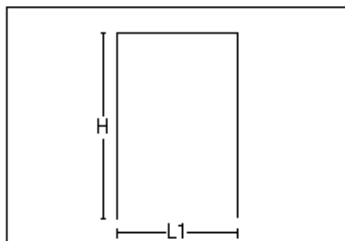
Tittel Wind load calculation		Side 1	
Prosjekt NMBU	Ordre	Sign MOHSHA	Dato 27-04-2017

Dataprogram: LastBeregning versjon 6.2.3 Laget av Sletten Byggdata AS

Standard NS-EN 1991-1-4: Vindlaster

Data er lagret på fil:

1. Geometri



H 12000 mm
L1 15600 mm

Byggets lengde, L2: 24000 mm
Takvinkel : 0,00 (grader)

Vertikalsnitt

2. Vindhastighet

Fylke: Hordaland Kommune: Bergen Referansevindhastighet: 26 m/s

Byggested, høyde over havet (m): 50 Calt: 1

Returperiode (år): 50 Cprob: 1

Årstidsfaktoren, Cseason: 1 hele året

Vindretning (region): Bruker retningsfaktoren C-ret: 1

Basisvindhastighet 26 m/s

Høyde Z over grunnivået: 12 m

BYGGSTEDETS TERRENGDATA

Terrengkategorikategori I: Kystnær, opprørt sjø. Åpne vidder og strandsoner uten trær eller busker.

Terrengkategorifaktoren K_t 0,17 Ruhetslengden Z_o (m): 0,01 Z_{min} (m): 2 V_m (m/s): 31,34 C_r : 1,21

TOPOGRAFI: Ingen topografisk påvirkning.

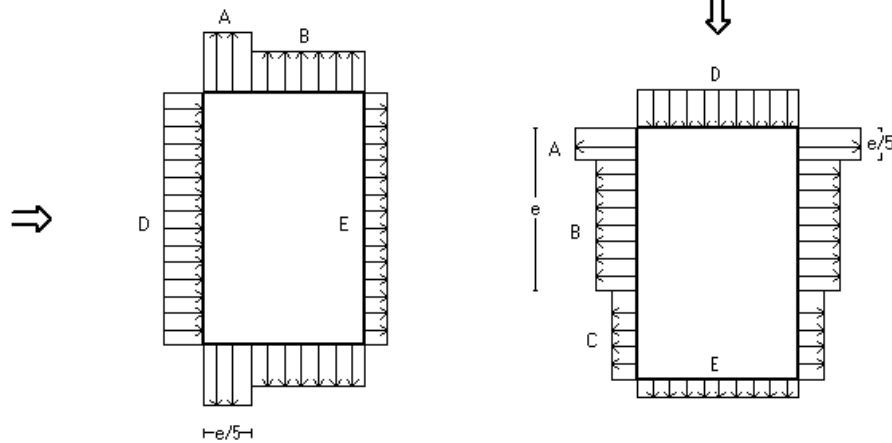
Terrengformfaktor $C_o(z)$: 1 Turbulensfaktor K_i : 1

V_{kast} : 44,18 m/s

Q_{kast} : 1,220 kN/m²

3. Yttervegger

3.1 Utvendig vindlast



Vindretning 0 grader. $e=24000$ mm

Vindretning 90 grader. $e=15600$ mm

Vindinnfallsretning på 0 grader.

	A	B	C	D	E
Formfaktor $C_{pe,10}$	-1,20	-0,80		0,77	-0,44
Utvendig last (kN/m ²)	-1,46	-0,98		0,94	-0,53
Formfaktor $C_{pe,1}$	-1,40	-1,10		1,00	-0,44
Utvendig last (kN/m ²)	-1,71	-1,34		1,22	-0,53
Utstrekning (mm)	4800	10800		24000	24000

Vindinnfallsretning på 90 grader.

	A	B	C	D	E
Formfaktor $C_{pe,10}$	-1,20	-0,80	-0,50	0,73	-0,37
Utvendig last (kN/m ²)	-1,46	-0,98	-0,61	0,89	-0,45
Formfaktor $C_{pe,1}$	-1,40	-1,10	-0,50	1,00	-0,37
Utvendig last (kN/m ²)	-1,71	-1,34	-0,61	1,22	-0,45
Utstrekning (mm)	3120	12480	8400	15600	15600

Positiv verdi for last gir trykk. Negativ verdi hvis last er sug.

3.2 Innvendig vindlast

Bygning uten dominerende vindfasade

Beregn innvendig vindlast for $u=0.2$ overtrykk og $u=-0.3$ (undertrykk)

	Undertrykk	Overtrykk
Formfaktor	-0,30	0,20
Innvendig last (kN/m ²)	-0,37	0,24

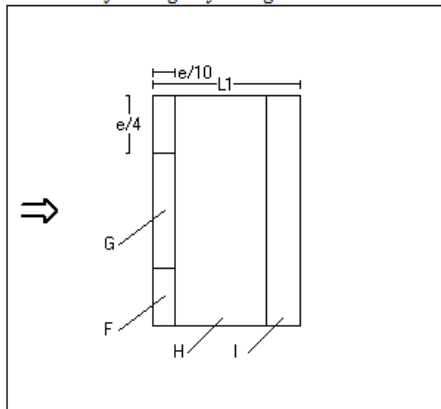
4 Overside av tak

Taktype: flatt tak

$L_1=15600$ mm $L_2=24000$ mm

$C_{pe,10}$ Gjelder for hele bygget. ($>=10m^2$)

Positiv verdi for last gir trykk. Negativ verdi hvis last er sug.



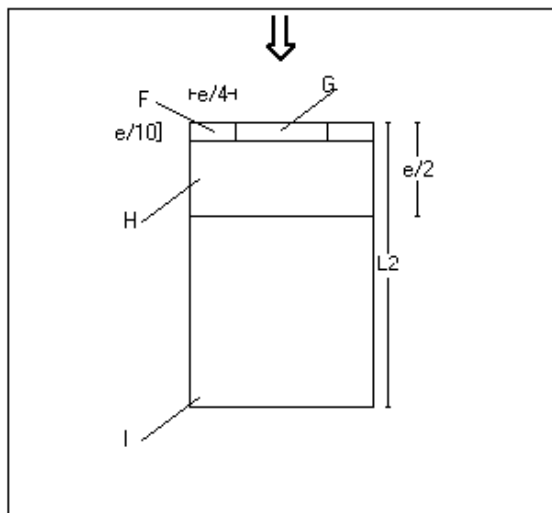
Utstrekning (mm)

$e=24000$

$e/4=6000$

$e/10=2400$

	$C_{pe,10}$	Last (kN/m ²)	Hor.prosjeksjon (mm)
F	-1,80	-2,20	6000x2400
G	-1,20	-1,46	12000x2400
H	-0,70	-0,85	24000x9600
I	+/-0,20	+/-0,24	24000x3600



Utstrekning (mm)

e=15600
e/4=3900
e/10=1560

	Cpe,10	Last (kN/m ²)	Hor.projeksjon (mm)
F	-1,80	-2,20	3900x1560
G	-1,20	-1,46	7800x1560
H	-0,70	-0,85	15600x6240
I	+/-0,20	+/-0,24	15600x16200

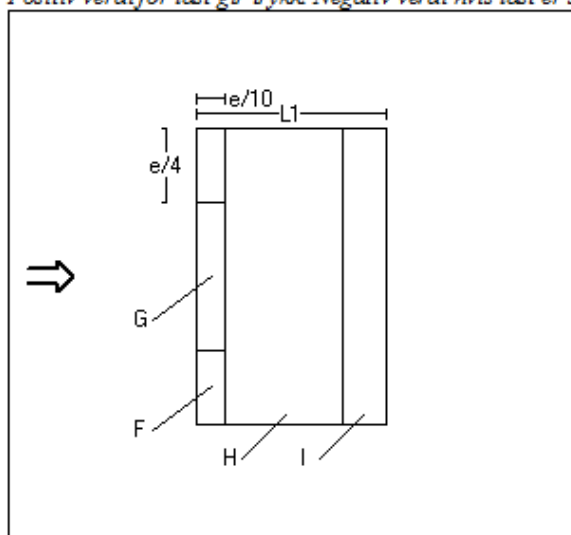
Taktype: Flatt tak

L1=15600 mm L2=24000 mm

Cpe,1 Gjelder for en lokal flate på 1m². Benyttes ved dimensjonering av limfuger, spikring, båndstål o.l.

Interpoleringsformel for belastet areal A mellom 1 og 10 m² : $Cpe = Cpe,1 + (Cpe,10 - Cpe,1) * \log_{10} A$

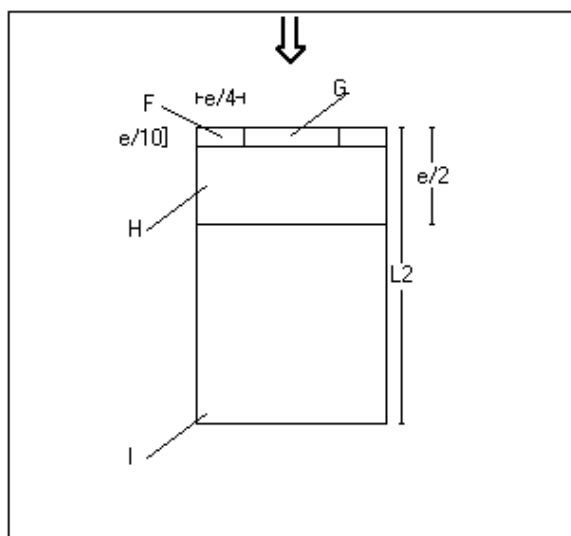
Positiv verdi for last gir trykk. Negativ verdi hvis last er sug.



Utstrekning (mm)

e=24000
e/4=6000
e/10=2400

	Cpe,1	Last (kN/m ²)	Hor.projeksjon(mm)
F	-2,50	-3,05	6000x2400
G	-2,00	-2,44	12000x2400
H	-1,20	-1,46	24000x9600
I	+/-0,20	+/-0,24	24000x3600



Utstrekning (mm)

e=15600
e/4=3900
e/10=1560

	Cpe,1	Last (kN/m ²)	Hor.projeksjon(mm)
F	-2,50	-3,05	3900x1560
G	-2,00	-2,44	7800x1560
H	-1,20	-1,46	15600x6240
I	+/-0,20	+/-0,24	15600x16200

APPENDIX D CLT FLOOR CALCULATION

CLTdesigner report where the deflection, vibration and capacity of CLT 240 C24 were calculated.

1 General

Service class 1

2 Structural system

Single span girder

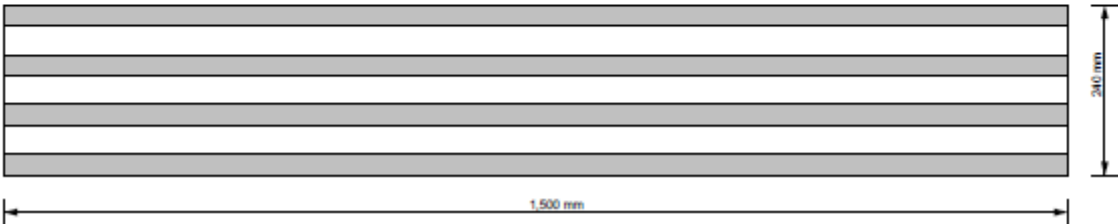


2.1 Width of supports

Support	x	Width
A	0.0 m	0.06 m
B	4.8 m	0.06 m

3 Cross section

Preferred cross section: 240 L7s
7 layers (width: 1,500 mm / thickness: 240 mm)



3.1 Layer composition

Layer	Thickness	Orientation	Material
# 1	30 mm	0	C24
# 2	40 mm	90	C24
# 3	30 mm	0	C24
# 4	40 mm	90	C24
# 5	30 mm	0	C24
# 6	40 mm	90	C24
# 7	30 mm	0	C24

3.2 Material parameters

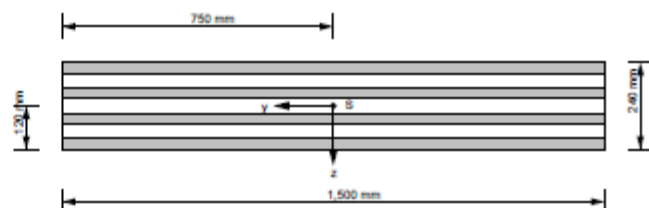
Partial safety factor $\gamma_M = 1.25$

Material parameters for C24	
bending strength	24.0 N/mm ²
tensile strength parallel	14.0 N/mm ²
tensile strength perpendicular	0.4 N/mm ²
compressive strength parallel	21.0 N/mm ²

Material parameters for C24	
compressive strength perpendicular	2.5 N/mm ²
shear strength	4.0 N/mm ²
rolling shear strength	1.0 N/mm ²
Youngs modulus parallel	11,000.0 N/mm ²
5%-quantile from Youngs modulus parallel	7,400.0 N/mm ²
Youngs modulus perpendicular	370.0 N/mm ²
shear modulus	690.0 N/mm ²
rolling shear modulus	69.0 N/mm ²
density	350.0 kg/m ³
density mean value	420.0 kg/m ³
in plane shear strength	5.0 N/mm ²
torsional strength	2.5 N/mm ²

3.3 Cross-sectional values

EA_{ef}	2.047E9 N
EI_{ef}	1.25E13 N-mm ²
GA_{ef}	3.559E7 N



4 Loads

Field	$g_{0,k}$	$g_{1,k}$	q_k	Category	s_k	Altitude/Region	w_k
1	1.98 kN/m	1 kN/m ²	2 kN/m ²	B	0.56kN/m ²	<1000m	

Partial safety factors:

$$\gamma_G = 1.35$$

$$\gamma_Q = 1.5$$

Load position:

Plate weight: Total

Permanent loads: Total

Imposed loads: Field-by-field

Snow: Field-by-field

Wind: Total

Combinations:

Combination factors: according to EN

5 Specification concerning structural fire design

No specifications are available

6 Information concerning vibrations

high requirements

Damping factor: 1.0 %

Support: 2-sided

Width perpendicular to the main load bearing direction: 1.5 m

7 Results

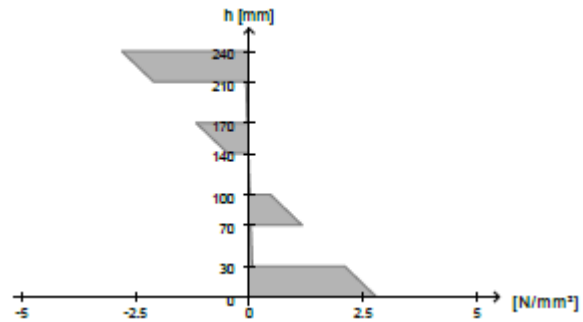
Referenced standards: EN 1995-1-1:2009, ON B 1995-1-1/NA:2014-11-15

Underlying calculation method: Timoshenko

7.1 ULS

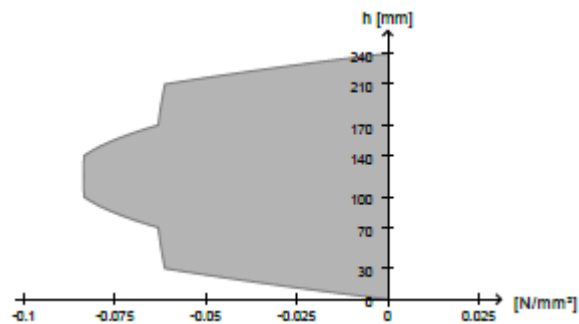
7.1.1 Bending

Utilisation ratio	16.6 %
k_{mod}	0.8
at x	2.4 m
Fundamental combination	$1.35 \cdot g_{0,k} + 1.35 \cdot g_{1,k} + 1.50 \cdot 1.00 \cdot q_k$



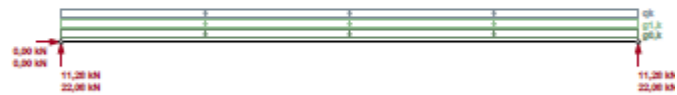
7.1.2 Shear

Utilisation ratio	13.1 %
k_{mod}	0.8
at x	4.8 m
Fundamental combination	$1.35 \cdot g_{0,k} + 1.35 \cdot g_{1,k} + 1.50 \cdot 1.00 \cdot q_k$



7.1.3 Bearing pressure

Utilisation ratio	8.8 %
k_{mod}	0.8
at x	4.8 m
Fundamental combination	$1.35 \cdot g_{0,k} + 1.35 \cdot g_{1,k} + 1.50 \cdot 1.00 \cdot q_k$



7.2 SLS

Limit values according to EN 1995-1-1

Instantaneous deformation $w_{inst} t = 0$: $l/300$

Final deformation $w_{fin} t = inf$: $l/150$

Final deformation $w_{net,fin} t = inf$: $l/250$

Limit values according to ON B 1995-1-1/NA:2014-11-15

Instantaneous deformation $w_{inst} t = 0$: $l/300$

Final deformation $w_{fin} t = inf$: $l/150$

Final deformation $w_{net,fin} t = inf$: $l/250$

Utilisation ratio	35.1 %
w_{max}	6.7 mm
k_{def}	0.85
at x	2.4 m
Final deformation $w_{net,fin} t = inf$ ($l/250$)	



7.2.2 Vibration

The verification is only valid for residential ceilings!

7.2.2.1 Verification corresponding to EN 1995-1-1

Eigenfrequency: $f_1 = 11.95 \text{ Hz} > 8.0 \text{ Hz}$

Stiffness: $w_{1kN} = 0.22 \text{ mm} < 1.0 \text{ mm}$

Velocity/Unit impuls: $v = 2.10 \text{ mm/s} < 12.1 \text{ mm/s}$

---> Vibration verification fulfilled

7.2.2.2 Verification corresponding to ON B 1995-1-1/NA:2014-11-15

Eigenfrequency: $f_1 = 11.95 \text{ Hz} > 8.0 \text{ Hz}$

Stiffness: $w_{1kN} = 0.22 \text{ mm} < 0.2 \text{ mm}$

---> Vibration verification fulfilled

7.2.2.3 Verification corresponding to DIN 1052

$w_{perm} = 2.8 \text{ mm} \leq 6.0 \text{ mm}$ ---> Vibration verification fulfilled

7.2.2.4 Verification according to Hamm/Richter

Eigenfrequency: $f_1 = 12.80 \text{ Hz} > 8.0 \text{ Hz}$

Stiffness: $w_{2kN} = 0.37 \text{ mm} < 0.5 \text{ mm}$

---> Vibration verification fulfilled

7.2.2.5 Verification according to modified Hamm/Richter

Eigenfrequency: $f_1 = 12.78 \text{ Hz} > 8.0 \text{ Hz}$

Stiffness: $w_{2kN} = 0.37 \text{ mm} < 0.5 \text{ mm}$

---> Vibration verification fulfilled

APPENDIX E MEASUREMENT INSTRUMENTS

Images of gravimeter, geophone and accelerometer:



Gravimeter – Source: Wikipedia



Geophones – Source: <http://www.sercel.com/products/Pages/sg-5.aspx>



A type of Accelerometer – Source: <https://www.passcal.nmt.edu/content/instrumentation/sensors/accelerometers>

APPENDIX F CLT VALUES FROM MARTINSON

Martinson's value used in FEM-DESIGN are as followed:

Karakteristiska, styvhets- och hållfasthetsvärden [MPa]

2017-01-23

KL-trä - Martinsons standardtjocklekar

Material:¹⁾ C24 till bitar i styv riktning

C14 till bitar i vek riktning

1. Styvhetsvärden för deformationsberäkningar (50%-fraktilen)

Tjocklek [mm] ²⁾	E-modul, böjning kring i- axeln, E _{mi,50}				E-modul, drag // i- axeln E _{ti,50}			E-modul, tryck // i- axeln E _{ei,50}			Skjuvmodul, G _{ij,50}		
	Z	X	Y ₁	Y ₂	X	Z	Y	X	Z	Y	XY	YZ	XZ
	Styv	Vek	Skivv.styv	Skivv.vek	Styv	Vek	Tvärdrag	Styv	Vek	⊥ Fibrema	Böj.styv	Böj.vek	Böj.skiv
60-3s	10 606	764	7 457	3 913	7 457	3 913	370				117	96	690
70-3s	10 152	892	6 384	3 211	6 384	3 211	310				95	108	582
80-3s	10 832	474	8 308	2 028	2 028	2 028	335				148	87	627
90-3s	10 601	616	7 410	2 580	7 410	2 580	323	Samma värden			117	96	606
100-3s	10 601	616	7 410	2 580	7 410	2 580	323	som för drag.			117	96	606
120-3s	10 601	616	7 410	2 580	7 410	2 580	323				117	96	606
140-3s	10 601	616	7 410	2 580	7 410	2 580	323				117	96	606
100-5s	8 760	1 749	6 692	3 022	6 692	3 022	314				100	104	590
120-5s	7 859	2 304	5 615	3 685	5 615	3 685	300				83	119	565
130-5s	9 451	1 324	7 686	2 410	7 686	2 410	327				125	93	613
140-5s	7 106	2 767	4 846	4 159	4 846	4 159	290				73	133	547
150-5s	8 760	1 749	6 692	3 022	6 692	3 022	314	Samma värden			100	104	590
160-5s	9 822	1 095	8 308	2 028	8 308	2 028	335	som för drag.			148	87	627
180-5s	7 859	2 304	5 615	3 685	5 615	3 685	300				83	119	565
200-5s	8 760	1 749	6 692	3 022	6 692	3 022	314				100	104	590
230-5s	8 760	1 749	6 692	3 022	6 692	3 022	314				100	104	590
210-7s	7 891	2 284	6 384	3 211	6 384	3 211	310				95	108	582
240-7s	9 401	1 354	8 308	2 028	8 308	2 028	335	Samma värden			148	87	627
270-7s	8 740	1 761	7 410	2 580	7 410	2 580	323	som för drag.			117	96	606
280-7s	7 891	2 284	6 384	3 211	6 384	3 211	310				95	108	582
300-7s	8 157	2 120	6 692	3 022	6 692	3 022	314				100	104	590

2. Styvhetsvärden för hållfasthetsberäkningar (5%-fraktilen)

Tjocklek [mm] ²⁾	E-modul, böjning kring i- axeln, E _{mi,05}				E-modul, drag // i- axeln E _{ti,05}			E-modul, tryck // i- axeln E _{ei,05}			Skjuvmodul, G _{ij,05}		
	Z	X	Y ₁	Y ₂	X	Z	Y	X	Z	Y	XY	YZ	XZ
	Styv	Vek	Skivv.styv	Skivv.vek	Styv	Vek	Tvärdrag	Styv	Vek	⊥ Fibrema	Böj.styv	Böj.vek	Böj.skiv
60-3s	7 126	274	4 933	2 467	4 933	2 467	-				-	-	-
70-3s	6 817	370	4 229	2 014	4 229	2 014	-				-	-	-
80-3s	7 284	73	5 550	1 175	5 550	1 175	-				-	-	-
90-3s	7 126	174	4 933	1 567	4 933	1 567	-	Samma värden			-	-	-
100-3s	7 126	174	4 933	1 567	4 933	1 567	-	som för drag.			-	-	-
120-3s	7 126	174	4 933	1 567	4 933	1 567	-				-	-	-
140-3s	7 126	174	4 933	1 567	4 933	1 567	-				-	-	-
100-5s	5 861	978	4 440	1 880	4 440	1 880	-				-	-	-
120-5s	5 242	1 371	3 700	2 350	3 700	2 350	-				-	-	-

130-5s	6 336	676	5 123	1 446	5 123	1 446	-				-	-	-
140-5s	4 725	1 699	3 171	2 686	3 171	2 686	-				-	-	-
150-5s	5 861	978	4 440	1 880	4 440	1 880	-	Samma värden			-	-	-
160-5s	6 591	514	5 550	1 175	5 550	1 175	-	som för drag.			-	-	-
180-5s	5 242	1 371	3 700	2 350	3 700	2 350	-				-	-	-
200-5s	5 861	978	4 440	1 880	4 440	1 880	-				-	-	-
230-5s	5 861	978	4 440	1 880	4 440	1 880	-				-	-	-
210-7s	5 264	1 357	4 229	2 014	4 229	2 014	-				-	-	-
240-7s	6 302	698	5 550	1 175	5 550	1 175	-	Samma värden			-	-	-
270-7s	5 847	986	4 933	1 567	4 933	1 567	-	som för drag.			-	-	-
280-7s	5 264	1 357	4 229	2 014	4 229	2 014	-				-	-	-
300-7s	5 446	1 241	4 440	1 880	4 440	1 880	-				-	-	-

3. Hållfasthetsvärden (5%-fraktilen)

Tjocklek [mm] ²⁾	Böjhållfasthet, $f_{m,k}$				Draghållfasthet, $f_{t,k}$			Tryckhållfasthet, $f_{c,k}$			Skjuvhållfasthet, $f_{ij,k}$		
	Z	X	Y ₁	Y ₂	X	Z	Y	X	Z	Y	XY	YZ	XZ
L / T ³⁾	Styv	Vek	Skivv.styv	Skivv.vek	Styv	Vek	Tvärdrag	Styv	Vek	⊥ Fibrema	Böj.styv	Böj.vek	Böj.skiv
60-3s	23,1	0,9	16,0	8,0	9,3	4,7	0,4	14,0	7,0	3,0	1,1	1,1	1,3
70-3s	22,1	1,1	13,7	6,0	8,0	3,4	0,4	12,0	6,9	3,0	1,1	1,1	1,3
80-3s	23,6	0,2	18,0	3,5	10,5	2,0	0,4	15,8	4,0	3,0	1,1	1,1	0,8
90-3s	23,1	0,5	16,0	4,7	9,3	2,7	0,4	14,0	5,3	3,0	0,7	0,7	1,0
100-3s	23,1	0,5	16,0	4,7	9,3	2,7	0,4	14,0	5,3	3,0	0,7	0,7	1,0
120-3s	23,1	0,5	16,0	4,7	9,3	2,7	0,4	14,0	5,3	3,0	0,7	0,7	1,0
140-3s	23,1	0,5	16,0	4,7	9,3	2,7	0,4	14,0	5,3	3,0	0,7	0,7	1,0
100-5s	19,0	2,9	14,4	5,6	8,4	3,2	0,4	12,6	6,4	3,0	1,1	1,1	1,2
120-5s	17,0	4,1	12,0	7,0	7,0	4,0	0,4	10,5	8,0	3,0	1,1	1,1	1,5
130-5s	20,6	2,0	16,6	4,3	9,7	2,5	0,4	14,5	4,9	3,0	1,1	1,1	0,9
140-5s	15,3	5,1	10,9	8,0	6,0	4,6	0,4	9,0	9,1	3,0	1,1	1,1	1,7
150-5s	19,0	2,9	14,4	5,6	8,4	3,2	0,4	12,6	6,4	3,0	0,7	0,7	1,2
160-5s	21,4	1,5	18,0	3,5	10,5	2,0	0,4	15,8	4,0	3,0	1,1	1,1	0,8
180-5s	17,0	4,1	12,0	7,0	7,0	4,0	0,4	10,5	8,0	3,0	0,7	0,7	1,5
200-5s	19,0	2,9	14,4	5,6	8,4	3,2	0,4	12,6	6,4	3,0	0,7	0,7	1,2
230-5s	19,0	2,9	14,4	5,6	8,4	3,2	0,4	12,6	6,4	3,0	0,7	0,7	1,2
210-7s	17,1	4,0	13,7	6,0	8,0	3,4	0,4	12,0	6,9	3,0	0,7	0,7	1,3
240-7s	20,4	2,1	18,0	3,5	10,5	2,0	0,4	15,8	4,0	3,0	1,1	1,1	0,8
270-7s	19,0	2,9	16,0	4,7	9,3	2,7	0,4	14,0	5,3	3,0	0,7	0,7	1,0
280-7s	17,1	4,0	13,7	6,0	8,0	3,4	0,4	12,0	6,9	3,0	1,1	1,1	1,3
300-7s	17,7	3,7	14,4	5,6	8,4	3,2	0,4	12,6	6,4	3,0	0,7	0,7	1,2

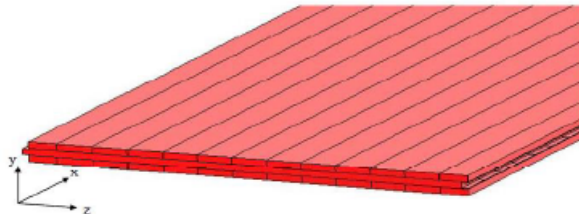
Värdena är rullerade till skivans totala tjocklek.

Styv riktning avser den riktning som är styvare med avseende på böjning.

1) Skiva 60-3s utförs av C24 även till bitar i vek riktning.

2) "60"=Tjocklek i mm. "3s"=Tre skikt.

3) "L"=Längsgående ytterskikt, "T"=Tvärgående ytterskikt.



BIBLIOGRAPHY

- A. Rønquist, Conrad Lindholm & Svein Remseth. (2012). *Earthquake engineering design practice in Norway: Implementation of Eurocode 8*. 15th World Conference on Earthquake Engineering, Lisbon: NTNU.
- Ansystuba.sk. (2016). *Harmonic Response Analysis*.
- BCA.GOV.SG. (2017). Cross Laminated Timber/ Glued Laminated Timber.
- Bell, K., Liven, H. & Norske limtreprodusenters, f. (2015). *Limtreboka*. Design of glulam structures. Bergen: John Grieg Norske limtreprodusenters forening.
- Bonomo. (2013). *CLT*. Energy Box is an earthquake-proof passive house built of cross-laminated timber. www.treehugger.com. Available at: <https://www.treehugger.com/green-architecture/energy-box-earthquake-proof-passive-house-built-cross-laminated-timber.html>.
- Brandner, R., Flatscher, G., Ringhofer, A., Schickhofer, G. & Thiel, A. (2016). Cross laminated timber (CLT): overview and development. *Holz als Roh- und Werkstoff*, 74 (3): 331-351.
- Byggforskserien. (2001). Massive trelementer. Typer og bruksområder.
- Byggforskserien. (2011). *Bjelker av tre. Dimensjonering*. Available at: https://www.byggforsk.no/dokument/304/bjelker_av_tre_dimensjonering.
- Chopra, A. K. & Goel, R. K. (2000). Building period formulas for estimating seismic displacements. *Earthquake Spectra*, 16 (2): 533-536.
- Chopra, A. K. (2012). *Dynamics of structures : theory and applications to earthquake engineering*. 4th ed. Upper Saddle River, N.J.: Prentice Hall. xxxiii, 944 p. pp.
- Clough, R. W. & Penzien, J. Dynamics of structures. 2003. *Computers and Structures, Inc., Berkeley*.
- Deierlein, G. G., Reinhorn, A. M. & Willford, M. R. (2010). Nonlinear structural analysis for seismic design. *NEHRP seismic design technical brief*, 4: 1-36.
- EC5. (1994). *Eurocode 5: Prosjektering av trekonstruksjoner = Eurocode 5: Design of timber structures. Part 1-1: General rules and rules for buildings : 1-1 : Generelle regler og regler for bygninger*. Norsk versjon. ed. Eurocode 5: Design of timber structures. Part 1-1: General rules and rules for buildings, vol. NL-ENV 1995-1-1. Oslo: Norges standardiseringsforbund.
- EC8. (2014). *Eurokode 8: prosjektering av konstruksjoner for seismisk påvirkning = Eurocode 8: Design of structures for earthquake resistance. Part 1: General rules, seismic actions and rules for buildings : Del 1 : allmenne regler, seismiske laster og regler for bygninger*. Eurocode 8: Design of structures for earthquake resistance. Part 1: General rules, seismic actions and rules for buildings, vol. NS-EN 1998-1:2004+A1:2013+NA:2014. Lysaker: Standard Norge.
- Elghazouli, A. (2009). *Seismic design of buildings to Eurocode 8*. London ; New York: Spon Press. xvi, 318 p. pp.
- Fardis, M. N. (2005). *Designers' guide to EN 1998-1 and EN 1998-5 Eurocode 8: design of structures for earthquake resistance: general rules, seismic actions, design rules for buildings, foundations and retaining structures*, vol. 8: Thomas Telford Services Limited.
- Fujita, M., Sakai, J., Oda, H. & Iwata, M. (2014). Building system for a composite steel-timber structure. *Steel Construction*, 7 (3): 183-187.
- HiØF. (2016). *Massetetthet og termiske egenskaper for noen stoffer*. Available at: <http://www.it.hiof.no/tressfysikk/scan/tabell1.pdf>.
- Jarrett, J., Zimmerman, R. & Charney, F. (2014). *Accidental Torsion in Nonlinear Response History Analysis*.
- Javed, P. D. M. (2015). *Introduction to Structural Dynamics and Earthquake Engineering*. Slideshare. Available at:

https://www.slideshare.net/javeduet?utm_campaign=profiletracking&utm_medium=ssite&utm_source=ssslideview.

- Jordskjelv.no. *Jordskjelv i Norge*. Available at: <https://www.jordskjelv.no/jordskjelv/om-jordskjelv/jordskjelv-i-norge/>.
- Khorasani, Y. (2011). *Feasibility study of hybrid wood steel structures*: University of British Columbia.
- Kirkegaard, P. H., Sorensen, J. D., Cizmar, D. & Rajcic, V. (2010). Robustness Analysis of a Wide-Span Timber Structure with Ductile Behaviour. *Proceedings of the Tenth International Conference on Computational Structures Technology*, 93.
- Kouskouna, V. & Makropoulos, K. (2004). Historical earthquake investigations in Greece. *Annals of Geophysics*.
- Koyluoglu, H. U., Nielsen, S. R. K., Cakmak, A. S. & Kirkegaard, P. H. (1997). Prediction of global and localized damage and future reliability for RC structures subject to earthquakes. *Earthquake Engineering & Structural Dynamics*, 26 (4): 463-475.
- Løset, Ø. & Rif, A. N. S. (2010). *Dimensjonering for jordskjelv : veileder til NS-EN 1998-1:2004+NA:2008*. Oslo: Rådgivende ingeniørers forening.
- Løset, Ø., Skau, H., Vinje, L., Lurén, H., Alexander, S., Knustad, R., Andersen, T. R. & Betongelementforeningen. (2011). *Dimensjonering for jordskjelv*. [Ny utg.]. ed., vol. H. Oslo: Betongelementforeningen.
- NS-EN338. (2016). *Konstruksjonstrevirke : styrkeklasser = Structural timber : strength classes*. Structural timber strength classes, vol. NS-EN 338. Oslo: Norges standardiseringsforbund.
- Seo, J., Hu, J. W. & Davaajamts, B. (2015). Seismic performance evaluation of multistory reinforced concrete moment resisting frame structure with shear walls. *Sustainability*, 7 (10): 14287-14308.
- SHARE. (2013). European Seismic Hazard Map 2013.
- Shrestha, R., Lewis, K. & Crews, K. (2014). *Introduction to cross laminated timber and development of design procedures for Australia and New Zealand*. Australasian Conference on the Mechanics of Structures and Materials (ACMSM23): Southern Cross University.
- Splinter, R. (2016). *Illustrated Encyclopedia of Applied and Engineering Physics*: CRC Press LLC.
- StoraEnso. (2016). *The Stora Enso CLT design software*: Stora Enso. Available at: <https://engineer.clt.info/Dokumentation/CLT-Engineer-Manual.pdf>.
- Taushanov, A. (2012). DEFINITION OF THE INFLUENCE VECTOR IN EARTHQUAKE ANALYSIS.
- TFD.com. (2016). *Fault*: The Free Dictionary.
- USGS.gov. *Earthquake Glossary*. Available at: <https://earthquake.usgs.gov/learn/glossary/?term=seismic%20moment>.
- Visual.ly. (2011). *Earthquake faults and zones*
- Wang, Y.-h., Nie, J.-g. & Cai, C. S. (2013). Numerical modeling on concrete structures and steel-concrete composite frame structures. *Numerical modeling on concrete structures and steel-concrete composite frame structures*, 51: 58-67.
- Øystad-Larsen, N. (2010). *Dimensjonering for jordskjelv : teorigrunnlag, regelverk og beregninger*. Oslo: N. Øystad-Larsen.
- Ås-Kommune. (2013). Nye spennende studentboliger åpnet. Available at: <http://www.as.kommune.no/nye-spennende-studentboliger-aapnet.5285626-125470.html>.



Norges miljø- og biovitenskapelig universitet
Noregs miljø- og biovitenskapelige universitet
Norwegian University of Life Sciences

Postboks 5003
NO-1432 Ås
Norway